HELLENIC REPUBLIC
National and Kapodistrian University of Athens
EST. 1837

Mass spectrometry based metabolomics for mapping and quality control of Extra Virgin Olive Oil (EVOO).
Evaluation of EVOO marker compounds in animal and human studies.

PhD thesis in Pharmacy

Theodora Nikou

Mass spectrometry based metabolomics for mapping and quality control of Extra Virgin Olive Oil (EVOO).
Evaluation of EVOO marker compounds in animal and human studies.

This research is co-financed by Greece and the European Union (European Social Fund- ESF) through the Operational Programme «Human Resources Development, Education and Lifelong Learning» in the context of the project “Strengthening Human Resources Research Potential via Doctorate Research” (MIS-5000432), implemented by the State Scholarships Foundation (IKY).

Mass spectrometry based metabolomics for mapping and quality control of Extra Virgin Olive Oil (EVOO).
Evaluation of EVOO marker compounds in animal and human studies.

Theodora Nikou

December 2019

Department of Pharmacognosy and Natural Products Chemistry

School of Pharmacy

National and Kapodistrian University of Athens

Examining Committee

Assistant Professor Maria Halabalaki[1]

Professor Leandros A. Skaltsounis[1]

Professor Emmanouil Mikros[2]

Senior Lecturer Emerson Ferreira Queiroz[3]

Professor Nikolaos Tentolouris[4]

Professor Sofia Mitakou[1]

Researcher A' Elissavet Dotsika[5]

[1]Department of Pharmacognosy and Naturals Products Chemistry, School of Pharmacy, National and Kapodistrian University of Athens.

[2]Department of Pharmaceutical Chemistry, School of Pharmacy, National and Kapodistrian University of Athens.

[3]Department of Phytochemistry and Bioactive Natural Products, Faculty of Pharmaceutical Sciences, University of Geneva.

[4]First Department of Propaedeutic and Internal Medicine, Department of Medicine, National and Kapodistrian University of Athens.

[5]Institute of Nanoscience and nanotechnology, National Center for Scientific Research Demokritos.

Table of Contents

Thesis Summary

Nature still remains an untapped source of bioactive molecules and an important driving force in drug discovery process. Natural products (NPs) are characterized by high degree of structural diversity and uniqueness which is incomparable to chemically synthesized molecules. Only in the area of cancer, from 1940s to 2007, 73% of the 155 small molecules are other than synthetic, with 42% actually being either NP or directly derived from NP [1]. The main sources of NPs are medicinal plants but also marine organisms and microorganism as well as edible plants and foods.

In our days much attention has been given to dietary and nutritional habits for the prevention as well as the treatment of human health complications and diseases. Dietary supplements have been introduced in the daily routine of the general population especially in western countries aiming to the improvement of life quality and health [2]. Nevertheless, the definition of dietary supplements differs from country to country and the general terminology includes natural health products, complementary medicines, food supplements or functional foods [3]. No global consensus exists for the classification of these products and their assortment into specific groups is difficult due to the existence of large number of products, their varying content and the large number of properties and claims.

The existing regulations concerning such products can be characterized as a grey zone, and in European Union (EU) dietary supplements are regarded as foods [2]. Many botanicals are also classified as dietary supplements and typically labelled as natural foods while health claims are often accompanying them. The lack of legislation allows for the marketing of many preparations without sufficient or solid scientific data, mainly related to quality, efficacy and safety. Even in cases that active compounds or entities are contained for which their activity and safety are

scientifically substantiated, it is not the case for the final product in the market. Moreover, despite efficacy and safety which are commonly underestimated, one of the most common limitation in supplements is the lack of knowledge for the bioavailability and generally ADMET properties, which are directly connected to efficacy. Finally, the absence of quality assessment of the dietary and/or food supplements is commonly observed.

Amongst foods, olive oil (OO) has attracted the scientific interest after the publication of two heath claims concerning its chemical composition and the respective positive impacts to human health [4,5]. Nowadays, OO has been established in the consciousness of people as one of the most superior nutritional and health promoting edible oils world-wide, with exceptional organoleptic and sensory properties. Responsible for health and nutrition beneficial effects as well as its recognition as superior edible oil is its unique chemical composition. OO composition is extremely variable and complex and depends on several exogenous factors like olive variety, microclimate conditions, cultivation practice, production procedure, storage etc. Such factors influence its content in the contained compounds [6]. Interestingly, till today there is not a satisfactory and generally accepted method for quality control of OO. Considering the economic value of OO for EU and especially for Mediterranean countries, the investigation of factors infusing the composition of OO, the identification of certain chemical markers as well as the establishment of a proper methodology for quality control purposes is of outmost importance.

Towards the elucidation of OO composition, numerous studies have been carried out aiming to the identification of its constituents but also the exploration of biological properties thereof. Recently, OO polyphenols, the small fraction of polar compounds of OO are in the center of research. It is worth noting that till today there are still compounds in OO which haven’t been structurally characterized and new ones are reported [7]. Especially, OO

polyphenols exert important biological properties and constantly new studies are published investigating their role. However, a critical drawback which complicates and delays significantly this process is the lack of reference compounds in the market for the investigation of their activity. For instance, oleocanthal (OLEA) and oleacein (OLEO) are two of the major secoiridoids in OO categorized in polyphenols group which according to recent studies exert a plethora of promising biological properties but they are not commercially available. Thus, the establishment of methods for the isolation in pure form as well as in satisfactory yield of such compounds is the basic step enabling their further investigation. This will allow the performance of *in vitro* but more importantly *in vivo* experiments which will facilitate significantly the elucidation of their biological role and consequently will assist to decipher the properties of OO itself.

Another field which is also overlooked in the area of NPs and it is affected from the lack of reference compounds in required yield and purity is the exploration of ADMET properties. Studies related to such properties are rare [8] also in well-established active natural entities despite the fact that Absorption, Distribution, Metabolism, Excretion and Toxicity of a compound influence the possible drug levels and kinetics and hence influence the performance and pharmacological activity of a compound as a drug. This fact, resulting to incomplete information for an active entity and it is decisive step for the development of a compound as a drug. Similar pattern is observed also in OO polyphenols and limited are the studied concerning the investigation of ADMET characteristics thereof. Despite, the numerous studies related to the activity of OO secoiridoids, the lack of such information is vast even though their unstable and highly reactive chemical nature is well-known. Therefore, the introduction of ADMET in the general workflow of drug discovery process in the area of NPs is a critical factor. ADMET

information together with complete isolation and identification data as well as biological profile can optimize significantly the entire process.

Among these lines, together with unknown or recently uncovered polyphenols, there are also well known compounds in OO with established biological and pharmacological properties. One of the most potent compound which is also generally considered as one of the most active NPs is hydroxytyrosol (HT) [9]. A lot effort has been made so far for the interpretation of its properties and its role mainly as a strong antioxidant agent has been proven. Special attention has been given after the EFSA health claim connecting HT and its derivatives in OO with protective effect of blood proteins from oxidation. HT but also its derivatives can been found in several dietary supplements in the market usually in OO or as an enrichment factor. However, very limited are the studies exploring the efficacy of such products, most of the cases the levels of individual constituents are not determined and even less are the interventions in humans. HT has been detected in urine, plasma and tissues (even in the brain) however it is easily biotransfomed [10]. Unfortunately, despite the commercialization of many products containing HT, there is limited information for the impact of HT to human metabolome. Most of the studies investigate the positive impact of HT supplementation for the prevention or treatment of a specific pathology or its concentration in human tissues and few studies have been published for the followed biosynthetic path in human organism. This situation which as mentioned before concerns the majority of supplements resulting to consumer or patient confusion and on the other hand doesn't allow truly beneficial products to be disclosed and further investigated and developed. Therefore, there is a strong need for solid scientific data for dietary supplements substantiating the complete composition as well as their efficacy. Most importantly human

studies are critical ensuring the potency against a clear complication or disease as well as safety; both critical factors for the general population.

In the current study, we tried to develop methods and approaches aiming to offer possible answers to certain complications, limitations and inadequacies in NPs drug discovery process and NPs applications and uses. As a model starting material olive oil was selected. Olive oil is a perfect candidate since it is characterized by insufficient methods for quality evaluation, is a rich source of highly potent, promising and unknown compounds while OO itself or its constituents in different forms and mixtures are circulated in the market. Moreover, limited are the studies relayed to the ADMET properties of OO constituents, *in vivo* evaluation towards specific targets and nearly absent controlled human studies. In the center of this effort was the development of chromatographic and analytical methods for the isolation of active compounds, quality control and quantitation of actives in different biological fluids. Especially, mass spectrometry was intensively used to accomplished these goals as well as metabolic profiling and metabolomic approaches.

Based on the above in the current study a complete work-flow was designed and established exploring OO and its constituents. Specifically, starting from a library of OO samples (approx. 300) from all over Greece, quality control aspects for OO were examined aiming to the determination of the effect of specific quality parameters to OO composition and identification of marker compounds. OO characteristic compounds, hydroxytyrosol (HT), tyrosol (T), oleacein (OLEA) and oleocanthal (OLEO) were quantified based on International Olive Council (IOC) HPLC-DAD method revealing important information. Moreover, taking advantage of the ultra high resolution and high accuracy of mass spectrometry platforms in combination with chemometric tools, statistical significant metabolites were determined and identified for their

final correlation with specific quality factors. This is the first time that a complete metabolic profiling approach is developed and applied in Greek EVOOs with two different HRMS platforms and a list of identified marker compounds were determined.

Secoiridoids were found to be one of the major chemical categories in the generated list of markers. Thus, selected secoiridoid derivatives and recently reported iridoid derivatives were isolated for the performance of *in vitro* and *in vivo* tests as well as a pharmacokinetics study. OLEO and OLEA were two of them, characterized by strong anti-inflammatory and antioxidant properties. Both of them as well as three polyphenols extracts (TPFs) with high, medium and low levels of these metabolites were tested *in vitro* for evaluation of their cytotoxicity effects and proteasome activity in human fibroblasts cells. Moreover, TPFs were administered as dietary supplement to a *Drosophilla in vivo* model for investigation of their impact to healthy aging. Both molecules as well as TPF revealed positive impact to healthy aging promoting cytoprotective pathways and suppressed oxidative stress in both mammalian cells and flies. Consequently, an *in vivo* mouse model was designed for determination of OLEO pharmacokinetic characteristics. OLEO metabolism and biotransformation *in vivo* was investigated for the first time.

Another statistical significant compound was HT which is also a constituent of several products in the market. Thus, an intervention study was designed and performed to investigate the effect of an enriched in HT soft capsule supplemented in two different doses (5mg/day and 15mg/day) based on suggested dose from EFSA, to obese/overweight women in double-blinded study for a six-month period. Capsule was firstly evaluated for its final quality; total ingredients were identified and the final HT concentration was accurately determined. A targeted UPLC-triple-quadropole methodology was developed and validated for quantitation of HT in urine

during the whole intervention period and excretion levels were established. Consequently, un untargeted high-resolution mass spectrometry method was developed for the exploration of blood and urine metabolome during intervention. Biotransformation reactions of HT were monitored and possible phase I and phase II metabolization products were identified. Statistical significant weight and fat loss was observed after six months of supplementation in high doss (15mg/day) and it is the first time that HT is related to obesity in a human cohort. Moreover, different pathways were seemed to be followed depending on the supplemented dose. Using metabolomics approaches novel data were provided concerning the association of certain endogenous metabolites with HT supplementation.

Bibliography

[1] D.J. Newman, G.M. Cragg, Natural products as sources of new drugs over the last 25 years., J. Nat. Prod. 70 (2007) 461–477. doi:10.1021/np068054v.

[2] C.W. Binns, M.K. Lee, A.H. Lee, Problems and Prospects: Public Health Regulation of Dietary Supplements, Annu. Rev. Public Health. 39 (2018) 403–420. doi:10.1146/annurev-publhealth-040617-013638.

[3] J.T. Dwyer, P.M. Coates, M.J. Smith, Dietary Supplements: Regulatory Challenges and Research Resources, Nutrients. 10 (2018) 41. doi:10.3390/nu10010041.

[4] N. and A. (NDA) EFSA Panel on Dietetic Products, Scientific Opinion on the substantiation of health claims related to foods with reduced amounts of saturated fatty acids (SFAs) and maintenance of normal blood LDL-cholesterol concentrations (ID 620 , 671 , 4332) pursuant to Article 13 (1) of Regula, EFSA J. 9 (2011). doi:doi:10.2903/j.efsa.2011.2062.

[5] N. and A. (NDA) EFSA Panel on Dietetic Products, Scientific Opinion on the substantiation of health claims related to polyphenols in olive and protection of LDL particles from oxidative damage (ID 1333 , 1638 , 1639 , 1696 , 2865), maintenance of normal blood HDL-cholesterol concentrations (ID 1639), 9 (2011) 1–25. doi:10.2903/j.efsa.2011.2033.

[6] A. Agiomyrgianaki, P. V Petrakis, P. Dais, Influence of harvest year , cultivar and geographical origin on Greek extra virgin olive oils composition : A study by NMR spectroscopy and biometric analysis, FOOD Chem. 135 (2012) 2561–2568. doi:10.1016/j.foodchem.2012.07.050.

[7] A. Angelis, L. Antoniadi, P. Stathopoulos, M. Halabalaki, L.A. Skaltsounis, Oleocanthalic and Oleaceinic acids : New compounds from Extra Virgin Olive Oil (EVOO), Phytochem. Lett. 26 (2018) 190–194. doi:10.1016/j.phytol.2018.06.020.

[8] K.L. Pang, K.Y. Chin, The biological activities of oleocanthal from a molecular perspective, Nutrients. 10 (2018) 1–22. doi:10.3390/nu10050570.

[9] A. Karkovi, T. Jelena, M. Barbaric, Hydroxytyrosol, Tyrosol and Derivatives and Their Potential Effects on Human Health, (2019).

[10] J. Rodríguez-morató, A. Boronat, A. Kotronoulas, A. Pastor, E. Olesti, C. Pérez-mañá, O. Khymenets, M. Farré, R. De Torre, A. Boronat, A. Kotronoulas, J. Rodr, Metabolic disposition and biological significance of simple phenols of dietary origin : hydroxytyrosol and tyrosol, Drug Metab. Rev. Metab. Rev. 48 (2016) 218–236. doi:10.1080/03602532.2016.1179754.

No quality control method available

Limited information on olive oil biophenols biological and ADMET properties

No data of HT administration in humans investigating MetS/obesity

- *Mapping of OO*
- *Quantification of biophenols*
- *HRMS based metabolic profiling*

- *Biophenols isolation*
- *In vitro evaluation (proliferation)*
- *In vivo evaluation (anti-ageing)*
- *Pk characteristics*
- *Metabolites identification*

- *LC-MS based quantitation of HT in urine and blood*
- *LC-MS based metabolomics*
- *Investigation of pathways*

Acknowledgments

This study was carried out at the laboratory of Pharmacognosy and Natural Products Chemistry in School of Pharmacy of National and Kapodistrian University of Athens. I feel grateful for having the opportunity to work in a laboratory equipped with state of the art instrumentation and be a member of a highly qualified research group. I would like to take the opportunity and acknowledge all collaborators who contributed to the accomplishment of the current thesis. Particularly,

I would like firstly to thank the members of the examining committee Ass. Prof. Maria Halabalaki, Prof. Leandros A. Sklatsounis, Prof. Emmanouil Mikros, Senior Lecturer Emerson Ferreira Queiroz, Prof. Nikolas Tentolouris, Prof. Sofia Mitakou and Researcher A' Elissavet Ntotsika for agreeing to participate in this procedure.

I would like also to thank the three-member scientific committee of my PhD Ass. Prof. Maria Halabalaki, Prof. Leandros A. Sklatsounis, Prof. Emmanouil Mikros for the scientific advices and guidance all these years. I appreciate a lot the continuous support and encouragement from my first day in the laboratory.

I would like also to acknowledge the State Scholarships Foundation (IKY) for the financial support. This research is co-financed by Greece and the European Union (European Social Fund-ESF) through the Operational Programme «Human Resources Development, Education and Lifelong Learning» in the context of the project "Strengthening Human Resources Research Potential via Doctorate Research" (MIS-5000432), implemented by the State Scholarships Foundation (IKY).

I sincerely feel grateful and would like to express my gratitude to Ass. Prof. Maria Halabalaki for being my scientific supervisor for all my postgraduate years. I would like to thank her for the scientific guidance, the advices and for transmitting me all her inspiration. She offered me freedom to explore the science of natural products and trust to explore my abilities. I would like also to thank her for introducing me in the world of analytical chemistry and metabolomics and the opportunity she gave to work with elite instrumentation of analytics. Ass. Prof. Maria Halabalaki was the person who always motivated and encouraged me to participate in international conferences, to become better and not to be afraid to expose my work and thoughts. I really appreciate all the time she invested for my scientific progress and for all of her moral support and assistance to accomplish me PhD. Also I would like to thank her for revising my thesis and all her helpful comments and guidance for writing my thesis.

I would like also to express my gratitude to Prof. Leandros A. Skaltsounis for his support and guidance all these years. I would like to thank him for giving me the opportunity to be a member of his scientific team, for all the opportunities he gave me all these years, to travel and participate in international conferences and the financial support. He also gave me the opportunity to participate in an organization of an international congress held in Athens, which was an outstanding experience.

I would like to acknowledge Prof. Emmanouil Mikros for accepting to supervise my thesis and all of his kindness and support all these years for accomplishing all the administrative procedures.

I would like to express my gratitude to Dr. Matthias Witt and Dr. Aiko Barsch for the conduction and their total contribution in MRMS experiments and their kind interest for my thesis all these years.

I would like to thank Prof. Ioannis Trougakos, Dr. Aimilia Sklirou and PhD candidate Vasiliki Liaki for the conduction of the *in vivo Drosophila* experiments. I would like also to thank PhD candidate Kalliopi Karampetsou for the conduction of the *in vivo* PK experiments and the team of Dr. Oreste Gualillo for the performance of the *in vitro* assays.

I would like to acknowledge Prof. Nicholas Katsilambros, Prof. Nikolaos Tentolouris and Christina Fytilli for the design and their contribution in the clinical trial and our nice collaboration. I would like also to thank Intermed S.A. for the kind offer of HT and placebo capsules and PhD candidate Eirini Bata for helping me with the protocol of capsule dialysis.

During my thesis I had the pleasure to work with experienced researchers with decisive role in my work and my progress in the laboratory and I would like to express special acknowledge to them. I would like to thank Dr. Panagiotis Stathopoulos for introducing me to the field of analytical chemistry and our fruitful and timeless discussions for understanding this field. For his help in all the quantification experiments and all his experimental and moral support all these years. I would like also to thank Dr. Apostolis Angelis for his significant contribution in my first steps in the laboratory, for his guidance for biophenols isolation, NMR structure elucidation and mainly for passing me his passion in phytochemistry.

Also feel grateful to Dr. Vincent Brieudes for transmitting me all of his knowledge about mass spectrometry and for sharing with me many ideas about sample preparation, data treatment and statistical analysis.

I feel also grateful to the secretary team of the laboratory, Foteini Kapsali, Maria Platania, Evita Klantzi, and Maria Katsatsou for their assistance in all administrative issues.

I would like also to thank all the past and present members of the laboratory for the pleasant atmosphere in the laboratory. It was a great pleasure to work and collaborate with them. Each one contributed in a different way in my thesis.

I want to express special thanks to some laboratory colleagues and close friends Marilena Sakavitsi, Georgia Sarikaki and Anastasia Liakakou. I would like to thank them for their support and their willingness to help in every way in my thesis. I will never forget our greatest moments in and out of Greece!

I would like to express my warmest gratefulness to Marilena, the first person I met in the laboratory, for helping me in my first steps, for passing me all of her passion and optimism. I feel lucky for sharing with her our good and difficult moments of our lives. Thank you for your friendship and support until today.

I would like to thank my dearest and childhood friends for their emotional support, their friendship and understanding all these years.

I would like to express my deepest gratitude to my family for their love and encouragement all these years. Specifically, I owe great thanks to my mother for her unconditional love, affection and support. For all of her help in every field of my life and keep me and make me stronger every day. Without her and my beloved brother I wouldn't have the opportunity to accomplish my PhD.

Lastly, I would like to express my warmest thanks to Dimitris for being the most beautiful and flourish collaboration all these years and for being my brace in laboratory and life.

Thank you,
Theodora Nikou

Chapter 1

Quality control aspects of olive oil using high resolution mass spectrometry (HRMS) metabolomic approaches

This chapter has been submitted for publication in Journal of "Frontiers in Public Health"

Abstract

Extra virgin olive oil (EVOO) consumption has globally been increased due to its superior nutritional and sensory properties. In combination with its importance for European Union's economy, it has been established as a product of high economic priority and the need for its quality and authenticity control is of outmost importance. Its chemical complexity and variability enhances the hassle in investigating the most suitable methodology and consequently numerous analytical methods have been suggested. However, a reliable methodology to ensure authenticity and quality of EVOO is still unavailable. In this study a collection of more than 300 EVOOs from the main producing regions of Greece was carried out for the investigation of their biophenols (polar constituents) and lipid part as well. Samples were extracted and then analysed via HPLC-DAD for the determination of certain biophenols namely hydroxytyrosol, tyrosol, oleacein and oleocanthal and then correlated with specific quality parameters e.g. geographical origin, production procedure and cultivation practice.

Subsequently, Fourier Transform High Resolution Mass Spectrometry (FT-HRMS) techniques were integrated under metabolomic profiling concept for analysis of EVOO and their corresponding biophenol extracts. In particular, Ultra High Performance Liquid Chromatography coupled to orbitrap mass analyser (UPLC-Orbitrap-MS) and Magnetic Resonance Mass Spectrometry (MRMS) (also known as Fourier Transform Ion Cyclotron Resonance Mass Spectrometer (FT-ICR-MS) using Flow Injection Analysis (FIA) method were incorporated providing novel data for EVOO chemical discrepancy and classification. Samples were analysed with both techniques and data were subjected to multivariate data analysis (MDA). Clear trends and clusters were observed correlating certain biomarkers with selected

discriminating factors (geographical region, cultivation practice and production procedure). To our knowledge this is the first time that two FT MS platforms combining LC and FIA methods were integrated to provide solutions to quality control aspects of EVOO. Moreover, this is the first time that both lipophylic components and polyphenols are analysed together providing a holistic quality control workflow for EVOO.

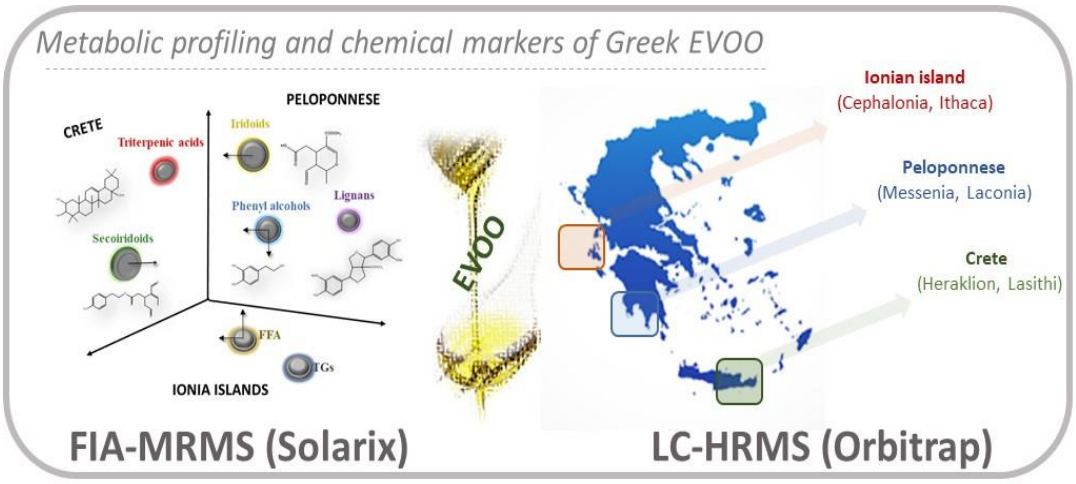

Abbreviations:

HPLC-DAD, High Performance Liquid Chromatography-Diode Array Detector; FIA-MRMS, Flow Injection Analysis-Magnetic Resonance Mass Spectrometry; LC-HRMS, Liquid Chromatography-High Resolution Mass Spectrometry; EVOO, extra virgin olive oil; OO, olive oil; IOC, Olive Oil Council; TGs, triacylglycerols; DGs, diglycerides; FFAs, free fatty acids; MUFA, monounsaturated fatty acid; FA, fatty acids; TPF, total phenolic fraction; HT, hydroxytyrosol; T, tyrosol; OLEA, oleacein; OLEO, oleocanthal; FT, Fourier-Transformed; MDA, multivariate data analysis; TPC, total phenolic content; PCA, Principal Component Analysis; OPLS-DA, Orthogonal Partial Least Squares-Discriminant Analysis; VIP, Variable Importance in Projection; QC, quality control.

1. Introduction

Since centuries olive oil (OO) is consumed raw or cooked, in considerable amounts from Mediterranean populations comprising if not the only, the main source of fat [1]. Especially virgin or extra virgin olive oil (VOO and EVOO, respectively) has been established in the consciousness of people as one of the most superior nutritional and health promoting edible oils world-wide with exceptional organoleptic and sensory properties. Together with other ingredients encompasses a main component of Mediterranean diet also widely recognized as one of the healthier dietetic patterns distinguished by UNESO and included in the Intangible Cultural Heritage List [2]. Consumers demand for OO is globally increasing according to International Olive Council (IOC) information [3]. Responsible for health and nutrition beneficial effects as well as its recognition as superior edible oil is its unique chemical composition.

Chemically, olive oil is an extremely multifaceted assembly of molecules. It is generally composed of two major parts, with the third being the volatiles which are critical for the particular aroma of OO. The main part is the glycerol fraction (90-99% of the total oil weight) which includes primarily triacylglycerols-TGs and secondarily diglycerides-DGs and free fatty acids-FFAs [4]. OO is rich in monounsaturated fatty acids (MUFA), especially oleic acid, which comprises almost 56-84% of the total fatty acids (FA) with the well-known activity in decreasing LDL-cholesterol complex and increasing of HDL-cholesterol in plasma [5].

The second part is the non-glycerol or unsaponified fraction (approx. 0.4-5% of the total oil weight) [6]. This fraction is characterized by high chemical complexity and consists the polar fraction (Total Phenolic Fraction – TPF) of OO with its components found to be biologically active [6,7]. These compounds are subdivided

into lipophilic and hydrophilic [8]. The lipophilic part contains hydrocarbons (e.g. squalene), tocopherols, sterols and pigments such as carotenoids. On the other hand, in the hydrophilic part an interesting class of compounds is the so-called OO polyphenols, phenols or biophenols. Numerous compounds belonging to more than 35 different chemical classes e.g. phenols, iridoids, secoiridoids, triterpenic acids, flavonoids, lignans constitute the OO unsaponified fraction (Figure 1) [9].

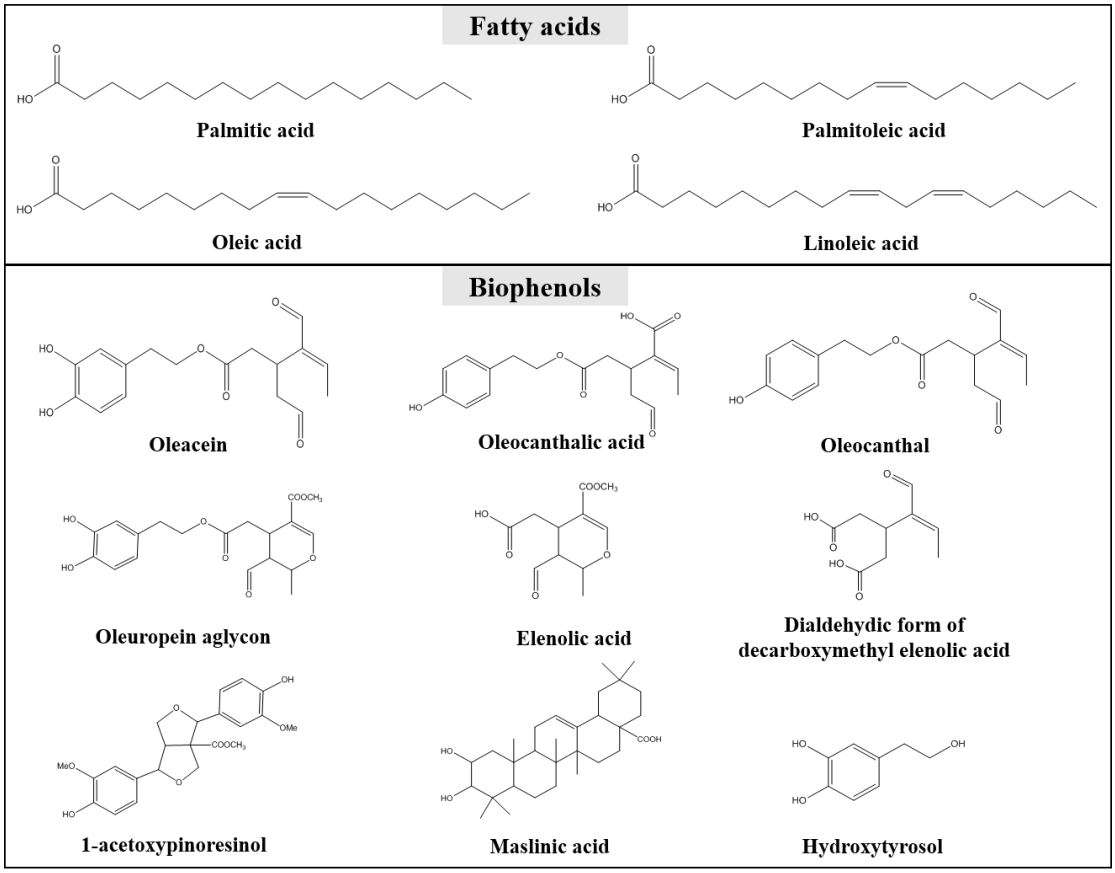

***Figure 1**: Representative compounds of OO glycerol fraction (upper part) and biophenols fraction (lower part).*

Although their total percentage is low, OO biophenols attracted the last decade great attention by scientists and experts in the field. The main reason is the increasing number of studies investigating the pharmacological properties of biophenols as single entities or in mixture; these studies yielded promising results such as antioxidant, antimicrobial, anti-inflammatory and hypoglycemic effects [10–13].

Furthermore, in 2011 the European Food Safety Authority (EFSA) recognized the positive correlation between certain OO polyphenols and protection of blood lipids from oxidative stress following a daily consumption of OO containing at least 5 mg of hydroxytyrosol (HT) and its derivatives per 20g of OO [14]. This development is important since it supplements another dimension to OO quality, namely the concentration levels of these specific compounds. The molecules which are implicated in the EFSA approved health claim are HT and its derivatives. The most characteristic are tyrosol (T), oleocanthal (OLEO), oleacein (OLEA), oleuropein and ligstroside aglycons.

Despite the plethora of reported studies, the complex nature of biophenols incommodes the complete elucidation of their composition as well as their analysis. The key reason is that OO is not *per se* a natural entity but the final product of a milling process. Furthermore, its chemical characteristics are influenced by several autogenous and exogenous factors such as the olive variety, cultivation practice, harvesting period, weather conditions, milling procedure itself, etc. [15]. Thus, the composition of phenolic fraction and the quantitative patterns could be highly diverse and the identification of (E)VOOs with high levels of biophenols is a difficult task which requires systematic and laborious analytical screening. Until now several analytical methodologies in terms of samples preparation and the employed analytical tool have been proposed for the qualitative and quantitative determination of biophenols. Usually, liquid-liquid extraction (LLE), solid-phase extraction (SPE) and ultra-sound assisted extraction (UAE) are incorporated for biophenols obtainment. Concerning the employed analytical tool, colorimetric analysis (Folin-Ciocalteu, DPPH), HPLC-DAD/UV, GC-FID/MS, LC-MS and ^{1}H-NMR analyses are used depending on the determinant factor (TPF or certain biophenols) [26–30]. Extract

complexity, discrepancies in results expression, absence of commercially available standards and other limitations lead to incomplete TPF characterizations and contradictory outcomes. As a result, great confusion among VOOs producers, consumers and even the legislative bodies is generated.

Being a food product of high added value for the European Union economy and mainly for the OO producing countries of Mediterranean basin, its quality is of outmost importance. The main categorization of OO regarding quality is principally based on free acidity expressed as oleic acid being the main quality parameter together with sensory and chemical characteristics which should be in accordance to specific standards. Thus, Extra Virgin Olive Oil (EVOO), Virgin Olive Oil (VOO), ordinary virgin olive oil, virgin olive oil not fit for consumption, refined olive oil, olive oil and olive oil pomace are the main quality categories [20].

Nevertheless, additional features contribute to OO quality and especially for EVOO and VOO, providing surplus value. As in other commodities and foodstuffs, PGI (protected geographical indication) and PDO (protected designation of origin) OO products whelm the global market. Moreover, the published health claims for the positive impact of OO regarding monounsaturated FAs [21] and polyphenols [22] [23], lead to more quality branches increasing the OO products variety in the market. Thus, the European Community has adopted a framework providing guidelines for PGI and PDO in order to enhance credibility and ensure quality [24].

However, OO quality is an extremely multifaceted issue. On one side stands it's unique, complex and highly variable composition and on the other side the "rules" of market. Its final quality in terms of organoleptic and health aspects, depends on several agronomic (e.g. microclimate, cultivation practice, olive tree cultivar, ripening

stage) and technological parameters (e.g. milling, malaxation, separation, storage) [25] which influence the final quality and price.

The use of wide definitions for PDO and PGI products and the elusive regulations for labelling concerning the employed analytical procedures for OO quality control have led to the increase of fraud and mislabeling incidences. Today, OO is in the top-5 fraudulent food products, worldwide [31].

Regarding authenticity purposes several analytical methods and techniques have been suggested for OO quality control. However, until now, no analytical procedure has been established for the verification of the information appears on the label. As a result, the need for the development of robust and reliable analytical strategies for ensuring OO quality and authenticity has risen as a priority issue for consumers, suppliers and regulatory agencies. The available relative studies target the lipophilic fraction, or they are fragmented and usually include inadequate sample size for meaningful correlations [15–19]. So far, the only analytical method which is suggested by IOC and generally adopted by regulation bodies is based on HPLC-UV and concerns the health claim of OO polyphenols. However, this method is suffering by certain limitations restricting its employment for accurate and complete quality control purposes [32].

Based on literature data, chromatographic techniques (GC, LC, CE) coupled to several detectors (diode array detection-DAD, mass spectrometry-MS) [33,34] are mostly employed taking the advantage of the separation of compounds in combination with the detection characteristics and sensitivity. In other approaches, authors suggest alternative techniques to reduce or even eliminate the required chromatographic analysis time, like Fourier Transformed Infra-Red (FT-IR) spectroscopy [35] and

Nuclear Magnetic Resonance (NMR) [4], but in all these cases with decreased sensitivity and accuracy [36,37].

Furthermore, many studies have been carried out under metabolic profiling concept employing different analytical platforms, mainly LC-MS and NMR [38,39]. Regardless the analytical method, usually multivariate data analysis (MDA) is applied to cope with the generated data [25]. Using this approach, projection and prediction models are generated for the classification of OO samples according to the question of the study. In rare cases, chemical groups or certain metabolites are suggested [15]. Additionally, the great majority of studies focuses either on the lipophilic or the hydrophilic part. Usually biophenols of the OOs under investigation fail evaluation of samples as whole or respond to the most quality parameters [38,39]. Additionally, other constrains exist in both LC-MS-based as well as in NMR-based metabolomic approaches. Laborious sample preparation procedures, long analysis time, selectivity, matrix effect etc in LC-MS studies and low sensitivity, high cost, identification issues etc in NMR-based limiting their applications. Based on the above, alternative methods which provide speed, efficiency and credibility are under investigation. Towards this direction, direct MS analysis of OO has been suggested and nowadays is in the center of the scientific interest for quality control purposes generally in food [40–42].

Another issue which complicates much more the analysis of OO is the accurate identification of compounds. Even today the complete composition of unsaponified fraction of OO is still unresolved and new compounds are suggested [43]. Especially in untargeted metabolic profiling studies many features remain unidentified or misidentified due to the lack of databases, the unavailability of reference standards and the limitations of analytical techniques used. Particularly for LC-MS based

metabolic profiling approaches the analyser is critical for the accurate identification of detected features and accurate interpretation of results [44].

Greece is the country possessing the highest OO consumption [45] and is the third OO production country globally. Thus, authentication and quality control of Greek OOs is a matter of high concern. Several approaches have been suggested since '80s based either on glycerol or biophenols fraction, using different experimental protocols and analytical techniques [46–50]. Additionally, several studies have been carried out for the classification of OOs coming from different Greek olive tree varieties [15,51–53]. To the best of our knowledge only two studies have been published for the influence of the employed cultivation practice in Greek OOs [54,55] and only one for the study of the production procedure methodology [56]. Both of the aforementioned factors have been found to influence OO quality [57,58], but until now they are not well studied in Greek OOs. Moreover, no previous study exists to investigate origin, cultivation and production procedure at the same time or to study simultaneously both chemical parts (lipophilic and hydrophilic) of OO.

Hence, the aim of the current study was the qualitative and quantitative determination of OO biophenols for the exploration of the influence of specific factors reported that affect quality characteristic. TPF and TPC were correlated to geographical origin, cultivation practice and production procedure methodology. In parallel, two different quantitative methodologies were developed for HT, T, OLEO and OLEA quantitative determination. Additionally, an untargeted, fast and highly accurate methodology was developed for the classification of EVOOs according to the same quality parameters. Specific compounds were revealed as markers for these quality parameters, both lipophylic and hydrophilic, taking advantage of the excellent identification competence of two FT analysers. Indeed, two analytical platforms were

employed for the analysis of EVOOs and specifically, a UPLC-HRMS/MS (orbitrap analyser) as more established method in parallel with flow injection analysis-magnetic resonance mass spectrometry (FIA-MRMS) to improve sensitivity, accuracy, speed and detection range. Thus, a rapid methodology of 2 and 8 minutes per sample was developed and applied for the analysis of intact EVOOs as well as their biophenol extracts, respectively. Data were processed using MDA and distinct clusters were revealed associating certain metabolites with geographical origin, production procedure and cultivation practice. To our knowledge, this is the first time that certain marker compounds abundant in EVOO are associated with three quality parameters employing at the same time FIA method and the identification confidence of MR analyzer.

2. Materials and Methods

2.1.1 Reagents and materials

Solvents for extraction and HPLC-DAD analysis were of analytical grade, MeOH, ACN and water were HPLC grade (Carlo-Erba). The analytical reference standards, syringaldehyde, HT and T were purchased from Chembiotin (Greece) with purity > 98%. Oleocanthal (OLEO) and oleacein (OLEA) were isolated from OO using the described methodology of chapter 2 (Section 2.2) with purity > 98%. For Folin Ciocalteu analysis, Folin Ciocalteu reagent and gallic acid were purchased from Sigma Aldrich (Missuri, USA). ACN and formic acid used for HRMS analysis were LC-MS grade (Fisher Chemical) and water (H_2O) was obtained from a milli-Q water purification system (Millipore, USA).

2.1.2 Instrumentation

For the HPLC-DAD quantification a Thermo Scientific system was used equipped with a pump SpectraSystem P4000, autosampler SpectraSystem AS3000, PDA SpectraSystem UV800 and column Discovery HS-C18, 25 cm, 4.6 mm, 5 μm. Data processing was performed with the ChromQuestTM 4.2 software. Metabolomic analysis of biophenols was accomplished to an H class Acquity UPLC system (Waters, USA) coupled to a LTQ-Orbitrap XL hybrid mass spectrometer (Thermo Scientific, USA). Metabolomics via MRMS of EVOOs and biophenols were performed to a solariX 7T MRMS system (Bruker Daltonik GmbH, Bremen, Germany).

2.2 Samples collection and registration

EVOO samples were obtained directly from OO producers and OO cooperatives during the harvesting period 2015-2016 from three producing areas of Greece. During sample collection, complete information accompanying each sample (metadata) were thoroughly assembled i.e. olive tree cultivar, production procedure, cultivation practice, exact location of olive grove, ripening stage, olive oil storage and the categorization of olive oil in the virginity index. The metadata are presented in Table A1 in appendix. The selection of the geographical regions was based on a previous study of our group, investigating the quantitative profile of certain biophenols in Greek EVOOs [59]. Over 300 EVOO samples were initially collected from Crete, Peloponnese and Ionian islands, OO producing regions of Greece, representing three production procedures and cultivation practices, respectively. Ultimately, after the implementation of certain acceptance criteria the number of samples narrowed down to 208. After the collection, all EVOOs were directly centrifuged and stored under nitrogen conditions in dark, glassy vials at 20°C to retain their chemical stability during storage [60].

2.3 Biophenols extraction

Samples were extracted following the IOC proposed protocol [61] after the employment of minor modifications for automation purposes. In brief, 1 g (±0.001) of EVOO was weighed and dissolved in 1 mL of *n*-hexane. The solution of oil and hexane was mixed and homogenized with MeOH:H_2O 80:20 (v/v) using a vortex mixer for 3 minutes and then centrifuged in 3.000 rpm for 3 minutes for phases separation. The same procedure was repeated twice. The extracts were defatted twice with *n*-hexane and evaporated under vacuum conditions and centrifugation at 30^{o}C

(GeneVac HT-4X). After evaporation, the dried extracts were stored in glassy vials at -20°C until use.

2.4 Total Phenolic Content (TPC) via colorimetric assay

As a widely used parameter Total Phenolic Content (TPC) was also evaluated for the derived extracts via Folin Ciocalteu colorimetric assay (or gallic acid equivalence method). Gallic acid calibration curve was plotted by preparing eight different concentration of gallic acid (2.5 μg/ml, 5 μg/ml, 10 μg/ml , 12.5 μg/ml , 20 μg/ml , 25 μg/ml , 40 μg/ml and 50 μg/ml) mixed with Folin Ciocalteu reagent (tenfold diluted) and sodium carbonate solution (7.5 % w/v). Extracts were prepared in the appropriate dilution with the same reagents and analysed in triplicates. The absorption was measured at 765 nm. TPC values were expressed as mg of gallic acid equivalent/Kg of EVOO using the resulted standard calibration curve of gallic acid (R^2=0.9982) (Figure A1). The detailed results of the biophenols extracts are presents in supplementary information in Table A2.

2.5 Quantitative determination of biophenols

2.5.1 HPLC-DAD method

For HPLC-DAD analysis, samples were dissolved in MeOH:H_2O 1:1 (v/v) and syrigaldehyde was added as internal standard (IS) in the final concentration of 50 μg/mL. For the quantification of HT and T a method proposed from IOC was applied, with some modifications. The separation was achieved with a gradient elution system starting with 98% water with 0.2% acetic acid (A) and 2% acetonitrile (B). In 40 minutes the concentration of acetonitrile was increased to 30% and maintained for 5 minutes. Subsequently, initial composition was reached in 5 minutes. The total run time was 50 minutes with a flow rate 1 mL/min. The injection volume was set at 20

μL. The column temperature was kept at 40ºC. Chromatograms were processed at 280 nm and both molecules, HT and T were quantified according to their 6-points calibration curves.

OLEO and OLEA were quantified according to the method proposed from Impellizzeri et al., 2006 [62]. A gradient elution system was used for the separation. The initial composition was 80% water (A) and 20% ACN (B). The concentration of ACN was increased after 20 minutes to 30% and maintained for 15 minutes. The system returned to initial conditions in 5 minutes. The total run time was 40 minutes with a flow rate 1 mL/min and the injection volume was set to 10 μL. The column temperature was kept at 25ºC. Chromatograms were processed at 235 nm and both molecules were quantified according to their respective 11-points calibration curves.

2.5.2 Preparation of standard solutions, calibration curves and quality control (QC) samples

Stock solutions of HT, T OLEO, OLEA and ES were prepared at the concentration level of 1 mg/mL in MeOH and stored at -20ºC. Working solutions were prepared by diluting appropriate volumes of each analyte and IS stock solutions in a solution of MeOH:H_2O 1:1 (v:v). Calibration points were built in matrix solution using 6 different concentrations of HT and T and 11 concentrations for OLEA and OLEO. The dynamic range of HT calibration curve was 2 μg/mL-150 μg/mL (2 μg/mL, 3 μg/mL, 20 μg/mL, 50 μg/mL, 100 μg/mL, 150 μg/mL); for T the dynamic range was 2 μg/mL-100 μg/mL (2 μg/mL, 3 μg/mL, 20 μg/mL, 50 μg/mL, 80 μg/mL, 100 μg/mL); for OLEO and OLEA the dynamic range was 50 μg/mL-1000 μg/mL (50 μg/mL, 100 μg/mL, 200 μg/mL, 300 μg/mL, 400 μg/mL, 500 μg/mL, 600 μg/mL, 700 μg/mL, 800 μg/mL, 900 μg/mL, 1000 μg/mL). In the four analyte solutions, S was added in the final concentration of 50 μg/mL. A standard mixture of T (1 mg/mL) was

used as quality control (QC) solution and injected evert eight runs to check the reliability of the system.

Three QC levels, low, medium and high were prepared for each analyte. For HT 50 μg/mL, 100 μg/mL and 150 μg/mL; for T 20 μg/mL, 50 μg/mL and 100 μg/mL for OLEA 500 μg/mL, 700 μg/mL, 1000 μg/mL; OLEO 500 μg/mL, 700 μg/mL, 1000 μg/mL.

2.5.3 Matrix preparation

For matrix preparation an OO sample characterized by completely absence of the four biophenols was used. Concisely, XAD7 resin was mixed overnight with OO in ratio 1:4 (w/v). After filtering resins were washed with *n*-hexane for fatty acids removal and then extracted with methanol. Matrix extract was evaporated until dryness. For QC and calibration points preparation matrix extract was prepared in the final concentration of 2 mg/mL diluted in a solution of MeOH:H_2O 1:1 (v/v).

2.5.4 Quantification and validation of the analytical methodology

For calibration curves construction the ratio of the area of analytes versus the area of the ES was used. The linearity was checked using partition least squares method and evaluation of the regression coefficient (R^2).

The validation of the method was performed in accordance to ICH quality guidelines "Validation of Analytical Procedures Q2 (R1)" [63] and FDA [64] by evaluating the stability, specificity, linearity, precision, accuracy, lower limit of quantification (LLOQ)-detection (LLOD) and the system suitability parameters.

2.5.4.1 Specificity-Recovery

Specificity was evaluated by injecting five individually prepared matrix samples and investigation of the presence of possible interference at the corresponding retention time (RT) of analytes and ES. Recovery was determined in the three QC levels of each analyte and comparing the concentrations of analytes from pre-spiked samples with post-spiked samples.

2.5.4.2 Lower limit of quantification (LLOQ) and detection (LLOD)

LLOQ and LLOD were calculated based on the standard deviation and the slope of the calibration curves. For the calculations, the equations below and a blank matrix sample were used.

LLOQ= $\frac{yblank+10\ \sigma}{b}$

LLOD= $\frac{yblank+3\ \sigma}{b}$

where yblank is the background signal, b is the slope estimated from the calibration curve and σ is the standard deviation of the response.

2.5.4.3 Repeatability, intermediate precision and accuracy

Repeatability (within-run) and intermediate precision (between run) of the assay were evaluated based on and the standard deviation (SD) and relative standard deviation (%RSD) of the three QC levels of QC run in five replicates. The rejection criteria was % RSD<2 for repeatability and % RSD<10-15% for intermediate precision. Within-run accuracy and between-run were determined for QCs as the % RSD which should be less than 15%.

2.5.4.4 Robustness

The robustness of the method was evaluated incorporating alterations in analysis conditions within ±5% changes. Firstly, column temperature was set at 38°C and 42°C and secondly autosampler temperature was set at 9.5°C and 10.5°C. All experiments were performed in the medium QC level (HT: 100 μg/mL, T: 50 μg/mL, OLEA: 500 μg/mL, OLEO: 500 μg/mL) calculating the chromatographic peak area of analyte and the RT. Results are expressed as % RSD.

2.6 UPLC-HRMS & HRMS/MS analysis

UPLC-HRMS and high resolution tandem MS (HRMS/MS) was employed only for the analysis of biophenol extracts. The extracts as well as the quality control (QC) pooled sample were prepared in the final concentration of 500 μg/ml diluted in MeOH:H_2O 1:1 (v/v). For the separation, H_2O with 0.1% formic acid (FA) was used as solvent A and acetonitrile (ACN) as solvent B. The elution method started with 2% of B and in 2 minutes reached 21%. In the next 4 minutes the percentage of B increased to 44.5%. Finally, at ninth minute, B reached 100% and maintained for 2 minutes. The next minute the system returned to the initial conditions and stayed for 3 minutes for system equilibration. A Thermo Hypersil Gold C-18 (50 mm x 2.1 mm, 1.9 μm) column was used for the separation, with a stable temperature of 40°C. The measurements were performed with a total acquisition time of 15 minutes and a flow rate of 400 μl/min. The injection volume was 10 μl and the autosampler temperature was at 7°C. Mass spectra were obtained in negative ion mode using an electrospray ionisation source (ESI). The capillary temperature was set at 350°C, capillary voltage at -10 V and tube lens at -40 V. Sheath and auxiliary gas were adjusted at 40 and 10 arb, respectively. Mass spectra were recorded in full scan mode in the range of 115-1000 *m/z*, with resolving power 30,000 at 500 *m/z* and scan rate 1 microscan/sec.

HRMS/MS experiments were obtained in data-depending method with collision energy 35.0% (q = 0.25). The system was calibrated externally every 50 injections.

2.7 FIA-MRMS analysis

MRMS analysis was employed for both intact EVOOs samples and their corresponding biophenol extracts. EVOO samples were dissolved 1:1000 in CH_2Cl_2:MeOH 50:50 containing 10 mM ammonium acetate. Spectra were acquired in the mass range of 147–3000 *m/z* with a resolving power of 450,000 at *m/z* 400. Spectra were externally calibrated with NaTFA cluster and additionally internally calibrated with a lock mass of deprotonated palmitic acid at *m/z* 255.23295. Mass spectra were obtained in negative ion mode with 24 scans/spectrum and the acquisition time was 0.75 min. A sample loop was filled with 20 µl sample solution and transferred to the electrospray ionisation source. During the spectra acquisition the flow was 10 µl/min. The total injection time was 2 minutes. Five repetitive measurements were performed for each sample.

The corresponding biophenol extracts were diluted 1:20 in 50% MeOH with 10 mM ammonium acetate. Spectra were acquired in the mass range of 107 – 3000 *m/z* with a resolving power of 300,000, at *m/z* 400. Spectra were externally calibrated with NaTFA cluster. Mass spectra were obtained in negative mode with 92 scans/spectrum and the acquisition time was 6 min. A sample loop was filled with 100 µl sample solution and transferred to the electrospray ion source. During the spectra acquisition the flow was 10 µl/min. The total injection time was 8 minutes. Three repetitive measurements were performed for each sample.

2.8 Statistical process and chemometrics

UPLC-MS data were recorded with Xcalibur 2.2. Raw files (.raw, Thermo) were imported to MZmine 2.26 software for data processing. Peak list was generated with centroid selection algorithm. For chromatogram building of the generated mass list, 0.05 minute was set as minimum time of span and 5 ppm for mass tolerance. Chromatogram deconvolution module was employed and spectra were processed with local minimum search algorithm using R package. The minimum retention time range was set at 0.1 minute and peak width 0.05-0.7 minutes. Chromatograms were aligned and spectra were normalized regarding retention time with 0.005 minute tolerance. Join align method which aligns detected masses using a match score, calculated based on the mass and detection time of each peak was used. Finally, gap filing was implemented, using peak finder method. MRMS data were recorded with ftmsControl 2.1 and processed with ProfileAnalysis 2.1. The mass lists of the mass spectra were imported as feature lists based on the average mass spectrum of all spectra. This list was exported as asc file for import in SIMCA.

Both of the generated data tables were imported to SIMCA 14.1 (Umetrics, Sweden) software for statistical analysis. Mainly, Principal Component Analysis (PCA) and Orthogonal Partial Least Squares-Discriminant Analysis (OPLS-DA) were implemented for sample discrimination and identification of statistically important metabolites responsible for observed trends and classifications. For this purpose, Variable Importance in Projection (VIP) values of OPLS-DA models which rank variable contribution were estimated and evaluated. VIP scores >1 were considered as statistically significant.

The generated models were evaluated for their R2 and Q2 parameters indicating the measure of fit and the predictability, respectively. Only models with R2 values

close to 1, Q2 values over 0.5 or models with lower R2 but close to Q2 value were accepted. Permutation test was also applied for further validation of the models. Similarly, only models which succeeded in the permutation test were used for data visualization and VIP calculations.

2.9 Structure elucidation workflow

Based on VIP calculations a list with significant features was created and subjected to identification process. Initially, LC-HRMS chromatograms and their corresponding HRMS spectra (< 2 ppm) were investigated. Extraction ion method was used in parallel with peak-to-peak selection affording the corresponding full scan spectra. Suggested Elemental Composition (EC) of each detected peak together with isotopic patterns and ring double bond equivalent (RDBeq) values were further used to confirm the proposed structures. Additionally, HRMS/MS spectra contributed to the identification of specific chemical entities based on in-house databases (Figures A6-11). Furthermore, on-line databases were used for additional structural information. Another factor witch assisted considerably the identification process was the MS spectra derived from FIA-MRMS analysis. Nonetheless, the ultra-high resolution of the MRMS instrumentation (< 1 ppm) and SmartFormula^{TM} (SF) tool enabled the identification of compounds with high confidence. The MRMS spectra were imported and processed in MetaboScape 4.0 (Bruker Daltonics). Using the T-Rex 2D algorithm possible adducts as well as isotope of a compounds are combined to one feature so that the detected masses belonging to the same elemental composition are presented only as one feature in the table. The import was conducted with a delta *m/z* of only 1 mDa with maximum possible charge state of 1 and an intensity threshold of 1000000 which corresponds to S/N 2. Molecular Formula were automatically assigned using the SF algorithm which also takes into account isotopic

fine structure information. Known and expected compounds in analysed samples were automatically annotated using custom AnalteLists.

3. Results and discussion

3.1 Samples selection and registration

Particularly important element in approaches with quantification and metabolomics purposes is sampling quality by means of samples size as well as complete and accurate sample information (metadata). Commonly, small number of samples is subjected for analysis diminishing significantly the statistical confidence of the obtained results or leading to fragmented and incomplete conclusions [55]. Therefore, comprehensive and precise metadata is the basis of data validity and ultimately results soundness since correlations with certain parameters of chemical composition, concertation levels and/or markers are expected. Despite the plethora of studies available, the quality of metadata is usually overlooked or underestimated.

In the current study special attention has been given to the sampling and precise metadata as well as the selection of the discriminating parameters. Given the fact that Koroneiki variety dominates Greece, only OO samples from the specific olive variety have been selected for quantification and metabolomics analyses. Koroneiki is considered as the most common and suitable tree cultivar for OO production in the south of Greece due to its adaption to dry and hot climates and the production of small drupes, with high ratio of skin/flesh, generating high yields of oil [54].

Following variety, the second selection criterion was extra virgin index since more than ¾ of the Greek oils are EVOOs. Only EVOO samples were included while other OO qualities were excluded. Ripening stage was the third inclusion parameter. It is well known that the olive drupe maturity is strongly associated with the chemical composition of OO [66]. Therefore, EVOO samples characterized by close ripening stage (November–December) were selected. Finally, OO samples with incomplete

metadata were also excluded. Thus, from the 300 initially collected samples only 243 were qualified to be further scrutinized.

The number of samples was further reduced taking into account the geographical origin. The two main regions, Peloponnese and Crete responsible for approx. 75% of the total production were rationally selected as more representative. Each region was further divided into two subareas i.e. Heraklion & Lasithi (Crete) and Messenia & Laconia (Peloponnese) based on the same rationale. Additionally, Crete and Peloponnese are the dominating OO producing areas of Greece and can consequently provide an adequate number of samples produced in different olive oil mills and with different cultivation practices. Considering that both origin and cultivation conditions are strongly related to climate conditions, it should be noted that both Crete and Peloponnese are characterized by high temperatures during the whole year and low precipitation levels. In order to explore in more detail these parameters, samples from Ionian islands (Cephalonia and Ithaca) were also included. Ionian islands is not an area of high OO production. However, these islands have a microclimate utterly different (low temperatures during the winter and high precipitation levels the whole year) from Crete and Peloponnese and can provide data with high significance.

For cultivation practice, conventional, integrated and organic farming were recorded. Conventional practice is mainly used in Greece for olive tree growing, while integrated has started to become more popular. In these two practices, synthetic fertilizers and pesticides are used and the difference concerns that in the second there are limitations in terms of the quantity of synthetics and propagation material. In organic farming, synthetic products are forbidden and soil regeneration is based on physical processes [67,68]. Regarding production procedure, two phases, three phases

and traditional mills were used for OO production. Nonetheless, samples produced with traditional pressing system were excluded from the analyses, due to the low number of samples. Nowadays, this kind of production is almost abandoned in Greece. Two phases and three phases centrifugation systems are the most common used methods and their difference lies in the amount of the added water during the step of oil separation from paste; two phases centrifugators are more evolved and require lower amount of added water in comparison to three phases [58]. These production procedures and cultivation practices are the most employed in Greece and in consequence disclose high interest for investigation. Samples coming from organic cropping that were not certified were excluded as well except samples produced from traditional pressing systems.

After the last examination of the OO samples based on the discriminating parameters under investigation, the number of valid samples to be forwarded for analyses was finally 208. Table 1 illustrates the total sample collection subjected to quantification and metabolic analysis.

Quality parameters	**Subclasses**	**Number of observations**
Geographical origin	Peloponnese	89
	Crete	85
	Ionian islands	34
Production procedure	Two phases	117
	Three phases	87
Cultivation practice	Conventional	104
	Integrated	38
	Organic	45

Table 1*: Representation of the total number of samples under investigation (n=208). Samples are grouped in three quality parameters: geographical origin (n=208), production procedure (n=204) and cultivation practice (n=187). Quality parameters are divided in subclasses and the respective number of samples is tabulated.*

3.2 TPF and TPC determination

The first inspected parameter in the derived biophenols extracts was the produced extraction yield (TPF) of EVOOs. Moreover, all TPFs were analysed with Folin-Ciocalteu colorimetric assay for TPC determination. Useful observations could be made when comparing the average values of TPF and TPC with respect to their geographical origin, production procedure and cultivation practice (Figures 2 and 3). The detailed results are shown in Table A2 in appendix.

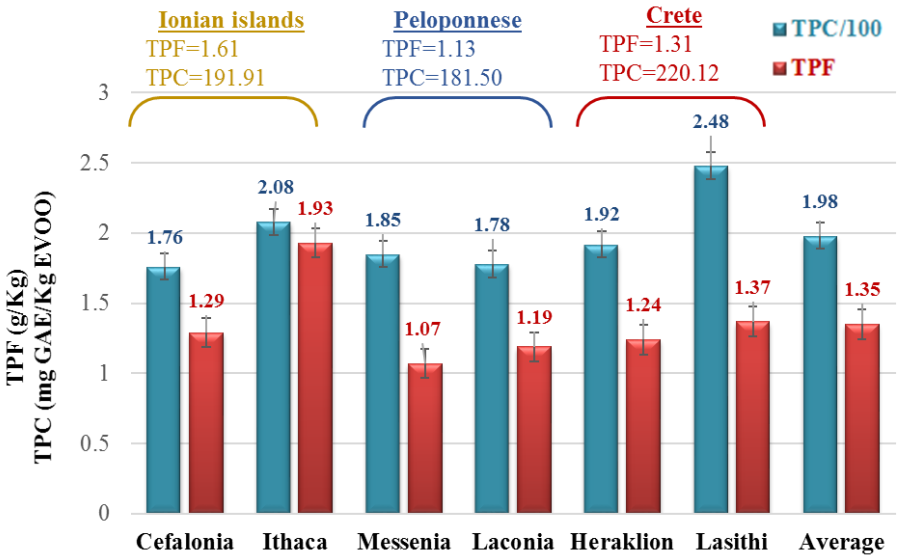

***Figure 2**: Mean values of TPF and TPC versus geographical origin. TPF results are expressed as g/Kg EVOO. TPC is presented as the ratio TPC/100 for axis normalization and expressed as mg GAE/kg EVOO. The basic geographical areas with the corresponding TPF and TPC values are indicated above each region. In parenthesis the number of samples of each geographical region is represented. The total number of analysed samples is 208.*

As it is obvious in the above figure there is a correlation between TPF and TPC levels. Higher TPFs result in higher TPC demonstrating the coherence of these two parameters. The TPCs mean values varied significantly among the different geographical regions and among samples originating from the same area as well. TPCs ranged from 63 to 607 mg GAE/Kg EVOO. The average value was calculated

at 198 mg GAE/Kg EVOO (Figure 2). These values are characteristics for Greek EVOOs and are in agreement to those reported by other authors [69]. Similarly, TPFs values indicated considerable variations between 0.54 and 3.01 g/Kg EVOO with an average value of 1.35 g/Kg EVOO [70]. In more detail, the highest TPC values were recorded in Crete and specifically in Lasithi region. Heraklion region of Crete showed both TPF and TPC values close to the calculated average, with some samples holding considerable high values for both parameters. Samples from Ionian islands possessed the next highest values for TPC. It has to be noted that Ithaca island held high the calculated TPC and TPF (highest TPF value of all regions) mean values of this region, while Cefalonia island was characterized by low TPFs and TPCs. Concerning Peloponnese even if a number of samples were characterized by high TPFs and TPCs values, the majority was at the limit of the calculated average. It is worth mentioning that the regions of Lasithi, Heraklion, Laconia and Messenia are the main olive oil production regions in Greece.

It is interesting that Ithaca samples possessed the highest TPF but not TPC. After investigation of the corresponding HPLC-DAD chromatograms, no significant additional peaks were found that could be responsible for the relatively high TPFs. A rational hypothesis could be that these samples could be characterized by high amounts of not UV absorbing compounds which at the same time are unable to react with the Folin-Ciocalteu reagent such as triterpenic and fatty acids (Peragon et al., 2015). At this point it has to be mentioned that the olive tree variety cultivated in Ionian Islands (even though has a common variety name) has been adapted to the utterly different microclimate conditions of these islands.

The same calculations were conducted for OO production system which is regarded as an important parameter which affects biophenols content. As it is

illustrated in figure 3A and indicated from both TPF and TPC values, the incorporation of two phase mills leads to higher preservation of biophenols in EVOO compared to the three phases mills which is in agreement with previous studies [71]. For the two phases system the calculated mean value of TPC was 211 mg GAE/KL EVOO and TPF 1.24 g/Kg EVOO. The corresponding values for three phases systems were lower from two phases and from the calculated mean values and specifically 182.46 mg GAE/Kg VOO and 1.18 g/Kg, respectively. Even if the difference in the determined values is not important, the trend is clear as indicated also from numerous previous published data [71,72]. These results could be explained by the different operation procedures of the two mill types. Specifically, in three-phases mills the addition of water during malaxation favors the removal of biophenols into waste [72]. TPC and TPF values of traditional press production systems were not included in the calculations due to the small numbers of samples.

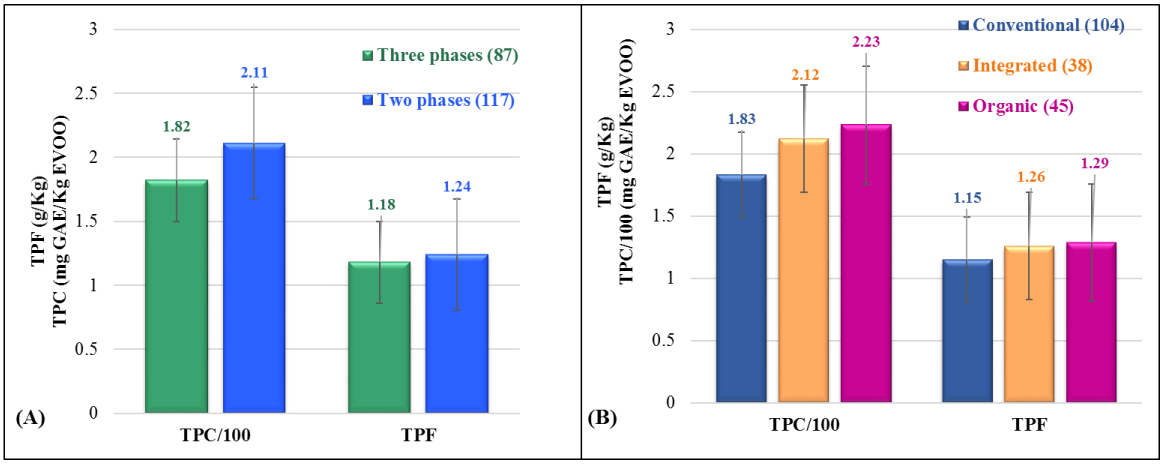

***Figure 3**: TPF-TPC average values versus **A)** production system (n=204) and **B)** cultivation practice (n=187). Traditional press systems (graph a-left) and organic-non certified (graph b-right) were not included. Results are expressed in g/Kg and mg GAE/Kg EVOO, respectively. Each system and practice is characterized by its number of samples. TPC values are represented as ration TPC/100 for axis normalization.*

Similarly, to milling process, cultivation practice was also analysed in relation to TPC and TPF values. Despite the fact that the last decades there is an increasing interest in producing and consuming (E)VOO coming from organic and generally from supervised cultivations, there are only few studies examining the nutritional characteristics of these OOs [73]. As can be observed in figure 3B, organic practice possessed the highest values for TPC and TPF, namely 223 mg GAE/Kg EVOO and 1.29 g/Kg, respectively; followed by integrated cultivation practice (212 mg GAE/Kg VOO and 1.26 g/Kg for TPC and TPF, respectively). The lowest values were calculated in TPFs from EVOOs derived from conventional cultivation practice (183 mg GAE/Kg VOO and 1.15 g/Kg for TPC and TPF, respectively). From the above results it can be inferred that supervised cultivations (organic and integrated) produce higher TPF and TPC values denoting the possible impact of the employed practices to phenols production in olive drupes and OO.

3.4 Quantitative determination of biophenols

Based on former studies of our group [74] as well as on information from the literature, amongst the major compounds abundant in TPFs of Greek EVOOs are OLEO and OLEA (Figure 1). There are also cases where oleuropein and ligstroside aglycons were found in considerable concentration levels. Moreover, HT and T are characteristic components of TPF while substantial data are available for their significant biological properties as mentioned already [75]. Based on the availability of reference standards, we proceeded with the quantification of OLEO, OLEA, HT and T.

Due to the different physicochemical characteristics of the analysed compounds, two HPLC-DAD methods were employed for the analysis of EVOO samples. Specifically, one method in acidic conditions was used for the quantification of HT

and T and another method in not acidified conditions for OLEO and OLEA. In both cases HPLC-DAD apparatus was employed according to already published methods with minor modifications [62].

3.4.1 Method development for HPLC-DAD

Quantification was performed with two different analytical methodologies, one for the quantification of HT and T and one for OLEA and OLEO. In both of them, testings for elution solvents selection and the appropriate column temperature were performed. MeOH and ACN were tested for the selection of organic phase and H_2O with and without AA for aqueous phase. ACN resulted in better peak shape for all analytes and thus selected as organic phase. In the case of OLEA and OLEO use of ACN for elution produced a double peak elute with better peak shape in comparison to the one peak elute of MeOH as elution solvent. H_2O with 0.2% AA improved also the chromatographic resolution, although in the case of OLEA and OLEO a different chromatographic behavior was observed. Addition of AA in aqueous phase resulted in the disappearance of the double peak and the elution of only one peak. For this reason, AA was used only for HT and T method and rejected for OLEA and OLEO. Concerning column temperature, use of 40^{o}C improved peak shape for HT and T and selected as analysis temperature. Though for OLEA and OLEO use of AA changed the ratio of the double peak and for this reason analysis was performed at 25^{o}C. In both methodologies the used gradient was tested and adjusted to avoid co-elution with other biophenols of the extracts.

3.4.2 Quantification and validation of the analytical methodology

For the quantification of the four biophenols syrigadelhyde was used as IS since it exhibits similar chemical structure with the analytes and high and repeatable

recovery. IS shows high stability during analysis and it has not been described as an OO constituent. Moreover, it does not interfere with the four analytes and for these reasons it was selected as IS of the employed quantification methodologies. Figure 4 illustrates the peaks of HT, T and IS in indicatives calibration points for each analyte.

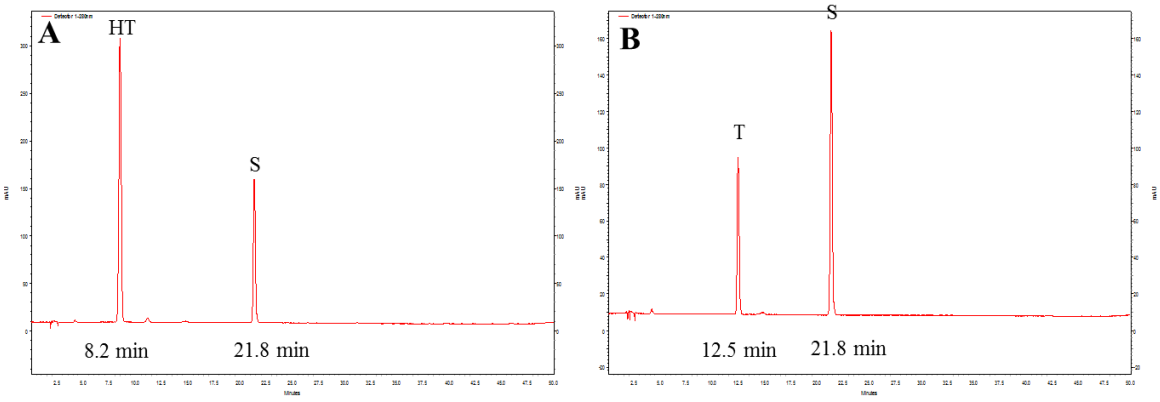

Figure 4: *HPLC-DAD chromatograms of hydroxytyrosol (HT) and tyrosol (T). A: HT at the concentration level of 20 μg/mL. B: T at the concentration level of 50 μg/mL. Chromatograms are obtained at 280 nm. Syrigaldehyde (S) and retention time are annotated.*

For the construction of HT and T calibration curves the ratio of analytes area to the area of IS was used. The linearity was checked using partition least squares method. The derived HT equation is: y = 0.0404x + 0.0043 with correlation coefficient R^2=0.9997 and for T is: y = 0.0251x + 0.0146 with correlation coefficient R^2=0.9999. The corresponding equation is presented in figure A2.

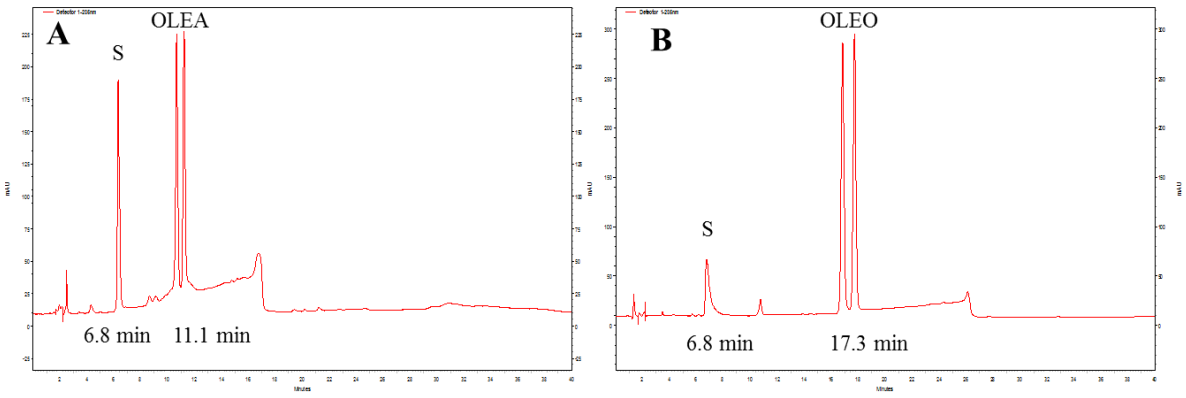

Figure 5: *HPLC-DAD chromatograms of oleacein (OLEA) and oleocanthal (OLEO). A: OLEA at the concentration level of 200 μg/mL. B: OLEO at the concentration level of 200 μg/mL. Chromatograms are obtained at 235 nm. Syrigaldehyde (S) and retention time are annotated.*

For OLEA and OLEO calibration curves were constructed using analytes area. ES was used only for the verification of injection and system stability. For OLEA the corresponding equation is: y = 42987x + 600597 with correlation coefficient R^2=0.9931 and for OLEO: y = 46773x + 124584 with correlation coefficient R^2=0.9934. The corresponding equation is presented in figure A3.

3.4.2.1 Specificity-recovery

Specificity was evaluated and no interference from the biophenol extract metabolites was found to the corresponding RT of HT, T, OLEA, OLEO and ES. The recovery was determined in the three QC levels of analytes in five replicates with use of the equation below:

$$\%R = \frac{pre - spiked\ average\ area}{post - spiked\ average\ area}\ x\ 100$$

Recoveries were estimated over 94% for all analytes and QC levels and render the employed methodologies suitable for HT, T, OLEA and OLEO quantification in OO biophenol extract.

3.4.2.2 Lower limit of quantification (LLOQ) and detection (LLOD)

LLOD and LLOQ were determined for each analyte based on given equations of section 2.5.4.2. Particularly, LLOQ were found for HT 0.04 mg/ml, for T 0.05 mg/mL, for OLEA 0.56 mg/mL and for OLEO 0.67 mg/mL.

The corresponding LLOD values were for HT 0.02 mg/mL, for T 0.03 mg/mL, for OLEA 0.25 mg/mL and for OLEO 0.33 mg/mL.

3.4.2.3 Repeatability, intermediate precision and accuracy

Repeatability, intermediate precision and accuracy were determined by analyzing five replicates at the three QC concentration levels of the analytes. Repeatability and intermediate precision did not exhibit values over 0.7% and 0.9% respectively. Measured accuracy displayed %RSD <12% for all QC levels and analytes.

3.4.2.4 Robustness

The altered conditions to evaluate system robustness resulted in % RSD< 2% in both deliberate changed conditions. Change of column temperature caused an RT shifting with RSD=1.82 %, while change of the autosampler temperature caused RSD=0.14% in peak area calculations.

3.4.3 Measurements of HT, T OLEO and OLEA in EVOO

Table 2 summarizes the average values of the quantification results of the four analytes as well as the sum of them, according to their geographical origin. The detailed results of each sample are given in Appendix Table A2.

***Table 2**: Mean values of HT, T, OLEA, OLEO concentrations according to their geographical origin. Results are expressed in mg/Kg EVOO. In bold the higher concentration values compared to the estimated average are presented.*

Geographical region		HT (mg/Kg EVOO)	T (mg/Kg EVOO)	OLEA (mg/Kg EVOO)	OLEO (mg/Kg EVOO)	Sum (mg/Kg)
Ionian islands	**Cephalonia**	4.88	**6.66**	40.98	44.25	96.78
	Ithaca	**7.08**	**8.02**	**68.95**	**114.30**	**198.34**
Peloponnese	**Messinia**	**9.39**	**7.75**	33.36	38.54	89.04
	Laconia	4.23	6.27	21.98	42.59	75.04
Crete	**Lasithi**	6.00	4.78	**47.43**	**60.54**	**129.66**
	Heraklion	**6.66**	6.26	**59.85**	58.48	**118.75**
Average		**6.37**	**6.62**	**45.43**	**59.78**	**117.94**

The concentration levels of HT ranged from not detectable to 29.9 mg/kg EVOO and for T ranged from not detectable to 58.0 mg/kg EVOO (see also, Appendix Table A2). Average values were found 6.37 and 6.62 mg/kg EVOO for HT and T, respectively. The highest values for HT were found in Peloponnese and specifically in Messenia region. Ithaca presents also high values followed by Heraklion. Concerning T the highest values are presented again from Messenia and Ithaca, followed by Cephalonia. All the other regions are characterized by lower levels of HT and T compared to the calculated mean values. Figure 6 illustrates superimposed chromatograms of two OO extracts with different concentrations of HT and T. These results are in agreement with those found in previous published studies where HT and T were studied and quantified [69,76].

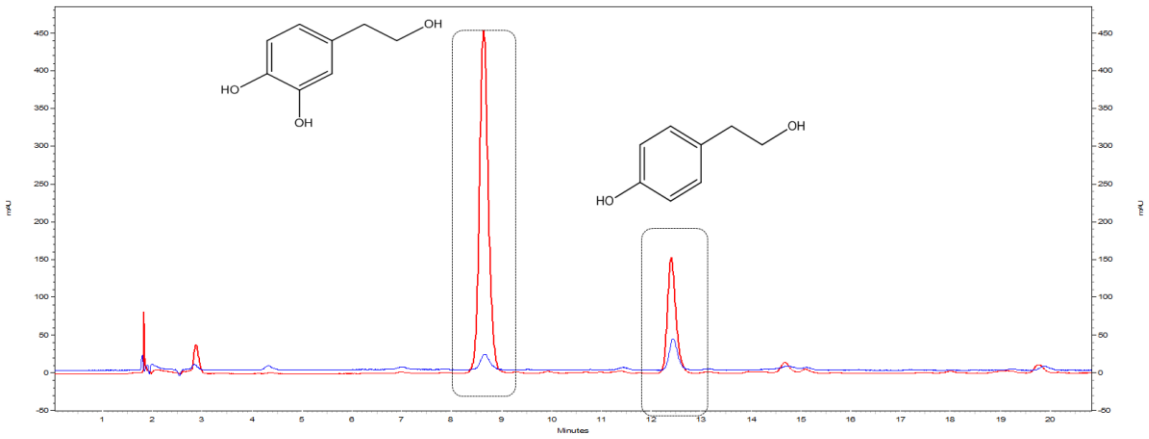

Figure 6: *HPLC-DAD chromatogram obtained at 280 nm representing an OO extract rich in HT and T (red annotation) and another poor in these analytes (blue annotation).*

For OLEO and OLEA a different pattern was found. It has to be noted that both compounds are secoiridoids that are hydrolyzed by endogenous enzymes during ripening of olive drupe and/or during malaxation releasing the corresponding simple phenols, HT and T respectively [77]. According to our data, the concentration of OLEA and OLEO ranged from not detectable to 157 and 181 mg/Kg EVOO,

respectively. Average values were also calculated and found 45.4 and 59.8 mg/Kg EVOO for OLEA and OLEO, respectively. The detailed results for each sample are given in Appendix Table A2. The calculated mean values and concentration range are similar with those reported previously [76,78]; although according to another study the concentration of OLEO and OLEA in Greek VOOs was found to be much higher for both compounds [79]. Nevertheless, in this latter study the compounds quantification was not performed by HPLC-DAD but with NMR and reference standards of the compounds were not used. Due to extended overlapping of aldehydic protons of OLEA and OLEO with other compounds bearing an aldehyde moiety as well, this method could lead to overestimations [80].

Ithaca island gave again the highest values for both compounds. Heraklion and Lasithi regions of Crete gave the nest higher values for OLEA, while for OLEO Heraklion was not over the calculated mean value but very close to it. Figure 7 illustrates an overlaid chromatogram of two OO extracts with different concentrations of OLEA and OLEO. It is intriguing that despite the fact that Ithaca and Cephalonia are islands very close each other, OO samples coming from them presented notable differences in their chemical composition; Ithaca presented high values for all of the four quantified compounds and high TPC levels as well, while Cephalonia did not indicate the same levels in those parameters. In both islands Koroneiki cultivar is cultivated but adapted in the microclimatic conditions of Ionian islands area. Although, another undefined factor except microclimate seems to differentiate the produced OO in these two islands. It has to be highlighted that OO samples coming from Ithaca are poorly studied concerning their biophenols content and to our knowledge this is the first time that EVOOs coming from Ithaca were quantified for the above four biophenols.

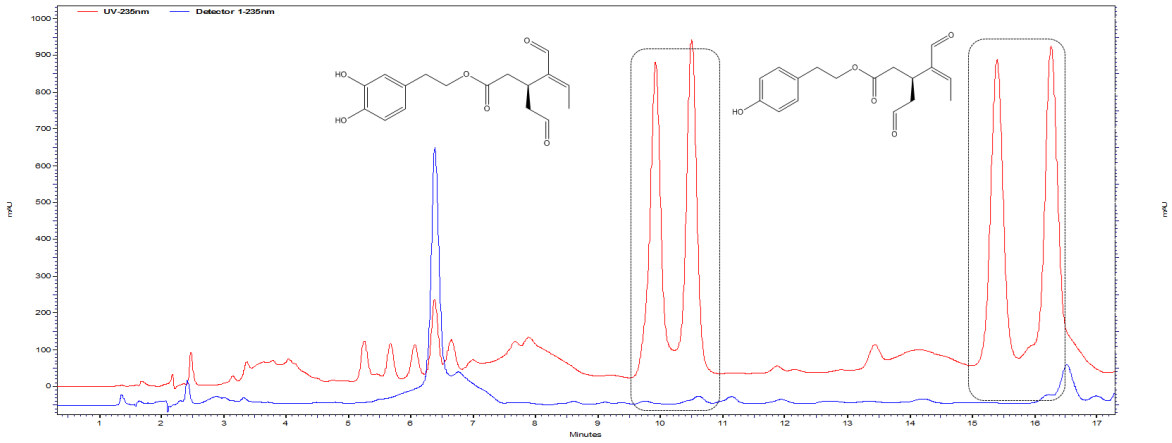

Figure 7: *HPLC-DAD chromatogram obtained at 235 nm representing an OO extract rich in OLEA and OLEO (red annotation) and another poor in these analytes (blue annotation).*

Additionally, the sum of the four determined compounds was estimated per origin in order to have an overview of their contribution in TPC (Table 2). The highest sum was observed in Ithaca as it was expected due to the occurrence of high levels in all of the four compounds. Continuously Crete region (Lasithi and Heraklion) presented the next higher sum. It is noteworthy that Ithaca and Crete possessed also the highest TPC values, although in reverse sequence indicating the higher contribution of these four compounds to Ithaca samples but not to Cretan. Cretan samples are possible rich in other secoiridoid compounds such as oleuropein and ligstroside aglycons that contribute to TPC values, but not quantified in this study.

3.5 UPLC-HRMS & HRMS/MS analysis

Being one of most popular and established method for quality control purposes, LC-MS was used first for the analysis of the samples. In this case only biophenol extracts were analysed due to well know restrictions in the analysis of intact oils with the LC-MS technique. Taking advantage of separation factor at the LC part and the

high resolving power and accuracy of the Orbitrap analyser, important data were generated. In total, for the 208 observations, 214 meaningful variables (*m/z*@Rt) were derived out of 1687 initially detected features. Primarily, unsupervised methods and specifically PCA was used (UV scaling). However, no specific patterns were observed.

Supervised methods were applied and OPLS-DA method after validation (Table A3) revealed distinct clustering information. Figure 8 illustrates the OPLS-DA scores plot and the generated groups according to geographical origin.

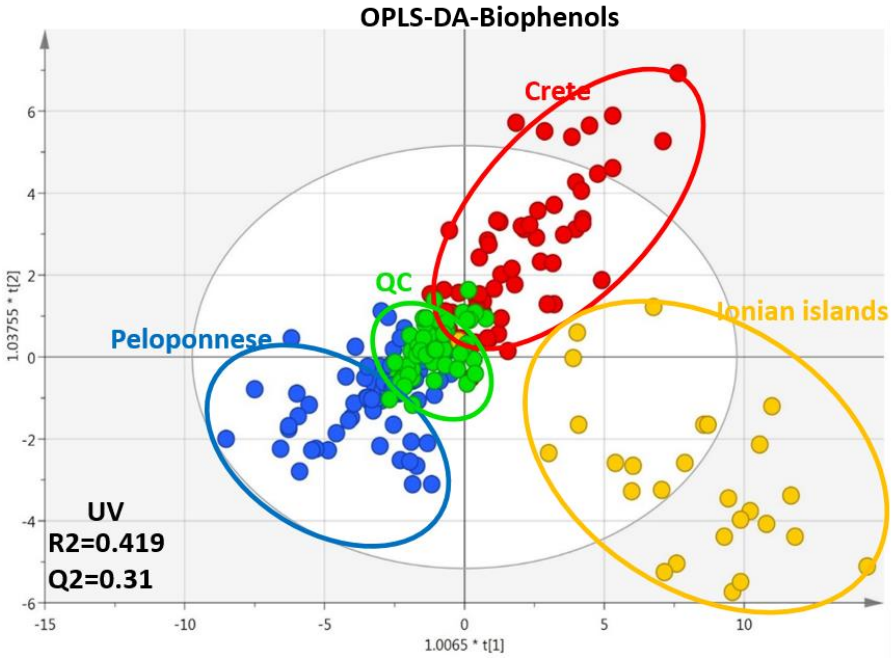

Figure 8: *OPLS-DA scores plot of the biophenol extract samples acquired via UPLC-HRMS. Plot includes the total number of observations in color scale according to geographical origin ClassID; Peloponnese (blue), Crete (red), Ionian islands (yellow). QC sample are also observed (green). On the left side of the plot the used scaling and the fitting parameters R=0.419 and Q2=0.310 are denoted.*

The generated model is not characterized by high fitting parameters (R2, Q2), although close values. Nevertheless, discrete clusters and trends were observed. Samples from Crete and Ionian islands were grouped separately from Peloponnese

samples at the first component, while they were differentially grouped amongst them at the second component. QC samples, as expected were centralized with limited dispersion indicating appropriate analytical procedure and good data fitting (Figure A5). Moreover, as illustrated in figure 8, the samples from Ionian islands were characterized by extensive dispersion while many of them could be considered as outliers (13/34). From VIP values, 55 features were selected as statistically significant with VIP>1 and were forwarded for identification. The detailed results are discussed in section 3.6.1 together with FIA-MRMS analysis.

As illustrated in figure 9, the LC dimension gives important information regarding the identity of compounds. For instance, based on RT and full scan MS, basic categorization could be achieved amongst the main chemical groups e.g phelylalcohols, iridoids, secoiridoids, flavonoids, triterpenic acids. Other features such as suggested EC and RDBeq. in combination with HRMS/MS facilitated significantly the identification process. An example of this process using extraction ion method as well as representative spectra of EVOO biophenols are given in appendix (figure A6-11). This information was coevaluated with MRMS data for accurate identification of metabolites.

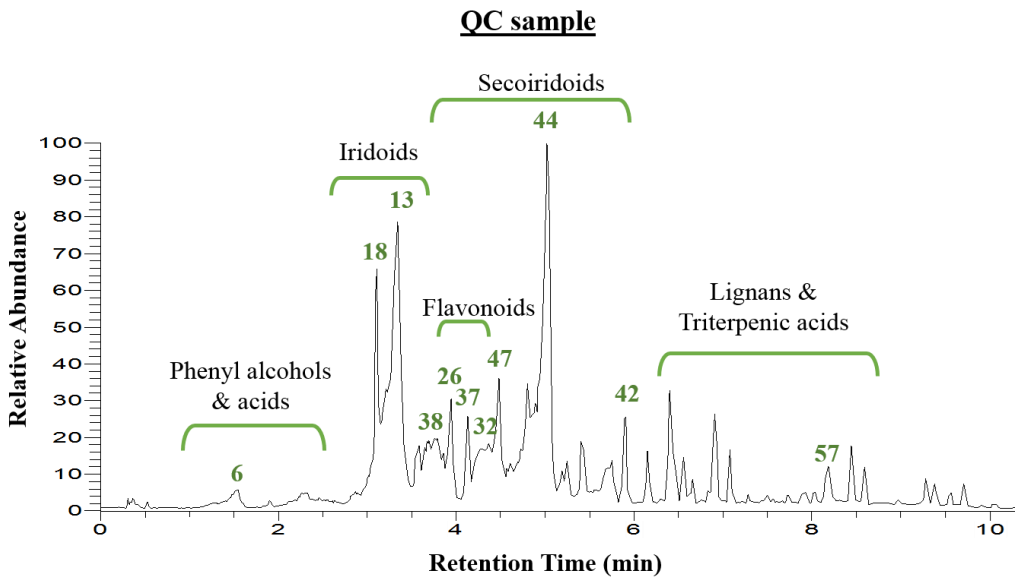

***Figure 9**: Base peak (BP) chromatogram of the QC (pooled sample). Certain metabolite groups are annotated.*

3.6 FIA-MRMS analysis

3.6.1 Geographical origin

In parallel to LC-MS, the 208 EVOO samples were analysed with FIA-MRMS. In this case both intact EVOO and biophenol extracts were analysed in 2 and 8 minutes, respectively. Similarly to LC-MS analysis, the spectral data were subjected to data processing prior MDA. Pareto scaling provided the best visualization and fitting results for intact EVOO samples while UV for the corresponding biophenol extracts. 2637 variables (*m/z*) were revealed from the EVOO dataset and 5079 from biophenols dataset. All the generated models using supervised methods (OPLS, OPLS-DA) succeeded in validation tests, holding higher scores for the corresponding R2 and Q2 parameters in comparison to UPLC-HRMS. Figure 10 illustrates representative scores plots using geographical origin as class parameter.

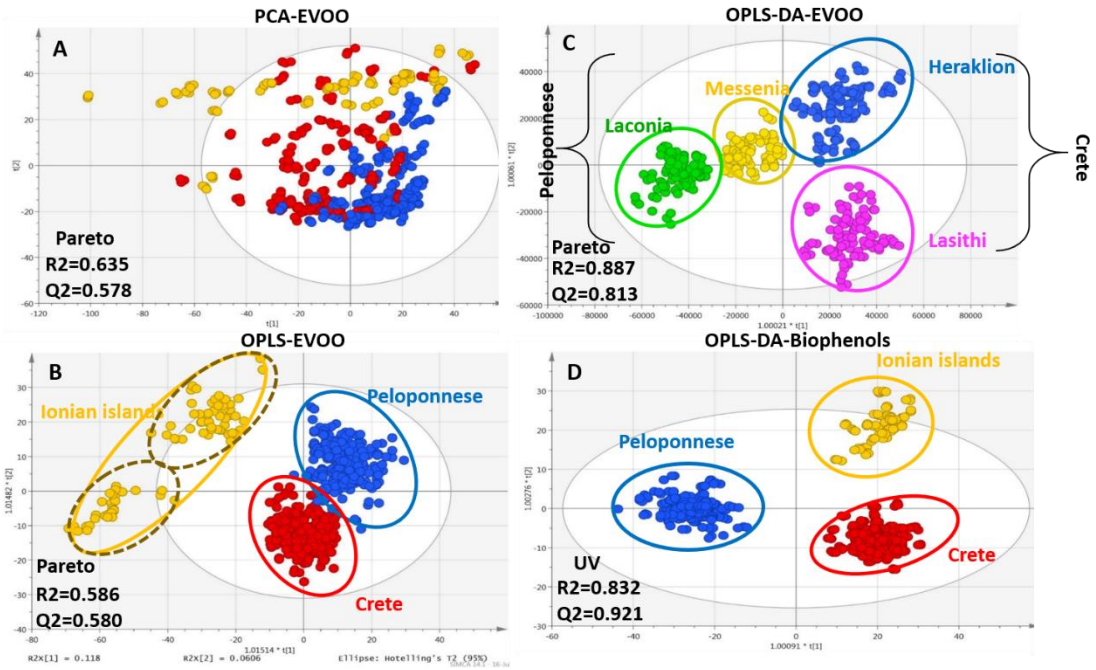

***Figure 10**: Scores plots of EVOOs and their corresponding biophenol extracts acquired via FIA-MRMS. Observations are colored coded according to geographical origin (A): PCA scores plot of EVOOs including all observations (pareto scaling); (B): OPLS scores plot of EVOOs including all observations (pareto scaling); (C): OPLS-DA plot of EVOOs excluding Ionian island samples (pareto scaling); and (D): OPLS-DA scores plot of biophenol extracts including all observations (UV scaling). Fitting parameters values (R2, Q2) are given (bottom- left).*

In PCA scores plot of intact EVOOs (Figure 10A), an unexpected clear tendency was observed separating the samples in the three basic areas; Peloponnese (blue), Crete (red) and Ionian islands (yellow). Similarly to LC-MS analysis, the majority of outliers originated from Ionian islands followed by samples of Crete while dispersion was obviously high. Interestingly, based on metadata most of the outliers corresponded to Ithaca island. In OPLS scores plot (Figure 10B) well-defined groups were revealed with acceptable fitting parameters. Especially for Ionian islands, two subgroups were clearly evident representing the two different collection islands i.e. Cephalonia (upper group) and Ithaca (lower group). Likewise, outliers corresponded to samples from Ithaca island. It is worth noting that the two islands are geographically very close, indicating the power and the sensitivity of the model.

Additionally, a distinct separation between the groups of Peloponnese/Crete and Ionian group was observed indicating the chemical discrepancy of Ionian samples in comparison to the other two areas. Excluding Ionian islands samples and using OPLS-DA method (Figure 10C), higher fitting parameters and clear clusters were disclosed. It is noteworthy that, there was a distinct separation between the two basic areas, Peloponnese and Crete, on the first component and apparent separation among the geographical subareas at the second component. For biophenols only OPLS-DA model passed the validation process (permutation test and acceptable fitting parameters). Distinct grouping of the three basic areas was attained (Figure 10D). Once more, Ionian islands were characterized by a number of outliers coming from Ithaca. It is worth noting that similar clustering trends in the separation of Ionian and Cretan samples with Peloponnese samples, in comparison to figure 8, was observed. Close inspection of the two plots (Figure 8 and Figure 10D) revealed that the absence of the LC dimension didn't affect at all the analysis performance. In contrast, the clustering was significantly improved with less dispersion and enhanced fitting.

Following the scores plots, the corresponding loading plots were thoroughly examined (Figure 11**)** for the identification of marker metabolites responsible for observed classification and correlation with geographical origin. VIP values were used to prioritize the detected variables. 297 features for EVOOs and 445 for biophenol extracts were determined with VIP>1. The ultra-high resolution and mass accuracy of MR analyzer contributed drastically to the identification of metabolites with high confidence and the detection of biophenols even in intact EVOOs analysis. The statistically significant identified compounds are presented in Table 3.

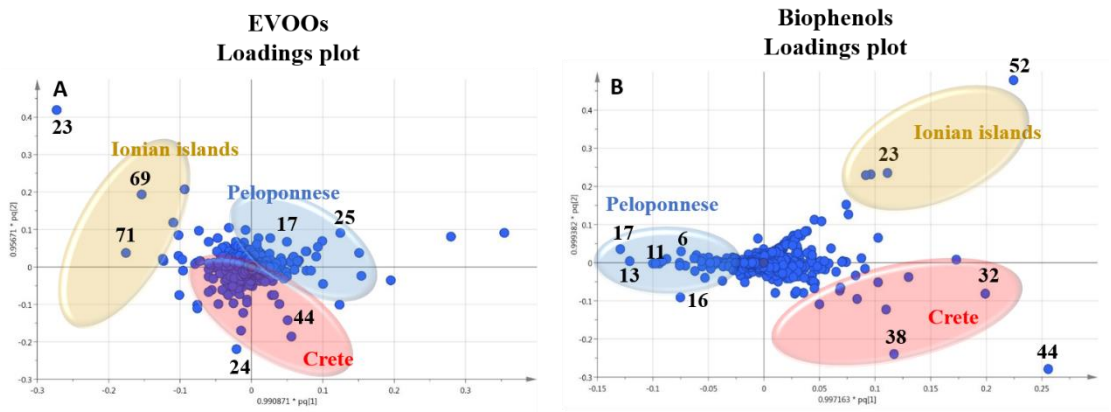

Figure 11: *OPLS-DA loadings plot for geographical origin identification generated by FIA-MRMS for intact EVOOs (A) and biophenols (B) dataset. Representative statistically significant loadings corresponding to certain marker compounds are annotated in areas of Peloponnese (blue), Crete (red) and Ionian islands (yellow).*

In total, 72 metabolites were identified both in EVOOs and biophenol extracts as geographical origin markers. The identification results denote that each geographical region was characterized by certain categories of compounds indicating their chemical discrepancy. Based on Table 3 (and Table A4 in appendix), EVOOs from Crete were mainly characterized by secoiridoid derivatives. Specifically, oleuropein aglycon (**44**) was present in almost all samples, revealing the highest relative levels amongst all groups (VIP=14.02). Also oleuropein aglycon derivatives i.e. 10-hydroxy oleuropein aglycon (**47**), hydroxy-O-decarboxymethyl oleuropein aglycon (**39**), oleacein (**38**) and oleocanthal (**32**) were characteristic secoiridoid markers of Crete. Other compounds strongly correlated were triterpenic acids (maslinic acid (**57**), oleanolic acid (**56**)) and long chain fatty acids (lignoceric acid (**43**), montanic acid (**55**), gondoic acid (**34**), arachidic acid (**35**)).

It is noteworthy that using metabolite-based projection method, oleic acid was clearly present in medium-high levels in Crete and Ionian in contrast to Peloponnese samples (Figure A12). Regarding, linoleic acid the opposite trend was observed while

for palmitic acid the trend of oleic acid was followed. Based on bibliographic data palmitic acid was formed from oleic acid [81], explaining the same trend in the two plots. Palmitic acid was found in significant intensities in Peloponnese as well. These observations are in agreement with previous studies using classical methods for acids determination ensuring the credibility of our approach [82].

In the case of Peloponnese, a different pattern was revealed. More chemical groups were represented i.e. flavonoids (apigenin (**20**), luteolin (**26**), luteolin-7-methyl ester (**29**)), lignans (acetoxypinoresinol (**51**), pinoresinol (**41**), syringaresinol (**53**)), phenyl acids (protocatehuic acid (**5**), benzoic acid (**2**)), phenylalcohols (hydroxytyrosol (**6**), tyrosol (**3**), hydroxytyrosol acetate (**9**)) and secoiridoids. It is worth noting that some compounds from the aforementioned groups have been previously suggested as Koroneiki variety markers [83]. Moreover, FA such as pentadecanoic acid (**14**), palmitoleic acid (**15**), margaric acid (**22**), lauric acid (**10**), margaroleic acid (**19**), stearic acid (**25**), octanoic acid (**4**) and characteristic triglycerides (triolein (**71**) and linolein (**70**)) were characteristic of Peloponnese EVOOs. Regarding the iridoids group, elenolic acid and its derivatives (elenolic acid methyl ester (**16**), elenolic acid ethyl ester (**21**), desoxyelenolic acid (**11**) were found as the most statistically significant markers together with ligstroside aglycon (**42**). Interestingly, high abundance of oleocanthal (**32**) found in some specific samples (Lakonia subarea) even if it was not statistically significant marker of Peloponnese EVOOs. In these cases, maybe other parameters such as altitude might be responsible for these high levels. In a previous published study, authors claim that the geographical prediction of origin regarding Lakonia and Crete is difficult, due to the same microclimatic conditions in these areas (high temperatures and low precipitation levels), associating their similar chemical profile with the biosynthetic pathway [48].

Contrary to the other areas, Ionian island samples uncovered completely different patterns. Linoleic acid derived as the most statistical significant marker of this region (Figure A13), while its levels in the other regions were significant low. Oleic acid (which is a considered as a predominant FFA of Koroneiki cultivar) retained its high levels, like Crete region. This fact can be explained from the activity of the enzyme oleate desaturase which has been found to convert oleic acid to linoleic [84]. Among the factors that regulate oleate desaturase activity is temperature [85]. It has been recently reported that low temperatures lead to higher content of C18:2 and C18:3 FA to maintain the fluidity of the biological membranes [86] Also it has been reported that higher temperatures increase oleic acid content in OO and its percentages depends on the mean environmental temperatures during fruit growth [87]. The high content of linoleic acid in Cephalonia have also been reported in another study where the authors calculated the FFA composition of different cultivars and locations of Ionian islands [50].

Additionally, Ionian samples as a total group displayed poor biophenol content and was mainly characterized by diglycerides and their derivatives. Besides, Ithaca samples uncovered high intensities in specific secoididoids, although not characterized as statistical significant. These findings are in accordance with previous results of our group confirming the significant chemical differences of Ionian OO with OOs produced in other regions of Greece [59]. The above findings may be explained by the different climate conditions in the three basic areas and the different adaption-behavior of Koroneiki cultivar in these microclimatic conditions. It has been generally proved that phenolic compounds content increase with the exposure to UV light and high temperatures [88]. The environmental stress of Crete and Peloponnese seems to lead to higher production of biophenols in comparison to Ionian islands. In

parallel, the relative lower temperatures of Ionian islands influence FFA composition and the saturation degree of OO [86]. Despite the clear markers for each region under study, some compounds are found significant for two regions, simultaneously but with different VIP values. For instance, oleic acid is important for the separation of Crete & Ionian samples from Peloponnese and palmitoleic acid could be used to differentiate Peloponnese & Ionian EVOOs from Cretan ones. Box-plots of characteristic phenols and their deviation between the three geographical origins are given in appendix (Figure A14).

3.6.2 Cultivation practice

The agronomical practices used for the cultivation of olive tree is a critical parameter affecting the composition of olive drupes and consequently of the produced OO [57]. In the current study three basic farming practices were investigated i.e. conventional, integrated and certified organic in order to reveal patterns and correlations with certain compounds. In this discriminating parameter only OPLS-DA models were valid for both EVOOs and biophenols samples. In biophenols scores plot once again the clusters were tighter with higher predictivity parameter (Q2) and better permutation test value (Table A3). Figure 12 illustrates the corresponding OPLS-DA scores plots.

In total, 309 variables were found with VIP >1 for EVOOs and 429 for biophenols for the entire number of observations. In figure 12A clear clustering with some overlappings between integrated and conventional practice were observed with a number of outliers originated from integrated practice (Figure A15 illustrates the corresponding loadings plot). It is interesting that integrated and conventional samples, which apply similar maintenance and fertilization practices, were separated

from organic farming on the first component, while integrated and conventional on the second component.

In a previous published study concerning the determination of FFA content between organic and non-organic VOO via GC-MS, authors denote that no difference was observed between the cultivation practices, pointing out that the existence of pesticides does effect the ratio of MUFA/PUFA [89]. In another study authors claim that the total FFA composition is the same and only the levels of oleic and linoleic acid varies between the same practices, with oleic acid possessing higher concentrations in organic treatments [73]. Although in our study we discovered a significant aggregation of FFAs in integrated practice, followed by conventional including oleic acid in significant content with the parallel substance of TGs. In organic farming mostly DGs, their derivatives and a number from FFAs were encountered. It should be highlighted that most of the organic practice samples used in the study originated from Ionian islands which might affect the results. Interestingly, integrated practice is poorly studied concerning the composition of OO (both lipophilic and hydrophilic part) and data are presented here for the first time.

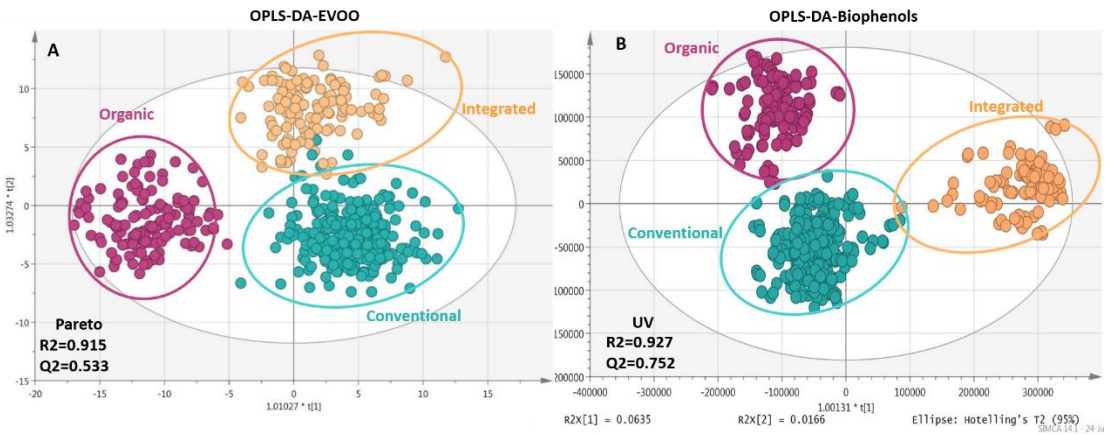

***Figure 12**: Scores plots of EVOOs and their corresponding biophenol extracts acquired via FIA-MRMS. Plots include the total number of observations and are colored coded according to cultivation practice classID; conventional (blue), integrated (light orange), and certified organic practices (magenta). (A): OPLS-DA*

scores plot of EVOOs with pareto scaling; (B): OPLS-DA scores plot of biophenols with UV scaling. Fitting parameters values (R2, Q2) are given (bottom- left).

Regarding biophenols a different trend was observed. In figure 12B organic and conventional samples are separated on the first component with integrated, while conventional and organic are separated on the second component (Figure A16 represents the corresponding loadings plot). Once more outliers originated from integrated practice.

Most of available studies report that organic practice produces higher TPC [54,57,90]. This was evident also from the current study as it is presented in figure 3B and Table A2 in appendix. However, due to the wide and sometimes unclear definitions of organic and conventional practices, the factors influencing TPC have not yet been substantiated. However, it is generally accepted that TPC production interrelates to the amount of the available water. Excess of water (usually provided to conventional practice) leads to low production of phenolic compounds [91] due to lower activity of L-phenylalanine ammonia lyase enzyme in olive fruits which is the key enzyme in phenolics biosynthesis [92]. In our study, VIP features revealed that conventionally grown trees emerged the majority of biophenolic classes such as secoiridoids, iridoids, phenyl alcohols, triterpenic acids, lignans, flavonoids. On the other hand, in organic practices we did not identify many biophenol groups, but in a considerable number of samples characteristic secoiridoids were identified i.e. oleacein (**38**), oleocanthal (**32**), ligstroside aglycon (**42**) and its derivatives as well as some oleuropein aglycon derivatives giving higher intensities in comparison to conventional practice. It should be noted that in organic practice we identified only a part of the secoiridoids groups, which appear in high concentrations in Greek OO [59] and in consequence constitute the main part of total biophenols.

In integrated practice only phenyl acids were identified. In figure 12A and B the displayed integrated outliers come from Ole 466 for biophenols and Ole 656 and 512 from EVOOs (all of them from Lasithi produced with three phases mill) possessed high intensities for linoleic acid and oleuropein aglycon, which were not found as statistical significant metabolites in integrated practice (Figure A17).

3.6.3 Production procedure

As mentioned already, samples of EVOO using traditional mills were not included in the study due to their low number since this production way has been almost abandoned nowadays. Models developed with unsupervised methods had low fitting parameters and did not pass the validation test. OPLS-DA models with pareto and UV scaling for EVOOs and biophenols respectively, were although valid with good fitting parameters. Figure 13 represents the OPLS-DA scores plots of EVOOs and their biophenol extracts.

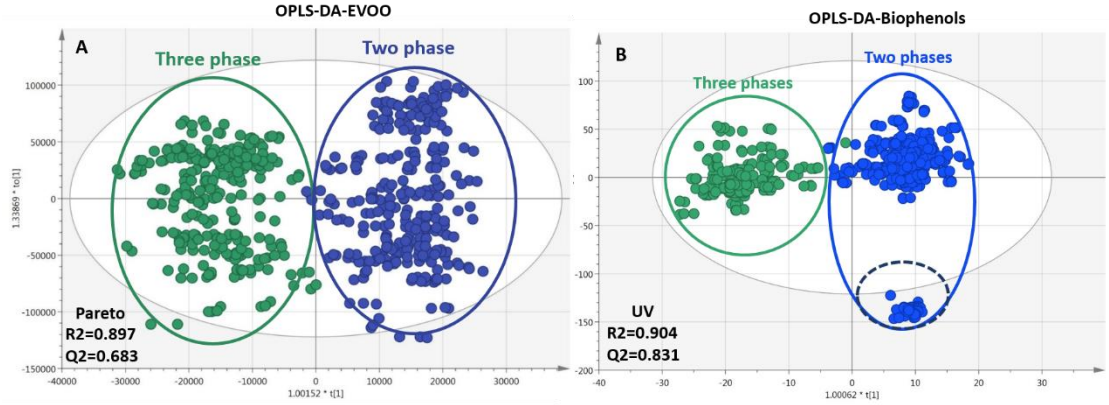

***Figure 13**: Score plots of EVOOs and their corresponding biophenol extracts acquired via FIA-MRMS and colored according to production procedure classID; three phases (green), two phases (blue). (A): OPLS-DA of EVOOs treated with pareto scaling. (B): OPLS-DA of biophenols treated with UV scaling. Fitting parameters R2 and Q2 are given (left-down).*

309 VIP features were calculated with values over 1 for EVOOs and 429 for biophenols (in figure A18 the corresponding s-plot is presented). Both plots had clear distinction between the two different procedures on the first component, while the model of biophenols showed higher fitting parameters R2, Q2, better permutation test results (Table A3) and tighter clusters in comparison to EVOOs model. In addition, two phases procedure (Figure 13B) uncovered a subgroup of outliers, interestingly all from the same producer.

Concerning the glycerol part (Figure 13A), two phases system contained most of the identified TGs, DGs and FFAs. Three phases system contained also some FFAs and DGs. This intersection of chemical groups between the two procedures may be the reason for the high diffusion of the two clusters and the low values in fitting scores. However, these findings concern only the identified compounds of the initial VIP list and in consequence no specific trend can be formed to support cluster separation. In a previous study, authors describe that FA variability is not influenced from production methodology [56] and therefore they can be regarded as an impotent factor of groups discrimination. In the same study, it is reported that two phases decanters resulted in OOs with higher content in phenyl alcohols and phenyl acids. Moreover, previous studies indicate that OOs produced in two phases mills contain higher phenolic content in comparison to three phases due to the removal of phenols into waste during the addition of water in the malaxation stage [58]. The same findings were uncovered in our study i.e. higher content of phenyl alcohols and their derivatives (hydroxytyrosol (**6**), tyrosol (**3**), hydroxytyrosol acetate (**9**), tyrosol acetate (**7**) and some secoiridoids (oleacein (**38**), oleocanthal (**32**), oleocanthal acid (**37**)) were observed as statistical significant biomarkers of two phases milling. On the other hand, the rest of secoiridoids, iridoids, lignans, flavonoids and triterpenic acids were

more present in three phases systems. Based on the above outcomes, it seems that two phases system congregated the more polar phenols.

Concerning the outliers in the two phases procedure group, all the samples come from the same oil production plant of Lakonia (Peloponnese) region, but different olive oil producers. These samples are characterized by phenyl acids (protocatehuic acid (**5**), benzoic acid (**2**)) and significant FFAs of OO (palmitic acid (**17**), myristic acid (**12**), pentadecanoic acid (**14**), palmitoleic acid (**15**), margaric acid (**22**), lauric acid (**10**), margaroleic acid (**19**), stearic acid (**25**), octanoic acid (**4**)). It should be noticed that these samples did not behave as outliers in the study case of geographical origin (EVOOs and biophenols), but only in the production procedure biophenols model. Outliers exposed a different biophenols composition from all the other samples produced with two phases mills, despite that in literature phenyl acids have been reported as biomarkers of two phases production procedure. The exact parameter influencing their composition is not clear. Although a special treatment (e.g. uncommon malaxation temperature or time) had possibly been implemented during oil production and consequently influenced their chemical profile. In brief, the existence of tighter clusters, higher fitting parameters, and stronger trends of figure 13B signify that the production procedure mainly affects biophenols composition in comparison to intact EVOO.

Table 3: Identified metabolites in EVOO and biophenol extracts by MRMS. All the metabolites are numbered according to the first column. Experimental m/z and elemental composition are given. Each metabolite is accompanied with the primary type of classID i.e. geographical region, production procedure and cultivation practice.

No	Experimental *m/z*	Suggested Molecule	Elemental Composition	Geographical region	Production procedure	Cultivation practice
1	119.034969	2-(2-hydroxyethoxy)acetic acid	$C_4H_8O_4$	Peloponnese	Two phases	Integrated
2	121.029503	Benzoic acid	$C_7H_6O_2$	Peloponnese	n.c.	Integrated
3	137.06081	Tyrosol	$C_8H_{10}O_2$	Peloponnese	Two phases	Integrated
4	143.107736	Octanoic acid	$C_8H_{16}O_2$	Peloponnese	Two phases	Integrated
5	153.01931	Protocatehuic acid	$C_7H_6O_4$	Peloponnese	Two phases	Integrated
6	153.055719	Hydroxytyrosol	$C_8H_{10}O_3$	Peloponnese	n.c.	Conventional
7	179.071361	Tyrosol Acetate	$C_{10}H_{12}O_3$	Ionian islands	Two phases	Conventional
8	183.066297	Dialdehydic form of decarboxymethyl Elenolic acid	$C_9H_{12}O_4$	Ionian islands	Two phases	Conventional
9	195.066278	Hydroxytyrosol Acetate	$C_{10}H_{12}O_4$	Peloponnese, Crete	Two phases	Conventional
10	199.170347	Lauric acid	$C_{12}H_{24}O_2$	Peloponnese	Two phases	Integrated
11	225.076859	desoxy elenolic acid derivative	$C_{11}H_{14}O_5$	Peloponnese	n.c.	Conventional
12	227.201648	Myristic acid	$C_{14}H_{28}O_2$	Peloponnese	Two phases	Integrated
13	241.071755	Elenolic acid	$C_{11}H_{14}O_6$	Peloponnese	Three phases	Conventional

14	241.21729	Pentadecanoic acid	$C_{15}H_{30}O_2$	Peloponnese	Two phases	Integrated
15	253.217315	Palmitoleic acid	$C_{16}H_{30}O_2$	Peloponnese, Ionian islands	Two phases	Integrated, Organic
16	255.087423	Elenolic acid methyl ester	$C_{12}H_{16}O_6$	Peloponnese	Three phases	Conventional
17	255.232958	Palmitic acid	$C_{16}H_{32}O_2$	Peloponnese	Two phases	Integrated
18	257.066694	Hydroxylated form of elenolic acid	$C_{11}H_{14}O_7$	Crete, Ionian islands	n.c.	Conventional
19	267.23293	Margaroleic acid	$C_{17}H_{32}O_2$	Peloponnese	Two phases	Integrated
20	269.045551	Apigenin	$C_{15}H_{10}O_5$	Peloponnese	Three phases	Conventional
21	269.103081	Elenolic acid ethyl ester	$C_{13}H_{18}O_6$	Peloponnese.		Conventional
22	269.248578	Margaric acid	$C_{17}H_{34}O_2$	Peloponnese	Two phases	Integrated
23	279.23298	Linoleic acid	$C_{18}H_{32}O_2$	Ionian islands	Two phases	Organic
24	281.248634	Oleic acid	$C_{18}H_{34}O_2$	Crete, Ionian islands	Two phases	Conventional, Integrated
25	283.264257	Stearic acid	$C_{18}H_{36}O_2$	Peloponnese	Two phases	Conventional, Integrated
26	285.040502	Luteolin	$C_{15}H_{10}O_6$	Peloponnese	Three phases	Conventional, Integrated
27	295.227889	Hydroxylinoleic acid	$C_{18}H_{32}O_3$	Crete	Two phases	Integrated
28	297.243504	Hydroxyoleic acid	$C_{18}H_{34}O_3$	Crete	Three phases	Conventional, Integrated

29	299.056138	Luteolin-7 methyl-ether	$C_{16}H_{12}O_6$	Peloponnese	Three phases	Conventional
30	299.20161	PUFA,C-20	$C_{20}H_{28}O_2$	Peloponnese	Two phases	Integrated
31	299.259173	Hydroxystearic acid	$C_{18}H_{36}O_3$	x	Three phases	Conventional
32	303.123779	Oleocanthal	$C_{17}H_{20}O_5$	Crete	Two phases	Organic, Conventional
33	303.232928	Arachidonic acid	$C_{20}H_{32}O_2$	x	x	Integrated
34	309.284317	Gondoic acid	$C_{20}H_{38}O_2$	Crete	Three phases	x
35	311.295541	Arachidic acid	$C_{20}H_{40}O_2$	Crete	Three phases	Conventional, Integrated
36	313.238436	Octadecanedioic acid	$C_{18}H_{34}O_4$	Crete	n.c.	Integrated
37	319.116536	Oleocanthalic acid	$C_{17}H_{20}O_6$	n.c.	Two phases	x
38	319.118731	Oleacein	$C_{17}H_{20}O_6$	Crete	Two phases	Organic, Conventional
39	335.113652	Hydroxy-O-decarboxymethyl oleuropein aglycon	$C_{17}H_{20}O_7$	Crete	n.c.	Conventional, Organic
40	339.232889	Docosanoic acid	$C_{23}H_{32}O_2$	Peloponnese	Three phases	Integrated
41	357.134425	Pinoresinol	$C_{20}H_{22}O_6$	Peloponnese	Three phases	Conventional
42	361.129246	Ligstroside aglycon	$C_{19}H_{22}O_7$	Peloponnese	Three phases	Conventional, Organic
43	367.361121	Lignoceric acid	$C_{24}H_{48}O_2$	Crete	Three phases	n.c.

44	377.124147	Oleuropein aglycon	$C_{19}H_{22}O_8$	Crete	Three phases	Conventional
45	389.290828	SFA	$C_{21}H_{42}O_6$	Ionian islands	Three phases	Conventional
46	391.139885	Methyl oleuropein aglycon	$C_{20}H_{24}O_8$	Crete	Three phases	Conventional
47	393.119148	10-Hydroxy oleuropein aglycon	$C_{19}H_{22}O_9$	Crete	Three phases	Conventional
48	393.155482	Ligstroside aglycon derivative (hydroxylated product)	$C_{20}H_{26}O_8$	Peloponnese	Three phases	Conventional, Organic
49	409.15044	Oleuropein aglycon derivative	$C_{20}H_{26}O_9$	Crete, Peloponnese	Three phases	Conventional
50	413.290878	TG	$C_{23}H_{42}O_6$	Ionian islands	Two phases	Organic
51	415.139887	Acetoxypinoresinol	$C_{22}H_{24}O_8$	Peloponnese	Three phases	Conventional
52	415.306484	MUFA ester	$C_{23}H_{44}O_6$	Ionian islands	Two phases	Organic
53	417.155523	Syringaresinol	$C_{22}H_{26}O_8$	Peloponnese	Three phases	Conventional
54	417.322155	SFA ester	$C_{23}H_{46}O_6$	Peloponnese	Two phases	Conventional
55	423.422612	Montanic acid	$C_{28}H_{53}O_2$	Crete	Two phases	n.c.
56	455.353111	Oleanolic acid	$C_{30}H_{48}O_3$	Crete	Three phases	Conventional
57	471.347941	Maslinic acid	$C_{30}H_{48}O_4$	Crete	Three phases	Conventional
58	611.525847	DG derivative	$C_{37}H_{72}O_6$	Ionian islands	Two phases	Organic
59	629.491862	DG	$C_{37}H_{70}O_5Cl$	Ionian islands	Two phases	Conventional, Organic
60	637.541557	Trilaurin	$C_{39}H_{74}O_6$	Ionian islands	Two phases	Organic

61	653.542317	DG derivative	$C_{39}H_{73}O_7$	Ionian islands	Two phases	Organic
62	655.515738	DG	$C_{39}H_{72}O_5Cl$	Ionian islands	Two phases	Conventional
63	679.554723	DG derivative	$C_{41}H_{75}O_7$	Peloponnese	Three phases	Organic
64	849.763319	TG derivative	$C_{53}H_{102}O_7$	Ionian islands	Two phases	Organic
65	867.725262	TG	$C_{53}H_{100}O_6Cl$	Ionian islands	Two phases	Conventional
66	875.774536	TG derivative	$C_{55}H_{104}O_7$	Ionian islands	Two phases	Organic
67	890.714835	Stearin	$C_{57}H_{110}O_6$	Ionian islands	Two phases	Conventional
68	891.725417	TG	$C_{55}H_{100}O_6Cl$	Ionian islands	Two phases	Conventional, Organic
69	893.742758	TG	$C_{55}H_{102}O_6Cl$	Ionian islands	Two phases	Conventional
70	895.732846	TG	$C_{55}H_{104}O_6Cl$	Peloponnese	Two phases	Integrated, Conventional
71	914.753581	Linolein	$C_{57}H_{98}O_6$	Peloponnese	Two phases	Conventional
72	919.754312	Triolein	$C_{57}H_{104}O_6Cl$	Ionian islands	Two phases	Conventional

[1] Metabolites marked with "x" are not found in the VIP list for the corresponding quality parameter. [2] Indication of "n.c." is referred to features that no conclusion could be made with due to the low number of samples. [3]SFA: saturated fatty acid; PUFA: polyunsaturated fatty acid.

4. Conclusions

In the present study a holistic analytical workflow was incorporated for mapping and quality control of Greek EVOO. Based on a methodical sample collection, EVOO samples were thoroughly selected from different areas of Greece and special attention was given to metadata qualifying the optimum ones subjected to the study. Essential phenolic parameters were evaluated using standard methodologies and in parallel two metabolic profiling approaches of intact EVOO and the corresponding biophenols were incorporated for the investigation of specific parameters i.e geographical origin, cultivation practice and production procedure.

More specifically, two HPLC-DAD methodologies were developed and applied for the quantification of two phenylalcohols (HT and T) and two secoiridoid derivatives (OLEA and OLEO), characterized by high pharmacological interest. Quantification results were combined with TPC and TPF values and then correlated with geographical origin, cultivation practice and production procedure. Studied parameters were associated with certain levels of analytes and phenolic content. Previous published data in combination with our results revealed the existence of certain levels of phenolic compounds in each geographical region and the impact each applied methodology of cultivation practice and production procedure to the phenolic content.

Subsequently, two different FT-HRMS methods were incorporated for quality control aspects of Greek EVOO using metabolic profiling approaches. Both, biophenols after extraction and native EVOOs were analysed using FIA-MRMS method and in parallel LC-Orbitrap methods were used for the analysis of polyphenols samples. Data derived from both techniques were subjected to MDA and correlated. Clear classification of EVOO samples was achieved in both types of samples with FIA-MRMS using for class discrimination all the parameters under investigation. Taking advantage of the excellent resolution and accuracy of MRMS as well as the

HRMS/MS capabilities of Orbitrap it was possible to identify specific compounds responsible for the observed classification with high confidence. It is the first time that two very important factors for EVOO quality, agronomical practice and procedure for its production are investigated under metabololic profiling concept for Greek samples. To our knowledge it is also the first time that certain markers belonging to lipophilic and polar constituents of EVOO are revealed, identified and correlated to specific parameter using a single technique. It was possible, with limited sample preparation and eliminating LC using just direct injection, to accomplish very fast analysis time of a few minutes without any negative impact of data quality. Therefore, FIA-MRMS is proven to be an excellent alternative for quality control purposes for such a complex and highly variable substrate such as EVOO.

Bibliography

[1] G. Buckland, C.A. Gonzalez, The role of olive oil in disease prevention: a focus on the recent epidemiological evidence from cohort studies and dietary intervention trials., Br. J. Nutr. 113 (2015) 94–101. doi:10.1017/S0007114514003936.

[2] UNESCO, Intangible Cultural Heritage, (n.d.). https://ich.unesco.org/en/lists.

[3] International Ollive Council, Market Newsletter, (2017) 1–6.

[4] P. Dais, E. Hatzakis, Quality assessment and authentication of virgin olive oil by NMR spectroscopy : A critical review, Anal. Chim. Acta. 765 (2013) 1–27. doi:10.1016/j.aca.2012.12.003.

[5] F. Visioli, A. Poli, C. Gall, Antioxidant and other biological activities of phenols from olives and olive oil., Med. Res. Rev. 22 (2002) 65–75.

[6] M. Servili, R. Selvaggini, S. Esposto, A. Taticchi, G. Montedoro, G. Morozzi, Health and sensory properties of virgin olive oil hydrophilic phenols: agronomic and technological aspects of production that affect their occurrence in the oil, J. Chromatogr. A. 1054 (2004) 113–127.

[7] H.K. Obied, P.D. Prenzler, S.H. Omar, R. Ismael, M. Servili, S. Esposto, A. Taticchi, R. Selvaggini, S. Urbani, Pharmacology of olive biophenols, 1st ed., Elsevier B.V., 2012. doi:10.1016/B978-0-444-59389-4.00006-9.

[8] D. Boskou, Olive Oil Composition. In Olive Oil Chemistry and Tecnology., AOC Press: Champaign, USA, 1996.

[9] A. Angelis, M. Hamzaoui, N. Aligiannis, T. Nikou, D. Michailidis, P. Gerolimatos, A. Termentzi, J. Hubert, M. Halabalaki, J.-H. Renault, A.-L. Skaltsounis, An integrated process for the recovery of high added-value compounds from olive oil using solid support free liquid-liquid extraction and chromatography techniques, J. Chromatogr. A. 1491 (2017) 126–136. doi:10.1016/j.chroma.2017.02.046.

[10] F. Visioli, E. Bernardini, Extra virgin olive oil's polyphenols: biological activities., Curr. Pharm. Des. 17 (2011) 786–804.

[11] S. Cicerale, L. Lucas, R. Keast, Antimicrobial, antioxidant and anti-inflammatory phenolic activities in extra virgin olive oil, Curr. Opin. Biotechnol. 23 (2012) 129–135.

[12] K. Hamden, N. Allouche, M. Damak, A. Elfeki, Hypoglycemic and antioxidant effects of phenolic extracts and purified hydroxytyrosol from olive mill waste in vitro and in rats., Chem. Biol. Interact. 180 (2009) 421–432. doi:10.1016/j.cbi.2009.04.002.

[13] S. Cicerale, L. Lucas, R. Keast, Biological Activities of Phenolic Compounds Present in Virgin Olive Oil, Int. J. Mol. Sci. 11 (2010) 458–479. doi:10.3390/ijms11020458.

[14] EFSA, EFSA Panel on Dietetic Products, Nutrition and Allergies (NDA); Scientific Opinion on the substantiation of health claims related to polyphenols in olive and protection of LDL particles from oxidative damage (ID 1333, 1638, 1639, 1696, 2865),

maintenance, EFSA J. 9 (2011) 2033–58. doi:10.2903/j.efsa.2011.2033.

[15] A. Agiomyrgianaki, P. V Petrakis, P. Dais, Influence of harvest year , cultivar and geographical origin on Greek extra virgin olive oils composition : A study by NMR spectroscopy and biometric analysis, FOOD Chem. 135 (2012) 2561–2568. doi:10.1016/j.foodchem.2012.07.050.

[16] A. Fernández-gutiérrez, Evaluating the potential of phenolic profiles as discriminant features among extra virgin olive oils from Moroccan controlled designations of origin, (2016). doi:10.1016/j.foodres.2016.03.010.

[17] R. Aparicio, M.T. Morales, R. Aparicio-Ruiz, N. Tena, D.L. García-González, Authenticity of olive oil: Mapping and comparing official methods and promising alternatives, Food Res. Int. 54 (2013) 2025–2038.

[18] M. Beltrán, M. Sánchez-Astudillo, D.L. Aparicio, Ramón García-González, Geographical traceability of virgin olive oils from south-western Spain by their multi-elemental composition., Food Chem. 169 (2015) 350–7.

[19] F. Camin, A. Pavone, L. Bontempo, R. Wehrens, M. Paolini, A. Faberi, R.M. Marianella, D. Capitani, S. Vista, L. Mannina, The use of IRMS, 1H NMR and chemical analysis to characterise Italian and imported Tunisian olive oils, Food Chem. 196 (2016) 98–105.

[20] International Ollive Council, Designations and definitions of olive oils, (n.d.). http://www.internationaloliveoil.org/estaticos/view/83-designations-and-definitions-of-olive-oils.

[21] N. and A. (NDA) EFSA Panel on Dietetic Products, Scientific Opinion on the substantiation of health claims related to foods with reduced amounts of saturated fatty acids (SFAs) and maintenance of normal blood LDL-cholesterol concentrations (ID 620 , 671 , 4332) pursuant to Article 13 (1) of Regula, EFSA J. 9 (2011). doi:doi:10.2903/j.efsa.2011.2062.

[22] N. and A. (NDA) EFSA Panel on Dietetic Products, Scientific Opinion on the substantiation of health claims related to polyphenols in olive and protection of LDL particles from oxidative damage (ID 1333 , 1638 , 1639 , 1696 , 2865), maintenance of normal blood HDL-cholesterol concentrations (ID 1639), 9 (2011) 1–25. doi:10.2903/j.efsa.2011.2033.

[23] European Union, Commission Regulation (EU) No 432/2012 establishing a list of permitted health claims made on foods, other than those referring to the reduction of disease risk and to children's development and health, (2012).

[24] E. Commision, Council Regulation (EC) No 510/2006, Off. J. Eur. Union. 2006 (2006) 12–25.

[25] A. M.Gómez-Caravaca, R. M.Maggio, L. Cerretanide, Chemometric applications to assess quality and critical parameters of virgin and extra-virgin olive oil . A review, Anal. Chim. Acta. 913 (2016) 1–21. doi:10.1016/j.aca.2016.01.025.

[26] G. Purcaro, R. Codony, L. Pizzale, C. Mariani, L. Conte, Evaluation of total hydroxytyrosol and tyrosol in extra virgin olive oils, Eur. J. Lipid Sci. Technol. 116

(2014) 805–811. doi:10.1002/ejlt.201300420.

[27] E. Karkoula, A. Skantzari, E. Melliou, P. Magiatis, Quantitative Measurement of Major Secoiridoid Derivatives in Olive Oil Using qNMR. Proof of the Artificial Formation of Aldehydic Oleuropein and Ligstroside Aglycon Isomers, J. Agric. Food Chem. 62 (2014) 600–607. doi:10.1021/jf404421p.

[28] A. Bajoub, E. Hurtado-Fernández, E.A. Ajal, N. Ouazzani, A. Fernández-Gutiérrez, A. Carrasco-Pancorbo, Comprehensive 3-Year Study of the Phenolic Profile of Moroccan Monovarietal Virgin Olive Oils from the Meknès Region, J. Agric. Food Chem. 63 (2015) 4376–4385. doi:10.1021/jf506097u.

[29] N. Mulinacci, C. Giaccherini, F. Ieri, M. Innocenti, A. Romani, F.F. Vincieri, Evaluation of lignans and free and linked hydroxy-tyrosol and tyrosol in extra virgin olive oil after hydrolysis processes, J. Sci. Food Agric. 86 (2006) 757–764. doi:10.1002/jsfa.2411.

[30] R. Mateos, J.L. Espartero, M. Trujillo, J.J. Ríos, M. León-Camacho, F. Alcudia, A. Cert, Determination of phenols, flavones, and lignans in virgin olive oils by solid-phase extraction and high-performance liquid chromatography with diode array ultraviolet detection, J. Agric. Food Chem. 49 (2001) 2185–2192. doi:10.1021/jf0013205.

[31] European Commission, Food authenticity and quality, (n.d.). https://ec.europa.eu/jrc/en/research-topic/food-authenticity-and-quality (accessed January 9, 2019).

[32] A. Mastralexi, N. Nenadis, M.Z. Tsimidou, Addressing Analytical Requirements To Support Health Claims on " Olive Oil Polyphenols " (EC Regulation 432/2012), J. Agric. Food Chem. 62 (2014) 2459–2461. doi:10.1021/jf5005918.

[33] A. Loubiri, A. Taamalli, N. Talhaoui, S. Nait, Usefulness of phenolic profile in the classification of extra virgin olive oils from autochthonous and introduced cultivars in Tunisia, Eur. Food Res. Technol. 243 (2017) 467–479. doi:10.1007/s00217-016-2760-7.

[34] I. Vulcano, M. Halabalaki, L. Skaltsounis, M. Ganzera, Quantitative analysis of pungent and anti-inflammatory phenolic compounds in olive oil by capillary electrophoresis, Food Chem. 169 (2015) 381–386. doi:10.1016/j.foodchem.2014.08.007.

[35] R.M. Maggio, L. Cerretani, E. Chiavaro, T.S. Kaufman, A. Bendini, A novel chemometric strategy for the estimation of extra virgin olive oil adulteration with edible oils, Food Control. 21 (2010) 890–895. doi:10.1016/j.foodcont.2009.12.006.

[36] C. Augusto, A. Dillenburg, R. Edward, H. Teixeira, Use of multivariate statistical techniques to optimize the simultaneous separation of 13 phenolic compounds from extra-virgin olive oil by capillary electrophoresis, Talanta. 83 (2011) 1181–1187. doi:10.1016/j.talanta.2010.07.013.

[37] R. Aparicio-ruiz, D.L. García-gonzález, M.T. Morales, A. Lobo-prieto, I. Romero, Comparison of two analytical methods validated for the determination of volatile compounds in virgin olive oil : GC-FID vs GC-MS, Talanta. 187 (2018) 133–141. doi:10.1016/j.talanta.2018.05.008.

[38] R. Gil-Solsona, M. Raro, C. Sales, L. Lacalle, R. Díaz, M. Ibáñez, J. Beltran, J.V. Sancho,

F.J. Hernández, Metabolomic approach for Extra virgin olive oil origin discrimination making use of ultra-high performance liquid chromatography e Quadrupole time-of- fl ight mass spectrometry ndez, Food Control. 70 (2016) 350–359. doi:10.1016/j.foodcont.2016.06.008.

[39] F. Longobardi, A. Ventrella, C. Napoli, E. Humpfer, B. Schütz, H. Schäfer, M.G. Kontominas, A. Sacco, Classification of olive oils according to geographical origin by using 1H NMR fingerprinting combined with multivariate analysis, Food Chem. 130 (2012) 177–183. doi:10.1016/j.foodchem.2011.06.045.

[40] F.J. Lara-ortega, M. Beneito-cambra, J. Robles-molina, J.F. García-reyes, Direct olive oil analysis by mass spectrometry : A comparison of different ambient ionization methods, Talanta. 180 (2018) 168–175. doi:10.1016/j.talanta.2017.12.027.

[41] M. Farré, Y. Picó, D. Barceló, Direct analysis in real-time high-resolution mass spectrometry as a valuable tool for polyphenols profiling in olive oil, Anal. Methods. 11 (2019) 472–482. doi:10.1039/C8AY01865K.

[42] L.-G. MJ, H.-M. JM, R.-R. G, S.-A. EF, Prediction of the genetic variety of Spanish extra virgin olive oils using fatty acid and phenolic compound profiles established by direct infusion mass spectrometry, Food Chem. 108 (2008) 1142–1148. doi:10.1016/j.foodchem.2007.11.065.

[43] A. Angelis, L. Antoniadi, P. Stathopoulos, M. Halabalaki, L.A. Skaltsounis, Oleocanthalic and Oleaceinic acids : New compounds from Extra Virgin Olive Oil (EVOO), Phytochem. Lett. 26 (2018) 190–194. doi:10.1016/j.phytol.2018.06.020.

[44] M. Suárez, M. Romero, A. Macià, R.M. Valls, S. Fernández, R. Solà, M. Motilva, Improved method for identifying and quantifying olive oil phenolic compounds and their metabolites in human plasma by microelution solid-phase extraction plate and liquid chromatography – tandem mass spectrometry, J. Chromatogr. B. 877 (2009) 4097–4106. doi:10.1016/j.jchromb.2009.10.025.

[45] International Ollive Council, Market Newsletter, (2016) 1–8.

[46] M. Tsimidou, R. Macrae, I. Wilson, Authentication of virgin olive oils using principal component analysis of triglyceride and fatty acid profiles: Part 1—Classification of greek olive oils, Food Chem. 25 (1987) 227–239. doi:http://dx.doi.org/10.1016/0308-8146(87)90148-8.

[47] A. PENELOPE FRONIMAKI, APOSTOLOS SPYROS, STELLA CHRISTOPHORIDOU, P. DAIS, Determination of the Diglyceride Content in Greek Virgin Olive Oils and Some Commercial Olive Oils by Employing 31 P NMR Spectroscopy, J. Agric. Food Chem. 50 (2002) 2207–2213. doi:10.1021/jf011380q.

[48] P. V. Petrakis, A. Agiomyrgianaki, S. Christophoridou, A. Spyros, P. Dais, Geographical characterization of Greek virgin olive oils (cv. Koroneiki) using 1H and 31P NMR fingerprinting with canonical discriminant analysis and classification binary trees, J. Agric. Food Chem. 56 (2008) 3200–3207.

[49] F. Longobardi, A. Ventrella, G. Casiello, D. Sacco, M. Tasioula-margari, A.K. Kiritsakis,

Characterisation of the geographical origin of Western Greek virgin olive oils based on instrumental and multivariate statistical analysis, Food Chem. 133 (2012) 169–175. doi:10.1016/j.foodchem.2011.09.130.

[50] I. Karabagias, C. Michos, A. Badeka, S. Kontakos, I. Stratis, M.G. Kontominas, Classification of Western Greek virgin olive oils according to geographical origin based on chromatographic, spectroscopic, conventional and chemometric analyses, Food Res. Int. 54 (2013) 1950–1958.

[51] E. Stefanoudaki, F. Kotsifaki, A. Koutsaftakis, The potential of HPLC triglyceride profiles for the classification of Cretan olive oils, Food Chem. 60 (1997) 425–432.

[52] E. Stefanoudaki, F. Kotsifaki, A. Koutsaftakis, Classification of Virgin Olive Oils of the Two Major Cretan Cultivars Based on Their Fatty Acid Composition, J. Am. Oil Chem. Soc. 76 (1999) 623–626.

[53] N.P. Kalogiouri, R. Aalizadeh, N.S. Thomaidis, Application of an advanced and wide scope non-target screening work fl ow with LC-ESI-QTOF-MS and chemometrics for the classi fi cation of the Greek olive oil varieties, Food Chem. 256 (2018) 53–61. doi:10.1016/j.foodchem.2018.02.101.

[54] E. Anastasopoulos, N. Kalogeropoulos, A.C. Kaliora, A. Kountouri, N.K. Andrikopoulos, The influence of ripening and crop year on quality indices , polyphenols , terpenic acids , squalene , fatty acid profile , and sterols in virgin olive oil (Koroneiki cv .) produced by organic versus non-organic cultivation method, Int. J. Food Sci. Technol. 46 (2011) 170–178. doi:10.1111/j.1365-2621.2010.02485.x.

[55] N.P. Kalogiouri, R. Aalizadeh, N.S. Thomaidis, Investigating the organic and conventional production type of olive oil with target and suspect screening by LC-QTOF-MS , a novel semi-quantification method using chemical similarity and advanced chemometrics, Anal. Bioanal. Chem. 409 (2017) 5413–5426. doi:10.1007/s00216-017-0395-6.

[56] N. Kalogeropoulos, A.C. Kaliora, A. Artemiou, I. Giogios, Composition , volatile pro fi les and functional properties of virgin olive oils produced by two-phase vs three-phase centrifugal decanters, LWT - Food Sci. Technol. 58 (2014) 272–279. doi:10.1016/j.lwt.2014.02.052.

[57] A. Rosati, C. Cafiero, A. Paoletti, B. Alfei, S. Caporali, L. Casciani, M. Valentini, Effect of agronomical practices on carpology , fruit and oil composition , and oil sensory properties , in olive (Olea europaea L .), FOOD Chem. 159 (2014) 236–243. doi:10.1016/j.foodchem.2014.03.014.

[58] M. Servili, A. Taticchi, S. Esposto, B. Sordini, S. Urbani, Technological Aspects of Olive Oil Production, in: Olive Germplasm- Olive Cultiv. Table Olive Olive Oil Ind. Italy, 2012. doi:10.5772/52141.

[59] T. Nikou, V. Liaki, P. Stathopoulos, A.D. Sklirou, N. Eleni, T. Jakschitz, G. Bonn, I.P. Trougakos, M. Halabalaki, L.A. Skaltsounis, Comparison survey of EVOO polyphenols and exploration of healthy agingpromoting properties of oleocanthal and oleacein, Food Chem. Toxicol. (2019). doi:10.1016/j.fct.2019.01.016.

[60] P. Inglese, F. Famiani, F. Galvano, M. Servili, S. Esposto, S. Urbani, Factors Affecting Extra-Virgin Olive Oil Composition, in: Hortic. Rev. (Am. Soc. Hortic. Sci)., 2011: pp. 83–147. doi:10.1002/9780470872376.ch3.

[61] International Olive Council, Determination of Biophenols in Olive Oils By Hplc, Int. Olive Counc. 29 (2009) 1–8.

[62] J. Impellizzeri, J. Lin, A Simple High-Performance Liquid Chromatography Method for the Determination of Throat-Burning Oleocanthal with Probated Antiinflammatory Activity in Extra Virgin Olive Oils, (2006) 3204–3208.

[63] A.I.C. on H. for Technical, R. Of, R. Pharmaceuticals, for human Use, Validation of Analytical Procedures: Text and Mthodology Q2 (R1), (2005).

[64] D. of H. and H.S. Food and Drug Administration, Bioanalytical Method Validation Guidance for Industry, (2013).

[65] E.M.A. (EMA), Concept/Recommendations Paper on the Need for a Guideline on the Validation of Bioanalytical Methods., (2008).

[66] S. Charoenprasert, A. Mitchell, Factors In fl uencing Phenolic Compounds in Table Olives (Olea europaea), J Agric Food Chem. 60 (2012) 7081–7095. doi:10.1021/jf3017699.

[67] G. Beaufoy, The Environmental Impact of Olive oil Production in the European Union: Practical Options for Improving the Environmental Impact, (2001) 1–73. http://ec.europa.eu/environment/agriculture/pdf/oliveoil.pdf.

[68] S. Misner, T.A. Florian, Organically Grown Foods versus Non-Organically Grown Foods, Univ. Arizona Coop. Ext. (2013) 1–3.

[69] N. Kalogeropoulos, M.Z. Tsimidou, Antioxidants in Greek Virgin Olive Oils, 3 (2014) 387–413. doi:10.3390/antiox3020387.

[70] F. Visioli, C. Galli, Olive Oil Phenols and Their Potential Effects on Human Health, J. Agric. Food Chem. 46 (1998) 4292–4296.

[71] M. Servili, A. Taticchi, S. Esposto, B. Sordini, S. Urbani, Technological Aspects of Olive Oil Production, in: Olive Germplasm – Olive Cultiv. Table Olive Olive Oil Ind. Italy, IntechOpen, 2012: pp. 151–172. doi:10.5772/52141.

[72] C. Petrakis, Olive Oil Extraction, in: D. Boskou (Ed.), Olive Oil Chemitry Technol., Second, 2006.

[73] F. Gutiérrez, T. Arnaud, M. a. Albi, Influence of ecological cultivation on virgin olive oil quality, J. Am. Oil Chem. Soc. 76 (1999) 617–621.

[74] A. Angelis, M. Hamzaoui, N. Aligiannis, T. Nikou, D. Michailidis, P. Gerolimatos, A. Termentzi, J. Hubert, M. Halabalaki, J.-H. Renault, A.-L. Skaltsounis, An integrated process for the recovery of high added-value compounds from olive oil using solid support free liquid-liquid extraction and chromatography techniques, J. Chromatogr. A. 1491 (2017). doi:10.1016/j.chroma.2017.02.046.

[75] S. Cicerale, L.J. Lucas, R.S.J. Keast, Antimicrobial, antioxidant and anti-inflammatory

phenolic activities in extra virgin olive oil., Curr. Opin. Biotechnol. 23 (2012) 129–135. doi:10.1016/j.copbio.2011.09.006.

[76] T. Nikou, V. Liaki, P. Stathopoulos, A.D. Sklirou, E.N. Tsakiri, T. Jakschitz, G. Bonn, I.P. Trougakos, M. Halabalaki, L.A. Skaltsounis, Comparison survey of EVOO polyphenols and exploration of healthy aging-promoting properties of oleocanthal and oleacein, Food Chem. Toxicol. 125 (2019). doi:10.1016/j.fct.2019.01.016.

[77] A. Bendini, L. Cerretani, A.M. Carrasco-Pancorbo, Alegria Gómez-Caravaca, A. Segura-Carretero, A. Fernández-Gutiérrez, G. Lercker, Phenolic Molecules in Virgin Olive Oils: a Survey of Their Sensory Properties, Health Effects, Antioxidant Activity and Analytical Methods. An Overview of the Last Decade, Molecules. 12 (2007) 1679–1719.

[78] S. Cicerale, L.J. Lucas, R.S.J. Keast, Oleocanthal : A Naturally Occurring Anti-Inflammatory Agent in Virgin Olive Oil, (2011).

[79] E. Karkoula, A. Skantzari, E. Melliou, P. Magiatis, Direct measurement of oleocanthal and oleacein levels in olive oil by quantitative (1)H NMR. Establishment of a new index for the characterization of extra virgin olive oils., J. Agric. Food Chem. 60 (2012) 11696–703.

[80] S. Christophoridou, P. Dais, L.-H. Tseng, M. Spraul, Separation and identification of phenolic compounds in olive oil by coupling high-performance liquid chromatography with postcolumn solid-phase extraction to nuclear magnetic resonance spectroscopy (LC-SPE-NMR)., J. Agric. Food Chem. 53 (2005) 4667–4679. doi:10.1021/jf040466r.

[81] V. Ninni, A statistical approach to the biosynthetic route of fatty acids in olive oil : cross-sectional and time series analyses, 2121 (1999) 2113–2121.

[82] S.E. Chatziantoniou, D.J. Triantafillou, P.D. Karayannakidis, E. Diamantopoulos, Traceability monitoring of Greek extra virgin olive oil by Differential Scanning Calorimetry, Thermochim. Acta. 576 (2014) 9–17. doi:10.1016/j.tca.2013.11.014.

[83] R. García-Villalba, A. Carrasco-Pancorbo, C. Oliveras-Ferraros, A. Vázquez-Martín, J.A. Menéndez, A. Segura-Carretero, A. Fernández-Gutiérrez, Characterization and quantification of phenolic compounds of extra-virgin olive oils with anticancer properties by a rapid and resolutive LC-ESI-TOF MS method, J. Pharm. Biomed. Anal. 51 (2010) 416–429. doi:10.1016/j.jpba.2009.06.021.

[84] F. Gutierrez, B. Jımenez, A. Ruız, M.A. Albi, Effect of Olive Ripeness on the Oxidative Stability of Virgin Olive Oil Extracted from the Varieties Picual and Hojiblanca and on the Different Components Involved, J. Agric. Food Chem. (1999) 121–127.

[85] M.L. Hernández, M.N. Padilla, M.D. Sicardo, M. Mancha, J.M. Martínez-rivas, Effect of different environmental stresses on the expression of oleate desaturase genes and fatty acid composition in olive fruit, Phytochemistry. 72 (2011) 178–187. doi:10.1016/j.phytochem.2010.11.026.

[86] S. Kesen, A. Amanpour, A.S. Sonmezdag, Effects of Cultivar , Maturity Index and Growing Region on Fatty Acid Composition of Olive Oils, Eurasian J. FOOD Sci. Technol. (n.d.) 18–27.

[87] B.D.P. Rondanini, D.N. Castro, P.S. Searles, M.C. Rousseaux, Fatty acid profiles of varietal virgin olive oils (Olea europaea L .) from mature orchards in warm arid valleys of Northwestern Argentina (La Rioja), Grasas Y Aceites. 62 (2011) 399–409.

[88] F.W. and Q.W. Li Yang, Kui-Shan Wen, Xiao Ruan, Ying-Xian Zhao, Response of Plant Secondary Metabolites to Environmental Factors, Molecules. 23 (2018) 1–26. doi:10.3390/molecules23040762.

[89] D.L. García-gonzález, R. Aparicio-ruiz, M.T. Morales, Chemical characterization of organic and non-organic virgin olive oils, OCL - Oilseeds Fats, Crop. Lipids. 21 (2014) D506.

[90] P. Ninfali, M. Bacchiocca, E. Biagiotti, S. Esposto, M. Servili, A. Rosati, G. Montedoro, A 3-year Study on Quality , Nutritional and Organoleptic Evaluation of Organic and Conventional Extra-Virgin Olive Oils, J. Am. Oil Chem. Soc. 85 (2008) 151–158. doi:10.1007/s11746-007-1171-0.

[91] M.J. Tovar, M.P. Romero, S. Alegre, J. Girona, M.J. Motilva, Composition and organoleptic characteristics of oil from Arbequina olive (Olea europaea L) trees under deficit irrigation, J. Sci. Food Agric. 82 (2002) 1755–1763. doi:10.1002/jsfa.1246.

[92] J.-R. Morelló, M.-P. Romero, T. Ramo, M.-J. Motilva, Evaluation of L -phenylalanine ammonia-lyase activity and phenolic profile in olive drupe (Olea europaea L .) from fruit setting period to harvesting time, Plant Sci. 168 (2005) 65–72. doi:10.1016/j.plantsci.2004.07.013.

Appendix

Table A 1: *Metadata of sample collection presenting geographical origin, olive tree variety, type of cultivation and production procedure methodology.*

Code	Origin	Variety	Type of cultivation	Production procedure
OLE410	Heraklion	Koroneiki	Integrated	Three phase
OLE411	Heraklion	Koroneiki	Integrated	Three phase
OLE412	Lasithi	Koroneiki	Organic	Two phase
OLE413	Lasithi	Koroneiki	Organic	Two phase
OLE416	Heraklion	Koroneiki	Integrated	Three phase
OLE417	Lasithi	Koroneiki	Integrated	Two phase
OLE418	Heraklion	Koroneiki	Conventional	Three phase
OLE419	Lasithi	Koroneiki	Organic	Two phase
OLE420	Lasithi	Koroneiki	Organic	Two phase
OLE421	Heraklion	Koroneiki	Organic	Three phase
OLE422	Heraklion	Koroneiki	Organic	Three phase
OLE423	Kefalonia	Koroneiki-Kefalonia	Conventional	Two phase
OLE424	Kefalonia	Koroneiki-Kefalonia	Conventional	Two phase
OLE425	Kefalonia	Koroneiki-Kefalonia	Conventional	Two phase
OLE426	Kefalonia	Koroneiki-Kefalonia	Conventional	Two phase
OLE427	Kefalonia	Koroneiki-Kefalonia	Conventional	Two phase
OLE428	Kefalonia	Koroneiki-Kefalonia	Conventional	Two phase
OLE429	Kefalonia	Koroneiki-Kefalonia	Conventional	Two phase
OLE430	Kefalonia	Koroneiki-Kefalonia	Conventional	Two phase
OLE431	Kefalonia	Koroneiki-Kefalonia	Conventional	Two phase
OLE432	Kefalonia	Koroneiki-Kefalonia	Conventional	Two phase
OLE433	Kefalonia	Koroneiki-Kefalonia	Conventional	Two phase
OLE434	Kefalonia	Koroneiki-Kefalonia	Conventional	Two phase
OLE435	Kefalonia	Koroneiki-Kefalonia	Conventional	Two phase
OLE436	Kefalonia	Koroneiki-Kefalonia	Conventional	Two phase
OLE437	Kefalonia	Koroneiki-Kefalonia	Conventional	Two phase
OLE438	Kefalonia	Koroneiki-Kefalonia	Conventional	Two phase
OLE439	Kefalonia	Koroneiki-Kefalonia	Conventional	Two phase
OLE440	Kefalonia	Koroneiki-Kefalonia	Conventional	Two phase
OLE441	Ithaki	Koroneiki- Thiaki	Organic	Two phase
OLE442	Ithaki	Koroneiki- Thiaki	Organic	Two phase
OLE443	Ithaki	Koroneiki- Thiaki	Organic	Two phase
OLE444	Ithaki	Koroneiki- Thiaki	Conventional	Two phase
OLE445	Ithaki	Koroneiki- Thiaki	Organic	Two phase
OLE446	Ithaki	Koroneiki- Thiaki	Organic	Two phase

OLE447	Ithaki	Koroneiki- Thiaki	Organic	Two phase
OLE448	Ithaki	Koroneiki- Thiaki	Organic	Two phase
OLE449	Ithaki	Koroneiki- Thiaki	Organic	Two phase
OLE450	Ithaki	Koroneiki- Thiaki	Organic	Two phase
OLE451	Lakonia	Koroneiki	Organic	Three phase
OLE452	Lakonia	Koroneiki	Organic	Three phase
OLE453	Lakonia	Koroneiki	Conventional	Three phase
OLE454	Lakonia	Koroneiki	Conventional	Three phase
OLE455	Lakonia	Koroneiki	Conventional	Three phase
OLE456	Lakonia	Koroneiki	Conventional	Three phase
OLE457	Lakonia	Koroneiki	Conventional	Three phase
OLE458	Lakonia	Koroneiki	Conventional	Three phase
OLE459	Lakonia	Koroneiki	Conventional	Three phase
OLE460	Lakonia	Koroneiki	Conventional	Three phase
OLE464	Heraklion	Koroneiki	Integrated	Three phase
OLE465	Lasithi	Koroneiki	Integrated	Three phase
OLE466	Lasithi	Koroneiki	Integrated	Three phase
OLE467	Lasithi	Koroneiki	Organic	Two phase
OLE468	Lasithi	Koroneiki	Integrated	Two phase
OLE469	Lasithi	Koroneiki	Integrated	Two phase
OLE470	Lasithi	Koroneiki	Organic	Two phase
OLE471	Lasithi	Koroneiki	Integrated	Three phase
OLE472	Lasithi	Koroneiki	Integrated	Two phase
OLE473	Lasithi	Koroneiki	Integrated	Two phase
OLE474	Lasithi	Koroneiki	Integrated	Two phase
OLE475	Lasithi	Koroneiki	Integrated	Two phase
OLE476	Heraklion	Koroneiki	Integrated	Two phase
OLE477	Lasithi	Koroneiki	Integrated	Three phase
OLE478	Lasithi	Koroneiki	Integrated	Three phase
OLE479	Lasithi	Koroneiki	Integrated	Three phase
OLE480	Heraklion	Koroneiki	Integrated	Three phase
OLE487	Messinia	Koroneiki	Conventional	Two phase
OLE488	Messinia	Koroneiki	Conventional	Two phase
OLE489	Messinia	Koroneiki	Organic	Two phase
OLE490	Messinia	Koroneiki	Organic	Two phase
OLE491	Messinia	Koroneiki	Conventional	Two phase
OLE492	Messinia	Koroneiki	Conventional	Three phase
OLE493	Messinia	Koroneiki	Conventional	Three phase
OLE494	Messinia	Koroneiki	Conventional	Two phase
OLE495	Messinia	Koroneiki	Organic	Two phase
OLE496	Messinia	Koroneiki	Conventional	Three phase

OLE497	Messinia	Koroneiki	Conventional	Three phase
OLE498	Messinia	Koroneiki	Organic	Two phase
OLE499	Messinia	Koroneiki	Conventional	Two phase
OLE500	Messinia	Koroneiki	Conventional	Two phase
OLE501	Messinia	Koroneiki	Conventional	Two phase
OLE502	Messinia	Koroneiki	Organic	Two phase
OLE503	Messinia	Koroneiki	Conventional	Two phase
OLE504	Messinia	Koroneiki	Conventional	Two phase
OLE505	Messinia	Koroneiki	Conventional	Two phase
OLE506	Messinia	Koroneiki	Conventional	Two phase
OLE509	Heraklion	Koroneiki	Conventional	Three phase
OLE510	Heraklion	Koroneiki	Conventional	Three phase
OLE511	Lasithi	Koroneiki	Integrated	Three phase
OLE512	Lasithi	Koroneiki	Integrated	Three phase
OLE513	Lasithi	Koroneiki	Conventional	Two phase
OLE514	Lasithi	Koroneiki	Conventional	Three phase
OLE515	Lasithi	Koroneiki	Organic	Two phase
OLE516	Heraklion	Koroneiki	Organic	Two phase
OLE517	Lasithi	Koroneiki	Conventional	Three phase
OLE518	Lasithi	Koroneiki	Conventional	Two phase
OLE519	Lasithi	Koroneiki	Conventional	Two phase
OLE520	Lasithi	Koroneiki	Conventional	Two phase
OLE521	Messinia	Koroneiki	Conventional	Traditional
OLE522	Messinia	Koroneiki	Conventional	Traditional
OLE523	Messinia	Koroneiki	Conventional	Traditional
OLE524	Messinia	Koroneiki	Conventional	Traditional
OLE534	Lasithi	Koroneiki	Conventional	Two phase
OLE535	Lasithi	Koroneiki	Organic	Two phase
OLE536	Lasithi	Koroneiki	Conventional	Three phase
OLE543	Messinia	Koroneiki	Conventional	Three phase
OLE544	Heraklion	Koroneiki	Conventional	Three phase
OLE545	Lasithi	Koroneiki	Conventional	Two phase
OLE546	Lasithi	Koroneiki	Conventional	Three phase
OLE547	Lasithi	Koroneiki	Organic-non certified	Two phase
OLE548	Lasithi	Koroneiki	Conventional	Two phase
OLE549	Lasithi	Koroneiki	Organic	Three phase
OLE550	Lasithi	Koroneiki	Organic	Two phase
OLE555	Messinia	Koroneiki	Conventional	Three phase
OLE556	Messinia	Koroneiki	Conventional	Three phase
OLE557	Lakonia	Koroneiki	Organic	Three phase
OLE558	Lakonia	Koroneiki	Organic	Three phase

OLE559	Lakonia	Koroneiki	Organic	Three phase
OLE560	Lakonia	Koroneiki	Organic	Three phase
OLE561	Lakonia	Koroneiki	Organic	Three phase
OLE569	Lakonia	Koroneiki	Organic-non certified	Two phase
OLE570	Lakonia	Koroneiki	Organic-non certified	Two phase
OLE571	Lakonia	Koroneiki	Organic-non certified	Two phase
OLE572	Lakonia	Koroneiki	Organic-non certified	Two phase
OLE573	Lakonia	Koroneiki	Organic-non certified	Two phase
OLE574	Lakonia	Koroneiki	Organic-non certified	Two phase
OLE575	Lakonia	Koroneiki	Organic-non certified	Two phase
OLE576	Lakonia	Koroneiki	Organic-non certified	Two phase
OLE577	Lakonia	Koroneiki	Organic-non certified	Two phase
OLE578	Lakonia	Koroneiki	Organic-non certified	Two phase
OLE579	Lakonia	Koroneiki	Organic-non certified	Two phase
OLE580	Lakonia	Koroneiki	Organic-non certified	Two phase
OLE581	Lakonia	Koroneiki	Organic-non certified	Two phase
OLE582	Lakonia	Koroneiki	Organic-non certified	Two phase
OLE589	Heraklion	Koroneiki	Organic	Three phase
OLE590	Heraklion	Koroneiki	Organic	Three phase
OLE591	Heraklion	Koroneiki	Organic	Three phase
OLE592	Heraklion	Koroneiki	Organic	Three phase
OLE593	Heraklion	Koroneiki	Conventional	Three phase
OLE594	Heraklion	Koroneiki	Conventional	Three phase
OLE595	Heraklion	Koroneiki	Organic	Three phase
OLE596	Heraklion	Koroneiki	Organic	Three phase
OLE597	Heraklion	Koroneiki	Conventional	Three phase
OLE598	Heraklion	Koroneiki	Conventional	Three phase
OLE599	Heraklion	Koroneiki	Conventional	Three phase
OLE600	Heraklion	Koroneiki	Conventional	Three phase
OLE601	Heraklion	Koroneiki	Conventional	Three phase
OLE602	Heraklion	Koroneiki	Conventional	Three phase
OLE607	Heraklion	Koroneiki	Conventional	Three phase
OLE608	Heraklion	Koroneiki	Conventional	Three phase
OLE609	Heraklion	Koroneiki	Conventional	Three phase
OLE612	Heraklion	Koroneiki	Integrated	Three phase
OLE613	Heraklion	Koroneiki	Conventional	Three phase
OLE614	Heraklion	Koroneiki	Conventional	Three phase
OLE615	Heraklion	Koroneiki	Conventional	Three phase
OLE616	Heraklion	Koroneiki	Conventional	Three phase
OLE617	Heraklion	Koroneiki	Conventional	Three phase
OLE618	Heraklion	Koroneiki	Conventional	Three phase

OLE635	Kefalonia	Koroneiki-Kefalonia	Organic-non certified	Two phase
OLE636	Kefalonia	Koroneiki-Kefalonia	Organic-non certified	Two phase
OLE637	Kefalonia	Koroneiki-Kefalonia	Organic-non certified	Two phase
OLE638	Kefalonia	Koroneiki-Kefalonia	Organic-non certified	Two phase
OLE639	Kefalonia	Koroneiki-Kefalonia	Organic-non certified	Two phase
OLE640	Kefalonia	Koroneiki-Kefalonia	Organic-non certified	Two phase
OLE647	Heraklion	Koroneiki	Conventional	Three phase
OLE648	Heraklion	Koroneiki	Conventional	Three phase
OLE649	Heraklion	Koroneiki	Conventional	Three phase
OLE650	Heraklion	Koroneiki	Conventional	Three phase
OLE651	Heraklion	Koroneiki	Conventional	Three phase
OLE652	Heraklion	Koroneiki	Conventional	Two phase
OLE653	Heraklion	Koroneiki	Conventional	Three phase
OLE654	Heraklion	Koroneiki	Conventional	Three phase
OLE655	Heraklion	Koroneiki	Conventional	Three phase
OLE656	Lasithi	Koroneiki	Integrated	Three phase
OLE657	Heraklion	Koroneiki	Conventional	Three phase
OLE677	Lakonia	Koroneiki	Integrated	Two phase
OLE678	Lakonia	Koroneiki	Conventional	Two phase
OLE679	Lakonia	Koroneiki	Integrated	Two phase
OLE680	Lakonia	Koroneiki	Integrated	Two phase
OLE681	Lakonia	Koroneiki	Integrated	Two phase
OLE682	Lakonia	Koroneiki	Integrated	Two phase
OLE683	Lakonia	Koroneiki	Integrated	Two phase
OLE684	Lakonia	Koroneiki	Integrated	Two phase
OLE685	Lakonia	Koroneiki	Integrated	Two phase
OLE687	Lakonia	Koroneiki	Integrated	Two phase
OLE688	Lakonia	Koroneiki	Integrated	Two phase
OLE689	Lakonia	Koroneiki	Conventional	Two phase
OLE690	Lakonia	Koroneiki	Integrated	Two phase
OLE691	Lakonia	Koroneiki	Conventional	Two phase
OLE692	Lakonia	Koroneiki	Conventional	Two phase
OLE693	Lakonia	Koroneiki	Integrated	Two phase
OLE694	Lakonia	Koroneiki	Integrated	Two phase
OLE695	Lakonia	Koroneiki	Integrated	Two phase
OLE696	Lakonia	Koroneiki	Organic	Two phase
OLE697	Lakonia	Koroneiki	Conventional	Two phase
OLE699	Lakonia	Koroneiki	Conventional	Two phase
OLE700	Lakonia	Koroneiki	Integrated	Two phase
OLE702	Messinia	Koroneiki	Organic	Two phase
OLE703	Messinia	Koroneiki	Organic	Two phase

OLE704	Messinia	Koroneiki	Organic	Two phase
OLE705	Messinia	Koroneiki	Organic	Two phase
OLE706	Messinia	Koroneiki	Conventional	Three phase
OLE707	Messinia	Koroneiki	Conventional	Three phase
OLE708	Messinia	Koroneiki	Conventional	Three phase
OLE709	Messinia	Koroneiki	Conventional	Three phase
OLE710	Messinia	Koroneiki	Conventional	Three phase
OLE711	Messinia	Koroneiki	Conventional	Three phase
OLE712	Messinia	Koroneiki	Conventional	Three phase

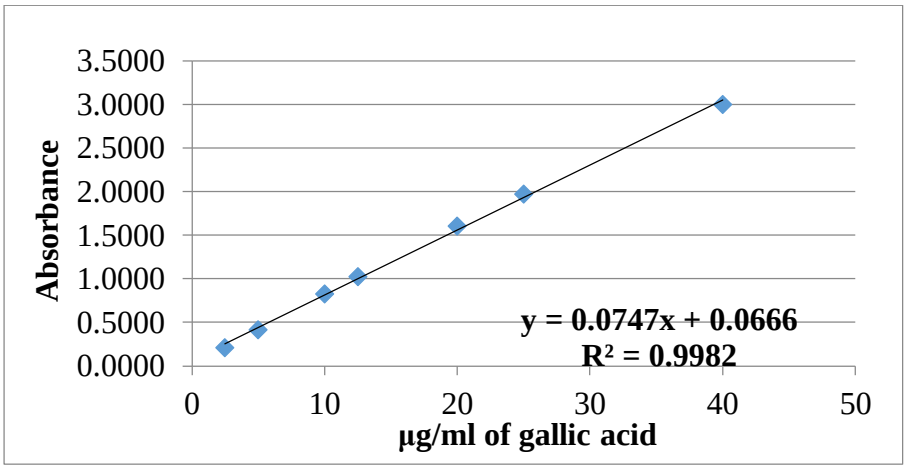

Figure A 1: *Standard calibration curve of gallic acid. The horizontal scale represents the used concentrations of gallic acid in µg/ml and the vertical scale the corresponding absorbances.*

Table A 2: *HPLC-DAD , TPC and TPF measurements. Results of hydroxytyrosol (HT), tyrosol (T), oleacein (OLEA) and oleocanthal (OLEO) are calculated in mg/Kg of olive oil (OO). TPC measurements are performed via Folin-Ciocalteu assay and expressed in mg GAE/Kg OO; values symbolized with ND are not determined and are out of the calibration curves. TPF represents the extraction yield and expressed in g/Kg OO.*

Code	HT (mg/Kg OO)	T (mg/Kg OO)	OLEA (mg/Kg OO)	OLEO (mg/Kg OO)	Total (mg/Kg OO)	TPC (mg GAE/Kg OO)	TPF (g/Kg OO)
OLE410	4.2	6.5	104	181	295	272	0.67
OLE411	2.5	4.4	69	105	181	380	1.02
OLE412	13.3	11.9	154	120	299	375	0.81
OLE413	5.0	4.9	112	118	240	317	0.86
OLE416	3.9	3.6	125	121	253	322	1.79
OLE417	2.4	3.8	79	123	208	172	1.50
OLE418	2.8	3.3	130	144	279	276	1.42
OLE419	8.7	5.1	157	102	272	470	1.89
OLE420	11.8	6.8	60	29	107	607	2.08
OLE421	1.7	2.4	25	39	68	194	1.53
OLE422	4.6	4.0	17	23	49	167	1.26
OLE423	6.9	4.8	20	22	54	190	0.97
OLE424	1.0	3.0	0	17	21	64	0.92
OLE425	8.2	6.3	0	0	15	160	1.62
OLE426	0.8	1.8	0	0	3	116	1.18
OLE427	2.2	2.4	10	4	18	194	1.22
OLE428	7.5	6.8	28	40	82	175	1.23
OLE429	1.5	1.3	22	20	44	126	1.06
OLE430	2.8	1.9	80	70	154	198	1.21
OLE431	3.0	3.2	65	60	132	275	2.17
OLE432	3.0	2.3	63	51	119	272	1.48
OLE433	2.2	3.5	28	44	78	146	1.19

OLE434	4.4	5.1	96	94	199	277	1.15
OLE435	3.6	3.5	85	61	154	216	0.96
OLE436	4.9	3.9	69	82	160	141	0.78
OLE437	10.8	7.8	104	152	274	266	1.60
OLE438	1.4	2.4	27	40	71	82	1.19
OLE439	18.5	58.0	0	0	77	129	1.26
OLE440	3.8	4.5	54	84	146	169	2.00
OLE441	5.9	8.2	119	136	269	239	2.45
OLE442	9.7	11.0	33	74	127	172	1.03
OLE443	13.5	13.0	111	158	295	259	1.33
OLE444	5.7	5.3	63	111	186	199	2.09
OLE445	13.2	13.4	90	154	270	276	1.68
OLE446	0.8	3.1	0	0	4	88	3.01
OLE447	8.2	11.5	61	134	214	191	1.58
OLE448	5.3	5.0	93	160	263	224	2.28
OLE449	3.1	3.7	35	71	112	139	2.31
OLE450	5.3	6.0	86	145	242	291	1.53
OLE451	2.0	2.5	27	62	93	200	1.23
OLE452	1.8	1.7	20	15	38	146	1.15
OLE453	1.0	1.4	0	0	2	133	0.98
OLE454	0.6	0.9	0	0	1	88	0.87
OLE455	0.5	1.0	0	0	2	73	0.86
OLE456	3.2	3.6	0	0	7	107	0.58
OLE457	1.8	1.8	16	0	19	167	0.80
OLE458	1.0	0.9	0	0	2	111	0.54
OLE459	3.1	3.1	26	0	32	ND	0.89
OLE460	1.3	1.4	17	0	19	137	1.12
OLE464	4.7	2.0	36	43	86	141	1.10

OLE465	7.6	2.6	108	86	204	263	1.48
OLE466	5.1	3.0	95	71	174	239	1.89
OLE467	6.3	3.5	83	64	157	272	1.53
OLE468	1.8	1.4	31	49	83	144	1.36
OLE469	4.5	2.5	64	70	141	190	1.39
OLE470	7.1	4.6	54	42	108	239	1.31
OLE471	4.7	2.6	54	67	129	204	1.08
OLE472	6.1	4.2	64	31	106	350	1.56
OLE473	7.2	4.8	36	27	74	186	1.48
OLE474	3.3	2.8	28	27	61	170	1.30
OLE475	6.6	3.5	37	35	82	163	1.45
OLE476	7.1	5.2	41	34	87	174	1.45
OLE477	6.7	4.1	63	81	155	197	1.51
OLE478	4.5	6.7	34	56	102	174	1.16
OLE479	2.2	4.5	16	33	55	141	0.63
OLE480	8.4	14.1	21	26	69	113	0.66
OLE487	9.2	13.9	59	74	156	243	0.97
OLE488	9.6	8.8	32	32	82	227	0.78
OLE489	21.2	32.1	24	42	120	178	0.82
OLE490	5.0	3.6	38	58	105	172	0.57
OLE491	16.3	8.9	85	51	161	234	0.86
OLE492	29.9	16.7	0	0	47	168	0.75
OLE493	16.5	11.5	38	37	103	186	0.74
OLE494	8.1	0.4	40	44	93	308	1.03
OLE495	2.7	6.3	17	32	58	115	0.75
OLE496	12.4	9.8	22	39	83	170	0.89
OLE497	8.2	5.2	35	27	75	140	0.94

OLE498	6.9	6.7	56	63	132	231	0.95
OLE499	6.3	9.2	12	16	43	164	0.80
OLE500	5.7	5.3	50	54	115	192	1.03
OLE501	5.6	4.9	42	48	101	175	0.89
OLE502	4.3	4.8	54	55	118	203	0.95
OLE503	8.7	10.3	75	82	176	267	1.24
OLE504	2.6	4.7	0	12	19	113	0.89
OLE505	7.7	7.2	51	48	114	198	1.01
OLE506	6.3	6.5	27	33	72	200	0.93
OLE509	5.6	6.6	36	43	92	120	1.19
OLE510	6.2	5.3	61	26	99	216	1.20
OLE511	4.8	5.3	40	49	99	185	1.14
OLE512	4.5	9.4	10	14	38	76	0.90
OLE513	6.7	6.3	60	59	132	254	1.7
OLE514	3.9	4.7	33	46	87	144	1.03
OLE515	12.6	8.2	84	83	188	372	1.45
OLE516	8.7	10.9	68	94	182	280	1.69
OLE517	21.8	4.9	46	27	100	208	1.41
OLE518	2.1	56.3	0	0	0	130	1.40
OLE519	8.2	6.8	32	32	79	185	1.30
OLE520	9.1	6.2	0	0	15	192	1.41
OLE521	3.5	2.9	60	58	125	217	1.20
OLE522	5.6	5.9	14	36	62	111	1.33
OLE523	3.9	5.6	24	57	90	274	1.57
OLE524	18.6	7.3	32	27	85	295	1.31
OLE534	3.9	3.5	50	43	101	220	1.16
OLE535	16.6	9.2	56	45	127	273	1.40

OLE536	3.5	2.0	53	46	104	ND	1.65
OLE543	1.2	2.6	10	13	27	125	0.98
OLE544	3.0	7.0	32	61	102	229	1.42
OLE545	7.5	4.6	90	70	172	ND	1.83
OLE546	5.4	4.9	42	35	87	588	1.60
OLE547	8.0	7.2	90	123	229	312	1.52
OLE548	6.7	3.5	47	42	99	ND	1.48
OLE549	2.8	3.6	62	135	204	199	1.28
OLE550	6.5	6.3	53	91	157	221	1.35
OLE555	5.6	3.7	54	59	122	224	1.25
OLE556	4.3	4.2	33	42	83	192	1.40
OLE557	4.1	5.1	21	53	83	198	1.15
OLE558	3.0	3.3	0	21	27	172	0.98
OLE559	3.8	6.6	10	20	41	131	0.96
OLE560	2.6	4.5	14	29	50	119	1.15
OLE561	5.9	26.6	11	37	81	186	1.39
OLE569	2.7	6.4	19	61	88	174	1.04
OLE570	1.8	2.1	21	50	75	133	0.99
OLE571	5.9	5.1	30	67	107	216	1.21
OLE572	2.4	6.2	29	63	101	136	1.09
OLE573	2.4	5.3	6	65	79	112	1.02
OLE574	4.5	7.9	46	103	162	180	1.57
OLE575	2.4	7.7	18	78	106	136	1.24
OLE576	3.3	8.1	29	98	138	172	1.14
OLE577	1.8	6.6	14	71	94	95	1.07
OLE578	5.7	9.2	40	97	151	97	1.38
OLE579	5.2	9.9	30	98	143	242	1.20

OLE580	4.8	4.4	68	122	200	197	1.26
OLE581	3.7	3.6	56	86	149	202	1.23
OLE582	1.6	1.9	18	63	85	189	1.13
OLE589	4.1	4.2	48	85	142	138	1.29
OLE590	8.4	7.1	53	88	157	191	1.59
OLE591	9.7	7.3	31	37	85	189	1.63
OLE592	11.2	9.3	52	67	139	271	1.56
OLE593	2.6	2.5	13	28	46	94	1.35
OLE594	6.7	2.2	59	46	113	217	1.23
OLE595	6.5	3.6	36	48	95	156	1.36
OLE596	4.9	3.6	24	41	74	132	1.25
OLE597	5.2	4.2	26	37	72	219	1.25
OLE598	6.1	5.6	33	35	79	212	1.43
OLE599	5.6	5.3	36	39	86	168	1.53
OLE600	8.2	6.4	54	39	108	203	1.50
OLE601	7.6	5.0	63	45	121	240	1.40
OLE602	5.4	4.4	56	47	113	207	1.30
OLE607	5.1	3.1	41	79	128	145	0.99
OLE608	5.1	3.1	41	79	128	145	0.99
OLE609	8.7	4.7	77	71	161	233	1.21
OLE612	15.7	11.8	81	106	214	227	1.47
OLE613	11.4	9.4	75	123	220	223	1.45
OLE614	7.8	6.0	13	20	47	145	1.20
OLE615	3.3	1.7	57	99	161	147	1.19
OLE616	4.1	1.5	23	36	65	114	1.31
OLE617	1.9	1.6	24	65	93	111	1.31
OLE618	9.8	8.1	40	68	125	249	1.46

OLE635	7.2	8.0	103	109	227	230	1.39
OLE636	4.2	6.8	0	0	11	98	1.21
OLE637	5.5	6.0	58	72	141	239	1.23
OLE638	3.1	5.0	14	0	22	132	1.28
OLE639	4.1	5.6	13	0	23	113	1.37
OLE640	6.7	6.3	44	42	99	214	1.39
OLE647	19.5	10.9	13	19	62	196	0.92
OLE648	3.4	1.9	29	62	96	133	0.78
OLE649	4.1	2.2	27	53	87	133	0.89
OLE650	4.1	1.9	59	49	113	159	1.13
OLE651	2.2	1.1	32	39	75	141	0.74
OLE652	2.1	1.2	36	47	86	164	0.83
OLE653	4.5	2.2	60	63	130	269	1.14
OLE654	6.0	3.2	49	44	102	250	0.98
OLE655	3.0	1.7	60	49	113	ND	0.98
OLE656	3.7	1.4	97	52	154	269	1.08
OLE657	4.4	1.1	45	53	104	120	1.05
OLE677	21.3	47.4	0	0	69	218	1.02
OLE678	3.1	3.1	29	36	71	180	1.05
OLE679	5.1	7.0	0	38	50	191	1.71
OLE680	14.4	9.5	16	0	39	251	1.67
OLE681	2.7	3.3	4	41	51	172	0.97
OLE682	3.1	3.6	0	0	7	196	1.05
OLE683	6.8	6.3	92	58	163	368	1.98
OLE684	8.2	8.1	35	73	124	306	1.86
OLE685	9.7	8.8	49	56	123	367	1.95
OLE687	3.2	4.1	17	27	51	146	1.52

OLE688	2.1	2.5	51	80	135	165	1.67
OLE689	6.6	7.4	74	61	149	314	1.27
OLE690	5.6	7.1	29	57	98	197	1.09
OLE691	3.6	4.2	11	32	51	120	0.95
OLE692	3.3	6.1	14	16	39	146	0.93
OLE693	3.8	4.0	46	57	111	173	1.18
OLE694	4.2	5.0	12	0	21	179	1.17
OLE695	7.5	8.9	22	44	83	281	1.38
OLE696	5.7	5.3	28	36	76	220	1.15
OLE697	3.4	5.6	15	21	45	209	1.33
OLE699	5.8	7.8	25	48	87	198	1.24
OLE700	2.9	6.6	13	37	60	106	1.02
OLE702	21.2	13.1	50	47	131	247	1.32
OLE703	19.1	20.9	0	0	40	181	1.04
OLE704	3.3	6.9	0	0	10	63	0.85
OLE705	8.0	6.4	21	29	64	161	1.06
OLE706	10.2	8.2	23	33	75	124	1.33
OLE707	13.4	5.1	24	22	65	148	1.53
OLE708	10.0	5.9	25	27	68	134	1.36
OLE709	13.4	6.6	55	50	125	235	1.59
OLE710	5.0	4.1	20	33	62	127	1.24
OLE711	6.4	4.6	29	44	84	112	1.20
OLE712	10.9	3.8	37	42	94	179	1.27

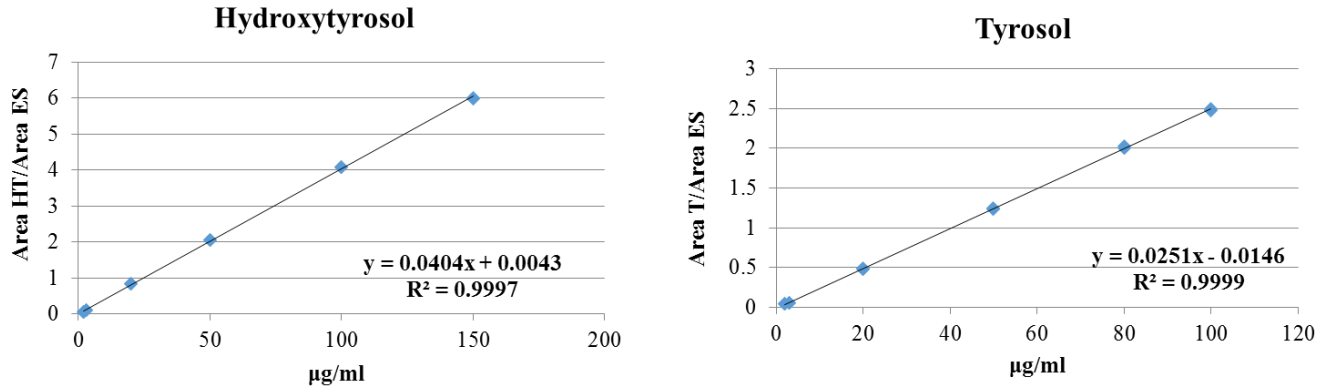

Figure A 2: *Standard calibration curves of hydroxytyrosol (HT) (left graph) and tyrosol (T) (right graph). The horizontal scale represents the concentration of calibration points in µg/ml and the vertical scale the area ratios of HT and T vs IS of the corresponding absorbances.*

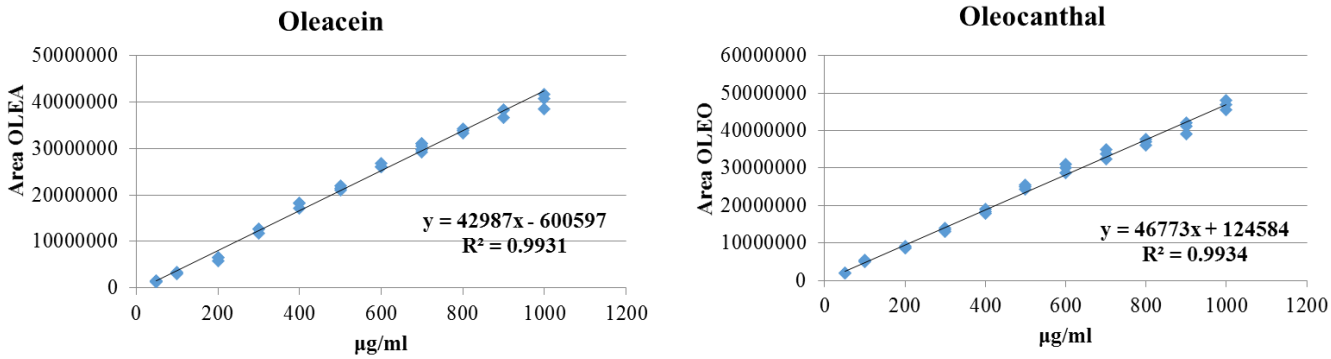

Figure A 3: *Standard calibration curves of oleacein (OLEA) (left graph) and oleocanthal (OLEO) (right graph). The horizontal scale represents the concentration of calibration points in µg/ml and the vertical scale the areas of OLEA and OLEO of the corresponding absorbances.*

***Table A 3**: Results of the performed permutation tests. 20 permutations were conducted for each Y- variable.*

Type of plot	Y-variable	R2 intercept	Q2 intercept
Figure 8	Crete	(0.0, 0.3130)	(0.0, -0.153)
	Peloponnese	(0.0, 0.3250)	(0.0, -0.141)
	Ionian	(0.0, 0.3060)	(0.0, -0.200)
Figure 10B	Crete	(0.0, 0.441)	(0.0, -0.257)
	Peloponnese	(0.0, 0.4140)	(0.0, -0.257)
	Ionian	(0.0, 0.3900)	(0.0, -0.258)
Figure 10C	Heraklion	(0.0, 0.2677)	(0.0, -0.282)
	Lasithi	(0.0, 0.2400)	(0.0, -0.265)
	Lakonia	(0.0, 0.2130)	(0.0, -0.223)
	Messinia	(0.0, 0.2430)	(0.0, -0.284)
Figure 10D	Crete	(0.0, 0.2650)	(0.0, -0.251)
	Peloponnese	(0.0, 0.2650)	(0.0, -0.272)
	Ionian	(0.0, 0.2820)	(0.0, -0.299)
	Three phases	(0.0, 0.3890)	(0.0, -0.493)
Figure 12A	Conventional	(0.0, 0.6610)	(0.0, -0.333)
	Integrated	(0.0, 0.7010)	(0.0, -0.354)
	Organic	(0.0, 0.6760)	(0.0, -0.366)
Figure 12B	Conventional	(0.0, 0.3610)	(0.0, -0.396)
	Integrated	(0.0, 0.3440)	(0.0, -0.414)
	Organic	(0.0, 0.3920)	(0.0, -0.415)
Figure 13A	Two phases	(0.0, 0.6240)	(0.0, -0.324)
	Three phases	(0.0, 0.7370)	(0.0, -0.353)
Figure 13B	Two phases	(0.0, 0.3730)	(0.0, -0.412)
	Three phases	(0.0, 0.3890)	(0.0, -0.493)

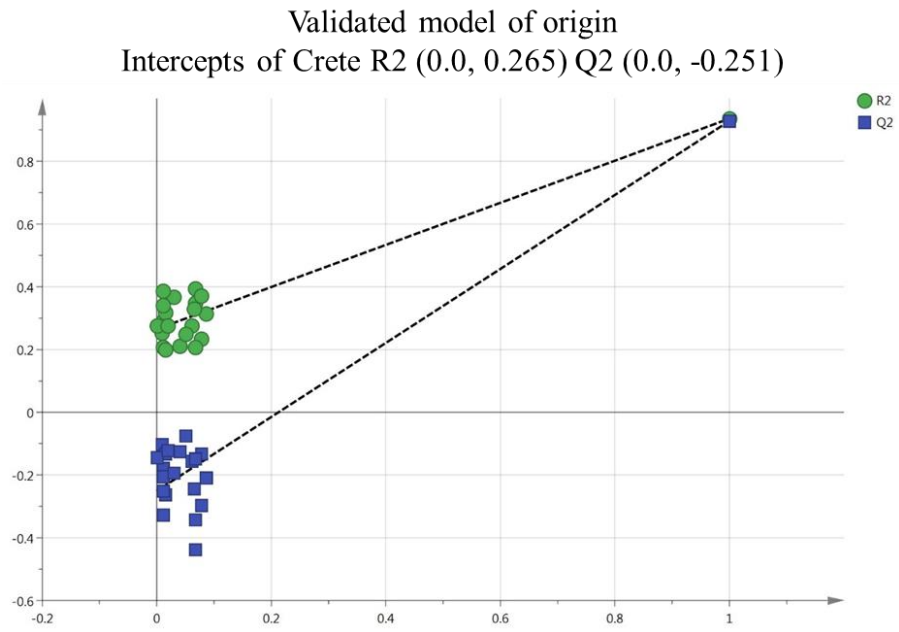

Figure A 4*: Permutation plot of biophenols OPLS-DA score plot for origin. The plot illustrates the permutation results conducted for figure 10D representing the intercepts of R2 and Q2 parameters for Crete classID.*

The permutation plot helps to estimate the validity of the current PLS or PLS-DA. The concept of this validation test is to compare the fitting (R2 and Q2) of the original model with the fitting of several models based on data where the order of Y-observations has been randomly permuted while X-matrix has been kept intact. The above plot shows for a selected Y-variable (origin-Crete) on the vertical axis the values of R2 and Q2 for the original model (far to the right) and of the Y-permutated models further to the left. The horizontal axis shows the correlation between the permuted Y-vectors and the original Y-vector for the selected Y. The original Y has the correlation 1 with itself, defining the high point on the horizontal axis. Figure 10D represents the results from 20 permutation tests conducted for Crete as Y-variable. In the vertical axis the intercepts for R2 (0.0, 0.265) and Q2 (0.0, -0.251) are represneted, indicating the validity and goodness of data fitting of the specific plot.

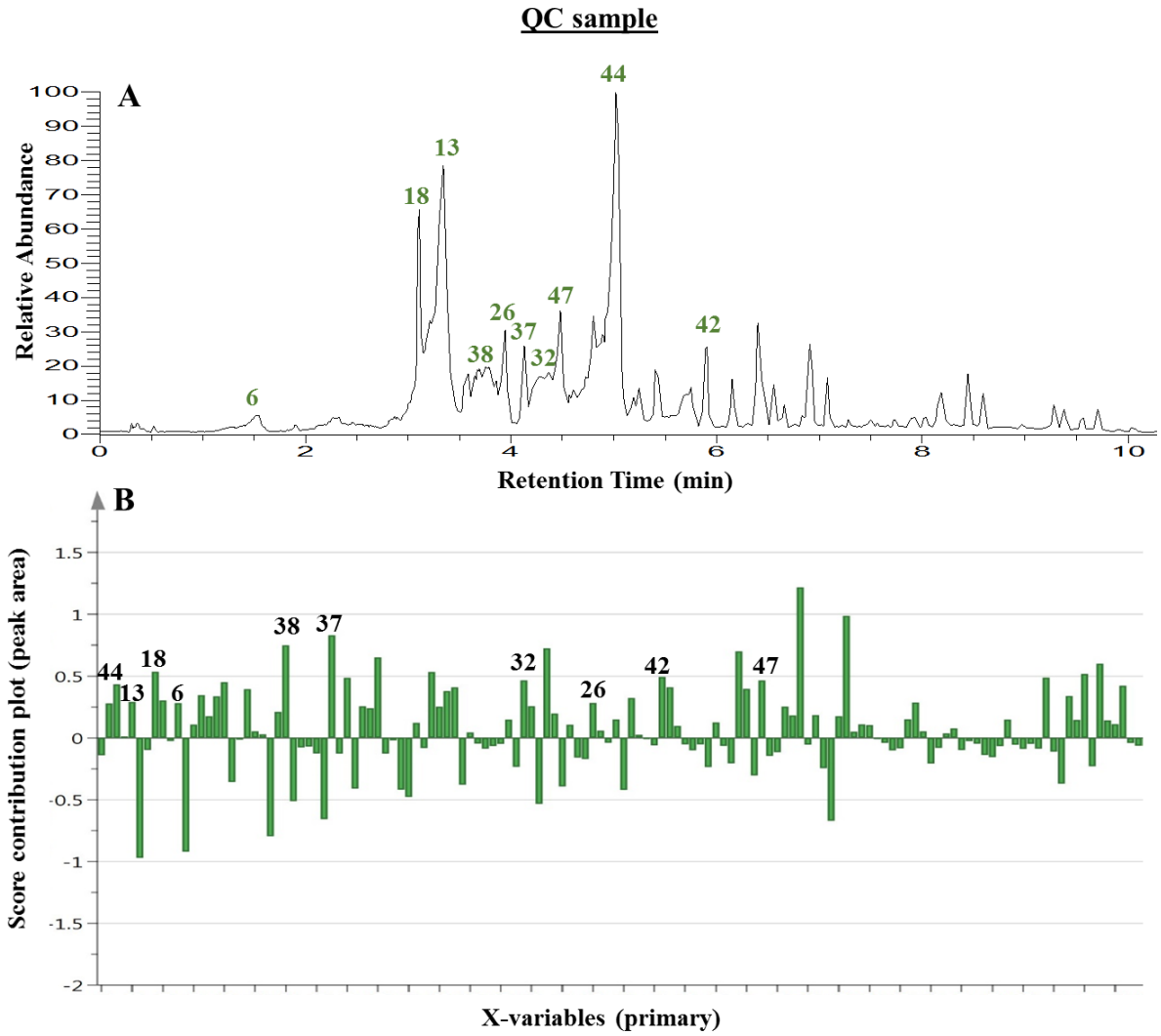

Figure A 5*: Score contribution plot and UPLC-HRMS chromatogram of QC samples. (A)UPLC-HRMS chromatogram of QC sample. (B) Score contribution plot of QC samples. The horizontal scale represents X-variables (m/z concatenated to retention time) and the vertical scale is in the units of standard deviations for peak areas of each variable. The sign of the bar (down=minus and up=plus) indicates in which direction the variable deviates. The marked peaks in A and B represent some of the identified biomarkers.*

Figure A5 associates the peaks of the UPLC-HRMS profile of QC samples with the contribution plot of the generated X-variables (m/z concatenated to retention time). Contribution plot (B) interprets the deviation of the variables in QC samples. The exclusively existence of green bars (no yellow bars indicating excess over 3rd standard deviation values) verifying the

good fitting and centralization of QCs in the corresponding OPLS-DA plot. The appeared numbering in both plots correspond compounds (presented in detail in Table A4**)**, which demonstrate high VIP scores for the discrimination of origin.

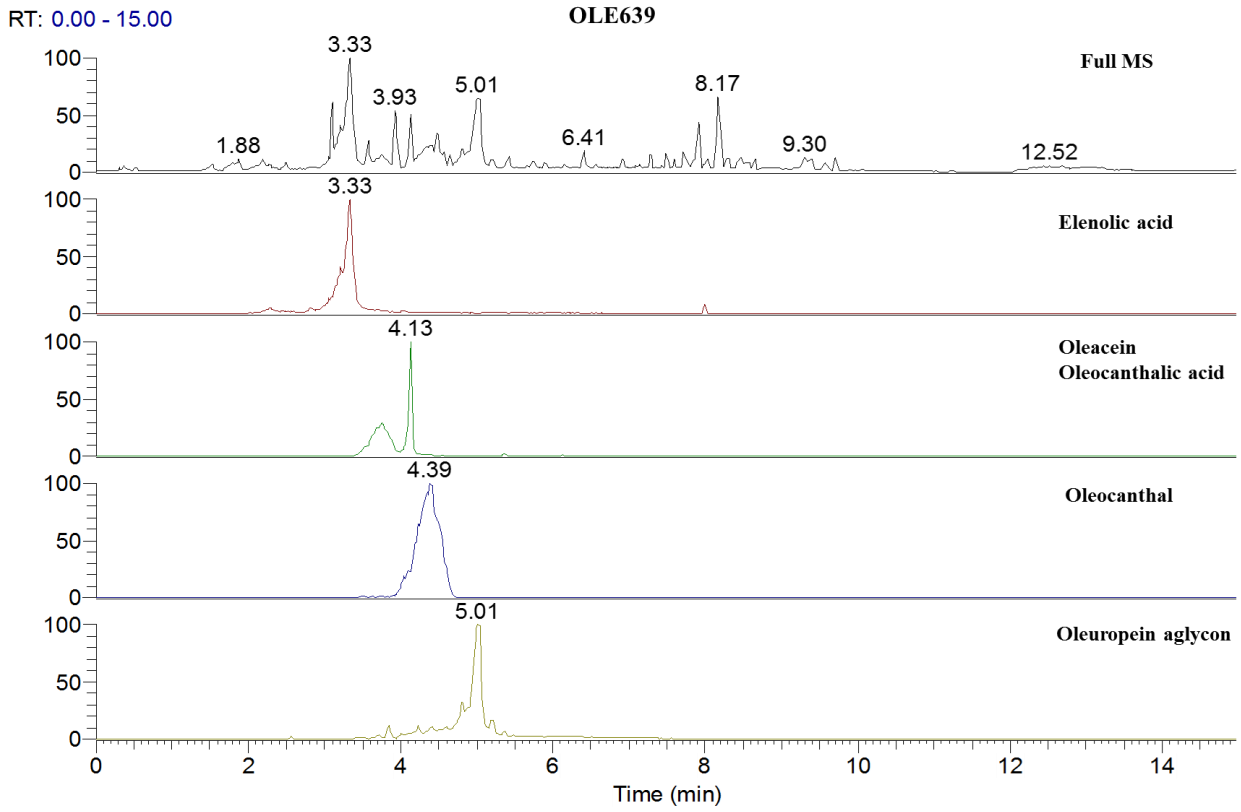

Figure A 6: *UPLC-HRMS chromatogram of the biophenolic extract OLE639. A: is the full scan chromatogram of the extract; B: is the extracted ion chromatogram of elenolic acid; C: is the extracted ion chromatogram of oleacein (broad peak) and oleocanthalic acid (sharp peak); D: is the extracted ion chromatogram of oleocanthal; E: is the extracted ion chromatogram of oleuropein aglycon.*

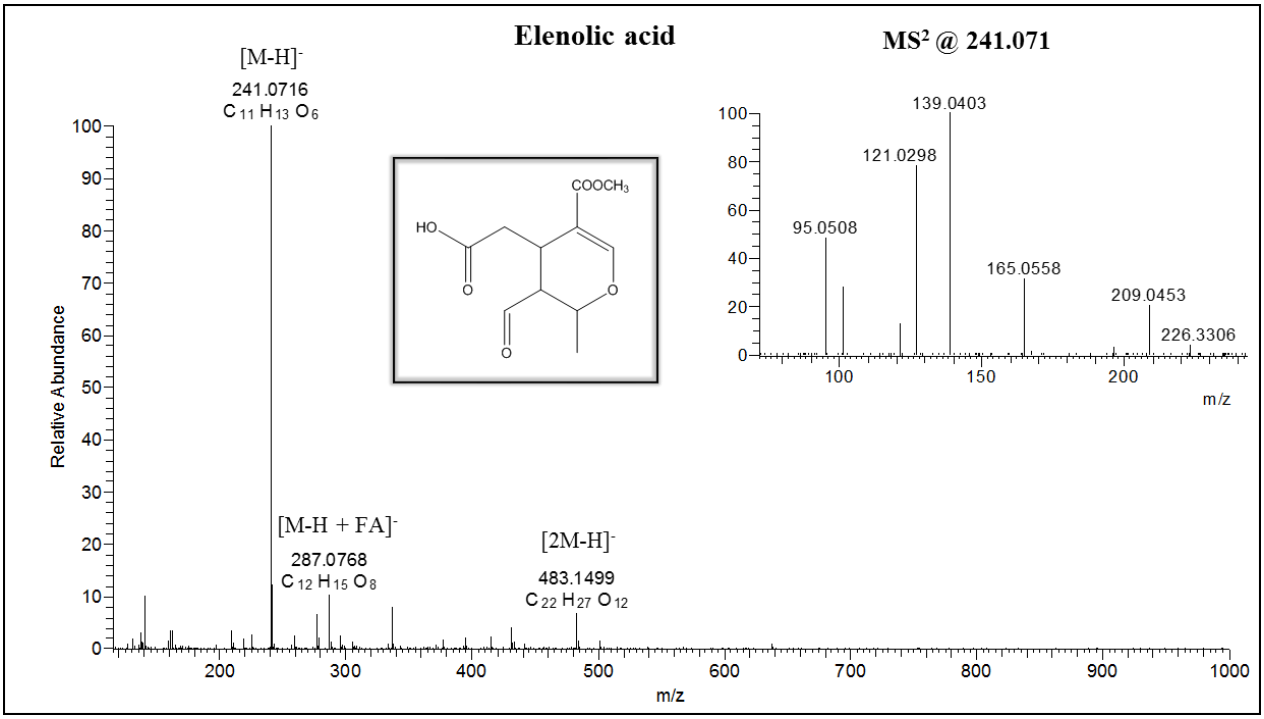

Figure A 7: *HRMS and HRMS/MS spectra of elenolic acid in negative ion mode. In the spectrum the characteristic adducts of elenolic acid are annotated and the HRMS/MS ion peaks of the corresponding pseudo-molecular ion.*

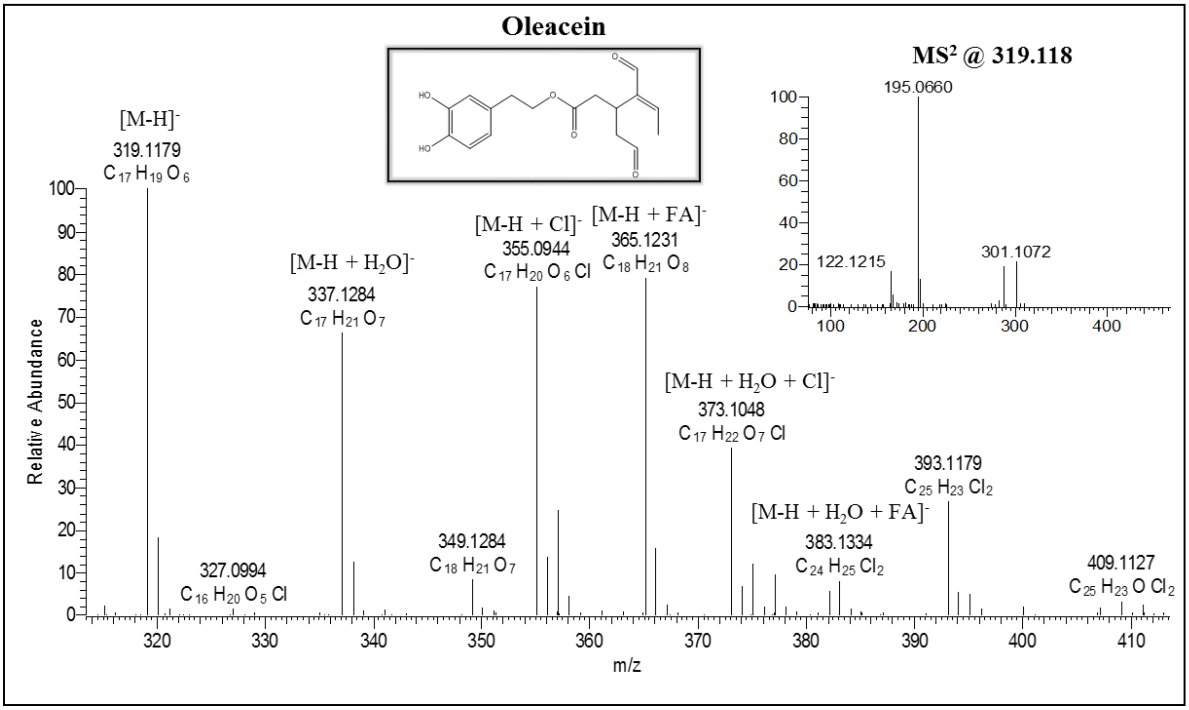

Figure A 8: *HRMS and HRMS/MS spectra of oleacein in negative ion mode. In the spectrum the characteristic adducts of oleacein are annotated and the HRMS/MS ion peaks of the corresponding pseudo-molecular ion.*

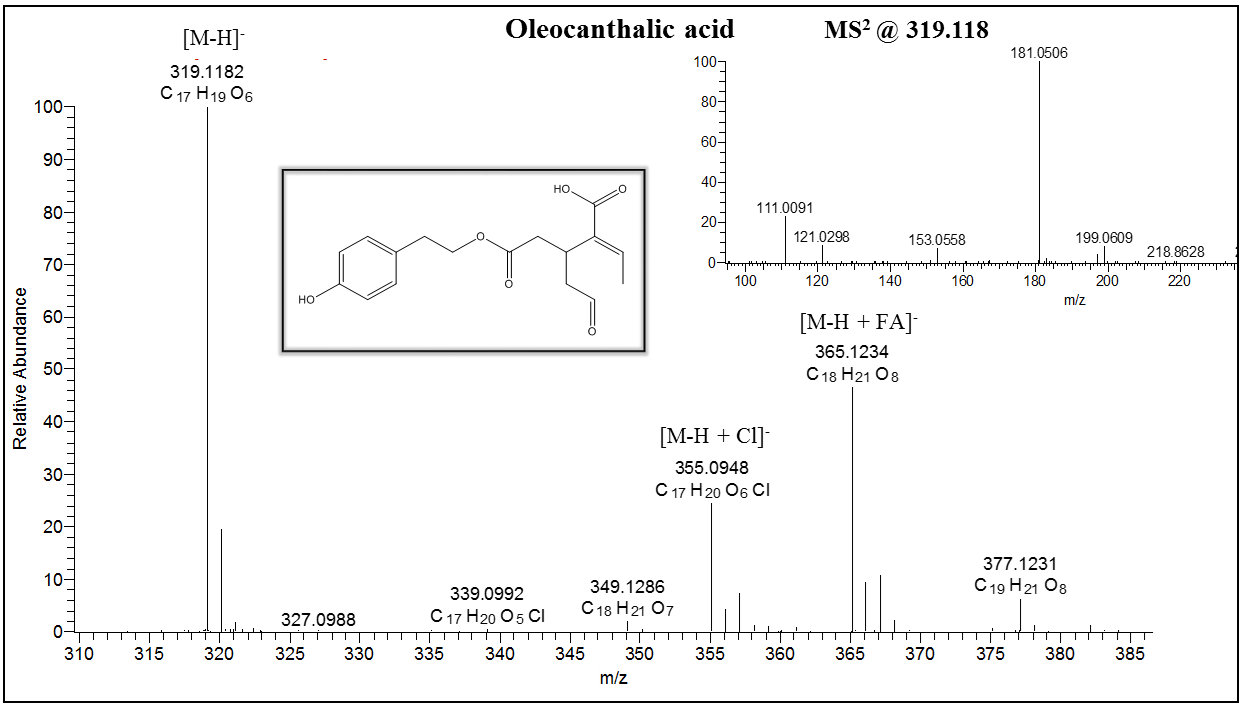

Figure A 9: *HRMS and HRMS/MS spectra of oleocanthalic acid in negative ion mode. In the spectrum the characteristic adducts of oleocanthalic acid are annotated and the HRMS/MS ion peaks of the corresponding pseudo-molecular ion.*

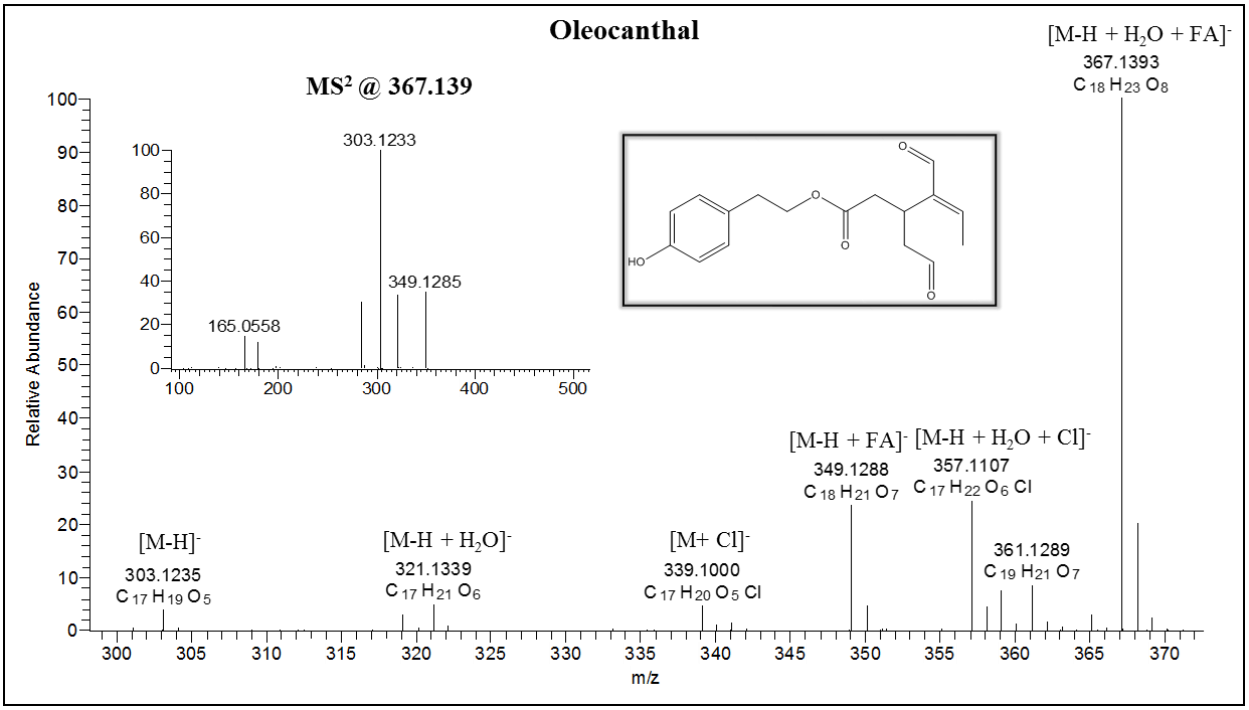

Figure A 10: *HRMS and HRMS/MS spectra of oleocanthal in negative ion mode. In the spectrum the characteristic adducts of oleocanthal are annotated and the HRMS/MS ion peaks of the corresponding pseudo-molecular ion.*

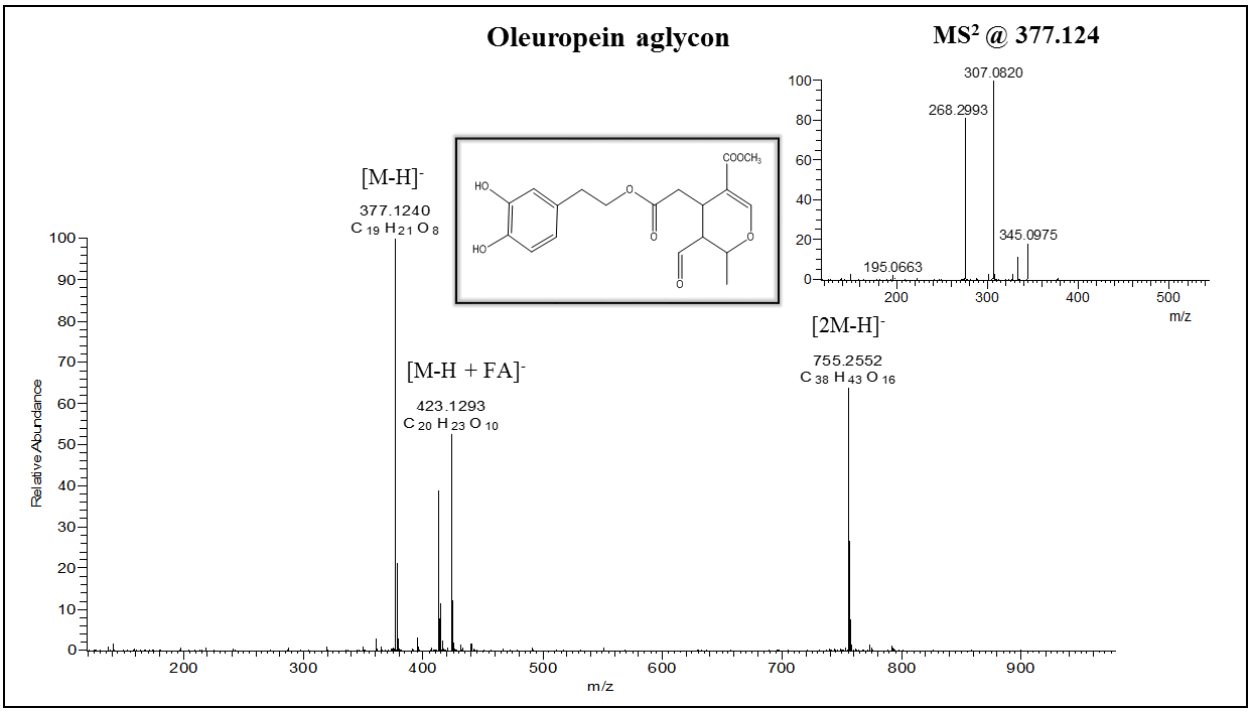

Figure A 11: *HRMS and HRMS/MS spectra of oleuropein aglycon in negative ion mode. In the spectrum the characteristic adducts of oleuropein aglycon are annotated and the HRMS/MS ion peaks of the corresponding pseudo-molecular ion.*

Table A 4: *Identified compounds with UPLC-Orbitrap-MS and FIA-MRMS. The identified compounds are numbered according to the first column. VIP scores are presented for each metabolite according to the studied Y-variable; origin, production procedure and cultivation practice. Mass error and mSigma values are generated by FIA-MRMS.*

No	Experimental m/z	Mass error [ppm]	mSigma	Compound name	Molecular formula	VIP origin	VIP production procedure	VIP cultivation Practice
1	119.034969	0.057	5.1	2-(2-hydroxyethoxy)acetic acid	$C_4H_8O_4$	5.22134	5.9023	5.92726
2	121.029503	0.071	∞	Benzoic acid	$C_7H_6O_2$	1.01405	-	1.09674
3	137.06081	0.077	1.9	Tyrosol	$C_8H_{10}O_2$	2.83547	3.1343	3.0046
4	143.107736	0.073	2.4	Octanoic acid	$C_8H_{16}O_2$	2.47795	2.86397	2.90721
5	153.01931	-0.002	4.8	Protocatehuic acid	$C_7H_6O_4$	4.19864	4.70888	4.8107
6	153.055719	0.031	2.4	Hydroxytyrosol	$C_8H_{10}O_3$	1.85303	2.10387	2.56499
7	179.071361	-0.061	5.3	Tyrosol Acetate	$C_{10}H_{12}O_3$	1.46927	1.4958	1.46246
8	183.066297	0.025	2.7	Dialdehydic form of decarboxymethyl Elenolic acid	$C_9H_{12}O_4$	1.94329	1.86022	1.93357
9	195.066278	-0.066	6.7	Hydroxytyrosol Acetate	$C_{10}H_{12}O_4$	5.84606	4.50373	4.5868
10	199.170347	-0.003	∞	Lauric acid	$C_{12}H_{24}O_2$	1.17209	1.24399	1.3038
11	225.076859	0.135	9.9	desoxy elenolic acid derivative	$C_{11}H_{14}O_5$	3.31405	1.57051	2.06128
12	227.201648	-0.025	6.5	Myristic acid	$C_{14}H_{28}O_2$	2.08587	2.20252	2.35945
13	241.071755	-0.072	6.1	Elenolic acid	$C_{11}H_{14}O_6$	6.52685	7.49337	7.9409
14	241.21729	-0.04	14.7	Pentadecanoic acid	$C_{15}H_{30}O_2$	1.628	1.76714	1.89093
15	253.217315	0.353	10.8	Palmitoleic acid	$C_{16}H_{30}O_2$	1.38489	1.27238	1.37402

16	255.087423	-0.104	8	Elenolic acid methyl ester	$C_{12}H_{16}O_6$	5.92739	5.10004	6.97496
17	255.232958	0.033	16.7	Palmitic acid	$C_{16}H_{32}O_2$	6.95458	5.94974	7.97047
18	257.066694	0.084	9.5	Hydroxylated form of elenolic acid	$C_{11}H_{14}O_7$	1.39886	1.73966	2.1057
19	267.23293	-0.120	∞	Margaroleic acid	$C_{17}H_{32}O_2$	1.03012	1.21267	1.19739
20	269.045551	0.009	11	Apigenin	$C_{15}H_{10}O_5$	2.17441	2.99418	2.66789
21	269.103081	0.213	∞	Elenolic acid ethyl ester	$C_{13}H_{18}O_6$	1.21439.	-	1.18804
22	269.248578	-0.098	9.2	Margaric acid	$C_{17}H_{34}O_2$	1.30501	1.35513	1.50447
23	279.23298	0.101	24.5	Linoleic acid	$C_{18}H_{32}O_2$	3.79235	1.50918	1.67573
24	281.248634	-0.095	5.7	Oleic acid	$C_{18}H_{34}O_2$	7.96697	3.60615	3.56477
25	283.264257	0.035	8.8	Stearic acid	$C_{18}H_{36}O_2$	3.94595	2.47538	4.2481
26	285.040502	0.166	16	Luteolin	$C_{15}H_{10}O_6$	2.55389	4.31307	1.81787
27	295.227889	-0.159	2.7	Hydroxylinoleic acid	$C_{18}H_{32}O_3$	9.94902	1.50918	1.99172
28	297.243504	-0.016	1.9	Hydroxyoleic acid	$C_{18}H_{34}O_3$	15.6066	11.8227	8.54964
29	299.056138	0.141	8.3	Luteolin-7 methyl-ether	$C_{16}H_{12}O_6$	1.59344	2.61407	2.29155
30	299.20161	-0.067	13.8	PUFA, C-20	$C_{20}H_{28}O_2$	3.11107	3.35868	3.53252
31	299.259173	-0.061	8.5	Hydroxystearic acid	$C_{18}H_{36}O_3$	3.3611	4.39046	3.35659
32	303.123779	-0.169	5.8	Oleocanthal	$C_{17}H_{20}O_5$	7.10945	6.12967	7.56752
33	303.232928	-0.083	∞	Arachidonic acid	$C_{20}H_{32}O_2$	-	-	1.05502
34	309.284317	-0.031	∞	Gondoic acid	$C_{20}H_{38}O_2$	1.26752	1.51175	-
35	311.295541	0.024	∞	Arachidic acid	$C_{20}H_{40}O_2$	1.82052	1.88345	1.12426

36	313.238436	-0.158	13.6	Octadecanedioic acid	$C_{18}H_{34}O_4$	3.99715	3.46563	2.50328
37	319.116536	-0.03	3.1	Oleocanthalic acid	$C_{17}H_{20}O_6$	2.05932	1.30741	-
38	319.118731	-0.064	3.7	Oleacein	$C_{17}H_{20}O_6$	8.37747	5.16096	6.61328
39	335.113652	0.091	18.7	Hydroxy-O-decarboxymethyl oleuropein aglycon	$C_{17}H_{20}O_7$	2.66469	1.72474	2.23065
40	339.232889	-0.108	41	Docosanoic acid	$C_{23}H_{32}O_2$	5.41017	6.1416	6.20101
41	357.134425	0.172	12.8	Pinoresinol	$C_{20}H_{22}O_6$	1.64706	3.62491	3.53953
42	361.129246	-0.074	5.6	Ligstroside aglycon	$C_{19}H_{22}O_7$	8.21102	14.1568	10.3804
43	367.361121	-0.080	3.3	Lignoceric acid	$C_{24}H_{48}O_2$	3.1083	3.60292	1.56055
44	377.124147	0.056	4.0	Oleuropein aglycon	$C_{19}H_{22}O_8$	14.0242	3.16452	13.6205
45	389.290828	-0.002	3.0	SFA	$C_{21}H_{42}O_6$	9.82473	8.88931	10.6974
46	391.139885	0.063	7.8	Methyl oleuropein aglycon	$C_{20}H_{24}O_8$	1.88511	4.59536	3.90901
47	393.119148	0.324	11.1	10-Hydroxy oleuropein aglycon	$C_{19}H_{22}O_9$	2.93417	2.94455	3.05225
48	393.155482	-0.045	3.2	Ligstroside aglycon derivative (hydroxylated product)	$C_{20}H_{26}O_8$	5.61589	9.73995	6.75293
49	409.15044	0.100	6.8	Oleuropein aglycon derivative	$C_{20}H_{26}O_9$	4.10616	5.18996	3.54232
50	413.290878	-0.262	9.5	TG	$C_{23}H_{42}O_6$	10.1037	7.23048	10.1697
51	415.139887	0.268	14.3	Acetoxypinoresinol	$C_{22}H_{24}O_8$	3.94367	6.18115	5.89184
52	415.306484	0.017	4.3	MUFA ester	$C_{23}H_{44}O_6$	21.0982	13.2781	16.8231
53	417.155523	-0.021	10.4	Syringaresinol	$C_{22}H_{26}O_8$	1.28993	2.63969	2.32783
54	417.322155	-0.005	7.4	SFA ester	$C_{23}H_{46}O_6$	6.60908	6.3243	7.14831

55	423.422612	0.018-	3.2	Montanic acid	$C_{28}H_{53}O_2$	1.50266	1.74077	1.43791
56	455.353111	0.045	11.8	Oleanolic acid	$C_{30}H_{48}O_3$	2.40333	4.08874	3.93516
57	471.347941	-0.263	10.3	Maslinic acid	$C_{30}H_{48}O_4$	5.51485	7.47799	6.80188
58	611.525847	0.334	64.2	DG derivative	$C_{37}H_{72}O_6$	1.2954	2.03549	2.25631
59	629.491862	-0.218	31.8	DG	$C_{37}H_{70}O_5Cl$	2.65682	2.95243	2.03171
60	637.541557	0.383	65.6	Trilaurin	$C_{39}H_{74}O_6$	1.08167	1.14146	4.05925
61	653.542317	-0.182	54.1	DG derivative	$C_{39}H_{73}O_7$	6.05454	5.15802	6.76803
62	655.515738	0.304	48.1	DG	$C_{39}H_{72}O_5Cl$	3.99641	4.21617	3.60206
63	679.554723	-0.07	3.1	DG derivative	$C_{41}H_{75}O_7$	7.93679	8.32565	9.20121
64	849.763319	-0.114	28.2	TG derivative	$C_{53}H_{102}O_7$	1.21126	1.17752	1.31861
65	867.725262	0.127	11.3	TG	$C_{53}H_{100}O_6Cl$	3.0872	3.7717	1.83018
66	875.774536	0.136	17.5	TG derivative	$C_{55}H_{104}O_7$	2.87357	2.56699	3.10146
67	890.714835	-0.07	2.6	Stearin	$C_{57}H_{110}O_6$	1.35101	1.7891	1.03562
68	891.725417	0.258	38.9	TG	$C_{55}H_{100}O_6Cl$	3.5948	5.35845	3.38906
69	893.742758	0.478	33.2	TG	$C_{55}H_{102}O_6Cl$	6.5368	2.63229	5.27303
70	895.732846	-0.380	52.3	TG	$C_{55}H_{104}O_6Cl$	3.65748	4.59915	2.93818
71	914.753581	-0.04	1.2	Linolein	$C_{57}H_{98}O_6$	1.62813	1.10354	1.40218
72	919.754312	0.05	5.8	Triolein	$C_{57}H_{104}ClO_6$	6.91628	7.65802	9.66812

[1]SFA: saturated fatty acid; PUFA: polyunsaturated fatty aci

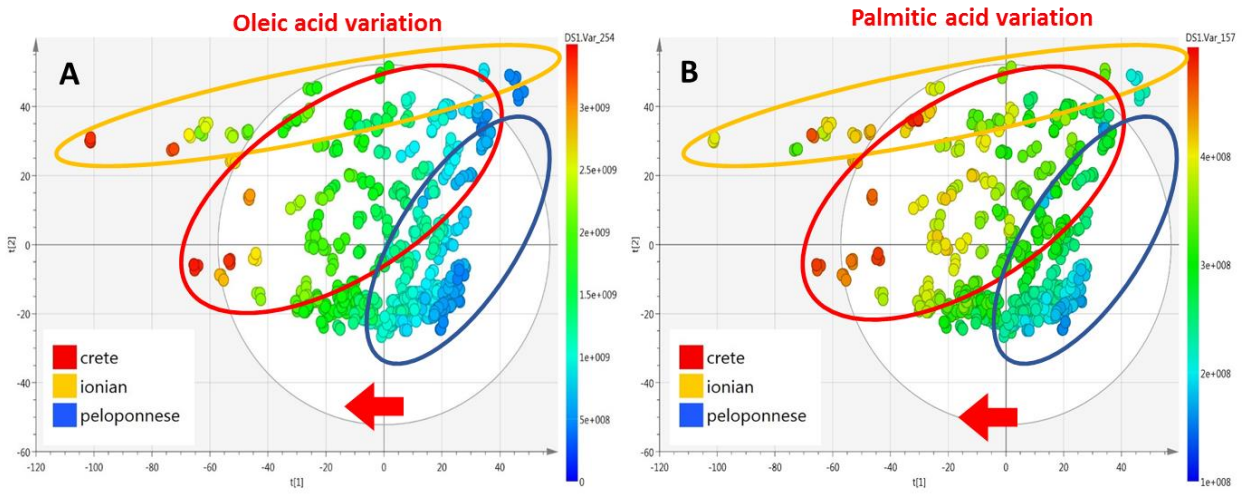

Figure A 12: *PCA plots of EVOOs colored according to specific X-variables; (A): PCA plot colored according to the intensity of oleic acid variable (var_254); (B): PCA plot colored according to the intensity of palmitic acid variable (var_157). Both plots are pareto scaled and include all observations.*

PCA plots in figure A12 represent the variation of intensities for oleic and palmitic acid. These metabolites have been derived as statistical significant biomarkers for the parameter of origin. The colored bar in the right side of plots (from blue - low intensities to red - high intensities) illustrates the intensities for oleic (A) and palmitic acid (B) of all observations. Both plots uncover an obvious trend of separation on the first component, based on compounds intensities. Observations on the right side of plots first component are characterized by low intensities for the fatty acids, while observations on the left side of the first component are characterized by high intensities for the compounds. Red, yellow and green spots in plot A reflect samples with high and medium intensities of oleic acid and mainly originate from Ionian islands and Crete. In these two areas oleic acid have been identified as statistical significant metabolite. Blue and light blue spots (samples with low intensities of oleic acid) mainly come from Peloponnese peninsula. For plot B the same trend is observed. Based on bibliographic data

palmitic acid is formed from oleic acid [81], explaining the same trend in the two plots. Palmitic acid is found in significant intensities in Peloponnese as well.

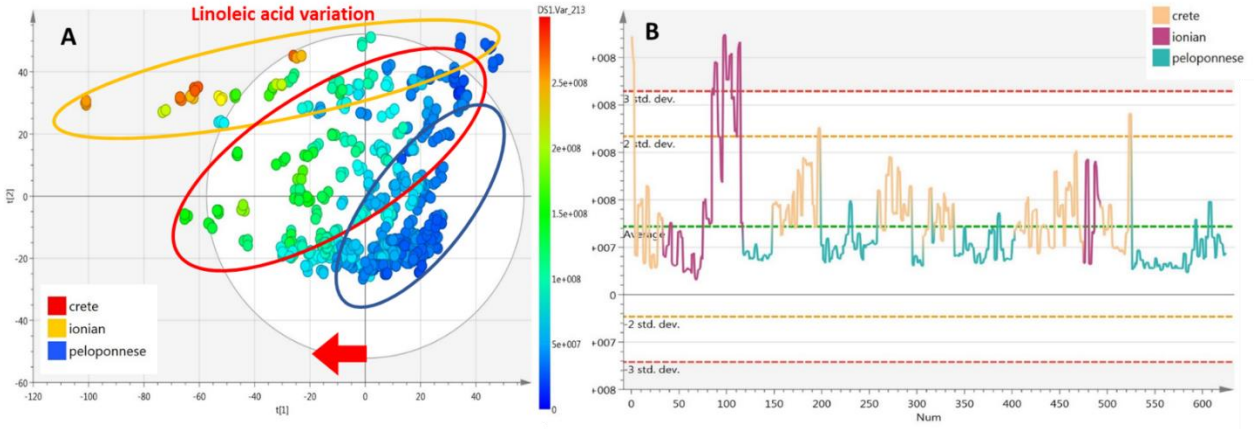

Figure A 13*: plots interpreting linoleic acid variation in all observations; (A) PCA plot colored according to linoleic acid intensity (pareto scaling); (B) Diagram illustrating the standard deviations (three standard deviations) of linoleic acid variable (var_213). Observations are colored according to the geographical origin; Crete with light orange, Ionian islands with magenta and blue for Peloponnese.*

Like palmitic acid, linoleic acid is formed from oleic acid after a desaturation reaction, having an antagonistic relation with palmitic acid formation [81]. In the PCA plot (A) red and yellow spots are samples originating from Ithaca island and green spots from Cefalonia, meaning that the two Ionian islands of sample collection hold the highest intensities for linoleic acid. On the other hand, Cretan and Peloponnese samples do not contain linoleic acid in considerable amounts, but only in oleic and palmitic acid (as it is shown in figure A12**)**. Diagram **(**B**)** evidence the previous finding, that only in Ionian samples linoleic acid intensities (magenta colored samples) exceed the third standard deviation.

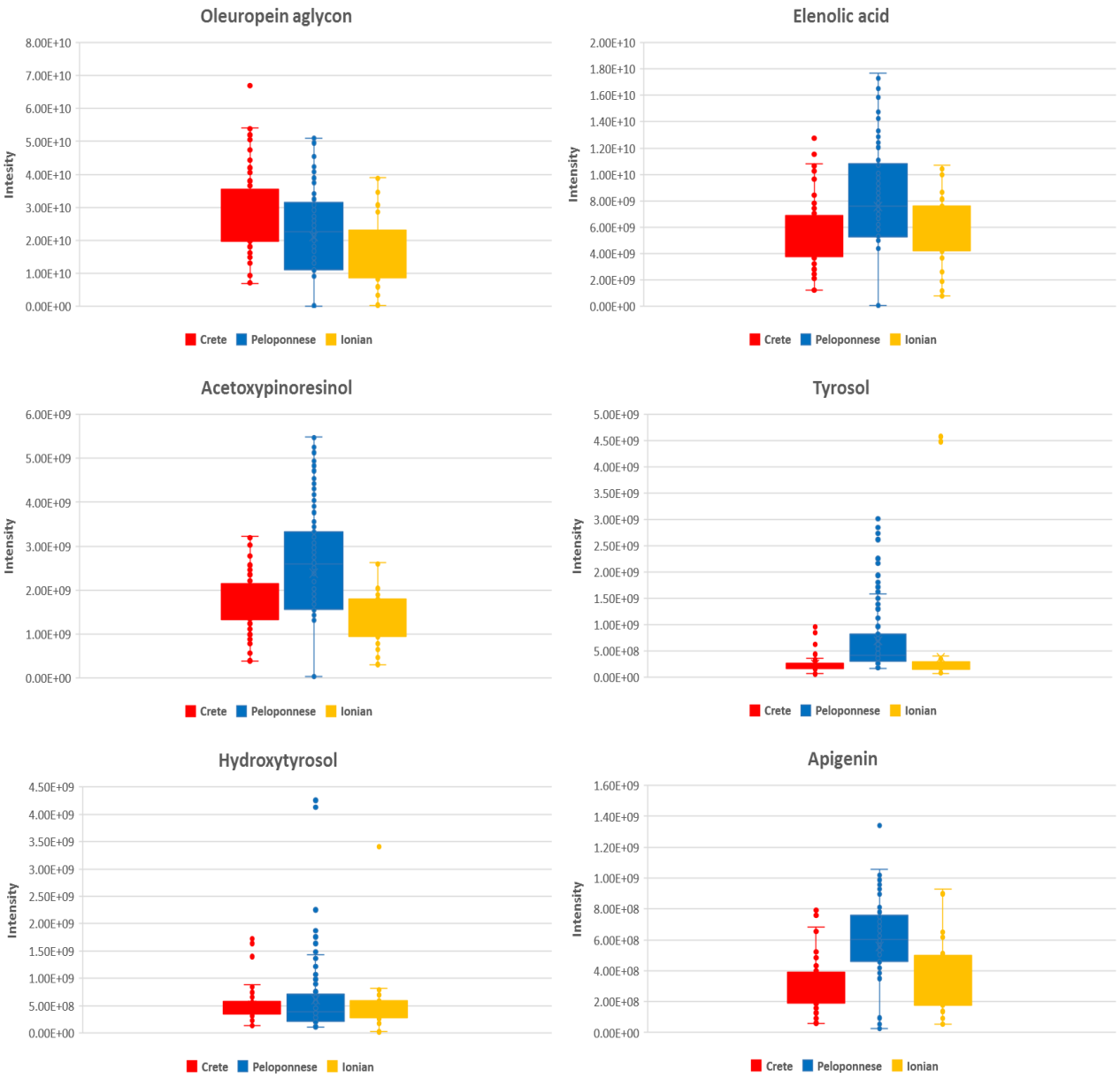

***Figure A 14**: Box-plots of oleuropein aglycon (44), elenolic acid (13), acetoxypinoresinol (51), tyrosol (3), hydroxytyrosol (6) and apigenin (20) representing their intensities in the three basic geographical regions; Crete (red boxes), Peloponnese (blue boxes) and Ionian Islands (yellow boxes).*

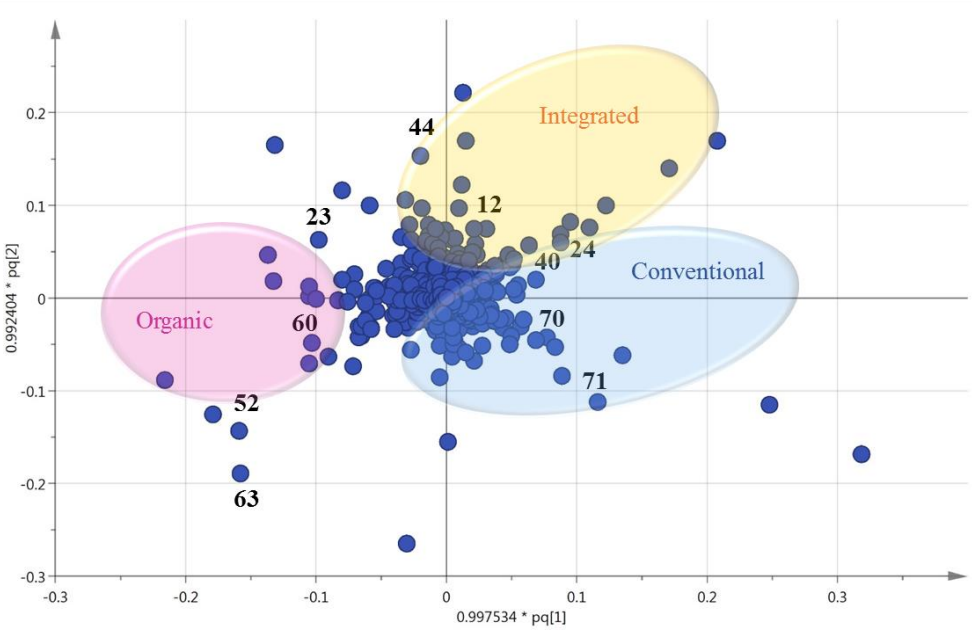

Figure A 15: *OPLS-DA loadings plot of cultivation practice generated by EVOOs dataset. In the plot are annotated statistical significant loadings for each cultivation practice; Conventional-blue annotation, Integrated-yellow annotation and organic-magenta annotation.*

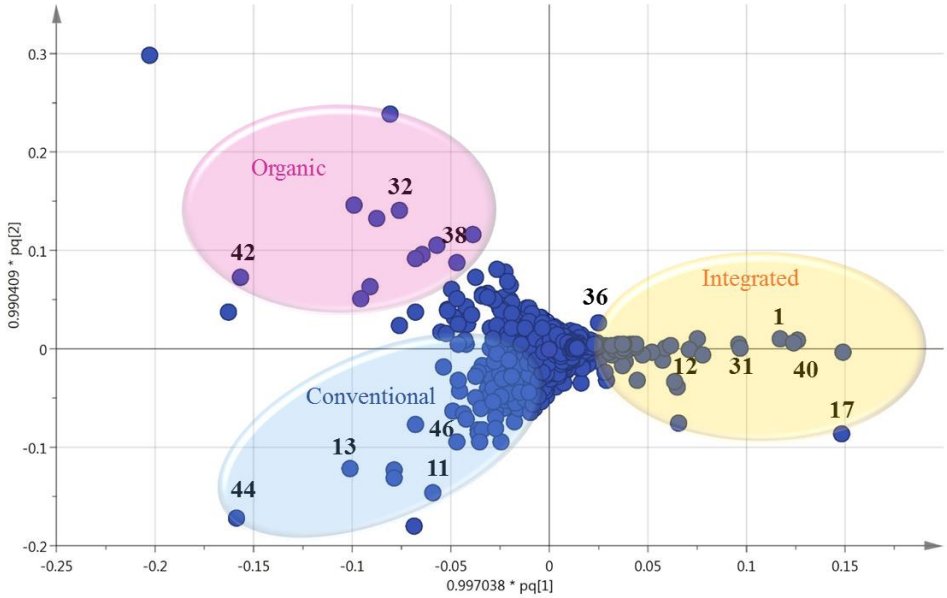

Figure A 16: *OPLS-DA loadings plot of cultivation practice generated by biophenols extracts dataset. In the plot are annotated statistical significant loadings for each cultivation practice; Conventional-blue annotation, Integrated-yellow annotation and organic-magenta annotation.*

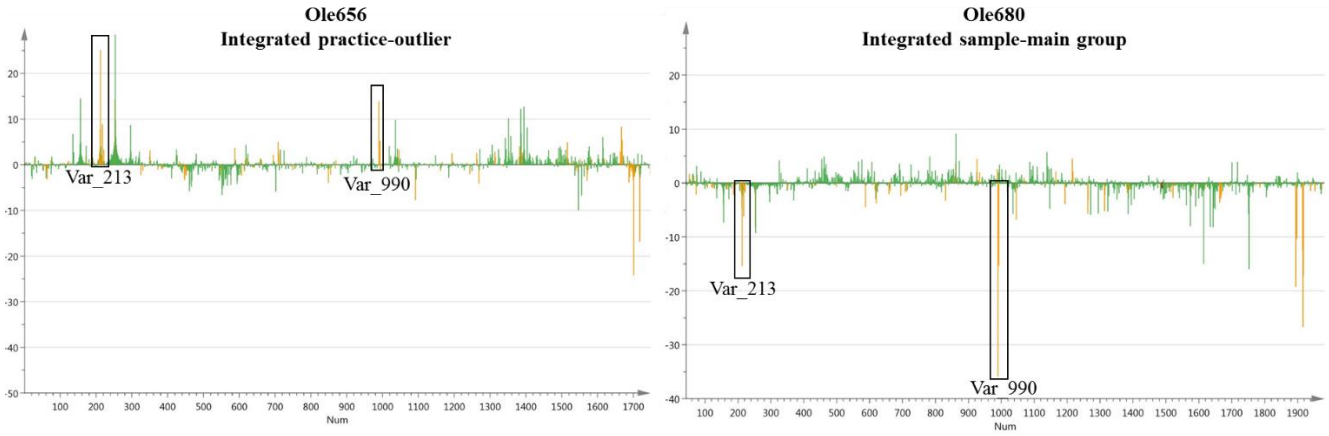

Figure A 17*: Contribution EVOOs plots of OLE656 – left plot (outliers of integrated cultivation practice) and OLE680- right plot (sample of the main group of integrated cultivation practice). The horizontal scale represents X-variables and the vertical scale is in the units of standard deviations. The sign of the bar (down=minus and up=plus) indicates in which direction the variable deviates. Yellow bars represent the variables that are out of the 3rd standard deviation. The variables in the black boxes are: variable 213 which corresponds to linoleic acid and variable 990 for oleuropein aglycon.*

The contribution plot shows why a point in a score plot deviates from the average. The plot shows the weighted difference between the data of the point and the average of the model. In figure A17 Ole656, which is an outlier of integrated practice, possess intensities higher from the 3rd standard deviation for linoleic acid (Var_213) and oleuropein aglycon (Var_990), which are not found as statistical significant metabolites for this practice. On the other hand, Ole680, which contributes to the main sample group of integrated practice, has the opposite profile concerning these metabolites and possess intensities lower from the 3rd standard deviation.

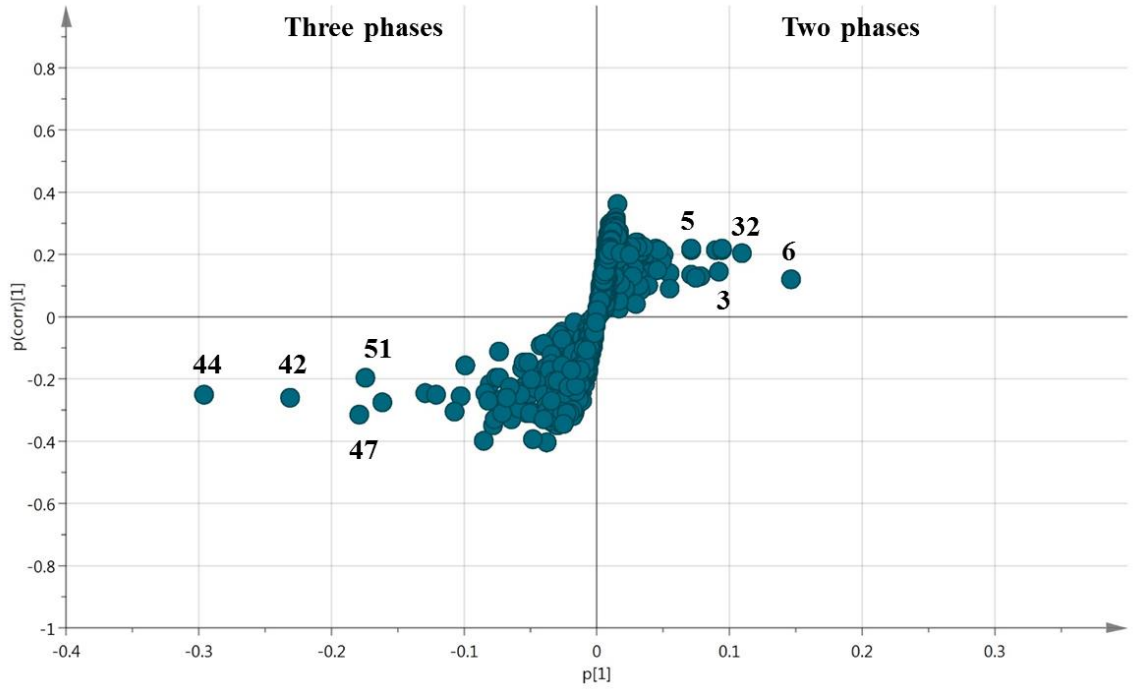

Figure A 18: *S-plot of production procedure generated by biophenols dataset. In the two treatments statistical significant metabolites are marked.*

The S-plot is used for covariance and correlation structure visualization between X-variables and the predictive score t[1]. It is a scatter plot of the p[1] vs p(corr)[1]vectors. This plot often shapes the letter 'S' unless the X-variables are scaled to UV. X-variables situated far out the wings of the S combine high model influence with high reliability. In the above S-plot X-variables right to p[1] influence two phases structure visualization, while X-variables left to p[1] influence three phases visualization. In the plot are marked identified compounds revealing high VIP scores for production procedure parameter.

Chapter 2

Isolation and biological evaluation of biophenols. In vitro, in vivo, PK & metabolization study

Part of this chapter has been published in journal of "Food and Chemical Toxicoly" (Nikou et al., 2019, 125:403-412) and Journal of "Chromatography A" (Angelis et al., 2017, 1491:126-136)

Abstract

Olive oil (OO) is widely accepted as a superior edible oil. Great attention has been given lately to OO secoiridoids which are linked to significant health beneficial effects. Despite the promising results of these compounds concerning their positive impact to human health, the lack of commercially available standards and their laborious isolation from OO, make their use for *in vivo* investigations and human applications almost infeasible. In the current study, selected OO, characterized by high concentration of secoiridoids was extracted and fractionated for the isolation of secoiridoids and other unexplored biophenols. Isolated compounds were tested with typical *in vitro* assays for cytotoxicity evaluation. Consequently, compounds with higher activity, namely oleocanthal and oleacein as well as selected OO extracts with high, medium and low levels of these compounds were bio-evaluated in mammalian cells and as a dietary supplement in a *Drosophila in vivo* model. Oleocanthal and oleacein were found to activate healthy aging-promoting cytoprotective pathways and suppressed oxidative stress in both mammalian cells and in flies. Ultimately, a pharmacokinetic (PK) experiment was carried out in mice model for determination of oleocanthal PK parameters. Compound metabolism was studied and relative content of selected metabolic products was determined.

Keywords

Biophenols; Oleacein; Oleocanthal; Aging; *Drosophila*, Pharmocokinetics

1. Introduction

Total phenolic fraction (TPF) of olive oil (OO), known also as "biophenols" or "polyphenols" is a biologically active element of OO characterized by strong antioxidant, anti-inflammatory and antimicrobial activities as well as other beneficial health effects [1,2]. Its chemical composition depends on many exogenous factors like olive tree variety, degree of ripeness, microclimatic conditions, processing techniques and storage, resulting to a highly variable mixture [3]. TPF is composed of a plethora of minor components and characterized by high chemical complexity [4]. The biophenol part can be divided into lipophilic and hydrophilic with the presence of a small amount of carotenoids [5]. The lipophilic part contains hydrocarbons (mainly squalene that is partially responsible for the chemoprevention of OO against certain types of cancer), tocopherols (α-tocopherol constitutes 90% of the total tocopherol content), sterols and triterpenic acids [6]. The contained biophenols in the hydrophilic part usually are grouped based on their structural similarity (approximately 36 different chemical structures have been isolated from virgin olive oil (VOO) unsaponified fraction [7]. Phenyl alcohols (hydroxytyrosol, tyrosol etc), phenolic acids (benzoic and cinnamic acid derivatives), secoiridoids (oleocanthal, oleacein, ligstroside aglycon, oleuropein aglycon etc), flavonoids (luteolin, apigenin), iridoids (elenolic acid, dialdehydic form of elenolic acid etc) and lignans (pinoresinol, acetoxypinoresinol) are the most common biophenols of TPF, with secoiridoids composing a considerable TPF part in Greek VOO [8].

Secoiridoids started to be more systematically studied in the recent past and are present exclusively in Oleaceae family which includes *Olea europaea* L. [9]. In OO, secoiridoids exist in their aglyconic form. Their basic skelotone is consisted of a phenolic part (hydroxytyrosol or tyrosol) linked to an iridoid part, elenolic acid (EA) or the dialdehydic form of elenolic acid

(EDA) forming secoiridoid aglycons or their dialdehydic forms respectively [10]. More specifically their production in OO is derived from two reactions in the glucosidic structures. Firstly, the activity of *β*-glucosidase produces aglycon forms with an aldehyde structure [9,10]. Subsequently, after the loss of glucose, a hydroxyl group is linked to the oxygenated ring of elenolic acid and an opening to the ring with a successive isomerization to dialdehyde open structure gives rise to this specific group of biophenols [9]. Secoiridoids are the main biophenols class in VOO extract and their concentration influences the sensory and organoleptic properties of OO [11]. Figure 14 depicts the basic chemical structures of secoiridoid aglycons.

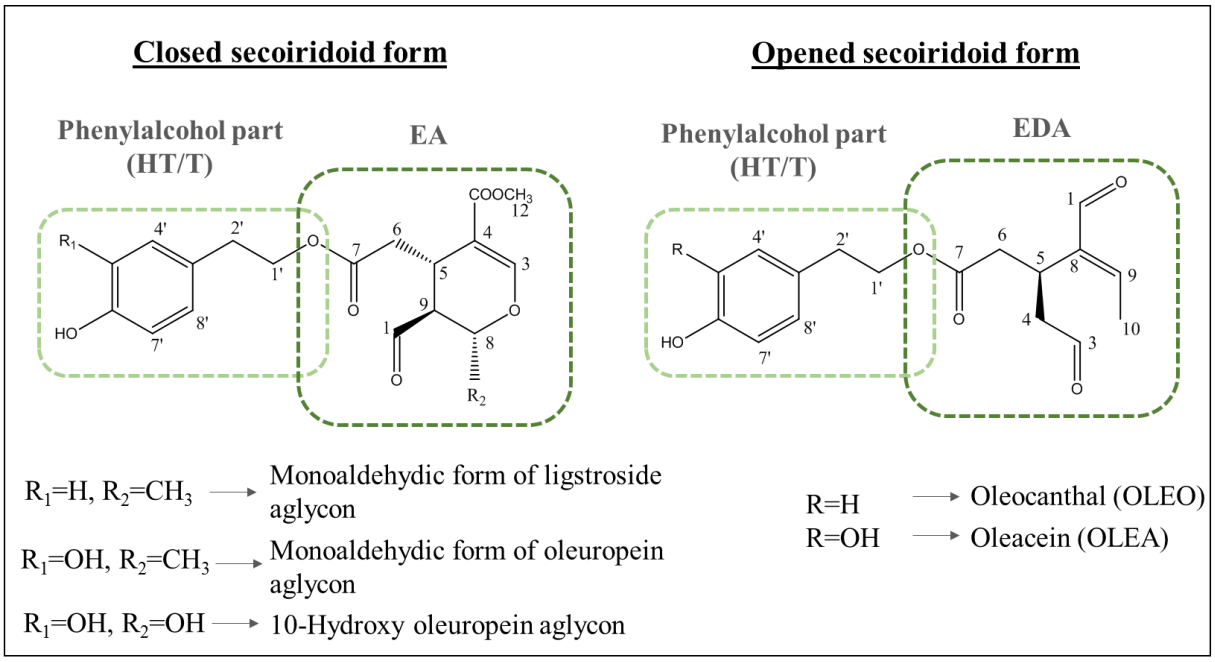

***Figure 14**: Secoiridoid aglycons basic skeleton. Left part represents closed forms of secoiridoids including elenolic acid (EA) in their chemical structures. Right part represents opened forms of secoiridoids including dialdehydic form of elenolic acid (EDA) in their structures. HT: hydroxytyrosol, T: tyrosol.*

Much attention has been given lately to the investigation of biological and pharmacological role of certain TPF secoiridoids and specifically, of oleocanthal (OLEO) and oleacein (OLEA)

[12,13]. OLEO has shown a strong anti-inflammatory *in vitro* activity by inhibiting COX-1 and COX-2 which are inflammatory enzymes involved in the biosynthesis of inflammatory prostaglandins. OLEO acts in a dose-dependent manner and is considered more effective to ibuprofen at equimolar concentrations [14]. Also attenuates other inflammatory mediators like iNOS, MMP-13 and ADAMTS-5 [15,16]. OLEO has also been recognized as a potent pharmacological agent in the treatment of neurodegenerative diseases [17]. *In vitro* and *in vivo* studies have revealed the great potential of OLEO in counteracting amyloid aggregation and toxicity [17]. Also, OLEO has the ability to prevent amyloid-β (Aβ) and tau aggregation *in vitro* and enhance Aβ clearance from the brain of wild-type mice *in vivo* [17]. It has been also shown that OLEO is implicated in pathogenesis of several cancer types. It inhibits the proliferation, migration and invasion of non metastatic and highly metastatic human breast and prostate cancer cell lines, mediated via inhibition of HGF-c-Met pathway and inhibits the tumor growth in an orthotic model of breast cancer *in vivo* [18,19]. Moreover, OLEO exerts antimicrobial activity against *Escherichia coli*, *Salmonela enterica*, *Listeria monocytogenes*, *Helicobacter pylori*, *Staphylococcus aureus* and *Enterococcus faecalis* [20].Several studies revealed that OLEA has a strong antioxidant activity with effect on the function of human neutrophils [21]. It reduces significantly myeloperoxidase (MPO), released from neutrophils, comparably with anti-inflammatory drug indomethacin [21]. Apart from antioxidant, however to a lesser extent, OLEA exhibited some effects on inflammatory mediators, MMP-9 and IL-8 [21]. It also indicates a protective action against abdominal fat accumulation, weight gain and liver steatosis, with improvement of insulin-dependent glucose and lipid metabolism [22]. Finally it exerts antimicrobial effect and the statistical correlation between oleacein concentration and Gram-positive and Gram-negative bacteria survival was found [23].

It is worth noting that these compounds are major components of biophenols fraction in many extra virgin olive oils (EVOOs). Thus, it can be hypothesized that a positive association exists between OLEO and OLEA levels and the beneficial effects of (E)VOOs. To our knowledge, there is limited information related to these two secoiridoids and the health benefits of Mediterranean diet. Over the last decade many epidemiological studies have associated the consumption of (E)VOO with advanced life expectancy and reduced incidences of age-related diseases [24–26]. Aging is a multifactorial process that is characterized by accumulating cellular damage and is promoted by both genetic and environmental factors [27]. Age-related genome and proteome damage seem to be interconnected. Specifically, non-functional or damaged proteins could affect the proper function of crucial cellular processes, such as DNA Damage Responses (DDR) resulting in genomic instability. On the other hand, genome damage impacts on the proper structure or function of proteins leading to disturbance of proteome homeodynamics [28]. The maintenance of proteostasis and proteome quality control is assured by the so-called proteostasis network (PN) [28].

The two main cellular proteolytic systems, namely the autophagy lysosome- (ALP) and ubiquitin-proteasome (UPP) pathways have crucial role to the PN functionality. ALP degrades long-lived proteins and damaged organelles, while UPP degrades both short-lived ubiquitinated normal proteins and non-functional polypeptides [29]. Molecular chaperones stabilize the proteome under conditions of stress, while the transcription factor Nuclear factor (erythroid-derived 2)-like 2 (NRF2) is important in the maintenance of proteostasis as, except from its, well known, regulation of antioxidant genes [via its binding to antioxidant response element (ARE) of target genes] it also regulates proteasomal genes; and is implicated in mitochondrial biogenesis and removal (Tsakiri et al., 2013a, 2018). Several studies have shown the dysfunction of UPP,

ALP, chaperones and NRF2 signalling during aging [30,31]. Interestingly, genetic or pharmacological activation of the PN modules seems to increase health- and/or life-span and to confer protection against agerelated diseases [32,33]. Also, several natural products (NPs) (e.g. extracts or pure compounds) from various sources have been found to activate cytoprotective mechanisms in human cells or to exert health- and/or life-span promoting effects at *in vivo* models [27].

Most of OO biophenols have been explored for their biological activities *in vitro, in vivo* [34,35] and few of them in clinical trials [36,37]. Though, their biological properties depend on their absorption and metabolism in biological systems. Hydroxytyrosol (HT) and tyrosol (T) have an extensively investigated metabolism, with determined metabolic products and pharmacokinetic (PK) parameters [38–40]. However, limited data exist for secoiridoids due to the lack of commercially available standards and their laborious isolation through TPF.

Despite OLEO and OLEA having strong evidences for their positive impact to human health [13] the low availability of standard compounds confines the investigation in human system and study of their metabolism and absorption. Besides, their peculiar chemical structure, composing of two aldehydes and a sensitive ester bond make their detection almost unfeasible in biological systems. Few experimental protocols have been proposed for their detection in biological systems and until now these two compounds have not yet been detected or dubious results are generated due to the absence of an appropriate and sensitive methodology for their detection [41].

In a previous *in vitro* research authors suggested that the inability to detect secoiridoids derives from the fact that they are not absorbed in biological systems in the parental form [42]. They uncovered glucuronide conjugates of reduction derivatives coming from the parental

compounds probably formed during enterocytic transfer [42]. Other metabolic reactions have also been proposed namely hydrogenation, hydroxylation, and hydration for phase I metabolism and the generated OLEO products are further metabolized via phase II metabolism, i.e., glucuronidation, sulfation and methylation [43]. In the literature is generally accepted that secoiridoid aglycons are hydrolyzed in the acidic gastric environment in the stomach, leading to the increase of HT/T only 30 minutes after incubation in an *in vitro* rat intestinal model. As can be expected higher amounts of HT/T may be present in jejunum and ilioum than would be expected [44]. Apparently, there are no information concerning PK parameters of OLEO or OLEA and only one study has been found studying several secoiridoids in human urine 2-6 hours after OO intake.

Herein, we report a study aiming the investigation of the positive impact of TPF and secoiridoids, OLEO and OLEA on healthy aging-promoting PN pathways and the further exploration of OLEO PK parameters in a mouse model. Towards this purpose fractionation of TPF was carried out for the isolation of secoiridoids and more specifically OLEO and OLEA. After the conduction of standard *in vitro* assays to the isolated compounds, three TPFs corresponding to low, intermediate and high levels of both secoiridoid compounds, along with pure OLEO and OLEA were evaluated for their potential to activate cytoprotective PN modules in normal human foreskin BJ fibroblasts and mouse highly differentiated C5N keratinocytes, as well as at the *in vivo* experimental model of *Drosophila melanogaster*. Subsequently, pure OLEO was provided to a standard dose via ingestion to mice and plasma samples were collected in 10 time points for determination of metabolites PK parameters. Plasma extracts were analyzed via UPLC-HRMS/MS for metabolites identification and determination of their relative content in plasma.

2. Materials and Methods

2.1 EVOO selection for *in vitro* and *in vivo* assays

The selection of the appropriate EVOOs for isolation of biophenols in order to perform *in vitro* and *in vivo* experiments was based on a library containing over 400 TPF collected the period 2014-2016. TPFs were selected according to their concentration in OLEA and OLEO and the presence of other secoiridoid derivatives as well. Biophenols quantification was employed as described in detail in section 2.5 of chapter 1.

2.2 Biophenols isolation

2.2.1 EVOO extraction using CPE liquid-liquid extraction

The extraction was carried out as described by Angelis *et al*., [45]. In brief, the mobile phase was prepared by mixing *n*-hexane and EVOO (ratio 3:2 v/v). The stationary phase was prepared by mixing EtOH and H_2O (ratio 3:2 v/v). The FCPE column was filed at a flow rate of 75 mL/min and 200 rpm in ascending mode with the aqueous phase. The rotation speed was then increased up to 1000 rpm and the mobile phase (EVOO/*n*-hexane) (2.5 L) was pumped into the column at a flow rate of 60 mL/min, for the extraction step. Afterwards, the pumping mode was switched to descending and a volume of 0.3 L of fresh aqueous phase was pumped at 60 mL/min and 1000 rpm. The extracting aqueous phase containing phenolic compounds was then recovered. This cycle of extraction and recovery steps was repeated 7 times, of about 47 minutes each. The obtained aqueous phase was then evaporated to dryness under vacuum at 40^{o}C and yielded a viscous extract. The latter was then partitioned between *n*-hexane and acetonitrile (ACN) to remove the traces of remaining fat and stored at 4^{o}C for further use.

2.2.2 TPF fractionation via FCPC1000 apparatus

The experiment was performed on a preparative CPC column (1000 mL). For the fractionation solvent system of *n*-hexane/EtOAc/EtOH/H_2O was used. The column was initially filled with the lower phase, EtOH/H_2O, in ratio 2:3 v/v at a flow rate of 30 mL/min and a rotation speed of 300 rpm, in the ascending mode. Then, the column rotation was set at 900 rpm and the first mobile phase (MP1) (Table 4) was pumped at a flow rate of 20 mL/min. When the equilibration of the two liquid phases inside the CPC column was established (Sf = 65%), the sample (5 g of TPF dissolved in 30 mL of the first system *n*-hexane/EtOAc/EtOH/H_2O in proportion of 4:1:2:3 v/v) was injected through the sample loop. Then, a sequential pumping of the upper mobile phases MP1, MP2, MP3 and MP4 was performed in volumes of 500 mL,1100 mL, 1400 mL and 1000 mL respectively (elution step). Subsequently, the system was changed in descending mode passing 750 mL of fresh stationary phase in order to extrude the remaining stationary phase (extrusion step). Fraction collector was set to collect 25 mL fractions during experiment. The experiment lasted 240 min while all collected fractions (190 fractions) were analyzed by Thin Layer Chromatography (TLC) and pooled, based on chemical composition similarity, giving finally 17 combined fractions.

***Table 4**: Mobile phases 1-4 of the used solvent systems for CPC fractionation of TPF.*

Mobile phase	***n*-hexane/EtOAc**
MP1	4/1
MP2	3/2
MP3	2/3
MP4	1/4

2.2.3 Purification of CPC fractions using the adsorption mode on silica gel or size exclusion chromatography

The combined CPC fractions were further analyzed using low pressure column chromatography. As stationary phase normal phase Silica gel60H® (0.04–0.06 mm) was used diluted in dichloromethane (DCM) while the sample was subjected to the column as dray powder mixture with Silica gel 60® (0.08–0.12 mm). Mixtures of DCM, ethyl acetate (EtOAc) and MeOH in increasing polarity mode were used for the elution (i.e. DCM 100%, DCM:EtOAc 98:2 – 96:4 – 92:8 – 84:16 –68:32 – 36:64 v/v, EtOAc 100%, EtOAc:MeOH 50:50 v/v). All collected fractions (10 mL) were evaluated by TLC and those with the same chemical profile were pooled. Selected fraction containing secoiridoids with minor presence of co-eluting compounds were analyzed using size exclusion column chromatography with Sephadex LH-20® as stationary phase. The samples, diluted in 0.5 mL ethanol, were subjected to the column and eluted with ethanol. Fractions of 0.5 mL were collected during analysis and combined based on their TLC profile.

2.2.4 TLC, NMR and HRMS analysis

The TLC analysis was performed on Merck 60 F254 pre-coated silica gel plates and developed with DCM:MeOH 95:5 (v/v). The revelation was firstly achieved by using UV light at 254 and 365nm. TLC plates were then sprayed by a vanillin (5% w/v in MeOH)– H_2SO_4(50% v/v in MeOH) solution and heated at 100–120ºC for 2–3 minutes.

Structure confirmation or elucidation of the isolated compounds were achieved by NMR and HRMS analysis. All ^{1}H,^{13}C (1D-2D) NMR experiments were performed on a 600 MHz on a Bruker Avance AVIII-600 spectrometer (Karlsruhe, Germany) equipped with a TXI cryoprobe (Wissembourg, France) in $CDCl_3$ and CD_3OD. For HRMS analysis of isolated compounds a

hybrid LTQ-Orbitrap Discovery Mass Spectrometer (Thermo Scientific, Brehmen, Germany) was employed. The mass spectrometer was equipped with electrospray ionization (ESI) source and operated in negative mode (HRMS data in appendix).

2.5 Cell viability assay

Two different protocols were applied for cell viability evaluation of the isolated biophenols. For ligstroside aglycon isomers, elenolic ethyl ester isomers, elenolic acid and oleuropein aglycon, ATDC-5 cells (8×10^3/well, seeded in 96-well plates) were pre-incubated for 12 hours with the isolated compounds and then stimulated with them (1–50 μ*M*) in 5% FBS medium for 24 hours at 37°C. Then, cells were incubated with 10 μL of MTT (5 mg/mL) for 4 hours at 37°C. After dissolving the formazan, the spectrophotometric absorbance was measured using a microtiter enzyme-linked immunosorbent assay reader at 550 nm (Multiskan EX; Thermo Labsystems).

The effect of TPF and of pure OLEO and OLEA was performed by MTT and trypan blue dye exclusion assay. For the MTT assay, cells were treated with different concentrations of TPF, OLEO or OLEA for 48 h and, after removal of the medium, cells were incubated with 1 mg/ml by 3-(4,5-dimethylthiazol-2-yl)-2,5-diphenyltetrazolium bromide (MTT, Sigma-Aldrich) dissolved in serum-free, phenol red–free medium for 3–4 h. Then, the MTT solution was discarded and the formazan crystals were dissolved by isopropanol. Cell survival was estimated using the ratio of OD570 of treated cells to the controls. Cell viability was also assayed with the trypan blue dye (Thermo Scientific) on a hemacytometer after trypsinization by performing the trypan blue dye exclusion assay; the cytotoxicity threshold was arbitrarily set to 80% survival rates for normal human diploid fibroblasts (see Supplementary Material for the cell lines used and cell culture conditions).

2.6 Drosophila lines and used antibodies

The Oregon R *Drosophila* strain was used in this study. Transgenic flies overexpressing constitutively active InR (UAS-InR^{A1325D}; express a mutated constitutively active insulin receptor) were obtained from the Bloomington *Drosophila* Stock Center. Tubulin-GeneSwitch-Gal4 (tubGSGal4) flies express RU486-regulated Gal4 [upon dietary administration of RU486 (30 μM)] under the control of the tubulin enhancer (a generous gift from Prof. D. Bohmann, University of Rochester Medical Center, NY, USA). Flies stocks were maintained at 23 °C, 60% relative humidity on a 12-h light: 12-h dark cycle and were fed standard medium [46]. In all presented experiments only somatic tissues (after the removal of the gonads) were analyzed [30]. Based on the study of Deshpande et al. (2014) we assume that flies consumed the following amounts of OLEO/OLEA per day: OLEO, 400 nM (0.233 ng-1.4 ng), 200 nM (0.1165–0.7 ng), 100 nM (0.05825–0.35 ng); OLEA 400 nM (0.245–1.47 ng), 200 nM (0.1225–0.735 ng) and 100 nM (0.06125–0.3675 ng).

Primary antibodies against the 20S-α (sc-65755, 1:1000) and Rpn7 (sc-65750, 1:1000) *Drosophila* proteasome subunits, Gapdh (sc-25778, 1:1000) and the HRP-conjugated secondary antibodies (1:2000) were from Santa Cruz Biotechnology (Heidelberg, Germany). The polyclonal antibody against the *Drosophila* proteasome β5 subunit (Prosβ5, 1:4000) was a generous gift from Dr. Maria Figueiredo-Pereira (Dept of Biological Sciences, Hunter College of the City University of NY, USA).

2.7 Climbing and longevity assays

Climbing assays were performed as described before [47]. Briefly, thirty flies were placed in a 100 ml glass cylinder and were gently tapped to the bottom of the cylinder. The number of

flies that climbed above a 66 ml mark after 20 s was recorded; trials were performed at least in triplicates.

For longevity assays female and male flies (equal numbers per sex) were collected and cultured in vials containing (or not) various concentrations of the VOOs (enriched in polyphenols). Flies were transferred to vials with fresh food every 3‑4 days and deaths were scored daily. Statistical analyses and numbers of flies per experiments are reported in Table A12. For other assays 10 flies in total were used; 5 males and 5 females.

2.8 RNA extraction, cDNA synthesis and quantitative real time PCR (QPCR) analysis

Total RNA was extracted using the RNAiso Plus [Total RNA extraction Reagent, (TAKARA)], quantified with BioSpec-nano spectrophotometer (Shimadzu Inc.) and converted to cDNA with the Maxima First Strand cDNA Synthesis Kit for RT-qPCR (Thermo Scientific). Realtime PCR was accomplished with the Maxima SYBR Green/ROX qPCR Master Mix (Thermo Scientific) and the PikoReal 96 Real-Time PCR System (Thermo Scientific) (see also appendix).

2.9 Immunoblotting analysis, measurement of proteasome, cathepsins B, L enzymatic activities and reactive oxygen species (ROS)

Immunoblotting studies in dissected flies' somatic tissues were done as previously described (Tsakiri et al., 2013b). Primary and horseradish peroxidase-conjugated secondary antibodies were applied for 1 h at room temperature and immunoblots were developed by using an enhanced chemiluminescence reagent kit (GE Healthcare Amersham, Pittsburgh, PA, USA).

Proteasome or cathepsin peptidase activities in cells or flies somatic tissues were measured at a VersaFluor™ Fluorometer System (Bio-Rad laboratories, Hercules, CA, USA), as described previously [32,47].

Measurement of ROS levels was done as described previously [30] by using the CM-H_2DCFDA (Invitrogen, Carlsbad, CA, USA) dye. Fluorescent dichlorodihydrofluorescein was measured using a VersaFluor TM Fluorometer System (Bio-Rad Laboratories, Hercules, CA, USA) at excitation, 490 nm, and emission, 520 nm.

2.10 Statistical analysis of the bio-assays

Experiments were performed at least in duplicates (biological replicates). For statistical analyses the MS Excel and the Statistical Package for Social Sciences (IBM SPSS; version 19.0 for Windows) were used. Statistical significance was evaluated using one-way analysis of variance (ANOVA). Data points correspond to the mean of the independent experiments and error bars denote standard deviation (S.D.); significance at $P < 0.05$ or $P < 0.01$ is indicated in graphs by one or two asterisks, respectively. For flies' longevity/survival curves and statistical analyses, the Kaplan-Meier procedure and log-Rank (Mantel- Cox) test were used (see Table A12).

2.13 Pharmacokinetic experiment

2.13.1 Animal treatment

Age-matched, 8 to 10-week-old female BALB/c mice (20–25 g) were obtained from the breeding unit of Hellenic Pasteur Institute (HPI, Athens, Greece). Experimental protocol was approved by the Animal Bioethics Committee of the HPI, according to the regulations of the National Law 56/2013. Briefly, mice were intraperitonealy treated with 5 mg/Kg body weight

(b.w.) of OLEO. Ten time points were selected for blood collection and specifically at 0, 5, 15, 30 minutes and 1 h, 4, 6, 8, 12 and 24 h after OLEO administration. Samples were directly centrifuged for plasma obtainment and then kept at -80^{o}C, until analysis day.

2.13.2 Plasma sample preparation

Plasma samples were thawed in ice. After homogenization 50 μL of plasma were vortexed with cold ACN in ratio 1:4 (v/v) for 1 minute. Solutions were centrifuged at 4^{o}C for 12 minutes at 12.000 rpm. Supernatants were evaporated under vacuum conditions and centrifugation at 25^{o}C until the complete dryness of the pellets. The derived residues were diluted in 120 μL MeOH:H_2O 60:40 and analyzed via UPLC-HRMS.

2.13.3 Plasma UPLC-HRMS analysis

Plasma extracts were analyzed with a LC gradient consisted of H_2O with 0.1% formic acid (FA) (solvent A) and ACN (solvent B). The elution method started with 2% of B which stayed for 2 minutes. In the next 16 minutes B reached 100% and stayed for 2 minutes. Finally, at 21st minute, system returned to the initial conditions and stayed for 4 minutes for system equilibration. An Acquity UPLC Peptide BEH C18 (50 mm x 2.1 mm, 1.7 μm) column was used for the separation, with a stable temperature of 40°C. Measurements were performed with a total acquisition time of 25 minutes and a flow rate of 400 μL/min. The injection volume was 10 μL and the autosampler temperature was at 7°C.

Mass spectra were obtained in negative ion mode using an electrospray ionization source (ESI). The capillary temperature was set at 350°C, capillary voltage at -10 V and tube lens at -40 V. Sheath and auxiliary gas were adjusted at 40 and 10 arb, respectively. For the ionization, capillary temperature was set at 350°C, capillary voltage at -30 V and tube lens at -100 V. Sheath

and auxiliary gas were adjusted at 40 and 10 arb, respectively. Mass spectra were recorded in full scan mode in the range of 115-1000 *m/z*, with resolving power 30,000 at 500 *m/z* and scan rate 1 microscan per second. HRMS/MS experiments were obtained in data-depending method with collision energy 35.0% (q = 0.25). The system was calibrated externally.

2.14 Structure elucidation workflow

Initially, full-scan chromatograms and their corresponding HRMS spectra (< 2 ppm) were investigated. Extraction ion method was used in parallel with peak-to-peak selection affording the corresponding full scan spectra. Suggested Elemental Composition (EC) of each detected peak together with isotopic patterns and ring double bond equivalent (RDBeq) values were further used to confirm the proposed structures. Additionally, HRMS/MS spectra contributed to the identification of specific chemical entities based on in-house databases. Furthermore, on-line databases were used for additional structural information. More specifically, Human Metabolome Data Base (HMDB) (http://www.hmdb.ca/), METLIN Metabolomics Database (https://metlin.scripps.edu/), Kyoto Encyclopedia of Genes and Genomes (KEGG) (https://www.genome.jp/kegg/) and ChemSpider free chemical structure database (http://www.chemspider.com/). The obtained data were compared with those previously reported in literature.

3. Results and Discussion

3.1 EVOO selection for biophenols isolation and performance of biological assays

In the current part of the study TPF and secoiridoid derivatives were evaluated with *in vitro* tests and *in vivo* models. A prerequisite for the conduction of the biological experiments is the isolation of compounds of interest in high amounts and purity. For this reason, an experimental workflow was designed, aiming the isolation of secoiridoid derivatives characterized by high pharmacological interest. Moreover, three different TPFs were tested characterized by different concentration in specific molecules (OLEO and OLEA).

The first step of our workflow was the selection the appropriate OO sample, which was rich in biophenols and consequently could provide different derivatives in high amounts. In more detail, for the biological evaluation of TPF as well as pure OLEO and OLEA, three TPFs were selected based on their concentration in these compounds. The selection was based on quantification results conducted for OLEO, OLEA, HT and T from an in house library containing over 400 OO from different areas of Greece and two harvesting periods. For this purpose, a TPF with high (OLE 110), medium (OLE166) and low (OLE 122) levels of OLEA and OLEO were selected for the performance of the *in vivo* biological experiments (figure 15). The quantification results are presented in detail in appendix (Table A5). Moreover, TLC analysis was carried out with the method described previously in section 2.2.4 for the observation of TPF biophenols composition in UV light and visible. Based on TLC and HPLC-DAD chromatograms, sample with code OLE 110 was also rich in ligstroside and oleuropein aglycons, which correspond to the close forms of OLEO and OLEA respectively. For this reason, OLE 110 was used as raw material for the isolation of open and close forms of secoiridoids. The figure below illustrates the HPLC-DAD chromatogram of the selected EVOOs.

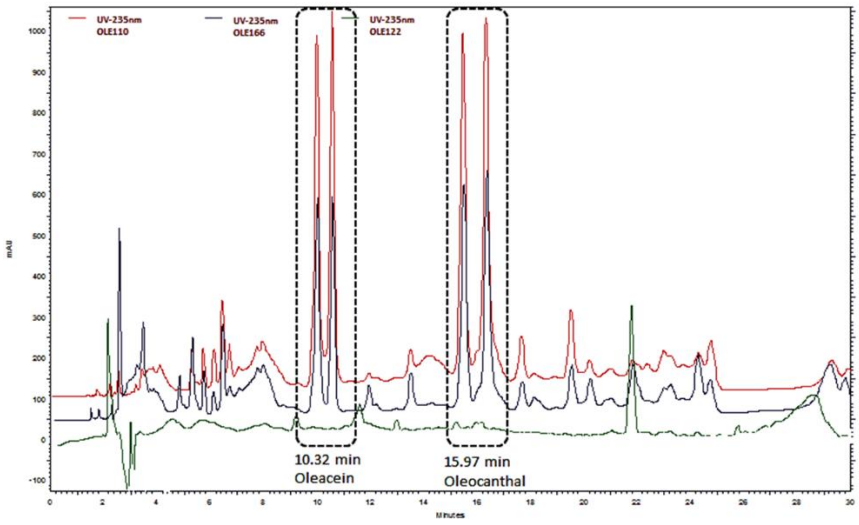

Figure 15: *HPLC-DAD chromatogram at 235 nm of the selected TPFs characterized by high-red line (OLE110), medium-blue line (OLE166) and low-green line (OLE122) levels of OLEO and OLEA.*

3.2 Isolation of biophenols

First step was the selection of EVOO rich in biophenols for the isolation of secoiridoids. Thus, OLE 110, which is characterized by high OLEO and OLEA content as well as other secoiridoid compounds was selected. After extraction and fractionation (section 2.2.1 and 2.2.2) targeted isolation of OLEO and OLEA as well as aglycons of ligstroside and oleuropein (opened and closed forms) was carried out. The purpose of this targeted isolation was the comparison of the activity of the opened and closed forms of secoiridoid derivatives. It is important to note that there limited studies for the biological properties of such compounds. Moreover, EA derivatives such as EA esters were isolated, due to their recent report and isolation from EVVO [48] and the absence of studies investigating its biological activities. EA was also isolated for comparison purposes.

From CPC performance, 17 phenolic fractions were derived based on elutes compositional similarities. Fractions were grouped according to their TLC results in UV light and visible. The

total number of fractions were analyzed via ^{1}H-NMR, UHPLC-HRMS and TLC for biophenols identification and subsequent targeted isolation of compounds. The figure below illustrates the TLC plate of the total number of CPC fractions annotated with the detected compounds intended for isolation.

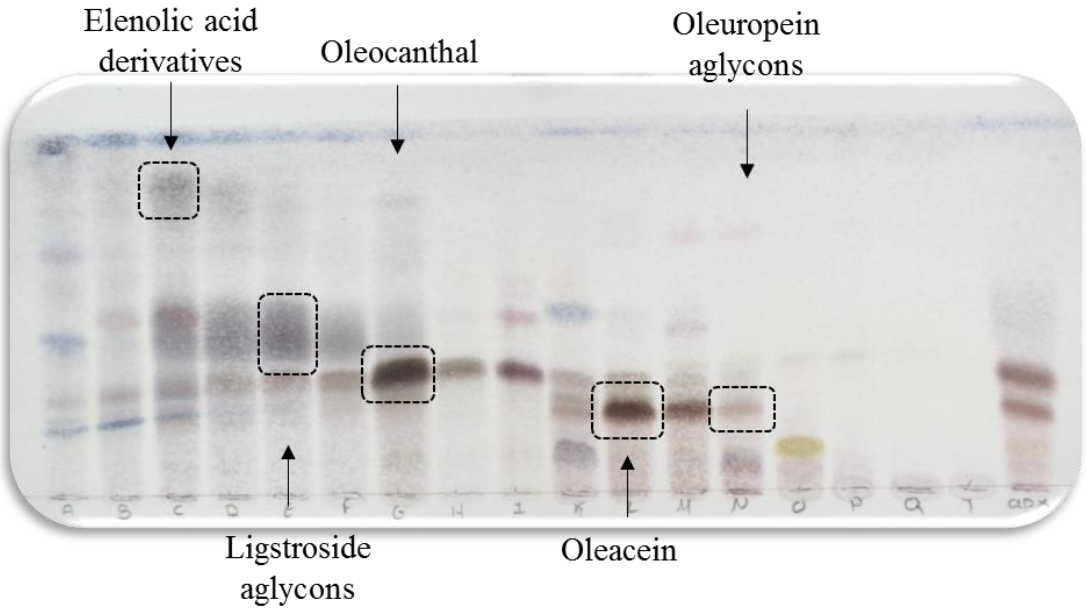

***Figure 16**: TLC analysis of CPC fractions. Plate is visualized after spraying with sulfuric vanillin and heating at 120°C.*

In order to isolate the annotated compounds of figure 16, the selected CPC fractions were subjected to further purification using silica gel and size exclusion column chromatography (section 2.2.3). In brief, fraction C was rich in iridoids and specifically in EA derivatives. Particularly EA and EA ethyl ester were isolated from this fraction. EA ethyl ester (5S, 8R, 9S) (PPh3) was isolated in high purity and as a mixture of two isomeric forms (5S, 8R, 9S / 5S, 8S, 9S 50/50) (PPh4). From the same fraction EA was isolated in high purity (PPh5).

Fraction E was rich in ligstroside aglycon derivatives. From this fraction, mixtures of two isomers of the monoaldehydic form of ligstroside aglycon (MFLA) were isolated. The one

fraction contained the isomer 5S, 8R, 9S and 5S, 8S, 9S in ratio 60/40 (PPh1) and the other fraction the two isomers in ratio 85/15 (PPh2). An isomer of monoaldehydic form of oleuropein aglycon (MFOA) was isolated from fraction N (PPh7).

Moreover, OLEO and OLEA were isolated from fractions G and K respectively. The figure below illustrates the chemical structures of the isolated compounds.

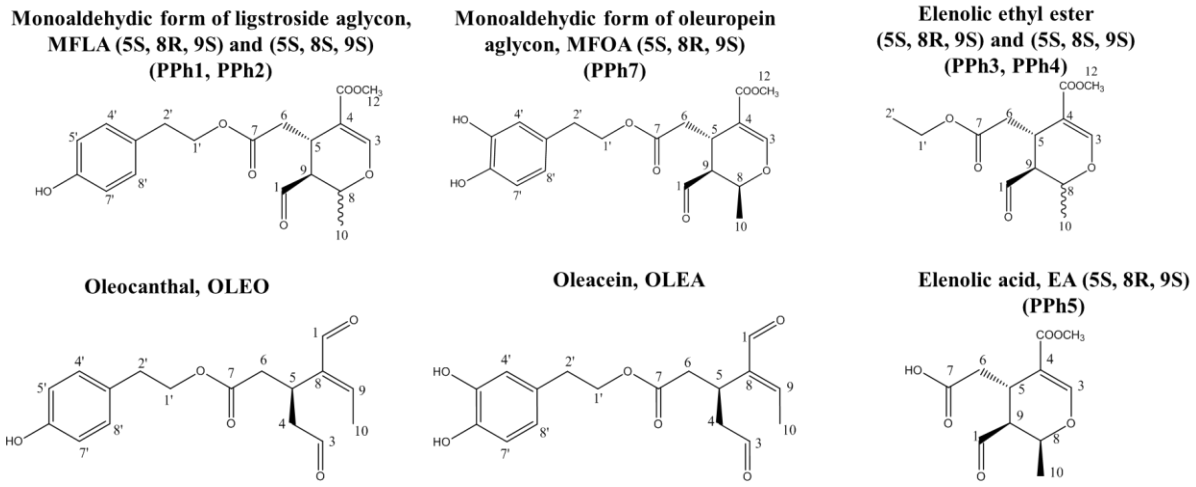

Figure 17*: Isolated compounds via CPC fractionation.*

The structure elucidation of the isolated compounds was achieved by (1D-2D) NMR and HRMS analysis. The table below presents in detail the ^{1}H-NMR spectroscopic data of the isolated isomeric forms 5S, 8R, 9S and 5S, 8R, 9S. Tables including the ^{1}H-NMR data of all the isolated compounds are presented in appendix (Tables A6-A11).

Table 5: *^{1}H-NMR data of 5S,8R,9S and 5S,8S,9S isomers of isolated elenolic acid and secoiridoid derivatives.*

	Elenolic acid	**Elenolic acid ethylester**		**MFLA**		**MFOA**	
Pr. No	**(5S,8R,9S)**	**(5S,8R,9S)**	**(5S,8S,9S)**	**(5S,8R,9S)**	**(5S,8S,9S)**	**(5S,8R,9S)**	**(5S,8S,9S)**
1	9.64 brd, *J*=2.0 Hz	9.63 brd, *J*=2.0 Hz	9.63 brd, *J*=2.0 Hz	9.48 brd, *J*=2.0 Hz	9.55 brs	9.54 brd, *J*=2.0 Hz	9.60 brd, *J*=2.0 Hz
3	7.59 brs	7.58 brs	7.64 brs	7.56 brs	7.61 brs	7.59 brs	7.65 brs
5	3.43 ddd, *J*=9.5/6.1/3.6 Hz	3.42 ddd, *J*=9.5/6.1/3.6 Hz	3.37 brd, *J*=11.1 Hz	3.38 ddd, *J*=9.5/6.1/3.6 Hz	3.33 brd, *J*=11.1 Hz	3.40 ddd, *J*=9.5/6.1/3.6 Hz	3.36 brd, *J*=11.1 Hz
6a	2.87 dd *J*=16.1/3.6 Hz	2.90 dd *J*=16.1/3.6 Hz	2.91 dd *J*=16.1/2.9 Hz	2.88 dd *J*=16.1/3.6 Hz	2.89 dd *J*=16.1/3.0 Hz	2.88 dd *J*=16.1/3.6 Hz	2.86 dd *J*=16.1/3.0 Hz
6b	2.54 dd *J*=16.1/9.5 Hz	2.56 dd *J*=16.1/9.5 Hz	2.24 dd *J*=16.1/11.1 Hz	2.53 dd *J*=16.1/9.5 Hz	2.20 dd *J*=16.1/11.1 Hz	2.55 dd *J*=16.1/9.5 Hz	2.20 dd *J*=16.1/11.1 Hz
8	4.49 qd *J*=6.7/6.1 Hz	4.41 qd *J*=6.7/6.1 Hz	4.20 qd *J*=6.7/2.0 Hz	4.41 qd *J*=6.7/6.1 Hz	4.14 qd *J*=6.7/2.0 Hz	4.48 qd *J*=6.7/5.7 Hz	4.20 qd *J*=6.7/2.0 Hz
9	2.72 td *J*=6.7/1.8 Hz	2.72 td *J*=6.7/1.8 Hz	2.64 ddd *J*=2.9/2.0/1.8 Hz	2.53 td *J*=6.1/1.8 Hz	2.48 ddd *J*=2.9/2.0/1.8 Hz	2.64 td *J*=5.7/1.8 Hz	2.62 ddd *J*=2.9/2.0/1.8 Hz
10	1.44, 3H, d *J*=6.7 Hz	1.42, 3H, d *J*=6.7 Hz	1.57, 3H, d *J*=6.7 Hz	1.37, 3H, d *J*=6.7 Hz	1.53, 3H, d *J*=6.7 Hz	1.41, 3H, d *J*=6.7 Hz	1.57, 3H, d *J*=6.7 Hz
12	3.73, 3H, s	3.72, 3H, s	3.73, 3H, s	3.71, 3H, s	3.72, 3H, s	3.75, 3H, s	3.78, 3H, s
1’		4.12, 2H, q, *J*=7.10 Hz	4.12, 2H, q, *J*=7.10 Hz	4.25, 2H, m	4.28, 2H, m	a)4.33, m b)4.23, m	a)4.38, m b)4.28, m
2’		1.24, 3H, t, *J*=7.10 Hz	1.26, 3H, t, *J*=7.10 Hz	2.84, 2H, t, *J*=7.10 Hz	2.85, 2H, t, *J*=7.10 Hz	2.82, 2H, m	2.82, 2H, m
4’				7.04 d, *J*=8.5 Hz	7.04 d, *J*=8.5 Hz	6.79 d, *J*=2 Hz	6.85 d, *J*=2 Hz
5’				6.76 d, *J*=8.5 Hz	6.76 d, *J*=8.5 Hz	-	-
7’				6.76 d, *J*=8.5 Hz	6.76 d, *J*=8.5 Hz	6.81 d, *J*=8.5 Hz	6.82 d, *J*=8.5 Hz
8’				7.04 d, *J*=8.5 Hz	7.04 d, *J*=8.5 Hz	6.63 dd, *J*=8.5/2.0 Hz	6.76 dd, *J*=8.5/2.0 Hz

3.3 Cell Viability assay

MTT assay was initially employed for the evaluation of the effect of the isolated biophenols in cell viability. Cells were treated with increasing concentrations of the isolated compounds from 0.1-50 μM. The table below represents the tested compounds and the corresponding labeling used in MTT assay.

Table 6*: List of the isolated compounds with the corresponding labeling used for MTT assay.*

Compound	**Code**
Aldehydic form of ligstroside aglycon 5S, **8R**, 9S 60% 5S, **8S**, 9S 40%	PPh1
Aldehydic form of ligstroside aglycon 5S, **8R**, 9S 85% 5S, **8S**, 9S 15%	PPh2
Elenolic acid ethyl ester 5S, 8R, 9S	PPh3
Elenolic acid ethyl ester 5S, **8R**, 9S 50% 5S, **8S**, 9S 50%	PPh4
Elenolic acid 5S, 8R, 9S	PPh5
Aldehydic form oleuropein aglycon 5S, 8R, 9S	PPh7

Figure 18 illustrates the results from MTT assay after 24 hours cells incubation with ligstroside aglycon derivatives (PPh1 and PPh2). As can be observed, the initial concentration affecting cells viability for both samples was found 1 μM for PPh1 and 10 μM for PPh2. At 10 μM PPh1 and PPh2 appeared to induce cell death while all the tested above concentrations i.g. 25 and 50 μM showed a significant decrease at cell number. It is interesting that PPh1,

containing the two isomers almost in the same percentage, at 50 μM is highly toxic for the cells (P< 0.001), while PPh2 was toxic but not in the same level. Presumably, the higher concentration of 8S isomer in PPh1 seems to be more important instigating that compared to 8R might be more potent. Both samples, PPh1 and PPh2 seem to affect ATDC5 cells in a dose-dependent manner.

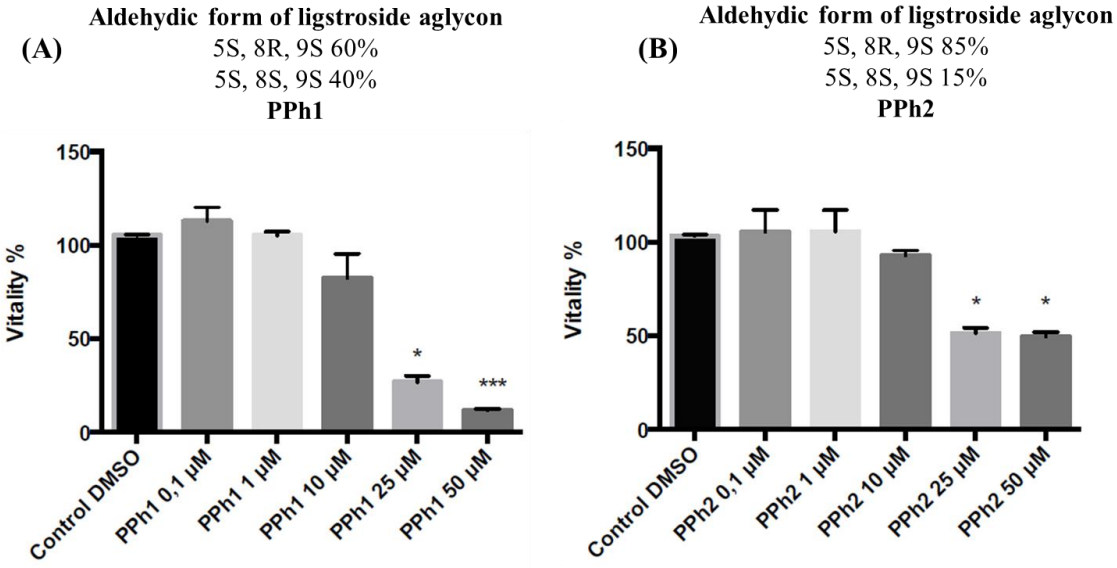

Figure 18: *MTT assay. (A): Relative (%) vitality of ATDC5 cells treated with increasing concentrations (0.1, 1, 10, 25 and 50 μM) of PPh1 for 24 h through MTT. (B): Relative (%) viability of ATDC5 cells treated with increasing concentrations (0.1, 1, 10, 25 and 50 μM) of PPh2 for 24 h through MTT. Values are the mean of 3 independent replicates. ***=P< 0.001, *=P<0.05.*

Continuously, EA ethyl ester isomers (PPh3 and PPh4) were tested. In has to be noted that there are not previously published studies investigating the biological properties as well as the cytotoxic effect of EA ethyl ester isomers. The exhibited concentrations of figure 19, demonstrated that both fractions (PPh3 & PPh4) had no toxicity effect to cells even at the highest concentration. The concentration of 10 μM PPh3 and PPh4 seemed to affect the viability but no significant results were uncovered for the pure compound and the mixture of isomers. Figure 19

illustrates the corresponding results.

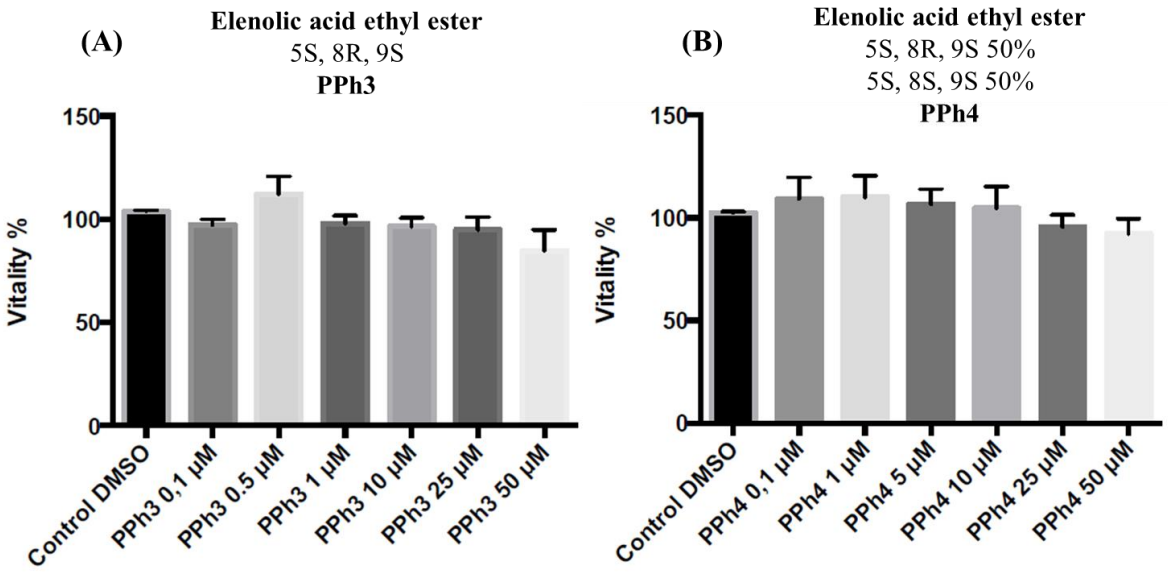

Figure 19: *MTT assay. (A): Relative (%) vitality of ATDC5 cells treated with increasing concentrations (0.1, 1, 10, 25 and 50 μM) of PPh3 for 24 h through MTT. (B): Relative (%) viability of ATDC5 cells treated with increasing concentrations (0.1, 1, 10, 25 and 50 μM) of PPh4 for 24 h through MTT. Values are the mean of 3 independent replicates.*

Lastly PPh5 and PPh7 were tested for their toxicity effect in ATDC5 cells. PPh5 as can be expected followed the same pattern like PPh3 and PPh4 due to their chemical structure similarities. The concentration of 10 μM PPh5 seem to induce cell proliferation up to the concentration of 100 μM, without showing any toxic affect. Concerning PPh7, it followed the similar pattern to PPh1 and PPh2. The concentration of 1 μM was found as critical, affecting cells vitality. At 5 μM a considerable decreased was observed, while 50 and 100 μM affected significantly cells vitality ($P<0.05$), following a dose response pattern.

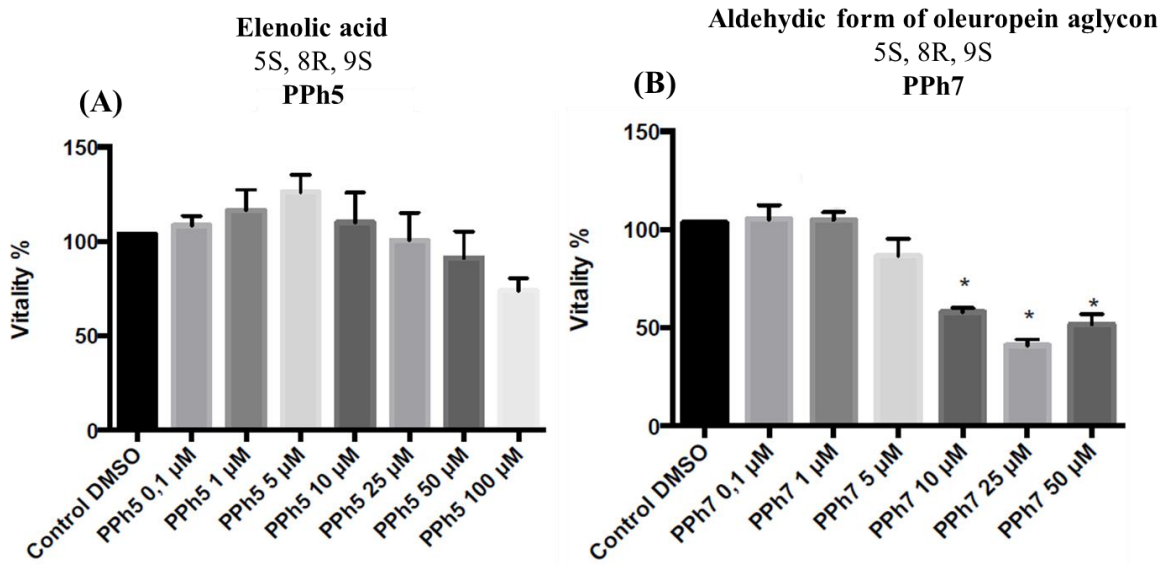

Figure 19': *MTT assay. (A): Relative (%) vitality of ATDC5 cells treated with increasing concentrations (0.1, 1, 10, 25 and 50 μM) of PPh5 for 24 h through MTT. (B): Relative (%) viability of ATDC5 cells treated with increasing concentrations (0.1, 1, 10, 25 and 50 μM) of PPh7 for 24 h through MTT. Values are the mean of 3 independent replicates. *=P<0.05.*

To summarize it seems that secoiridoid aglycons (oleuropein and ligstroside aglycons) were characterized by the highest cytotoxicity to ATDC5 cells in comparison to the other tested compounds missing the phenylalcohol part, instigating their effect. More specifically, MFLA found to be the most potent compound of all tested samples. EA and EA ethyl ester found to be inactive in any concentration. Exploring the role of 8R vs 8S isomers, the testing of isomeric forms (5S, 8R, 9S / 5S, 8S, 9S) in 50/50 ratio found as more effective in cells, while pure 5S, 8R, 9S isomers or in fractions with this isomer in high ratio were not found so active. Based on the above outcomes, it can be hypothesized that the existence of the phenylalcohol part in biophenols seems to induce the death of ATDC5 cells, and more specifically 8S diastereoisomer engendered a more notable decreased in cells number. Thus, it can be assumed that 8S diastereoisomer of secoiridoid aglycons could behave as more potent agent for decreasing

ATDC5 cells number. Concerning, the substitution of the benzol ring, 8R isomer of MFOA (existence of two hydroxyl groups in the benzol ring) were found more active in comparison to the sample with high ratio of 8R isomer of MFLA. Generally, 3,4-dihydroxy substitution in phenols have been previously reported as stronger antioxidants agents in comparison to 4-hydroxy substitution [49]. Overall, 8S isomers and 3,4-dihydroxy substitution in the benzol ring can be suggested as factors affecting secoiridoids aglycon activity. The no cytotoxic selected doses for the tested compounds were: 1 μM for PPh1, PPh2, PPh7 and 10 μM for PPh3, PPh4, PPh5. The isolated oleacein and oleocanthal were tested via MTT assay and discussed in more detail below in section 3.4.1

3.4 Effects of EVOOs on cellular and *in vivo* models

Mediterranean diet is considered as one of the healthiest diets and its cardioprotective role is well documented [50]. EVOO consumption is directly associated with MD comprising the main source of fat in MD. Studies have shown that adherence to MD reduce the expression of oxidative stress and inflammation markers [51] and is also associated with reduced incidences of metabolic syndrome [52] and type 2 diabetes [53]. Given the reported health-promoting effects of EVOOs and of Mediterranean diet, as well as that genetic or pharmacological activation of the PN modules suppressed cellular senescence or enhanced healthy aging in various models [32,33] we asked whether EVOOs also affect cytoprotective proteostatic cellular modules. Bio-guided studies of TPFs with different levels of OLEO and OLEA and of pure compounds were performed in both mammalian cells, as well as after oral administration in *Drosophila* flies.

3.4.1 Analysis of TPF, OLEO and OLEA effects in mammalian cells

We initially studied the effect of TPF (Ole110) on the viability of normal human skin fibroblasts (BJ cells) by using the MTT and trypan blue dye exclusion assays. To this end, cells

were incubated with increasing concentrations of TPF (0.1, 1, 5 and 10 μg/mL) for 48 h and, as shown in both figure $A25_{A1}$ and $A25_{A2}$, TPF did not exert any toxicity in BJ cells. Then, we sought to examine the effect of TPF on PN modules related genes. Thus, BJ cells were incubated with TPF at the maximum (non toxic) concentration of 10 μg/mL for 24 h. As can be seen in figure $A25_B$, Q-PCR analyses showed that TPF upregulated the proteasomal subunits genes *PSMA7*, *PSMB2*, *PSMB5* and *RPN11* and the autophagylysosome related gene *CTSD*. Moreover, incubation of cells with TPF resulted in the upregulation of molecular chaperones genes (*HSP70* and *CLU*) and also of genes being involved in cellular antioxidant responses, namely *NRF2* along with downstream transcriptional targets of NRF2, i.e. the *KEAP1* and *TXNRD1* genes (figure $A25_C$). Considering the induction of the PN modules, we then asked whether TPF could protect cells from H_2O_2-mediated oxidative stress toxicity. Cells were exposed to 200 μM H_2O_2 for 24 h in the presence or absence of 10 μg/mL TPF and the viability was measured by the MTT assay. As can be seen in figure $A25_D$, TPF conferred significant protection against H_2O_2-mediated toxicity. In previous studies, olive oils which contained the two phenolic compounds OLEO and OLEA showed increased H_2O_2 scavenging activity [54]. Furthermore, according to other studies, natural compounds or peptides, such as Platanoside, Tiliroside and Hexapeptide-11 have been found to enhance the proteasome activity, reduce the oxidative stress and thus, have anti-aging properties [32,55].

Furthermore, BJ cells were treated with different concentrations (50, 100, 150 and 200 μ M) of OLEO or OLEA for 48 hours and, by MTT (figure $A26_{A1}$ and $A26_{B1}$) and trypan blue dye exclusion (figure $A26_{A2}$ and $A26_{B2}$) assays, we found that both OLEO and OLEA were relatively not toxic (toxicity threshold was set to 80% viability) in BJ cells up to 50 μM as revealed by both assays; OLEO exerted significant toxicity on BJ cells only at increased concentrations (IC50 106

μM) (figure $A26_{A1}$). To examine if the compounds alter the proteasome activity, BJ cells were treated with 30 μM OLEO and/or 30 μM OLEA for 24 hours. As shown in figure $A26_C$, OLEO did not affect the three peptidase activities of proteasome, whereas OLEA was found to induce the rate limiting for protein breakdown proteasome peptidase activity, i.e. the chymotrypsin-like activity (CTL). In line with this finding, Q-PCR analyses revealed that treatment of BJ cells with OLEA at the concentration of 30 μM for 24 hours promoted the upregulation of PN related genes, i.e. proteasome (*PSMB2, PSMB5* and *RPN11*), ALP (*HDAC6*, *BECN1*, *LC3B* and *CTSD*), antioxidant responses (*NQO1*, *TXNRD1* and *KEAP1*) and molecular chaperones (*HSF1*, *HSP27*, *HSP70*, *CLU* and *STUB1*) genes (figure A27). Thus, as reported before [56] and shown herein the induction of proteasome due to OLEA could be (among others) attributed to NRF2 activation. Finally, we sought to evaluate whether these compounds could protect (similarly to the TPF extract) cells against H_2O_2 (oxidative stress) toxicity. To this end, BJ cells were treated with 200 μM H_2O_2 for 24 hours in the presence or absence of 30 μM OLEO or 30 μM OLEA and the viability was measured by the MTT assay. As it can be seen in figure $A26_D$, OLEA largely rescued BJ cells from H_2O_2-mediated oxidative stress toxicity.

We then examined the effects of OLEO and OLEA in an additional mammalian cellular model, namely mouse skin immortalized (highly differentiated) C5N cells. Cells were treated with increasing concentrations of OLEO (5, 15, 25, 50 and 100 μM) or OLEA (5, 25, 50 and 100 μM) for 48 hours and survival was estimated by MTT (figure $20A_1$ and $20B_1$) and trypan blue dye exclusion (figure $20A_2$ and $20B_2$) assays. Neither OLEO nor OLEA were significantly toxic in C5N cells up to a concentration of ~10 μM (figure 20A and 20B), as revealed by both cell viability assays. The IC50 for OLEO and OLEA was estimated to be 30 and 40 μM, respectively, for C5N cells by performing MTT assay. Also, both OLEO and OLEA activated the three

proteasomal peptidases activities after 48 hours of incubation (figure 20C) and tended to increase the lysosomal cathepsin peptidases activities; however, this increase was not statistically significant (figure 20D). Thus, proteasome activation by OLEO and OLEA is not cell- or species-specific.

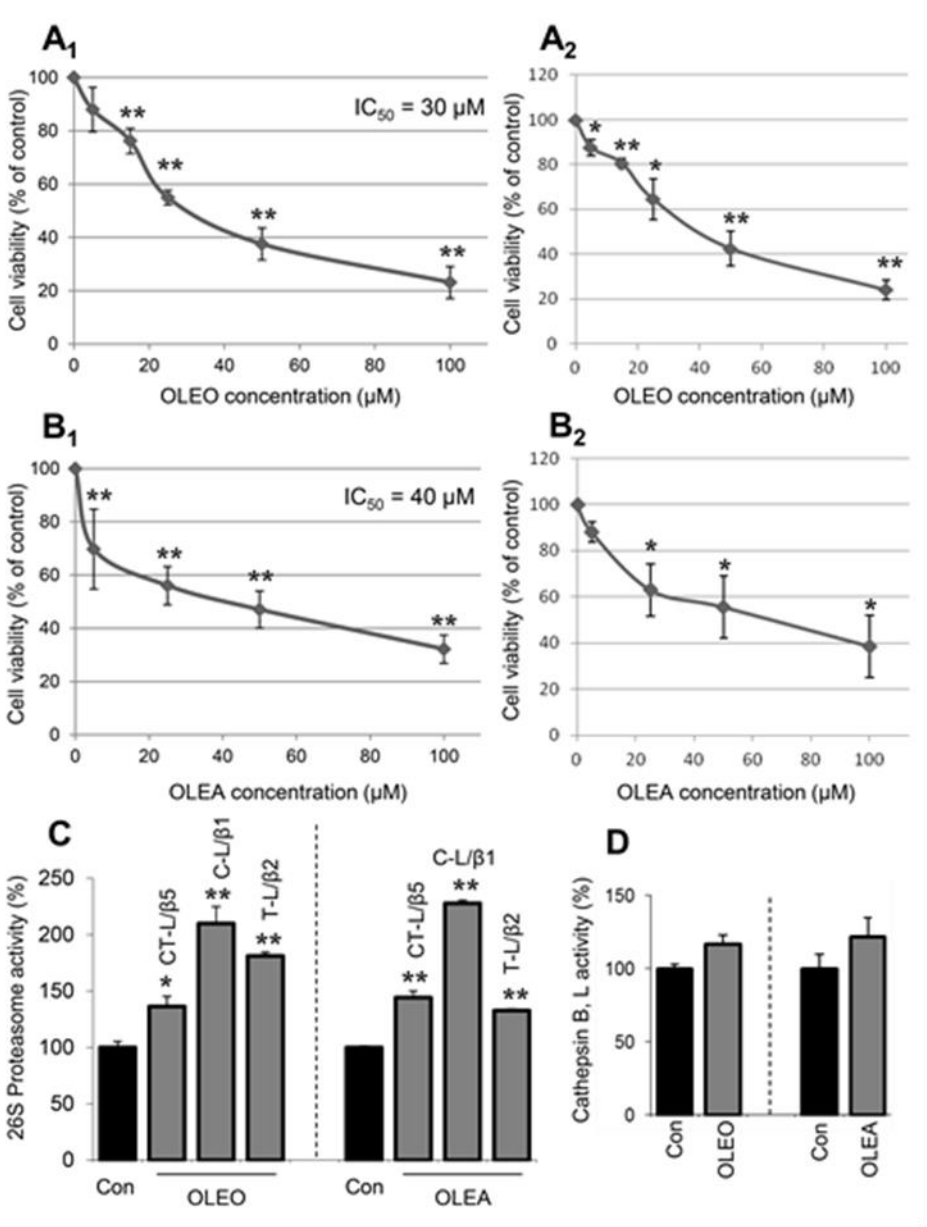

Figure 20: *Exposure of C5N cells to OLEO or OLEA does not exert toxicity (at low concentrations) in C5N cells and it activates proteasome. (A) Relative (%) cell viability of C5N cells incubated with increasing concentrations (5, 15, 25, 50 and 100 µM) of OLEO for 48 h*

*through MTT (A_1) and trypan blue dye exclusion (A_2) assays. (B) Relative (%) survival of C5N cells treated with increasing concentrations (5, 25 50 and 100 μM) of OLEA for 48 h through MTT (B_1) and trypan blue dye exclusion (B_2) assays. (C) Enzymatic activities of the three (CT-L/β5, C-L/β1 and T-L/β2) proteasomal peptidases activities in C5N cells treated with 30 μM OLEO or 40 μM OLEA for 48 h. Shown controls refer to control values of CT-L/β5 of the sample OLEO or OLEA. In all cases, standard deviation did not affect the shown significance of the other samples. (D) Relative (%) cathepsin B, L activities following exposure of C5N cells to 30 μM OLEO or 40 μM OLEA for 48 h. Proteasome and cathepsin activities were expressed in fluorescence units per μg of input protein vs. controls set to 100%. Bars, ± SD. *, P<0.05; **, P<0.01.*

3.4.2 Analysis of short- and long-term effects of OLEO or OLEA after oral administration in *Drosophila* flies

We then investigated the *in vivo* effects of OLEO and OLEA (added in the culture medium as food supplements) on proteostatic modules activity and physiology of *Drosophila* flies. *Drosophila* could be considered as a suitable organism to evaluate the biological properties of compounds or extracts. *Drosophila melanogaster* has similar metabolic pathways and proteasomes to mammalian organisms and also a large number of population can be cultured in a short period. Additionally, it is characterized by a short lifespan which is easily controlled. Due to the fact that the administration is carried out through food, *Drosophila* could serve as a model organism to investigate supplements and generally orally administered active entities.

OLEO had no effect on flies' appetite (gustatory assay), whereas for OLEA we noted a mild reduction (not shown). We observed that dietary administration of OLEO or OLEA increased the CT-L proteasome activity (figure $A28_A$) and the expression of 20 S (Prosβ5 and α-type subunits) and 19 S (Rpn7) proteasomal subunits (figure $A28_B$); notably, OLEA induced a stronger activation effect on proteasome than OLEO. Moreover, feeding of flies with OLEO or OLEA led to a significant decrease of ROS levels (in almost all tested concentrations) in somatic tissues of *Drosophila* flies (figure $A28_C$). The protective effects of these compounds were also

evident by the noted delay of the age-related decline of flies' locomotor performance (figure $A28_D$). Thus, dietary OLEO and OLEA at the doses used activate cytoprotective and healthy-aging promoting mechanisms.

Considering these findings and given the reported anti-atheroclerotic and anti-diabetic action of VOO [57] we focused on the model of transgenic flies expressing ubiquitously a constitutively active form of InR ($InRA^{1325D}$). This genetic intervention increased triglycerides in flies' fat body and promoted inflammatory responses [58]; thus, this model phenocopies some of the features seen in mammalian obesity and diabetes type 2. We found that flies with aberrant insulin signalling had a significantly reduced longevity (figure 21A).

Interestingly, addition of TPFs enriched with increased concentration of OLEO or OLEA resulted in higher proteasomes activities in the somatic tissues of flies fed with 10 μg/mL OLE 166 (medium levels of OLEO and OLEA) or with either 1 or 10 μg/mL of OLE 110 (high levels of OLEO and OLEA) (figure 21B). Moreover, sustained feeding of flies with 10 μg/mL OLE 122 (medium levels of OLEO and OLEA), OLE 166 (medium levels of OLEO and OLEA) and OLE 110 extended the lifespan of $InRA^{1325D}$ overexpressing transgenic flies (figure 21C); notably, OLE 166 and OLE 110 suppressed the toxic effects of InRA1325D overexpression more effectively than OLE 122 (low levels of OLEO and OLEA). In support to the herein reported anti-inflammatory activity of EVOOs rich in polyphenols, it has previously been found that OLEO inhibited COX-1, COX-2, Tumor necrosis factor-alpha (TNF-a) and Interleukin-1 beta (IL-1b) activity, as well as nitric oxide (NO) production in macrophages [59]. Additionally, OLEO causes necrotic and apoptotic cell death in cancer cell lines, reduces invasive capacity of breast cancer cell lines and inhibits proliferation of multiple myeloma cells [60]. Finally, it has been found that OLEO reduces Aβ accumulation both *in vitro* and *in vivo*, inhibits Tau

fibrilization and protects neurons from the synaptopathological effects of toxic oligomers [59]. Therefore, OLEO has been suggested as a lead compound for development in Alzheimer's disease therapeutics; our finding of OLEO-mediated proteasome activation reveals a novel mechanism that could contribute to anti-neurodegenerative effects of EVOOs. TPFs with different contents of OLEO or OLEA increase proteasome activity and partially rescue the longevity of a *Drosophila* model of reduced lifespan due to overexpression of a constitutively active InR.

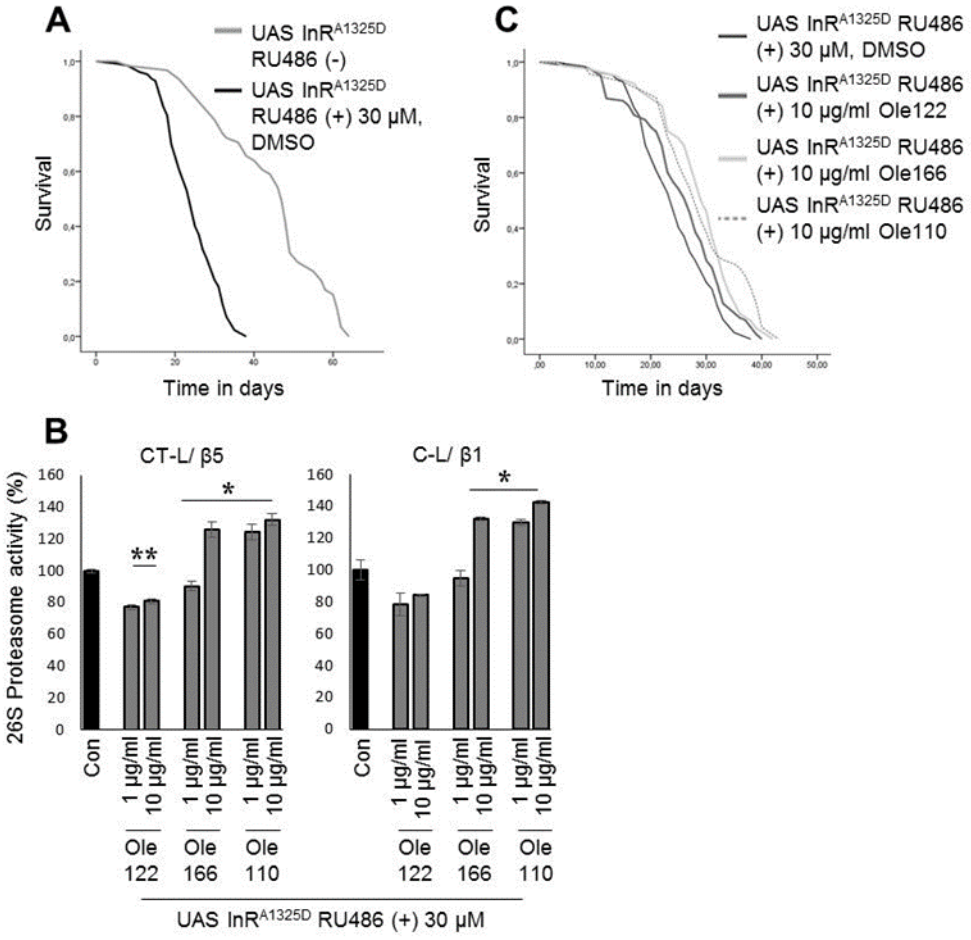

Figure 21*: (A) Longevity curves of transgenic flies overexpressing or not a constitutively active InR. (B) Relative (%) chymotrypsin-like activity (CT-L/β5) and caspase-like (C-L/β1) proteasomal activities in somatic tissues of young transgenic flies following exposure to the indicated concentrations of TPFs for 18 days. (C) Longevity curves of transgenic flies overexpressing a constitutively active InR and fed with 10 µg/ml of TPFs. The transgene was*

switched on by the addition of 30 μM RU486 in fly food. Flies median lifespan and comparative statistics are reported in Table S3; the longevity curves of UAS InR^{A1325D} RU486(+) 30 μM, DMSO in (A), (C) are the same. TPFs with low (122), medium (166) and high (110) content of OLEO or OLEA are reported as OLE 122, OLE 166 and OLE 110, respectively.

In this study, we provide novel data for the healthy aging-promoting effects (e.g. proteasome activation or delay of age-related locomotion decline) of TPFs (OLE 122, 166 or 110) or pure compounds (OLEO or OLEA) in the fly model. In support, it was shown by Parzonko et al. (2013) [56] that OLEA decreased the intracellular ROS formation, since its biological action has been related to NRF2 activation. In consistence with the aforementioned findings, we observed decreased levels of ROS in OLEA-treated flies and also upregulation of proteasome protein subunits; the reduced oxidative stress and the increase of proteasome expression in OLEA- (and OLEO-) treated flies could be possibly due to NRF2 activation, as NRF2 is a main regulator of antioxidant response and proteasome in flies [47]. It was also recently proposed that OLEO can act as HSP90 inhibitor [61]. This finding could explain the partially rescue of TPFs in transgenic flies that overexpress a constitutively form of InR, as HSP90 seems to be indispensable to the homodimerization of monomeric InR precursor [62,63]. Therefore, in TPFs treated transgenic flies the active forms of InR were probably less than those in non-treated transgenic flies resulting in reduced insulin signalling. The reduced insulin signalling is a well-known intervention that confers lifespan extension in various model organisms.

3.5 Pharmacokinetic/metabolization study

PK studies are performed to describe the relationship between the dose of a drug and its concentration in body fluids and tissues over time [64]. Absorption, distribution, metabolism and excretion (ADME) studies are critical for the evaluation of metabolite profiles in plasma and aim

in obtaining an early estimate of pharmacokinetic characteristics and can easily reflect the diversity and complexity of biological systems [65]. In the current part of the study, a suitable mice model based protocol was set in standard OLEO dose of 5mg/Kg. Our goal was to study PK characteristics of OLEO such as Tmax and/or Cmax. For this purpose, an UPLC-Orbitrap-MS methodology was developed for OLEO detection in plasma. In parallel, we were interested in investigating the possible metabolites of OLEO and the determination of their relative content in plasma over time.

3.5.1 Method development for plasma UPLC-HRMS analysis

For the evaluation of the sample preparation procedure 50 μg/mL of OLEO were spiked in plasma and recovery was calculated, resulting in values from 93-101 %. Spiked sample was used for the development of the UPLC and HRMS conditions. The figure below illustrates the UPLC-HRMS chromatogram of the spiked sample.

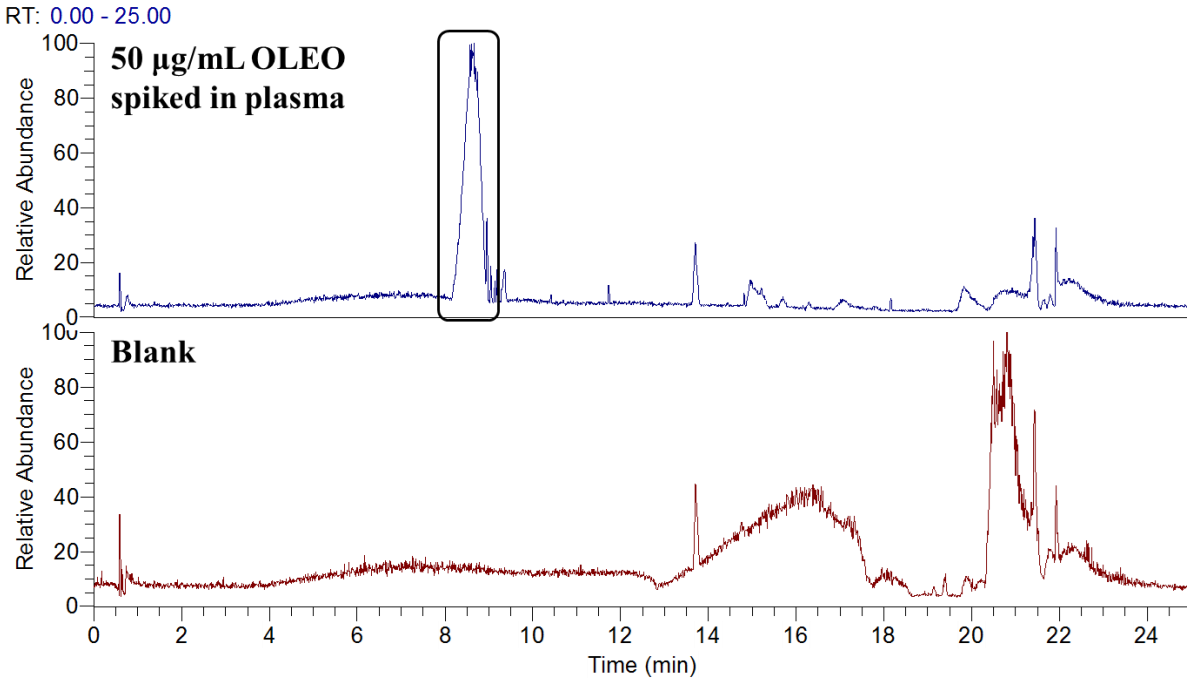

Figure 22: *UPLC-HRMS chromatogram of 50 µg/mL OLEO spiked in plasma (upper chromatogram) and a blank injection (lower chromatogram).*

For the development of the UPLC conditions, elution solvents, column temperature, and column characteristics were investigated. MeOH and ACN were tested as organic solvents and H_2O with and without FA were tested as aqueous phase. ACN resulted in better peak shape, together with acidified water and column temperature at 40°C. Two different columns were tested; an Acquity UPLC Peptide BEH C18 (100 mm x 2.1 mm, 1.7 µm) and a Thermo Hypersil Gold C-18 (50 mm x 2.1 mm, 1.9 µm). The first column produced chromatograms with higher resolution.

Mass spectrometer parameters were optimized for the ionization of secoiridoid derivatives and other biophenols after infusion of a TPF extract (OLE 110) with high content of OLEA and OLEO. The aim was to achieve optimal ionization to oleocanthal and other possible metabolic derivatives of this compound in order to detect oleocanthal as well as other metabolic derivatives

based on previous reported studies. Negative ion mode resulted in better ionization of secoiridoids and for this reason was selected for plasma analysis. The optimized tuning was then tested with the spiked OLEO sample (figure 22).

3.5.2 OLEO determination in plasma

OLEO is a molecule that concentrated the scientific interest the last years and a lot of research focuses on its pharmacological properties exploration [20]. However, its metabolism and PK characteristics in *in vivo* models and human system, is poorly studied due to its sensitive and unstable chemistry which triggers easy and fast decomposition or equilibration reactions in biological systems [66]. OLEO is characterized by two reactive hydrogens belonging to two aldehydes and a sensitive and easily hydrolyzed ester bond associating the T part with EDA (figure 14). Due to this nature it is expected to be fastly bio-transformed in biological systems and thus its detection in biological fluids and tissues is regarded as a challenging task [41]. OLEO undergoes several reactions in human body [43]. The ester bond could be easily hydrolyzed and generate corresponding products T and EDA as major metabolites [41]. Metabolic products are produced via phase I and phase II metabolic reactions. Usually phase I incorporates oxidation, hydrogenation, dehydrogenation, hydration, decarboxylation, methylation and hydroxylation reactions. Phase II reactions are usually known as conjugation reactions and engender glucuronidation, sulfoconjugation, acetylation and glutamination [43].

PK and/or ADME studies of OLEO in human are inadequate and poor data are present concerning the generated metabolic products and their corresponding content in human biological fluids. Only two studies were found investigating human biological fluids (plasma and urine) metabolic profile after VOO intake [43,67]. In brief, both studies incorporate mass spectrometry analysis for the detection and identification of secoiridoids in human biological

fluids after acute intake of VOO. OLEO was present in both cases in VOO, though not detected in biological fluids. Only products of phase I and phase II metabolization were identified. However, in both studies the lack of MS/MS experiments, in combination with the absence of standard compounds raise questions for the identification process.

In the current study, UPLC-HRMS/MS methodology was employed for the detection of OLEO and the identification of OLEO metabolic products as well as their relative content in plasma in specific time points, as described in section 2.13.1. Metabolites identification was based on extraction ion method in parallel with peak-to-peak selection affording the corresponding full scan spectra. Unfortunately, OLEO was not detected in none of the time points and for this reason attention was given to the identification of OLEO metabolites.

3.5.3 Identification of OLEO metabolites

For the investigation of structurally related compounds that could be rationally derived from OLEO, the appeared peaks on chromatograms after OLEO ingestion were investigated. For this reason, unrelated peaks were excluded and RT window from 1-12 minutes in which the peaks of interest appeared, was thoroughly investigated. The rest of the chromatogram included mainly matrix compounds and no significant difference were observed from 12-25 minutes. The figure below represents the UPLC-HRMS chromatograms of mice plasma in two different time points.

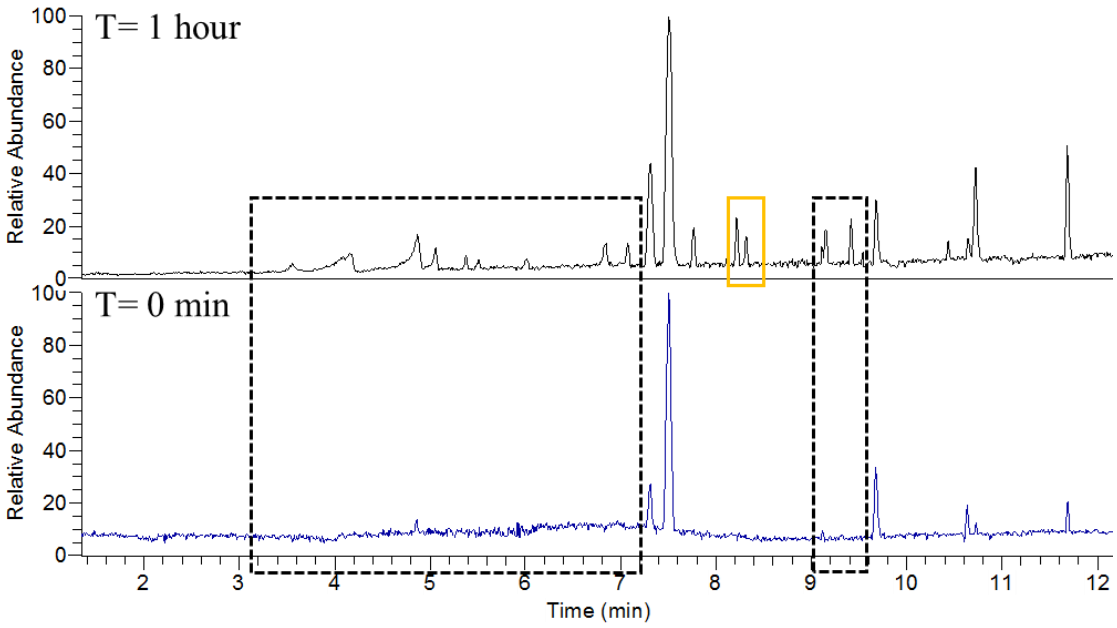

Figure 23: *UPLC-HRMS chromatogram of mice plasma. Upper part (T=1hour) illustrates the metabolic profile 1 hour after OLEO administration and lower part (T=0 min) the time of the administration.*

In figure 23, the upper chromatogram (T=1 hour) represents plasma metabolic profile 1 hour after OLEO ingestion and the lower part of figure the respective chromatogram the time of the ingestion (T=0 min) and could be considered as blank. As it is obvious and already mentioned the identification step focused on injection time 1-12 minutes where differences were observed. The elution areas including the generated compounds after OLEO ingestion are annotated. The area marked in yellow corresponds to two chromatographic peaks which appear at the same RT with spiked OLEO in blank sample (figure 22).

For the identification step, phase I and phase II metabolic reactions occurred in *in vivo* systems were studied for the determination of possible generated metabolic derivatives and interpretation of the results. In parallel, PK studies of other biophenols were studied in order to observe the biotransformation path of compounds with similar chemical structures [38,68,69] in

human systems or *in vivo* experiments. Ultimately, 21 metabolic derivatives of OLEO were assigned. Fourteen of them were totally identified and their chemical structures are presented in figure 24.

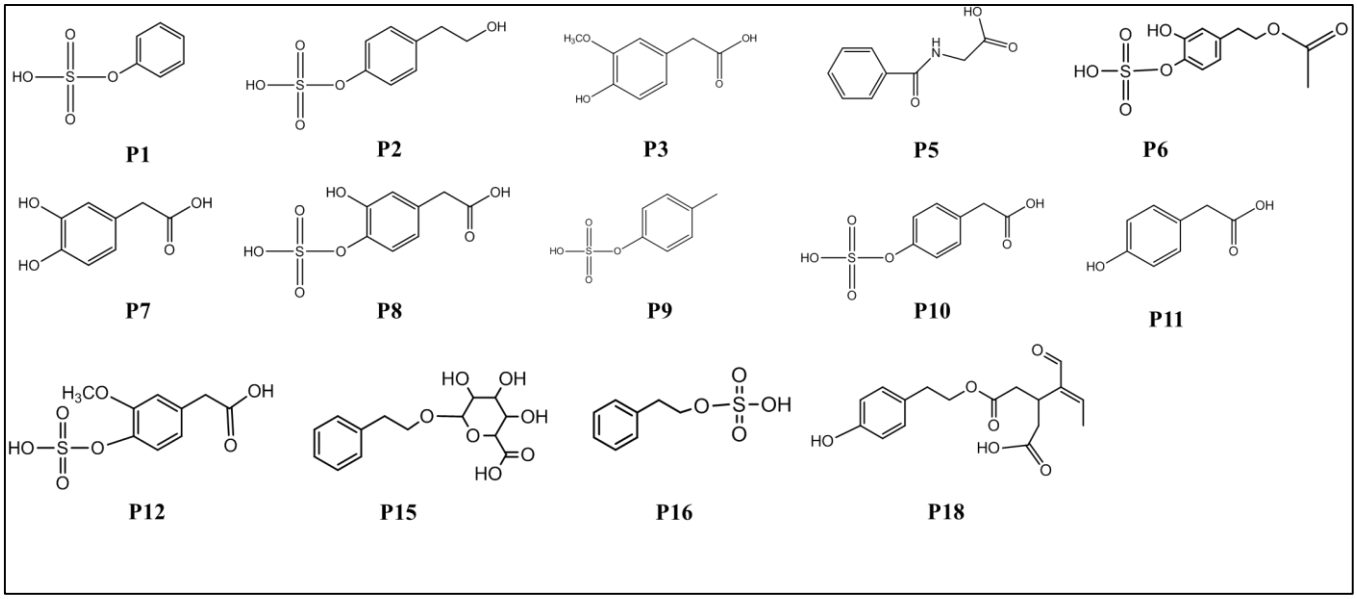

Figure 24: *Identified metabolites attributed to OLEO metabolization in plasma.*

Unfortunately, 7 chemical structures remain unresolved however their elemental composition was determined. Table 7 presents the identified metabolites in plasma 1 hour after OLEO administration.

Table 7: *Identified metabolites in human plasma. Experimental and theoretical m/z, Elemental Composition (EC), Ring and Double Bond equivalent (RDB), Δ in ppm, Retention Time (RT) and HRMS^n fragments are represented.*

#	name	RT	*m/z* experimental	*m/z* theoretical	EC	RDB	Δ (ppm)	HRMS^n (EC, RDB)
P1	Benzol sulfate	4.16	172.9917	172.9903	$C_6H_5O_4S$	4.5	1.777	93.0352 (C_6H_5O, 4.5)
P2	Tyrosol sulfate	4.17	217.0173	217.0165	$C_8H_9O_5S$	4.5	1.1509	196.4058
P3	Homovanillic acid	4.26	181.0508	181.0495	$C_9H_9O_4$	5.5	1.415	
P4	Unknown	4.85	212.0025	212.0012	$C_8H_6O_4NS$	6.5	1.03	196.4132, 80.9659
P5	Hippuric acid	5.04	178.0513	178.0499	$C_9H_8O_3N$	6.5	1.593	134.0615 (C_8H_8ON, 5.5)
P6	HT acetate sulfate-H_2	5.27	273.0075	273.0063	$C_{10}H_9O_7S$	6.5	2.351	193.0509 ($C_{10}H_9O_4$, 6.5)
P7	3,4-Hydroxyphenylacetic acid	5.85	167.0352	167.0339	$C_8H_7O_4$	5.5	1.365	-
P8	3,4-Hydroxyphenylacetic acid sulfate	5.85	246.9918	246.9907	$C_8H_7O_7S$	5.5	1.664	167.0353 ($C_8H_7O_4$)
P9	Crezol sulfate	6.01	187.0073	187.006	$C_7H_7O_4S$	4.5	1.376	107.0506 (C_7H_7O, 4.5)
P10	4-Hydroxyphenylacetic acid sulfate	6.04	230.9969	230.9958	$C_8H_7O_6S$	5.5	0.035	151.0403 ($C_8H_7O_3$, 5.5)
P11	4-Hydroxyphenylacetic acid	6.04	151.0404	151.039	$C_8H_7O_3$	5.5	2.268	136.0169 ($C_7H_4O_3$, 6)

P12	Homovanillic acid sulfate	6.22	261.0076	261.0063	$C_9H_9O_7S$	5.5	0.818	181.0508 ($C_9H_9O_4$, 5.5)
P13	Unknown	6.85	333.0076	333.0063	$C_{15}H_9O_7S$	11.5	0.371	253.0509 ($C_{15}H_9O_4$, 11.5)
P14	Unknown	6.98	417.1184	417.1180	$C_{21}H_{21}O_9$	11.5	-1.739	286.4811, 196.4267
P15	Benzol-ethanol glycuronide	7.07	297.098	297.0969	$C_{14}H_{17}O_7$	6.5	0.148	121.0664 (C_8H_9O, 4.5)
P16	Benzol-ethanol sulfate	7.31	201.0231	201.0216	$C_8H_9O_4S$	4.5	1.827	121.0666 (C_8H_9O, 4.5)
P17	Unknown	7.76	433.1143	433.1129	$C_{21}H_{21}O_{10}$	11.5	0.554	287.1794, 196.3327
P18	Oleocanthalic acid	8.11	319.1189	319.1176	$C_{17}H_{19}O_6$	8.5	0.872	153.0558 ($C_8H_9O_3$, 4.5)
P19	Unknown	8.12	353.0335	353.0326	$C_{15}H_{13}O_8S$	9.5	1.465	273.0762 ($C_{15}H_{13}O_5$, 9.5)
P20	Unknown	8.22, 8.31	507.2239	507.2225	$C_{26}H_{35}O_{10}$	9.5	0.669	331.1911 ($C_{20}H_{27}O_5$, 7.5), 287.1791, 196.3295
P21	Unknown	9.42	491.2292	491.2276	$C_{26}H_{35}O_9$	9.5	1.026	315.1962, 196.3320

As it is already mentioned intact OLEO was not detected in none of the time points, possible due to its unstable nature or rapid biotransformation in plasma. However, possible structures deriving from decomposition or equilibria of OLEO were identified. Due to unavailability of reference standards, it was not possible to proceed to absolute quantitation of the identified metabolites. However, their relative abundance in time was determined. The figure bellow illustrates the relative abundance of metabolites appearing high structural similarity with OLEO.

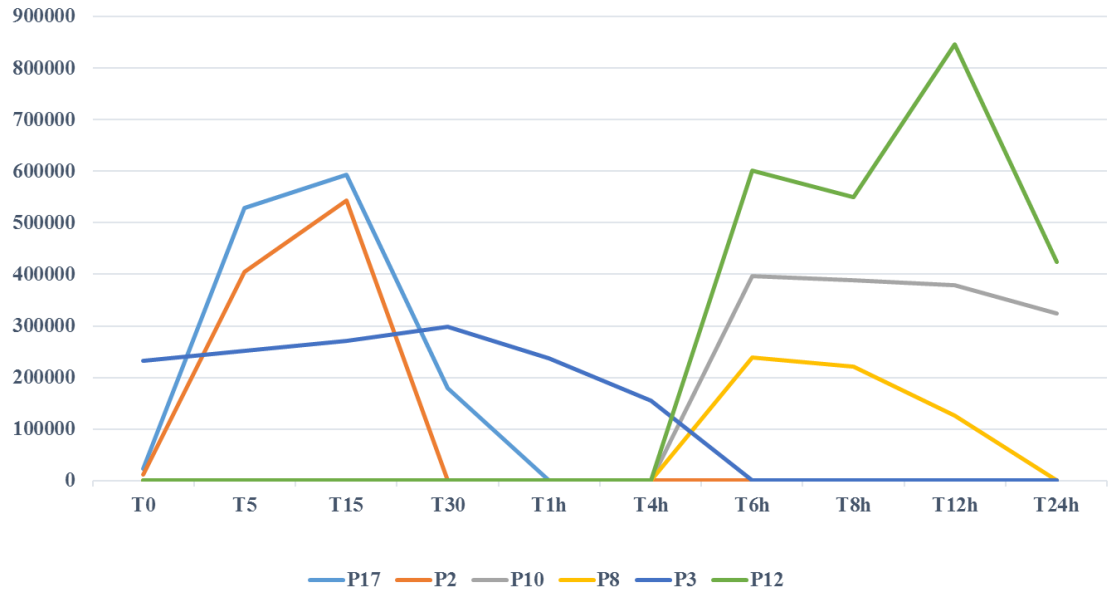

Figure 25: *Relative abundance of metabolites P18, P2, P10, P8, P3 and P12 in time.*

Oleocanthalic acid (P18) and T sulfate (P2) were identified as the first generated metabolic derivatives. T has been already described and detected as ligstroside aglycon metabolite subjected to hydrolysis in the acidic environment of stomach [70]. Tyrosol has also been identified as an endogenous metabolite of human system, produced by a minor pathway of tyramine metabolism [70]. T sulfate is regarded as the most abundant T metabolite of phase II

reactions generated in liver and studies have shown that it retains the biological activities of the parent compound [38]. On the other hand, oleocanthalic acid has been recently identified and isolated from OO [71] and thus never mentioned before as OLEO metabolite in biological fluids. The figure below illustrates the corresponding metabolic reactions producing P18 and P2 metabolites.

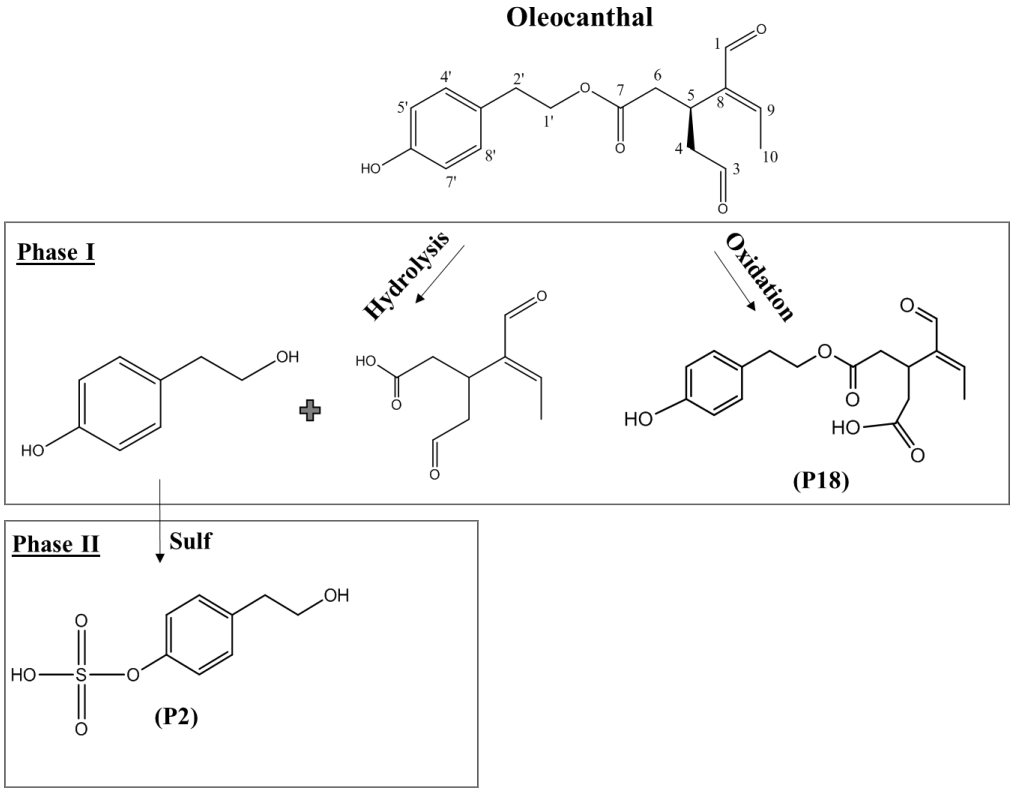

***Figure 26**: Basic reactions of phase I and phase II metabolism of oleocanthal. Sulf: sulfation.*

Continuously the relative content of these two metabolites was determined according to the integrated peak area in each time point. Figure 27 illustrates the corresponding relative abundance of metabolites in plasma in the time points.

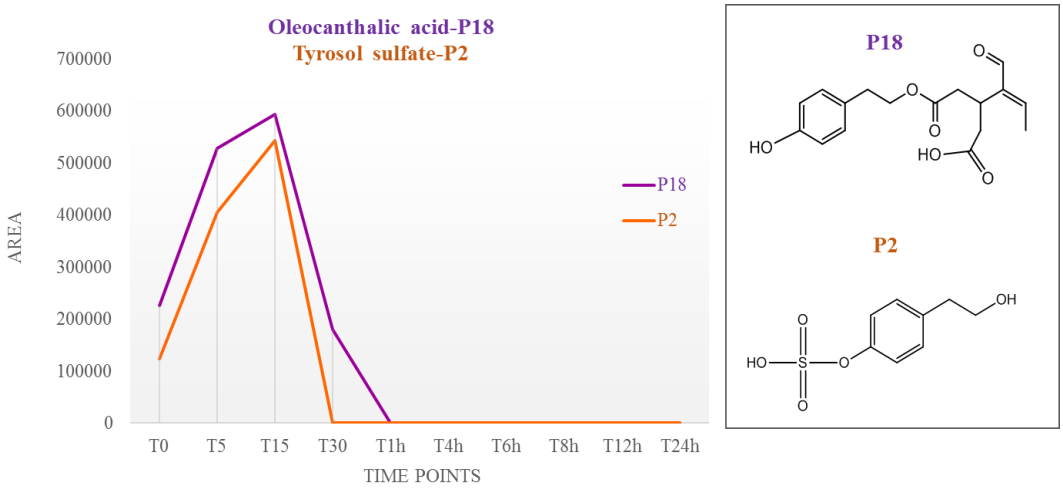

***Figure 27**: Relative abundance of oleocanthalic acid (P18) and tyrosol sulfate (P2) in mice plasma. Vertical axis corresponds to the integrated area of each metabolite and horizontal axis to the respective time point. Right of the graph the respective chemical structures are represented.*

As can be observed from the figure, both compounds were not present in T0 (ingestion time) in plasma. At T5 an obvious increase was observed and P18 existed in relative higher amount comparable to P2, possible due to its faster transformation reaction (aldehyde oxidation). P2 requires a hydrolysis of OLEO or P18 and then a sulfation of the corresponding product. Both compounds presented an increase in time with the highest peak (Tmax) observed at 15 minutes after ingestion (T15). One hour after ingestion (T1) both metabolites were almost undetectable. It has to be noted that, P2 despite being an endogenous metabolite, the corresponding increase and decrease of its content between T15 and T1 is a strong evidence of its association with OLEO administration. The observed Tmax is in agreement with previous published data [38] confirming their rapid metabolism and absorption in biological systems.

Two other identified OLEO metabolites were 4-Hydroxyphenyl acetic acid sulfate (P10) which is the sulfate conjugate of the acidic form of T and 3,4-Dihydroxyphenylacetic acid sulfate (P8), bibliographically known as DOPAC sulfate, which is the sulfate conjugate of the acidic

form of HT. DOPAC is an abundant endogenous metabolite and is generally regarded as a typical dopamine biomarker [72]. The two compounds have been mentioned before as metabolic products of secoiridoids [70]. The generated T from OLEO hydrolysis suffers from oxidation and produces the corresponding acidic product. Also it has been reported that T could be interconverted to HT in liver microsomes by the activity of cytochrome P450 (CYP) and act as a precursor of HT [73]. Both metabolites are endogenous formed in biological matrices in minor biosynthetic pathways [72]. The figure bellow depicts the fluctuation of their relative abundance in plasma.

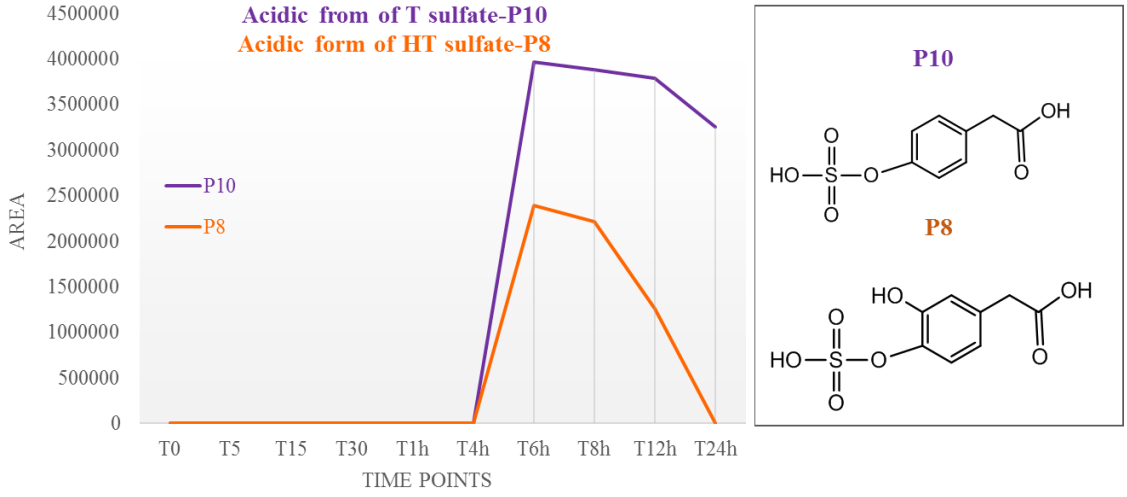

Figure 28: *Relative abundance of oxidized tyrosol sulfate (P10) and oxidized hydroxytyrosol sulfate (P8) in mice plasma. Vertical axis corresponds to the integrated area of each metabolite and horizontal axis to the respective time point. Right of the graph the respective chemical structures are represented.*

It is noteworthy that P10, produced from P2 oxidation, was present in plasma after the disappearance of P2 (Figures 28 & 27). Particularly, it was detected at the sixth hour after ingestion (T6) which was also the Tmax and then started to decrease. After 24 hours which is the last time point of plasma collection it continued to exist, indicating low rate of excretion in

comparison to the precursor. Likewise, Tmax of P8 appeared at T6, followed by the same decrease. The existence of the same trend in combination with its relative lower levels in comparison to P10 could be a sign of its production from P10. However, P8 was not present at the last time point. Also P11 metabolite was detected and has been previously described in literature but not identified [38]. In our study, P11 appeared in the same RT with P10 and for this reason it is thought as an ion fragment of P10. MS/MS data contributed to the identification of its chemical structure.

Apparently homovanillic acid (P3), which is considered as the major metabolite of phenol derivatives in biological matrices [72] was investigated as well. P3 is also a normally formed metabolite of dopamine metabolism [72]. Its sulfate conjugate (P12) was also detected and correlated with its precursor. As it is shown on the figure below, the two metabolic products appeared an inverse relationship in their content in time. P3 existed from T0 revealing its higher relative content in T30. After 6 hours is completely absent in plasma. Contrary, the corresponding sulfate conjugate started its production in the fourth hour with Tmax 12 hours after OLEO injection (T12).

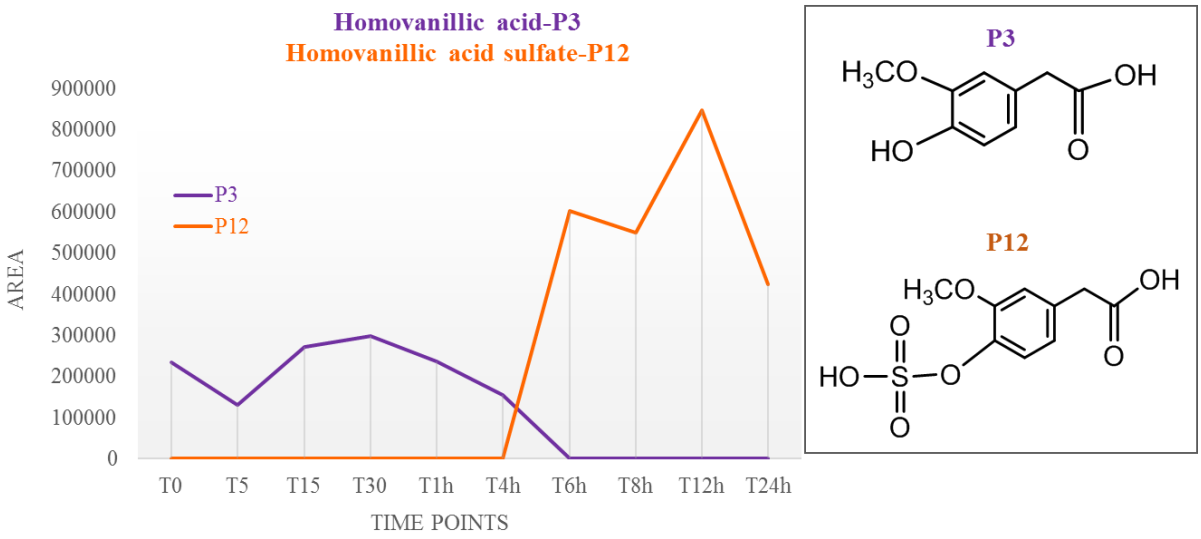

***Figure 29**: Relative abundance of homovanillic acid (P3) and homovanillic acid sulfate (P12) in mice plasma. Vertical axis corresponds to the integrated area of each metabolite and horizontal axis to the respective time point. Right of the graph the respective chemical structures are represented.*

It has to be highlighted that figure 29 speculates an inverse relationship between phase I and II metabolites of OLEO. In the figure the sulfated product (P12) appears its Tmax after the disappearance of the phase I metabolite (P3). The same trend of metabolites is also observed in figure 25; all sulfate products with exception P2 metabolite start to be produced after T4, presenting their Tmax between T4 and T12.

Two other interesting identified compounds of our study were metabolites P14 and P15. These metabolites are characterized by absence of hydroxy groups in the benzol ring. Sulfate and glucuronide conjugates were detected and not the precursor benzolethanol possible due to the poor ionization of this compound. Both compounds were detected after T6 like all previous phase II metabolization products. Compounds were not included in the figures of relative abundance, because their poor ionization or low content affect axis normalization Dihydroxylation is a common reaction in biological systems caused by dihydroxylases and has

been previously reported [40]. Both of them are possible generated by the produced T after hydrolysis of OLEO ester bond. Benzol sulfate was also detected possible generated after α-oxidation and dihydroxylation of P11.

Moreover, P6 metabolite was detected. P6 is attributed to HT acetate sulfate after a dihydrogenation reaction. Acetyltransferase catalyzes the transfer of acetyl group to HT, forming HT acetate. This compound is characterized by a more lipophilic character and with easier transportation through the lipophilic cell membranes [74]. Previous studies have uncovered hydroxylated or hydrated products of this metabolite in human urine after EVOO intake [43]. P6 was present in traces and for this reason the estimation of its relative content in plasma was not possible. However, its most intense peak appeared at T12.

Hippuric acid (P5) and cresol sulfate (P9) were also detected. P5 is the glycine conjugate of benzoic acid possible generated by T after α-oxidation and dihydroxylation. Previous studies have revealed that phenols consumption is associated with increased levels of hippuric acid in humans [75]. P5 presented increasing levels in accordance to time with exception time points T4 and T6. Its higher area was recorded at T12. P9, a metabolite produced from *p*-crezol in the liver, is normally produced from tyrosine pathway in human body [76]. Although it has never been associated before with secoiridoids administration. P9 appeared also increasing levels with exception time point T6 and T12. Its highest content was recorded at T4. The existence of increasing levels of both compounds is a possible indication of their association with OLEO administration.

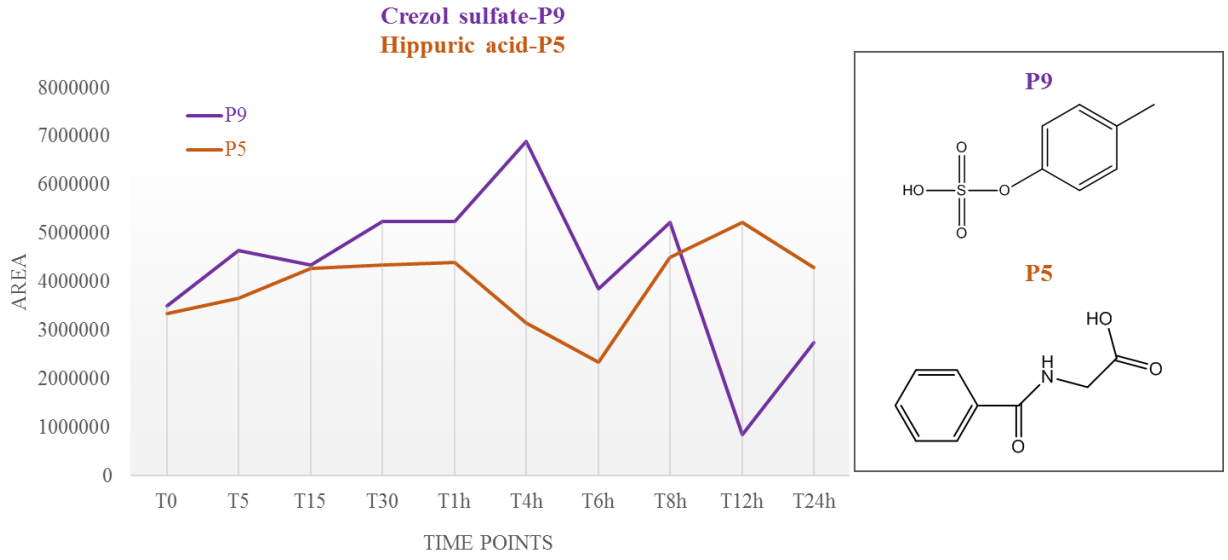

Figure 30: *Relative abundance of cresol sulfate (P9) and hippuric acid (P5) in mice plasma. Vertical axis corresponds to the integrated area of each metabolite and horizontal axis to the respective time point. Right of the graph the respective chemical structures are represented.*

The rest peaks of the chromatogram after OLEO administration unfortunately were not identified. However, their EC was determined. The interesting finding in these compounds is that many of them were characterized by common MS/MS fragments; fragments with *m/z* 196.3220 and 287.1791 were the most frequently identified. In this case belonged metabolite P19, which existed in two identical peaks at the same RT with OLEO spiked in blank sample, which after the first hour they disappeared. In figure 23 the corresponding area is marked in yellow box.

The qualitative and quantitative variations of plasma profile in time were remarkable and have to be underlined. The figure below depicts plasma profile and its qualitative differentiation 1 and 24 hours after OLEO ingestion.

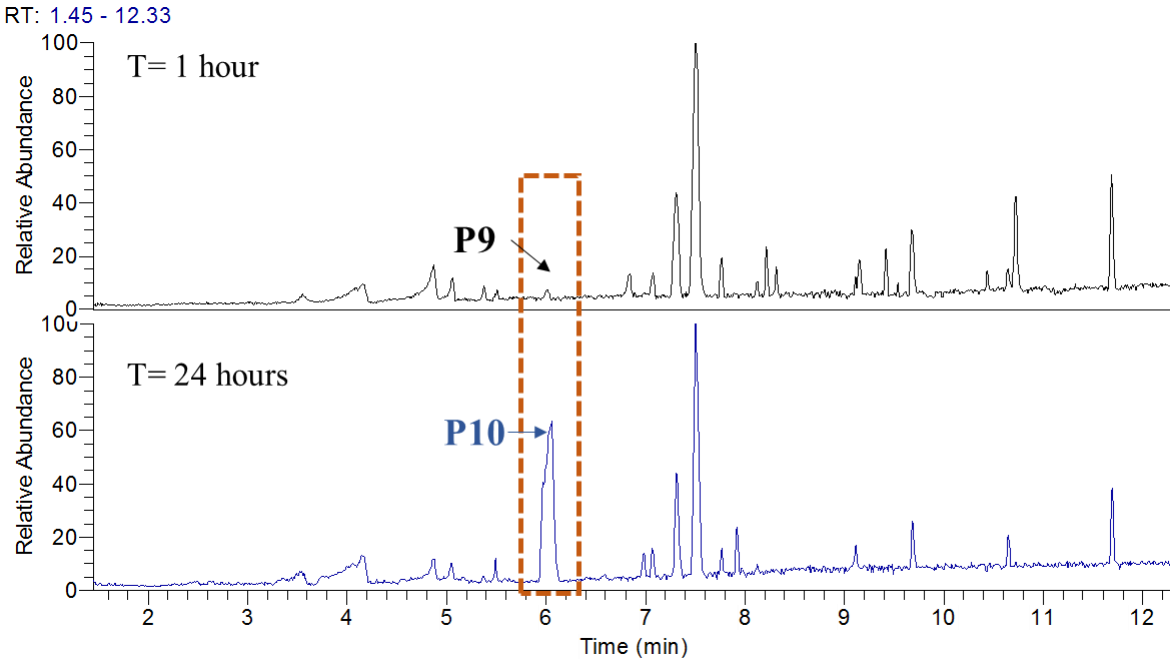

Figure 31: *UPLC-HRMS chromatogram of plasma profile 1 hour after OLEO ingestion (upper chromatogram) and 24 hours after OLEO ingestion (lower chromatogram).*

In the figure the most characteristic qualitative change is annotated. The existence of a peak at 6.04 minutes which increased 24 hours after OLEO ingestion is annotated. However, this peak did not correspond to the same metabolite 1 hour and 24 hours after ingestion. At T1 peak was assigned to P9, which as it already mentioned started to decline at T4. Interestingly at T24 the same peak corresponded to P10, which revealed its Tmax at T4 and then presented a small decline in time until T24.

To conclude, relative Tmax of compounds of interest were determined to understand the metabolism of OLEO and its products in plasma. The determined Tmax of the above discussed metabolites are in accordance with previous outcomes studying PK parameters of other OO biophenols [38,68,69]. Figures 27-30 indicating Tmax of selected compounds uncovered that metabolic production of sulfate conjugates (phase II metabolites) started four hours after OLEO ingestion and are characterized by longer existance in plasma, possible due to their more stable

chemical structures. Contrary according to the estimated Tmax of phase I metabolites, the higher relative content exists at 15-30 minutes after OLEO ingestion and they generally present for shorter period in plasma, characterized by completely disappearance 1-4 hours after secoiridoid ingestion.

Ultimately, hydrolysis of OLEO ester bond and aldehydes oxidation could be characterized as the most important metabolic reactions of OLEO followed by sulfation. No methylation products of OLEO or T were identified. This observation has been already been reported due to the lack of catecholic structure required for the activity of Catechol-O-methyl transferase (COMT) [70]. It can be assumed that oleocanthalic acid and T sulfate are the metabolic markers of OLEO metabolism and thus can be used for the detection and further investigation of OLEO metabolism in biological systems.

4. Conclusions

In this study, biological evaluation of OO biophenols was carried out with *in vitro* tests and *in vivo* models. The first step of the experimental workflow was the isolation of compounds for the performance of the biological experiments. For this reason, an OO rich in secoiridoids was extracted and fractionated for the isolation of selected biophenols. The selection of the isolated compounds was based either on their reported biological activities or the gap in bibliography for specific compounds. Some of them like OLEO and OLEA are characterized by high pharmacological interest and a plethora of biological activities, while no experiments have been reported for elenolic acid ethyl ester due to its recently reported existence in OO. Eventually, eight compounds, three iridoids and five secoiridoids were detected and then isolated from OO some of them with purity over 98% and others in mixtures with different ratios of 8S and 8R isomers. Isolated compounds were firstly tested *in vitro* with MTT assay for cell viability evaluation. Results indicated that secoiridoids were more potent, contrary to iridoids which were found not so effective. Moreover, 8S isomers revealed higher activity, while the existence of 8R isomeric forms in the mixtures reduced potency.

Subsequently, secoiridoids found more active with *in vitro* testing, OLEO and OLEA were evaluated in parallel with selected OO extracts characterized by low, medium and high content in these compounds in mammalian cells and as a dietary supplement in a *Drosophila in vivo* model. Novel data were provided concerning their promising results both to mammalian cells and flies. Furthermore, the positive effects of OO extracts and the purified compounds, on cytoprotective proteostatic modules at cell-based and *in vitro* models, as well as on their long-term protective effect in a model of aberrant activation of the insulin receptor in the fly model adding thus further mechanistic knowledge on the reported healthy aging-promoting properties of EVOOs.

Ultimately, due to the lack of PK data for OLEO, a PK experiment was designed and oleocanthal was administered to a mouse model. Ten different time points were selected for the investigation of OLEO time-dependent metabolism and plasma samples were obtained in every time point. Oleocanthal was not detected in plasma samples. However specific metabolic derivatives of the parent compound were identified. Oleocanthalic acid and tyrosol sulfate were identified as first formed metabolites of OLEO and suggested as possible biomarkers for monitoring OLEO in plasma. Fourteen more phase I and phase II metabolites were identified and their relative content was determined. Results indicated that sulfated metallization products presented their Tmax at least 4 hours after OLEO ingestion, while phase I metabolites revealed their Tmax 15-30 minutes after OLEO ingestion. For the first time an experiment was designed for monitoring OLEO existence and/or biostransfromation in plasma. The derived data could be used for the design of more targeted experiments and the exact quantitation of the suggested compounds.

Bibliography

[1] S. Cicerale, L. Lucas, R. Keast, Antimicrobial, antioxidant and anti-inflammatory phenolic activities in extra virgin olive oil, Curr. Opin. Biotechnol. 23 (2012) 129–135.

[2] H.K. Obied, P.D. Prenzler, S.H. Omar, R. Ismael, M. Servili, S. Esposto, A. Taticchi, R. Selvaggini, S. Urbani, Pharmacology of olive biophenols, 1st ed., Elsevier B.V., 2012. doi:10.1016/B978-0-444-59389-4.00006-9.

[3] M. Servili, R. Selvaggini, S. Esposto, A. Taticchi, G. Montedoro, G. Morozzi, Health and sensory properties of virgin olive oil hydrophilic phenols: agronomic and technological aspects of production that affect their occurrence in the oil, J. Chromatogr. A. 1054 (2004) 113–127. doi:10.1016/J.CHROMA.2004.08.070.

[4] P. Kanakis, A. Termentzi, T. Michel, E. Gikas, M. Halabalaki, A.-L. Skaltsounis, From olive drupes to olive oil. An HPLC-orbitrap-based qualitative and quantitative exploration of olive key metabolites., Planta Med. 79 (2013) 1576–1587. doi:10.1055/s-0033-1350823.

[5] D. Boskou, Olive Oil Composition. In Olive Oil Chemistry and Tecnology., AOC Press: Champaign, USA, 1996.

[6] F. Visioli, C. Galli, Biological Properties of Olive Oil Phytochemicals, Crit. Rev. Food Sci. Nutr. 42 (2002) 209–221. doi:10.1080/10408690290825529.

[7] A. Angelis, M. Hamzaoui, N. Aligiannis, T. Nikou, D. Michailidis, P. Gerolimatos, A. Termentzi, J. Hubert, M. Halabalaki, J.-H. Renault, A.-L. Skaltsounis, An integrated process for the recovery of high added-value compounds from olive oil using solid

support free liquid-liquid extraction and chromatography techniques, J. Chromatogr. A. 1491 (2017) 126–136. doi:10.1016/j.chroma.2017.02.046.

[8] T. Nikou, V. Liaki, P. Stathopoulos, A.D. Sklirou, E.N. Tsakiri, T. Jakschitz, G. Bonn, I.P. Trougakos, M. Halabalaki, L.A. Skaltsounis, Comparison survey of EVOO polyphenols and exploration of healthy aging-promoting properties of oleocanthal and oleacein, Food Chem. Toxicol. 125 (2019). doi:10.1016/j.fct.2019.01.016.

[9] G. Montedoro, M. Servili, M. Baldioli, R. Selvaggini, E. Miniati, A. Macchioni, Simple and hydrolyzable compounds in virgin olive oil. 3. Spectroscopic characterizations of the secoiridoid derivatives., J. Agric. Food Chem. 41 (1993) 2228–2234. doi:10.1021/jf00035a076.

[10] P. Gariboldi, G. Jommi, L. Verotta, Secoiridoids from Olea europaea, Phytochemistry. 25 (1986) 865–869. doi:10.1016/0031-9422(86)80018-8.

[11] M. Servili, S. Esposto, R. Fabiani, S. Urbani, A. Taticchi, F. Mariucci, R. Selvaggini, G.F. Montedoro, Phenolic compounds in olive oil: Antioxidant, health and organoleptic activities according to their chemical structure, Inflammopharmacology. 17 (2009) 76–84. doi:10.1007/s10787-008-8014-y.

[12] A. Filipek, M.E. Czerwińska, A.K. Kiss, M. Wrzosek, M. Naruszewicz, Oleacein enhances anti-inflammatory activity of human macrophages by increasing CD163 receptor expression, Phytomedicine. 22 (2015) 1255–1261. doi:https://doi.org/10.1016/j.phymed.2015.10.005.

[13] L. Parkinson, R. Keast, Oleocanthal, a Phenolic Derived from Virgin Olive Oil: A Review of the Beneficial Effects on Inflammatory Disease, Int. J. Mol. Sci. 15 (2014) 12323–

12334.

[14] G.K.. K. Beauchamp R. S. J.; Morel, D.; Lin, J.; Pika, J.; Han, Q.; Lee, C-H.; Smith, A. B.;, P.A.S. Breslin, Ibuprofen-like activity in extra-virgin olive oil, Nature. 437 (2005) 45–46. doi:10.1038/437045a10.1038/437046a.

[15] M. Scotece, J. Conde, V. Abella, V. López, V. Francisco, C. Ruiz, V. Campos, F. Lago, R. Gomez, J. Pino, O. Gualillo, Oleocanthal Inhibits Catabolic and Inflammatory Mediators in LPS-Activated Human Primary Osteoarthritis (OA) Chondrocytes Through MAPKs/NF-κB Pathways, Cell. Physiol. Biochem. 49 (2018) 2414–2426. doi:10.1159/000493840.

[16] A. Iacono, R. Gómez, J. Sperry, J. Conde, G. Bianco, R. Meli, J.J. Gómez-Reino, A.B. Smith III, O. Gualillo, Effect of oleocanthal and its derivatives on inflammatory response induced by lipopolysaccharide in a murine chondrocyte cell line, Arthritis Rheum. 62 (2010) 1675–1682. doi:10.1002/art.27437.

[17] A.H. Abuznait, H. Qosa, B.A. Busnena, K.A. El Sayed, A. Kaddoumi, Olive-Oil-Derived Oleocanthal Enhances β-Amyloid Clearance as a Potential Neuroprotective Mechanism against Alzheimer's Disease: In Vitro and in Vivo Studies, ACS Chem. Neurosci. 4 (2013) 973–982. doi:10.1021/cn400024q.

[18] A.Y. Elnagar, P.W. Sylvester, K.A. El Sayed, (-)-Oleocanthal as a c-Met inhibitor for the control of metastatic breast and prostate cancers., Planta Med. 77 (2011) 1013–1019. doi:10.1055/s-0030-1270724.

[19] M.R. Akl, N.M. Ayoub, M.M. Mohyeldin, B.A. Busnena, A.I. Foudah, Y.-Y. Liu, K.A.E.I. Sayed, Olive Phenolics as c-Met Inhibitors: (-)-Oleocanthal Attenuates Cell

Proliferation, Invasiveness, and Tumor Growth in Breast Cancer Models, PLoS One. 9 (2014) e97622. https://doi.org/10.1371/journal.pone.0097622.

[20] K.L. Pang, K.Y. Chin, The biological activities of oleocanthal from a molecular perspective, Nutrients. 10 (2018) 1–22. doi:10.3390/nu10050570.

[21] M. Naruszewicz, M.E.C. and A.K. Kiss, Oleacein. Translation from Mediterranean Diet to Potential Antiatherosclerotic Drug, Curr. Pharm. Des. 21 (2015) 1205–1212. doi:http://dx.doi.org/10.2174/1381612820666141007141137.

[22] G.E. Lombardo, S.M. Lepore, V.M. Morittu, B. Arcidiacono, C. Colica, A. Procopio, V. Maggisano, S. Bulotta, N. Costa, C. Mignogna, D. Britti, A. Brunetti, D. Russo, M. Celano, Effects of Oleacein on High-Fat Diet-Dependent Steatosis, Weight Gain, and Insulin Resistance in Mice , Front. Endocrinol. . 9 (2018) 116. https://www.frontiersin.org/article/10.3389/fendo.2018.00116.

[23] E. Medina, A. de Castro, C. Romero, M. Brenes, Comparison of the Concentrations of Phenolic Compounds in Olive Oils and Other Plant Oils: Correlation with Antimicrobial Activity, J. Agric. Food Chem. 54 (2006) 4954–4961. doi:10.1021/jf0602267.

[24] G. Buckland, C.A. Gonzalez, The role of olive oil in disease prevention: a focus on the recent epidemiological evidence from cohort studies and dietary intervention trials., Br. J. Nutr. 113 (2015) 94–101. doi:10.1017/S0007114514003936.

[25] M.-I. Covas, V. Konstantinidou, M. Fito, Olive oil and cardiovascular health., J. Cardiovasc. Pharmacol. 54 (2009) 477–482. doi:10.1097/FJC.0b013e3181c5e7fd.

[26] F. Perez-Jimenez, J. Ruano, P. Perez-Martinez, F. Lopez-Segura, J. Lopez-Miranda, The

influence of olive oil on human health: not a question of fat alone., Mol. Nutr. Food Res. 51 (2007) 1199–1208. doi:10.1002/mnfr.200600273.

[27] A. Argyropoulou, N. Aligiannis, I.P. Trougakos, A.-L. Skaltsounis, Natural compounds with anti-ageing activity, Nat. Prod. Rep. 30 (2013) 1412–1437. doi:10.1039/C3NP70031C.

[28] I.P. Trougakos, F. Sesti, E. Tsakiri, V.G. Gorgoulis, Non-enzymatic post-translational protein modifications and proteostasis network deregulation in carcinogenesis, J. Proteomics. 92 (2013) 274–298. doi:https://doi.org/10.1016/j.jprot.2013.02.024.

[29] E.N. Tsakiri, I.P. Trougakos, Chapter Five - The Amazing Ubiquitin-Proteasome System: Structural Components and Implication in Aging, Int. Rev. Cell Mol. Biol. 314 (2015) 171–237. doi:https://doi.org/10.1016/bs.ircmb.2014.09.002.

[30] E.N. Tsakiri, G.P. Sykiotis, I.S. Papassideri, V.G. Gorgoulis, D. Bohmann, I.P. Trougakos, Differential regulation of proteasome functionality in reproductive vs. somatic tissues of Drosophila during aging or oxidative stress, FASEB J. 27 (2013) 2407–2420. doi:10.1096/fj.12-221408.

[31] E.N. Tsakiri, S. Gumeni, K.K. Iliaki, D. Benaki, K. Vougas, G.P. Sykiotis, V.G. Gorgoulis, E. Mikros, L. Scorrano, I.P. Trougakos, Hyperactivation of Nrf2 increases stress tolerance at the cost of aging acceleration due to metabolic deregulation, Aging Cell. 18 (2019) e12845. doi:10.1111/acel.12845.

[32] A.D. Sklirou, M. Ralli, M. Dominguez, I. Papassideri, A.-L. Skaltsounis, I.P. Trougakos, Hexapeptide-11 is a novel modulator of the proteostasis network in human diploid fibroblasts, Redox Biol. 5 (2015) 205–215.

doi:https://doi.org/10.1016/j.redox.2015.04.010.

[33] A.D. Sklirou, N. Gaboriaud-Kolar, I. Papassideri, A.-L. Skaltsounis, I.P. Trougakos, 6-bromo-indirubin-3′-oxime (6BIO), a Glycogen synthase kinase-3β inhibitor, activates cytoprotective cellular modules and suppresses cellular senescence-mediated biomolecular damage in human fibroblasts, Sci. Rep. 7 (2017) 11713. doi:10.1038/s41598-017-11662-7.

[34] C. Santangelo, R. Vari, B. Scazzocchio, P. De Sanctis, C. Giovannini, M. D'Archivio, R. Masella, Anti-inflammatory Activity of Extra Virgin Olive Oil Polyphenols: Which Role in the Prevention and Treatment of Immune-Mediated Inflammatory Diseases?, Endocr. Metab. Immune Disord. Drug Targets. 18 (2018) 36–50. doi:10.2174/1871530317666171114114321.

[35] R. Fuccelli, R. Fabiani, P. Rosignoli, Hydroxytyrosol Exerts Anti-Inflammatory and Anti-Oxidant Activities in a Mouse Model of Systemic Inflammation, Molecules. 23 (2018) 3212. doi:10.3390/molecules23123212.

[36] C. Colica, L. Di Renzo, D. Trombetta, A. Smeriglio, S. Bernardini, G. Cioccoloni, R. Costa De Miranda, P. Gualtieri, P. Sinibaldi Salimei, A. De Lorenzo, Antioxidant Effects of a Hydroxytyrosol-Based Pharmaceutical Formulation on Body Composition, Metabolic State, and Gene Expression: A Randomized Double-Blinded, Placebo-Controlled Crossover Trial, Oxid. Med. Cell. Longev. 2017 (2017) 1–14. doi:10.1155/2017/2473495.

[37] A. Boronat, N. Soldevila-Domenech, J.A. Mateus, P. Díaz, M. Pérez, A. Rovira, R. De la torre, Generation of the Antioxidant Hydroxytyrosol from Tyrosol Present in Beer in a Randomized Clinical Trial (P06-003-19), Curr. Dev. Nutr. 3 (2019) nzz031.P06-003-19.

doi:10.1093/cdn/nzz031.P06-003-19.

[38] D.-H. Lee, Y.-J. Kim, M.J. Kim, J. Ahn, T.-Y. Ha, S.H. Lee, Y.J. Jang, C.H. Jung, Pharmacokinetics of Tyrosol Metabolites in Rats, Molecules. 21 (2016) E128–E128. doi:10.3390/molecules21010128.

[39] S. D'Angelo, C. Manna, V. Migliardi, O. Mazzoni, P. Morrica, G. Capasso, G. Pontoni, P. Galletti, V. Zappia, Pharmacokinetics and metabolism of hydroxytyrosol, a natural antioxidant from olive oil., Drug Metab. Dispos. 29 (2001) 1492–1498.

[40] M.-C. López de las Hazas, C. Piñol, A. Macià, M.-P. Romero, A. Pedret, R. Solà, L. Rubió, M.-J. Motilva, Differential absorption and metabolism of hydroxytyrosol and its precursors oleuropein and secoiridoids, J. Funct. Foods. 22 (2016) 52–63. doi:https://doi.org/10.1016/j.jff.2016.01.030.

[41] M. Suárez, M. Romero, A. Macià, R.M. Valls, S. Fernández, R. Solà, M. Motilva, Improved method for identifying and quantifying olive oil phenolic compounds and their metabolites in human plasma by microelution solid-phase extraction plate and liquid chromatography – tandem mass spectrometry, J. Chromatogr. B. 877 (2009) 4097–4106. doi:10.1016/j.jchromb.2009.10.025.

[42] J. Pinto, F. Paiva-Martins, G. Corona, E.S. Debnam, M. Jose Oruna-Concha, D. Vauzour, M.H. Gordon, J.P.E. Spencer, Absorption and metabolism of olive oil secoiridoids in the small intestine, Br. J. Nutr. 105 (2011) 1607–1618. doi:10.1017/S000711451000526X.

[43] R. García-Villalba, A. Carrasco-Pancorbo, E. Nevedomskaya, O.A. Mayboroda, A.M. Deelder, A. Segura-Carretero, A. Fernández-Gutiérrez, Exploratory analysis of human urine by LC-ESI-TOF MS after high intake of olive oil: Understanding the metabolism of

polyphenols, Anal. Bioanal. Chem. 398 (2010) 463–475. doi:10.1007/s00216-010-3899-x.

[44] G. Corona, X. Tzounis, M.A. Dessì, M. Deiana, E.S. Debnam, F. Visioli, J.P.E. Spencer, The fate of olive oil polyphenols in the gastrointestinal tract: Implications of gastric and colonic microflora-dependent biotransformation, Free Radic. Res. 40 (2006) 647–658. doi:10.1080/10715760500373000.

[45] A. Angelis, M. Hamzaoui, N. Aligiannis, T. Nikou, D. Michailidis, P. Gerolimatos, A. Termentzi, J. Hubert, M. Halabalaki, J.H. Renault, A.L. Skaltsounis, An integrated process for the recovery of high added-value compounds from olive oil using solid support free liquid-liquid extraction and chromatography techniques, J. Chromatogr. A. 1491 (2017) 126–136. doi:10.1016/j.chroma.2017.02.046.

[46] I.P. Trougakos, L.H. Margaritis, Immunolocalization of the Temporally "Early" Secreted Major Structural Chorion Proteins, Dvs38 and Dvs36, in the Eggshell Layers and Regions of Drosophila virilis, J. Struct. Biol. 123 (1998) 111–123. doi:https://doi.org/10.1006/jsbi.1998.4028.

[47] E.N. Tsakiri, G.P. Sykiotis, I.S. Papassideri, E. Terpos, M.A. Dimopoulos, V.G. Gorgoulis, D. Bohmann, I.P. Trougakos, Proteasome dysfunction in Drosophila signals to an Nrf2-dependent regulatory circuit aiming to restore proteostasis and prevent premature aging, Aging Cell. 12 (2013) 802–813. doi:10.1111/acel.12111.

[48] A. Angelis, M. Hamzaoui, N. Aligiannis, T. Nikou, D. Michailidis, P. Gerolimatos, A. Termentzi, J. Hubert, M. Halabalaki, J.-H. Renault, A.-L. Skaltsounis, An integrated process for the recovery of high added-value compounds from olive oil using solid support free liquid-liquid extraction and chromatography techniques, J. Chromatogr. A.

1491 (2017). doi:10.1016/j.chroma.2017.02.046.

[49] M. Servili, B. Sordini, S. Esposto, S. Urbani, G. Veneziani, I. Di Maio, R. Selvaggini, A. Taticchi, Biological Activities of Phenolic Compounds of Extra Virgin Olive Oil, Antioxidants. 3 (2014) 1–23. doi:10.3390/antiox3010001.

[50] C.-M. Lăcătușu, E.-D. Grigorescu, M. Floria, A. Onofriescu, B.-M. Mihai, The Mediterranean Diet: From an Environment-Driven Food Culture to an Emerging Medical Prescription, Int. J. Environ. Res. Public Health. 16 (2019) 942. doi:10.3390/ijerph16060942.

[51] M.A. Martinez-Gonzalez, J. Salas-Salvado, R. Estruch, D. Corella, M. Fito, E. Ros, Benefits of the Mediterranean Diet: Insights From the PREDIMED Study., Prog. Cardiovasc. Dis. 58 (2015) 50–60. doi:10.1016/j.pcad.2015.04.003.

[52] J. Salas-Salvado, J. Fernandez-Ballart, E. Ros, M.-A. Martinez-Gonzalez, M. Fito, R. Estruch, D. Corella, M. Fiol, E. Gomez-Gracia, F. Aros, G. Flores, J. Lapetra, R. Lamuela-Raventos, V. Ruiz-Gutierrez, M. Bullo, J. Basora, M.-I. Covas, Effect of a Mediterranean diet supplemented with nuts on metabolic syndrome status: one-year results of the PREDIMED randomized trial., Arch. Intern. Med. 168 (2008) 2449–2458. doi:10.1001/archinte.168.22.2449.

[53] E. Kopel, Y. Sidi, S. Kivity, Mediterranean diet for primary prevention of cardiovascular disease., N. Engl. J. Med. 369 (2013) 672. doi:10.1056/NEJMc1306659.

[54] M.N. Franco, T. Galeano-Díaz, Ó. López, J.G. Fernández-Bolaños, J. Sánchez, C. De Miguel, M.V. Gil, D. Martín-Vertedor, Phenolic compounds and antioxidant capacity of virgin olive oil, Food Chem. 163 (2014) 289–298.

doi:https://doi.org/10.1016/j.foodchem.2014.04.091.

[55] S. Chatzigeorgiou, Q.D. Thai, J. Tchoumtchoua, K. Tallas, E.N. Tsakiri, I. Papassideri, M. Halabalaki, A.-L. Skaltsounis, I.P. Trougakos, Isolation of natural products with anti-ageing activity from the fruits of Platanus orientalis, Phytomedicine. 33 (2017) 53–61. doi:https://doi.org/10.1016/j.phymed.2017.07.009.

[56] A. Parzonko, M.E. Czerwińska, A.K. Kiss, M. Naruszewicz, Oleuropein and oleacein may restore biological functions of endothelial progenitor cells impaired by angiotensin II via activation of Nrf2/heme oxygenase-1 pathway, Phytomedicine. 20 (2013) 1088–1094. doi:https://doi.org/10.1016/j.phymed.2013.05.002.

[57] F. Vlavcheski, M. Young, E. Tsiani, Antidiabetic Effects of Hydroxytyrosol: In Vitro and In Vivo Evidence, Antioxidants (Basel, Switzerland). 8 (2019) 188. doi:10.3390/antiox8060188.

[58] J.R. DiAngelo, M.L. Bland, S. Bambina, S. Cherry, M.J. Birnbaum, The immune response attenuates growth and nutrient storage in Drosophila by reducing insulin signaling, Proc. Natl. Acad. Sci. 106 (2009) 20853–20858. doi:10.1073/pnas.0906749106.

[59] M. Scotece, R. Gómez, J. Conde, V. Lopez, J.J. Gómez-Reino, F. Lago, A.B. Smith, O. Gualillo, Further evidence for the anti-inflammatory activity of oleocanthal: Inhibition of MIP-1α and IL-6 in J774 macrophages and in ATDC5 chondrocytes, Life Sci. 91 (2012) 1229–1235. doi:https://doi.org/10.1016/j.lfs.2012.09.012.

[60] O. LeGendre, P.A. Breslin, D.A. Foster, (-)-Oleocanthal rapidly and selectively induces cancer cell death via lysosomal membrane permeabilization., Mol. Cell. Oncol. 2 (2015) e1006077. doi:10.1080/23723556.2015.1006077.

[61] L. Margarucci, M.C. Monti, C. Cassiano, M. Mozzicafreddo, M. Angeletti, R. Riccio, A. Tosco, A. Casapullo, Chemical proteomics-driven discovery of oleocanthal as an Hsp90 inhibitor, Chem. Commun. 49 (2013) 5844–5846. doi:10.1039/C3CC41858H.

[62] R.R. Ramos, A.J. Swanson, J. Bass, Calreticulin and Hsp90 stabilize the human insulin receptor and promote its mobility in the endoplasmic reticulum, Proc. Natl. Acad. Sci. 104 (2007) 10470 LP-10475. doi:10.1073/pnas.0701114104.

[63] T. Saitoh, T. Yanagita, S. Shiraishi, H. Yokoo, H. Kobayashi, S. Minami, T. Onitsuka, A. Wada, Down-Regulation of Cell Surface Insulin Receptor and Insulin Receptor Substrate-1 Phosphorylation by Inhibitor of 90-kDa Heat-Shock Protein Family: Endoplasmic Reticulum Retention of Monomeric Insulin Receptor Precursor with Calnexin in Adrenal Chromaffin, Mol. Pharmacol. 62 (2002) 847 LP-855. doi:10.1124/mol.62.4.847.

[64] E. Flynn, Pharmacokinetic Parameters, in: S.J. Enna, D.B.B.T.T.C.P.R. Bylund (Eds.), Elsevier, New York, 2007: pp. 1–3. doi:https://doi.org/10.1016/B978-008055232-3.60034-0.

[65] J. Vrbanac, R. Slauter, Chapter 3 - ADME in Drug Discovery, in: A.S.B.T.-A.C.G. to T. in N.D.D. (Second E. Faqi (Ed.), Academic Press, Boston, 2017: pp. 39–67. doi:https://doi.org/10.1016/B978-0-12-803620-4.00003-7.

[66] G. Corona, X. Tzounis, M. Assunta DessÌ, M. Deiana, E.S. Debnam, F. Visioli, J.P.E. Spencer, The fate of olive oil polyphenols in the gastrointestinal tract: Implications of gastric and colonic microflora-dependent biotransformation, Free Radic. Res. 40 (2006) 647–658. doi:10.1080/10715760500373000.

[67] S. Silva, M. Garcia-Aloy, M.E. Figueira, E. Combet, W. Mullen, M.R. Bronze, High

Resolution Mass Spectrometric Analysis of Secoiridoids and Metabolites as Biomarkers of Acute Olive Oil Intake-An Approach to Study Interindividual Variability in Humans., Mol. Nutr. Food Res. 62 (2018). doi:10.1002/mnfr.201700065.

[68] N. Lemonakis, V. Mougios, M. Halabalaki, A.-L. Skaltsounis, E. Gikas, A novel bioanalytical method based on UHPLC-HRMS/MS for the quantification of oleuropein in human serum. Application to a pharmacokinetic study., Biomed. Chromatogr. 30 (2016) 2016–2023. doi:10.1002/bmc.3779.

[69] S. Angelo, C. Manna, V. Migliardi, O. Mazzoni, P. Morrica, G. Capasso, G. Pontoni, P. Galletti, V. Zappia, Pharmacokinetics and Metabolism of Hydroxytyrosol, a Natural Antioxidant from Olive Oil, Drug Metab. Dispos. 29 (2001) 1492–1498. http://dmd.aspetjournals.org/content/29/11/1492.abstract.

[70] A. Karkovi, T. Jelena, M. Barbaric, Hydroxytyrosol, Tyrosol and Derivatives and Their Potential Effects on Human Health, (2019).

[71] A. Angelis, L. Antoniadi, P. Stathopoulos, M. Halabalaki, L.A. Skaltsounis, Oleocanthalic and Oleaceinic acids : New compounds from Extra Virgin Olive Oil (EVOO), Phytochem. Lett. 26 (2018) 190–194. doi:10.1016/j.phytol.2018.06.020.

[72] J. Rodríguez-morató, A. Boronat, A. Kotronoulas, A. Pastor, E. Olesti, C. Pérez-mañá, O. Khymenets, M. Farré, R. De Torre, A. Boronat, A. Kotronoulas, J. Rodr, Metabolic disposition and biological significance of simple phenols of dietary origin : hydroxytyrosol and tyrosol, Drug Metab. Rev. Metab. Rev. 48 (2016) 218–236. doi:10.1080/03602532.2016.1179754.

[73] J. Rodriguez-Morato, P. Robledo, J.-A. Tanner, A. Boronat, C. Perez-Mana, C.-Y. Oliver

Chen, R.F. Tyndale, R. de la Torre, CYP2D6 and CYP2A6 biotransform dietary tyrosol into hydroxytyrosol., Food Chem. 217 (2017) 716–725. doi:10.1016/j.foodchem.2016.09.026.

[74] L. Rubio, A. Macia, R.M. Valls, A. Pedret, M.-P. Romero, R. Sola, M.-J. Motilva, A new hydroxytyrosol metabolite identified in human plasma: hydroxytyrosol acetate sulphate., Food Chem. 134 (2012) 1132–1136. doi:10.1016/j.foodchem.2012.02.192.

[75] D. Krupp, N. Doberstein, L. Shi, T. Remer, Hippuric Acid in 24-Hour Urine Collections Is a Potential Biomarker for Fruit and Vegetable Consumption in Healthy Children and adolescents, J. Nutr. Nutr. Epidemiol. 142 (2012) 1314–1320. doi:10.3945/jn.112.159319.A.

[76] N. Korytowska, A. Wyczałkowska-Tomasik, A. Wiśniewska, L. Pączek, J. Giebułtowicz, Development of the LC-MS/MS method for determining the p-cresol level in plasma, J. Pharm. Biomed. Anal. 167 (2019) 149–154. doi:https://doi.org/10.1016/j.jpba.2019.01.041.

Appendix

Table A 5*: HPLC-DAD quantification results for hydroxytyrosol (HT), tyrosol (T), oleocanthal (OLEO) and oleacein (OLEA). Results are expressed as mg/Kg of OO. Total phenolic content (TPC) and total phenolic fraction(TPF) are also presented and expressed as mg GAE/Kg of OO and g/Kg of OO respectively.*

Code	HT (mg/Kg OO)	T (mg/Kg OO)	OLEO (mg/Kg OO)	OLEA (mg/Kg OO)	TPC (mg GAE/Kg OO)	TPF (g/Kg OO)
OLE 110	1.3	1.6	83	116	166	1.8
OLE 122	37.3	16.9	< LOD[1]	< LOD[1]	128	2.14
OLE 166	11.1	9.8	57	71	142	1.31

[1]LOD: lower limit of detection

Table A 6: *[1]H-NMR data of elenolic acid (600 MHz,$CDCl_3$).*

Proton	Number of protons	δ (ppm)	Multiplicity	*J* coupling (Hz)
1	1H	9.70	d	*J*=2.0
3	1H	7.70	s	-
5	1H	3.40	dd	*J*=2.5/2.0
6	2H	a)2.95 b) 2.28	dd dd	*J*=16.5/3.0 *J*=16.5/11.1
8	1H	4.28	qd	*J*=6.7/2.0
9	1H	2.75	m	-
10	3H	1.58	d	*J*=7.0
12	3H	3.72	s	-
-COOH	1H	9.92	s (br)	-

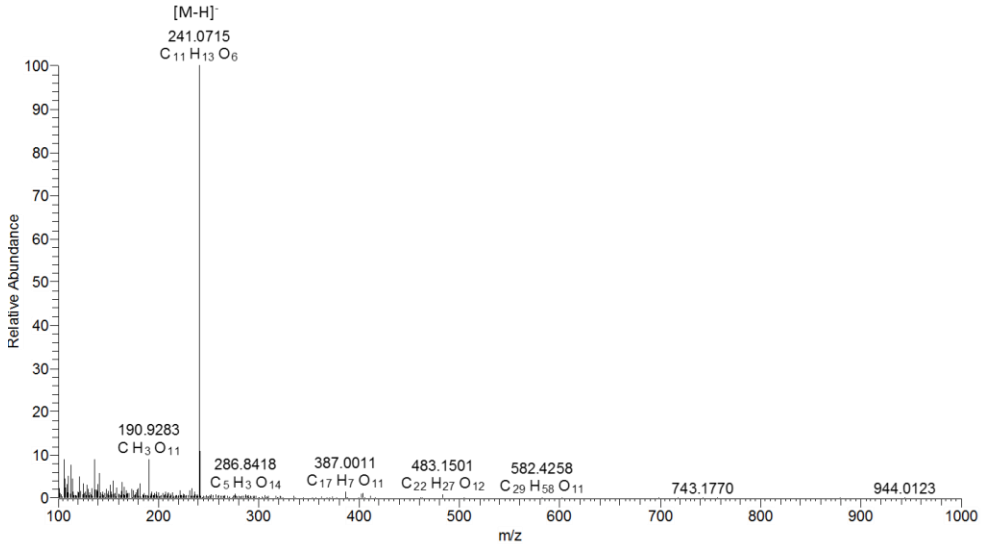

Figure A 19: *HRMS spectrum of elenolic acid in negative ionization. [M-H]- corresponds to the pseudomolecular ion. Experimental m/z and elemental composition are also depicted.*

Table A 7: *^{1}H-NMR data of monoaldehydic form of oleuropein aglycon (600 MHz,$CDCl_3$).*

Proton	Number of protons	δ (ppm)	Multiplicity	*J* coupling (Hz)
1	1H	9.52	d	*J*=1.7
3	1H	7.57	s (br)	-
5	1H	3.34	m	-
6a/2’	3H	2.86	m	-
6b/9	1H	2.55	m	-
8	1H	4.45	p	*J*=6.4
10	3H	1.39	d	*J*=6.7
12	3H	3.75	s	-
1’	2H	4.24	m	-
4’	1H	6.75	d	*J*=2.0
7’	1H	6.50	d	*J*=8.0
8’	1H	6.79	dd	*J*=8.0/2.0

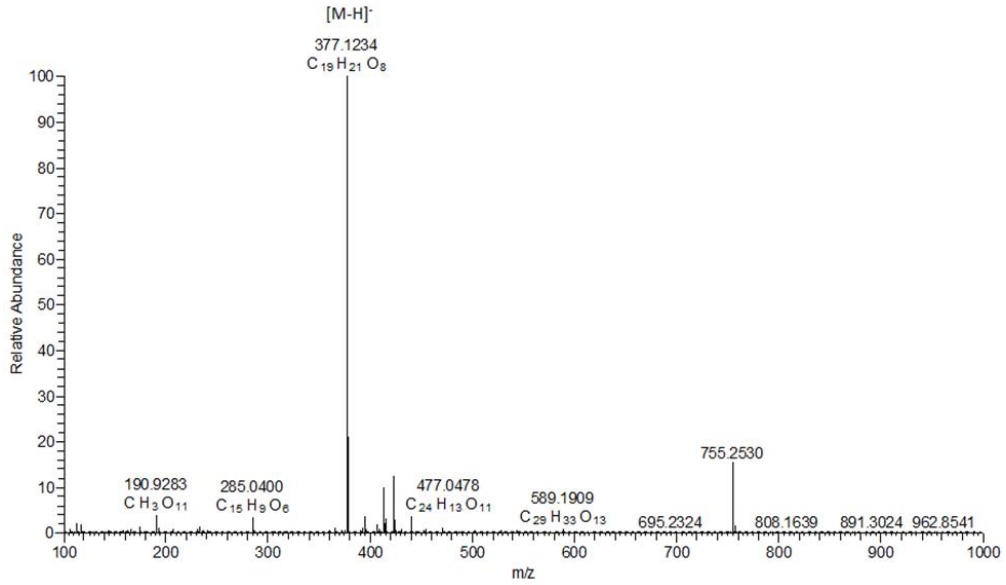

Figure A 20: *HRMS spectrum of monoaldehydic form of oleuropein aglycon in negative ionization. [M-H]- corresponds to the pseudomolecular ion. Experimental m/z and elemental composition are also depicted.*

Table A 8: *^{1}H-NMR data of oleacein (600 MHz,$CDCl_3$).*

Proton	Number of protons	δ (ppm)	Multiplicity	*J* coupling (Hz)
1	1H	9.17	d	*J*=1.9
3	1H	9.61	s (br)	-
4a	1H	2.92	ddd	*J*=18.4/8.3/1.0
4b	1H	2.73	m	-
5	1H	3.60	m	-
6a	1H	2.69	dd	*J*=15.6/8.7
6b	1H	2.59	dd	*J*=15.6/6.5
9	1H	6.63	d	*J*=7.1
10	3H	2.04	d	*J*=7.1
1'a	1H	4.22	dt	*J*=10.8/6.7
1'b	1H	4.15	dt	*J*=10.8/6.4
2'	2H	2.76	m	-

4’	1H	6.69	d	*J*=2.0
7’	1H	6.77	d	*J*=8,0
8’	1H	6.75	dd	*J*=8,1/2.0

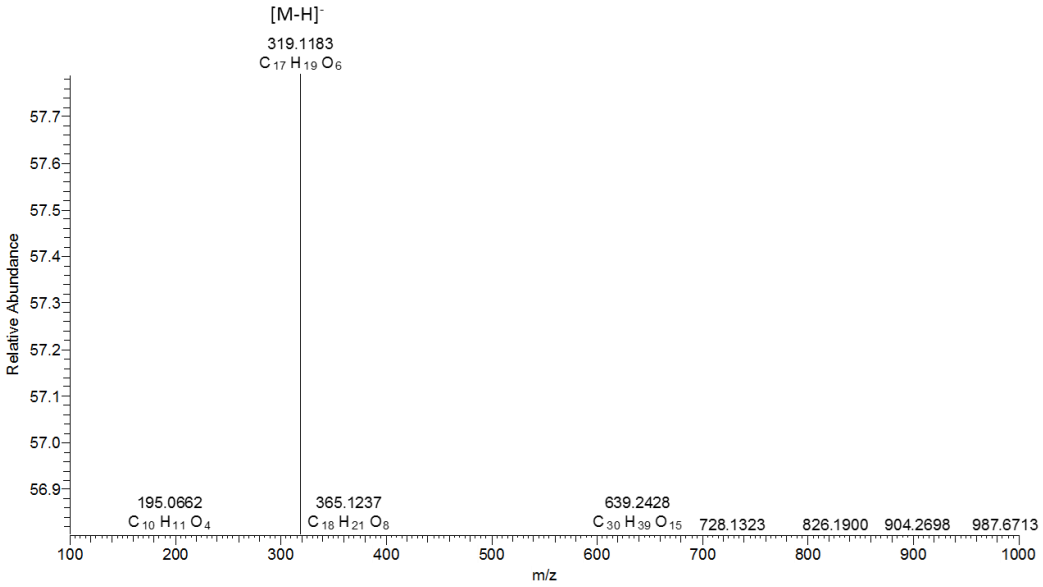

Figure A 21: *HRMS spectrum of oleacein in negative ionization. [M-H]- corresponds to the pseudomolecular ion. Experimental m/z and elemental composition are also depicted.*

Table A 9: *^{1}H-NMR data of ligstroside aglycon (600 MHz,$CDCl_3$).*

Proton	Number of protons	δ (ppm)	Multiplicity	*J* coupling (Hz)
1	1H	9,50	d	J=1,8 Hz
3	1H	7,56	s (br)	-
5	1H	3,35	m	-
6a	1H	2,89	dd	J=16,1/ 3,7
6b/9	2H	2,54	m	-

8	1H	4,41	p	J=6,5 Hz
10	3H	1,38	d	J=6,7 Hz
12	3H	3,72	s	-
1’	2H	4,27	m	-
2’	2H	2,85	t	J=7,1 Hz
4’/8’	2H	7,06	d	J=8,5 Hz
5’/7’	2H	6,76	d	J=8,5 Hz

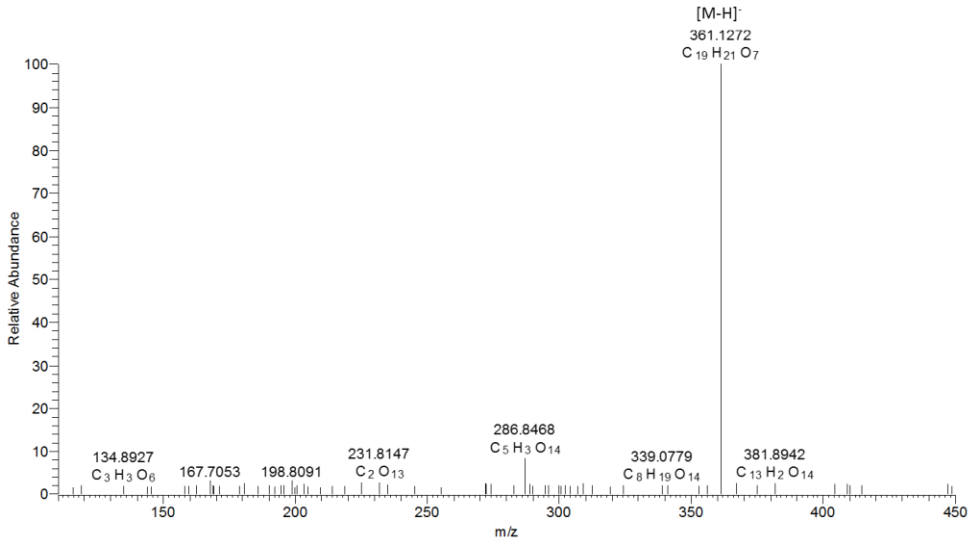

***Figure A 22**: HRMS spectrum of monoaldehydic form of ligstroside aglycon in negative ionization. [M-H]- corresponds to the pseudomolecular ion. Experimental m/z and elemental composition are also depicted.*

***Table A 10**: ^{1}H-NMR data of oleocanthal (600 MHz,$CDCl_3$).*

Proton	Number of protons	δ (ppm)	Multiplicity	*J* coupling (Hz)
1	1H	9.21	d	J=1.9
3	1H	9.61	s (br)	-
4a	1H	2.97	ddd	J=18.3/8.7/1.3
4b	1H	2.73	ddd	J=18.3/5.5/0.8

5	1H	3.60	m	-
6	1H	2.64	m	-
9	1H	6.63	q	J=7.1
10	3H	2.06	d	J=7.1
1’	2H	4.20	m	-
2’	2H	2.81	t	J=6.9
4’/8’	2H	7.03	d	J=8.5
5’/7’	2H	6.75	d	J=8.5

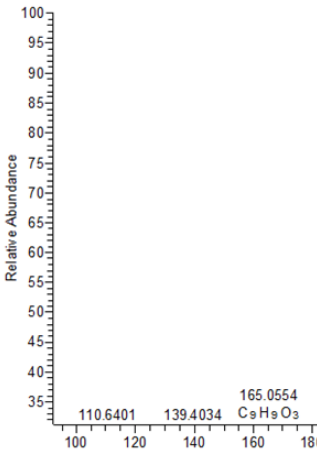

Figure A 23: *HRMS spectrum of oleocanthal in negative ionization. $[M-H]^-$ corresponds to the pseudomolecular ion. Experimental m/z and elemental composition are also depicted.*

Table A 11*: ^{1}H-NMR data of elenolic ethyl ester (600 MHz,$CDCl_3$).*

Proton	Number of protons	δ (ppm)	Multiplicity	*J* coupling (Hz)
1	1H	9.64	d	*J*=1.8
3	1H	7.58	s	-
5	1H	3.42	ddd	*J*=9.5/6.1/3.6
6	2H	a) 2.90 b) 2.56	dd dd	*J*=16.1/3.6 *J*=16.1/9.5
8	1H	4.41	qd	*J*=6.7/6.1
9	1H	2.72	td	*J*=6.1/1.8

10	3H	1.43	d	*J*=6.6
12	3H	3.73	s	-
1’	2H	4.13	q	*J*=7.10
2’	3H	1.25	t	*J*=7.10

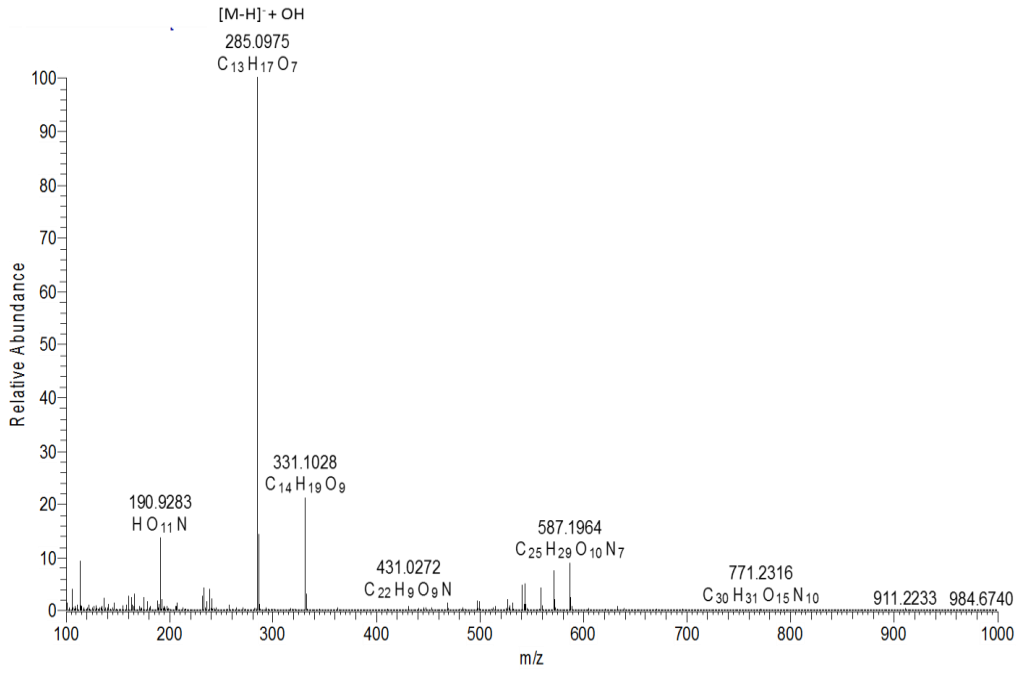

Figure A 24*: HRMS spectrum of elenolic acid ethyl ester in negative ionization. [M-H]⁻ corresponds to the pseudomolecular ion. Experimental m/z and elemental composition are also depicted.*

Cell lines and cell culture conditions

Human newborn foreskin diploid fibroblasts (BJs) were obtained from the American Tissue Culture Collection and were maintained in Dulbecco's modified Eagle's medium (Gibco Life Technologies), supplemented with 10% (v/v) fetal bovine serum, 2 mM glutamine and 1% non-essential amino acids. The non-tumorigenic immortalized mouse skin keratinocytes (C5N)

cells were a kind donation of Dr. V. Zoumpourlis (National Hellenic Research Foundation) (Zoumbourlis et al., 2003). C5N cells were cultured in Dulbecco's modified Eagle's medium (Gibco Life Technologies) containing 10% (v/v) fetal bovine serum and 2 mM glutamine. Both cell lines were maintained in a humidified incubator at 5% CO_2 and 37°C.

Quantitative Real Time PCR (Q-PCR) analysis

Primers were designed using the primer-BLAST tool (http://www.ncbi.nlm.nih.gov/tools/primer-blast/) and were the following (F: forward, R: reverse, Sequence: 5'→3'):

H-*PSMA7*-F: TAC-ATC-ACC-CGC-TAC-ATC-GC, H-*PSMA7*-R:AGA-GCC-TAG-GAG-TGC-CAT-CA; H-*PSMB1*-F: GGA-TGC-AGC-GGT-TTT-CAT-GG, H-*PSMB1*-R: AAT-TGC-CCC-CGT-AGT-CAT-GG; H-*PSMB2*-F: CTG-CTC-CGC-CCT-CCA-TTA-AC, H-*PSMB2*-R: GCC-AAG-CAT-GGA-GTA-GAA-CG; H-*PSMB5*-F: TCA-AGT-TCC-GCC-ATG-GAG-TC, H-*PSMB5*-R: CTT-CTT-CAC-CGT-CTG-GGA-GG; H-*RPN6*-F: TCA-AAC-TCT-CCA-AGG-CCG-AC, H-*RPN6*-R: CTC-CCC-CTG-GTC-CAA-AAT-CC; H-*RPN11*-F: ACG-GAA-GCC-GAA-GCA-AAC-TA, H-*RPN11*-R: GCA-AAC-CGG-CGA-TGA-ATC-AG; H-*BECN1*-F: CAG-AGC-GAT-GGT-AGT-TCT-GGA, H-*BECN1*-R: TTG-GAC-GTC-TTA-GAC-CCT-TCC; H-*HDAC6*-F: GAC-CAT-CCA-AGT-CCA-TCG-CA, H-*HDAC6*-R: ACC-TAG-GTT-TGG-CTG-GTT-GG; H-*LC3B*-F: GCTATCGCCAGAGTCGGAT, H-*LC3B*-R: CTTTGTTCGAAGGTGCGGC; H-*CTSL*-F: ACA-GGG-AAG-GGA-AAC-ACA-GC, H-*CTSL*-R: TTC-ACA-GGA-GTC-ACG-TAG-CC; H-*CTSD*-F: ACC-TTC-ATC-GCA-GCC-AAG-TT, H-*CTSD*-R: AGC-ACG-TTG-TTG-ACG-GAG-AT; H-*HSF1*-F: TAT-GGC-TTC-CGG-AAA-GTG-GT, H-*HSF1*-R: GGA-ACT-CCG-TGT-CGT-CTC-TC; H-*HSP27/HSPB1*-F: CCA-CCC-AAG-TTT-CCT-CCT-C, H-*HSP27/HSPB1*-R: GAC-TGG-GAT-GGT-GAT-CTC-GT; H-

HSP70/HSPA1A-F: AGG-CCA-ACA-AGA-TCA-CCA-TC, H-*HSP70/HSPA1A*-R: TCG-TCC-TCC-GCT-TTG-TAC-TT; H-*HSP90*-F: GGC-AGA-GGC-TGA-TAA-GAA-CG, H-*HSP90*-R: CTG-GGG-ATC-TTC-CAG-ACT-GA; H-*CLU*-F: AAA-CGA-AGA-GCG-CAA-GAC-AC, H-*CLU*-R: TGT-TTC-AGG-CAG-GGC-TTA-CA; H-*STUB1*-F: TAC-GGC-CGC-GCG-ATC-A, H-*STUB1*-R: GAA-GTG-CGC-CTT-CAC-AGA-CT; H-*NRF2*-F: CAT-CCA-GTC-AGA-AAC-CAG-TGG, H-*NRF2*-R: GCA-GTC-ATC-AAA-GTA-CAA-AGC-AT; H-*KEAP1*-F: AGT-TCA-TGG-CCC-ACA-AGG-TG, H-*KEAP1*-R: AAT-GGA-CAC-CAC-CTC-CAT-GC; H-*NQO1*-F: AGC-AGA-CGC-CCG-AAT-TCA-AA, H-*NQO1*-R: AGA-GGC-TGC-TTG-GAG-CAA-AA; H-*TXNRD1*-F: TTG-GAG-TGC-GCT-GGA-TTT-CT, H-*TXNRD1*-R: TTT-GTT-GGC-CAT-GTC-CTG-GT. The beta-2-microglobulin gene (H-*B2M*-F: ACT-GAA-TTC-ACC-CCC-ACT-GA, H-*B2M*-R: AAG-CAA-GCA-AGC-AGA-ATT-TGG) was used as Q-PCR normalizer.

Treatment of *Drosophila* flies with EVOOs

EVOOs were directly added in flies' culture medium before its solidification and when the temperature of the medium had dropped to ~50-60°C; the preparation was then thoroughly mixed. The doses and duration of flies' exposure to EVOOs are indicated in figure legends. In all experiments fresh culture medium containing the pure compounds or EVOOs was prepared every 3 days.

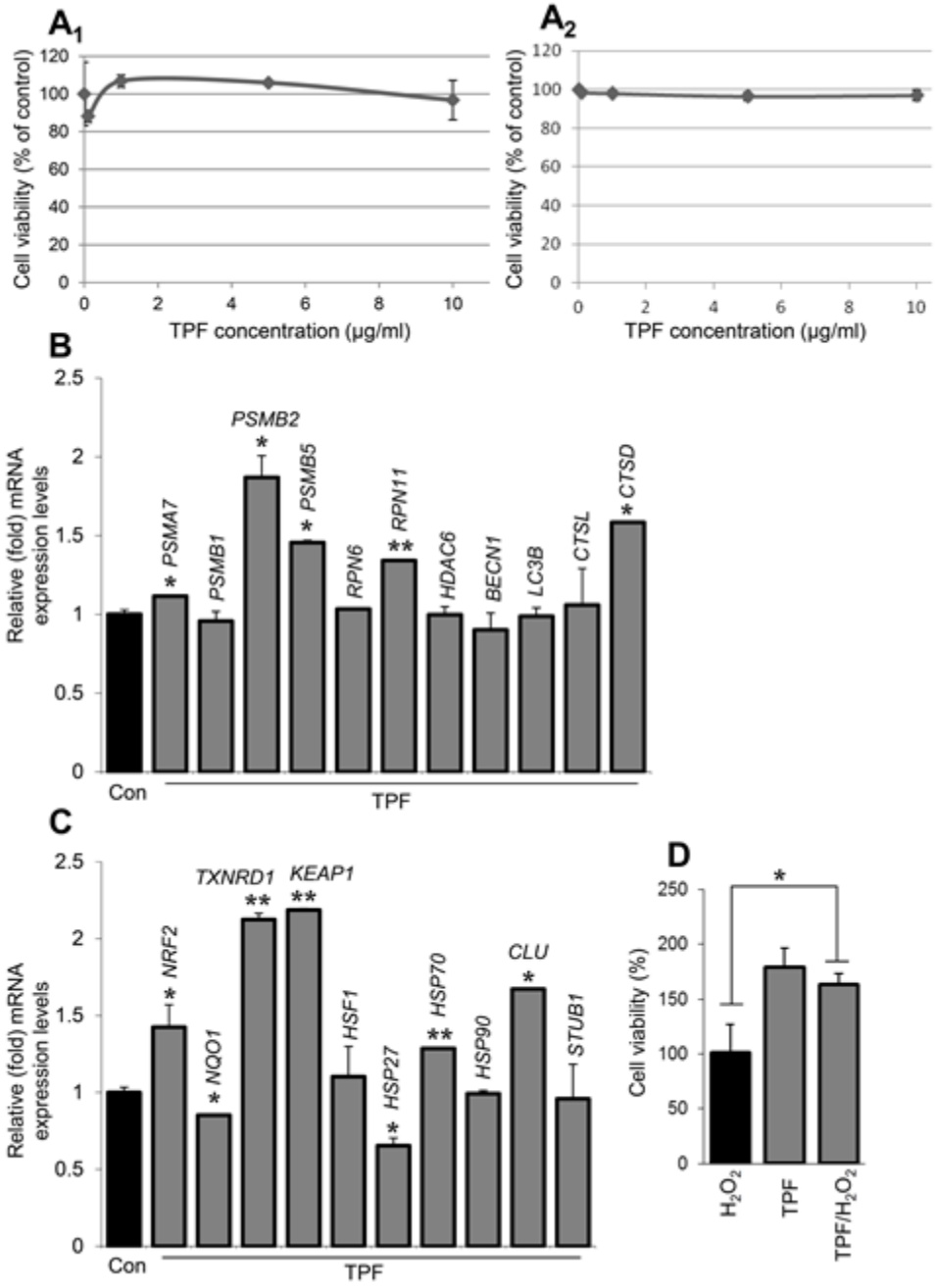

Figure A 25*: OLE 110 does not exert any significant toxicity in normal human diploid skin fibroblasts; upregulates genes involved in the proteostasis network regulation, as well as in cellular antioxidant responses, and protects cells from H_2O_2-mediated toxicity. (A) Relative (%) cell viability of early passage human skin (BJ) fibroblasts exposed to the indicated concentrations (0.1, 1, 5 and 10 μg/ml) of OLE 110 (TPF with high content of OLEO or OLEA) for 48 h through MTT (A_1) and trypan blue dye exclusion (A_2) assays. (B) Q-PCR mRNA expression analyses of proteasome genes (PSMA7, PSMB1, PSMB2, PSMB5, RPN6 and RPN11) and of genes involved in ALP functionality (HDAC6, BECN1, LC3B, CTSL and CTSD). Shown control refers to control values of the PSMA7 gene; in all other cases, standard deviation did not*

*affect the shown significance of the other samples. (C) Q-PCR mRNA expression levels of genes involved in antioxidant responses (NRF2, NQO1, TXNRD1 and KEAP1), as well as of molecular chaperones genes (HSF1, HSP27, HSP70, HSP90, CLU and STUB1). Shown control refers to control values of the NRF2 gene; in all other cases, standard deviation did not affect the shown significance of the other samples. (D) Relative (%) survival (MTT assay) of BJ fibroblasts exposed to 200 μM H_2O_2 for 24 h in the presence or absence of 10 μg/ml OLE110. In (A) and (D) controls were set to 100%, whereas in (B) and (C) controls were set to 1. In gene expression analyses the beta-2-microglobulin (B2M) gene expression was used as normalizer. Bars, ± SD. *, P<0.05; **, P<0.01.*

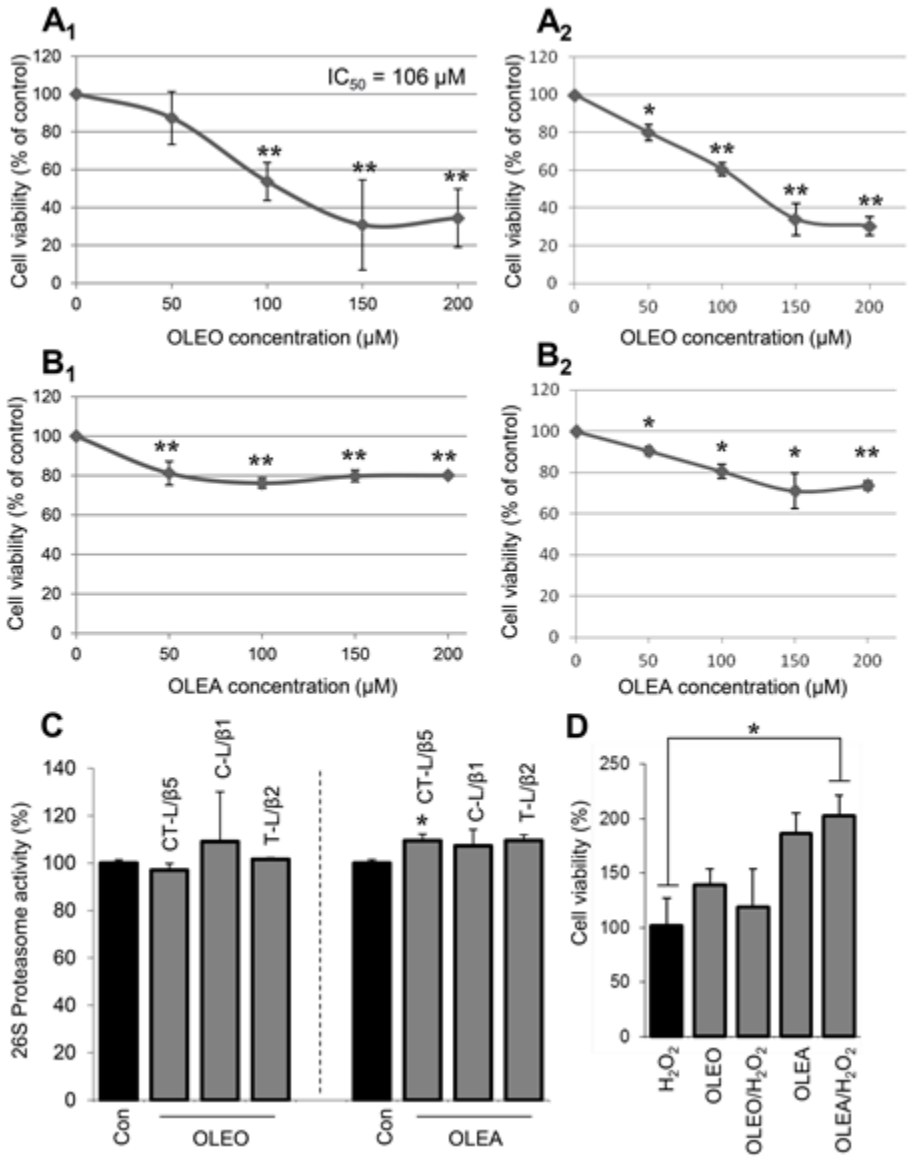

***Figure A 26**: OLEO and OLEA are relatively not toxic (at low concentrations) in human fibroblasts; OLEA induces the main proteasome peptidase activity and confers protection against H_2O_2-mediated toxicity. (A) Relative (%) viability of proliferating human diploid skin (BJ) fibroblasts treated with increasing concentrations (50, 100, 150 and 200 µM) of OLEO for 48 h through MTT (A_1) and trypan blue dye exclusion (A_2) assays. (B) Relative (%) survival of proliferating human skin (BJ) fibroblasts incubated with increasing concentrations (50, 100, 150 and 200 µM) of OLEA for 48 h through MTT (B_1) and trypan blue dye exclusion (B_2) assays. (C) (%) 26S proteasome activity (CT-L/β5, C-L/β1 and T-L/β2) in BJ cells following treatment with 30 µM OLEO or 30 µM OLEA for 24 h. Shown control refers to control values of the OLEO or OLEA CT-L/β5; in all other cases, standard deviation did not affect the shown significance of the other samples. (D) Relative (%) survival (MTT assay) of BJ fibroblasts exposed to 200 µM H_2O_2*

*for 24 h in the presence or absence of 30 μM OLEO or 30 μM OLEA for 24 h. In (A)-(D) controls were set to 100%. Bars, ± SD. *, P<0.05; **, P<0.01.*

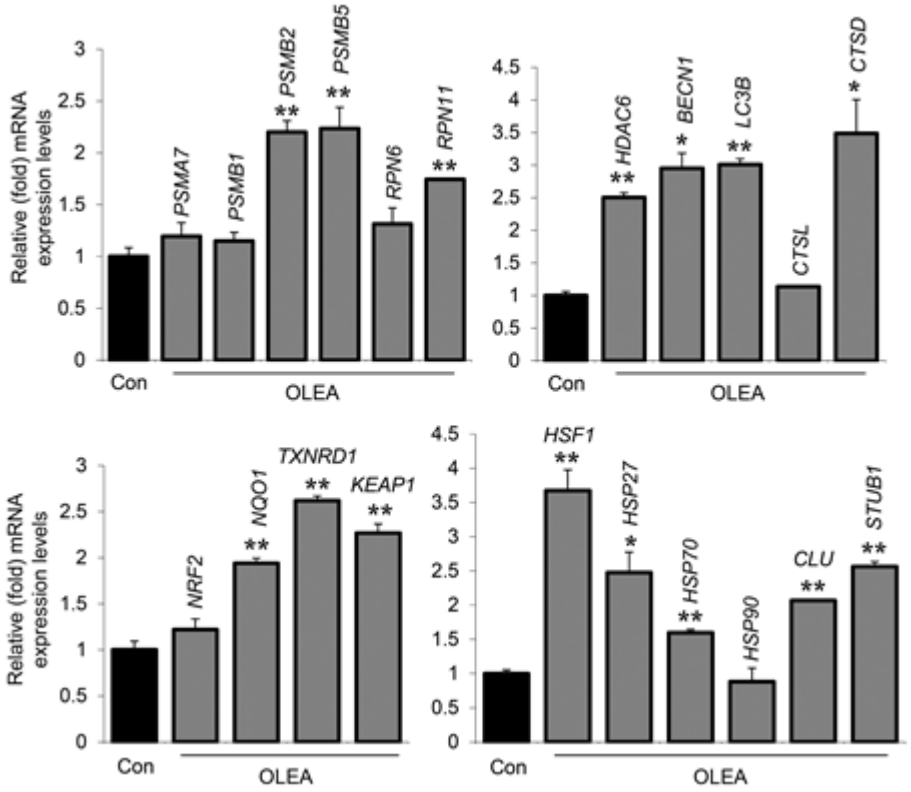

***Figure A 27**: Exposure of skin fibroblasts (BJ cells) to 30 μM OLEA for 24 h induces genes involved in the proteostasis network regulation, as well as in cellular antioxidant responses. Shown Q-PCR gene expression studies refer to proteasomal genes (PSMA7, PSMB1, PSMB2, PSMB5, RPN6 and RPN11), to genes involved in ALP functionality (HDAC6, BECN1, LC3B, CTSL and CTSD), as well as to genes involved in antioxidant responses regulation (NRF2, NQO1, TXNRD1 and KEAP1) and to molecular chaperones genes (HSF1, HSP27, HSP70, HSP90, CLU and STUB1). Shown controls refer to the control values of the samples PSMA7, HDAC6, NRF2 and HSF1, respectively. In all cases, standard deviation did not affect the shown significance of the other samples. The beta-2-microglobulin (B2M) gene expression was used as normalizer. ars, ± SD. *, P<0.05; **, P<0.01 vs. controls set to 1.*

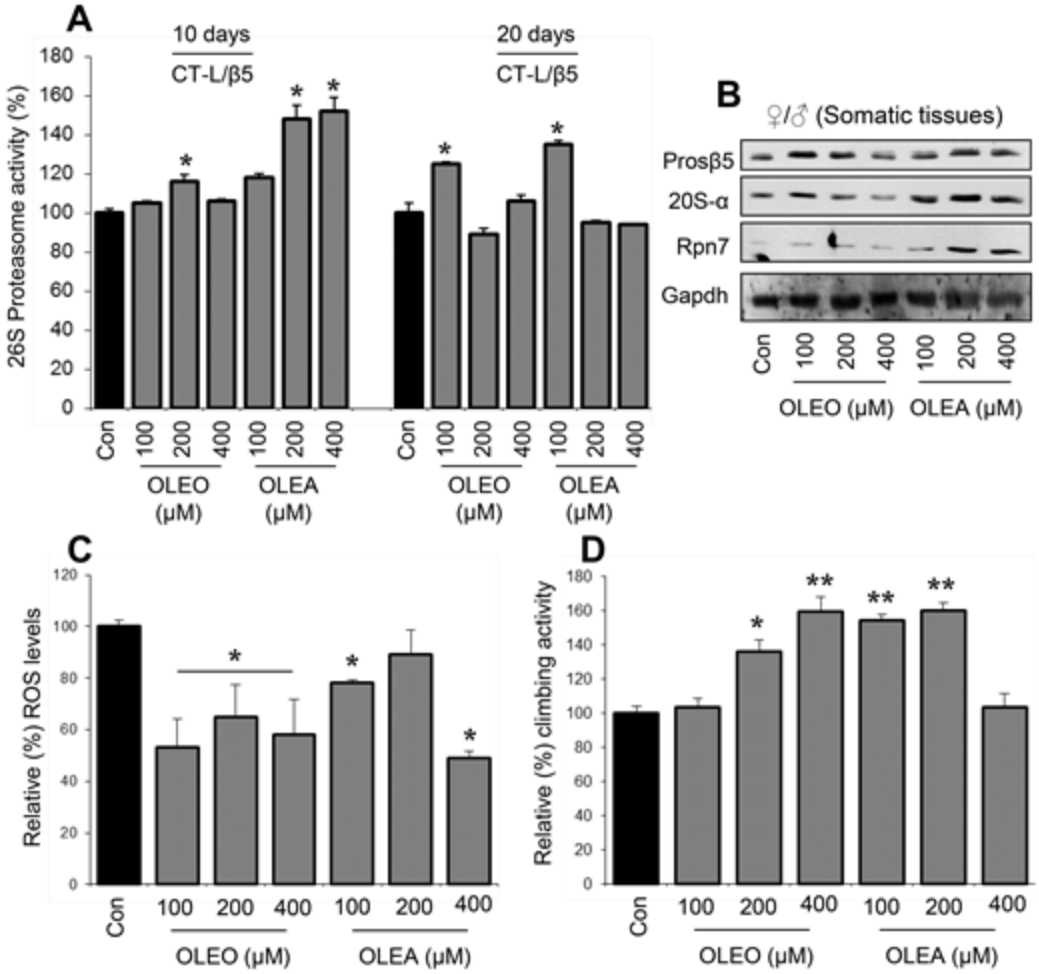

Figure A 28: *Oral administration of OLEO or OLEA in wild type Drosophila flies enhances proteasome activity and expression, decreases ROS levels and delays the age-related decline of locomotor (climbing) activity. (A) Relative (%) CT-L activity in somatic tissues of flies that were exposed for 10 and 20 days to the indicated concentrations of OLEO or OLEA. Proteasome activities were expressed in fluorescence units per μg of input protein vs. controls set to 100%. (B) Representative immunoblotting analyses of proteasome β5 subunit (Prosβ5), proteasome α-type subunits (20S-α) and Rpn7 expression following treatment of young wild type flies to the indicated concentrations of OLEO or OLEA for 10 days. Gapdh probing was used as reference for protein input. (C) ROS levels in somatic tissues of young flies after treatment with the indicated concentrations of OLEO or OLEA for 20 days (control samples were set to 100%). (D) Relative climbing activity (%) (vs. controls) of flies that were exposed to OLEO or OLEA for 20 days at the indicated concentrations. Bars, ± SD (n = 3). *P<0.05; **P<0.01.*

***Table A 12**: Summary of* Drosophila *lifespan experiments.*

	Genotype	Mean Lifespan (LF) +/- s.e.m. (Days)		Median Lifespan +/- s.e.m. (Days)		% Median LF vs. control	Max (Days)	Log Rank P Value		
								RU486 (-)	RU486 (+)	*Total Animals Died/Total*
	UAS InR^{A1325D}	43.932	1.764	47	1.392	100.00	64		0.000	60/62
	UAS InR^{A1325D}	23.981	0.595	24	0.803	51.06	38	0.000		127/128

								RU486 (+)	RU486 (+) - Ole122	RU486 (+) - Ole166	RU486 (+) - Ole110
	UAS InR^{A1325D}	23.981	0.595	24	0.803	100.00	38		0.012	0.000	0.000
	UAS InR^{A1325D}	25.462	0.742	27	1.02	112.50	40	0.012		0.022	0.003
	UAS InR^{A1325D}	28.576	0.818	30	0.868	125.00	42	0.000	0.022		0.327
	UAS InR^{A1325D}	28.686	1	28	1.14	116.67	43	0.000	0.003	0.327	

ere used
npounds was used as a control
ncentration of 10 µg/ml

Chapter 3

Mass spectrometry based investigation of hydroxytyrosol effect in human obesity

Abstract

Based on World Health Organization recent data, obesity is regarded as a major public health problem. So far, several *in vivo* studies and experimental models investigate the effect of olive oil (OO) biophenols and particular hydroxytyrosol (HT), a strong antioxidant entity of OO, in metabolic diseases. Promising results have been uncovered and nowadays research focuses on the exploration of HT effects on human metabolome.

In this study two different UPLC-HRMS platforms were incorporated for the quantification of HT in human biological fluids and the identification of metabolites-biomarkers thereof, after the administration of an encapsulated biophenol extract enriched in HT. In particular, urine and blood samples were collected in three time points from 30 overweight/obese women, randomized in three groups according to HT intake (A–15mg HT/day, B-5mg HT/day, C-placebo) in a double-blinded study. After investigation and application of the appropriate extraction protocols, a UHPLC-triple-quadrupole method was developed and validated for HT detection and quantification in human urine, using multiple reaction monitoring mode. Maximum HT excretion levels were determined for each group in all time points and further correlated with the corresponding weight and fat loss. Successively, blood and urine extracts were subjected to untargeted metabolomics via UPLC-Orbitrap-MS in negative ionization mode using full scan and data-depended methods. After pre-treatment, data were subjected to multivariate statistical analysis assisted by chemometric tools. Well-defined groups were revealed and statistical significant metabolites-biomarkers were identified among groups. The determined HT concentrations and weight loss of each group were correlated with the identified biomarkers and associated with specific metabolic pathways. Significant interrelations were observed associating

HT administration with a positive impact to weight and fat loss in overweight/obese women characterized by specific metabolic markers.

Keywords

Hydroxytyrosol; human intervention; HRMS; biological fluids; quantification; metabolomics; biomarkers

1. Introduction

Obesity is regarded as a major public health problem and based on World Health Organization (WHO) most recent data it affects more than 39% of world population [1]. Overweight and obesity are defined as abnormal or excessive fat accumulation that may impair health and are measured by body mass index (BMI) [1]. BMI is determined as weight in kilograms (Kg) divided by the square of height in meters (Kg/m^2). Overweight is considered someone with BMI ranging from 25-29.9 Kg/m^2 and obese someone with BMI>30 Kg/m^2 [2]. Obesity usually is accompanied with chronic low-grade inflammation and other metabolic disorders such as type 2 diabetes, disorders of lipid and glucose homeostasis, cardiovascular diseases (CVD) and hepatic steatosis [3].

Obesity is induced both by genetic and lifestyle factors. Generally is caused due to the imbalance between calories intake and expenditure, usually due to the consumption of energy-dense foods and lack of physical activity [4]. Lately, a growing number of studies focus also on gut microbiome and specifically in changes of symbiotic bacteria population in the gastrointestinal tract and the impact of such changes in human metabolic disorders [5]. Gut microbiome has a recognized contribution to digestion and metabolism by regulating energy production and fatty acid tissue composition. Investigation of gut microbiome population and its effects to human health are nowadays in the center of scientific interest [6].

These two determinant factors, calories intake and microbiota composition, are affected by populations' and personal dietary habits. Mediterranean Diet (MD) is considered as one of the healthiest diets and its cardioprotective effect is well documented. Nevertheless, based on literature data, greater adherence to MD is associated with lower abdominal adiposity in Mediterranean populations [7,8], prevention of obesity, metabolic syndrome and its related

disorders [9]. Olive products are major components of MD containing a plethora of phenol and secoiridoid derivatives, known for its antioxidant and anti-inflammatory properties [10]. One of these compounds is hydroxytyrosol (3,4-dihydroxyphenylethanol, HT) which is a bioactive catecholic compound of olive products with confirmed strong antioxidant, antinflammatory and antimicrobial properties [11]. Likewise HT is associated with metabolic syndrome and its disorders [12], while it was recently found that it improves obesity and insulin resistance by modulating gut microbiota [3]. Also it has been found that HT prevents inflammation and hyperglycemia produced by a high fat diet [13,14] and decreases lipid steatosis [14].

HT is a characteristic and biological important phenol of olive oil (OO) strongly associated with the protection of blood lipids from oxidative stress. After European Food Safety Authority (EFSA) investigation, the above positive effect was recognized, following a daily consumption of OO containing at least 5 mg of HT and its derivatives per 20 g of OO [15]. HT shows also high concentration in olive drupes and leaves [16,17] and it is also present in red wine [18] and several other species of *Oleaceae* family [19]. Nevertheless, HT can be found in considerable high concentrations in the generated by-products of OO mechanic extraction, in both solid residue (pomace) and aqueous known as olive mill wastewater (OMWW). Another source of high HT amount is the by-products from debittering process of edible olives (OWW). Its concentration in these by-products depends on several factors such as production procedure system (two, three, two and a half phases decanters) for OO production, extraction conditions, olive cultivar, agronomic practices and storage conditions [16].

It has to be highlighted that HT is normally synthesized in human body, formed through dopamine metabolic pathway [20]. Figure 32 describes the corresponding pathway for the formation of HT. Initially, dopamine is metabolized by monoaminooxidase B (MAO-B), which

removes the amine group and generates the corresponding aldehydic derivative 3,4-dihydroxyphenylacetaldehyde (DOPAL) [20]. Due to its unstable nature, DOPAL can be easily oxidized by mitochondrial aldehyde dehydrogenase (ALDH) to the corresponding acidic metabolite 3,4-dihydroxyphenylacetic acid (DOPAC). DOPAC is considered as the major metabolite of dopamine in biological matrices and the above pathway is known as the dopamine oxidative metabolism [21]. DOPAC can be further methylated by catechol-O-methyltransferase enzyme (COMT) to form homovanillic acid. However, another minor metabolic pathway can be followed after DOPAL generation. DOPAL reduction by aldehyde/aldose reductases (ALR) gives rise to 3,4-dihodroxyphenylethanol, known as HT. The latter reaction can also happens reversely by alcohol dehydrogenase (ADH) [21]. 4-hydroxy-3-methoxyphenylethanol or homovanillic alcohol is the corresponding methylated metabolite of HT after COMT activity [20]. Furthermore, DOPAC can be transformed to HT by DOPAC reductase [22]. HT and homovanillic alcohol are physiologically present in low concentrations in biological matrices, while DOPAC and homovanillic acid are more abundant. The latter compounds are regarded as typically dopamine biomarkers. It is notable that HT, which is a normally formed metabolite in human body, is considered as one of the most bioactive natural products [23].

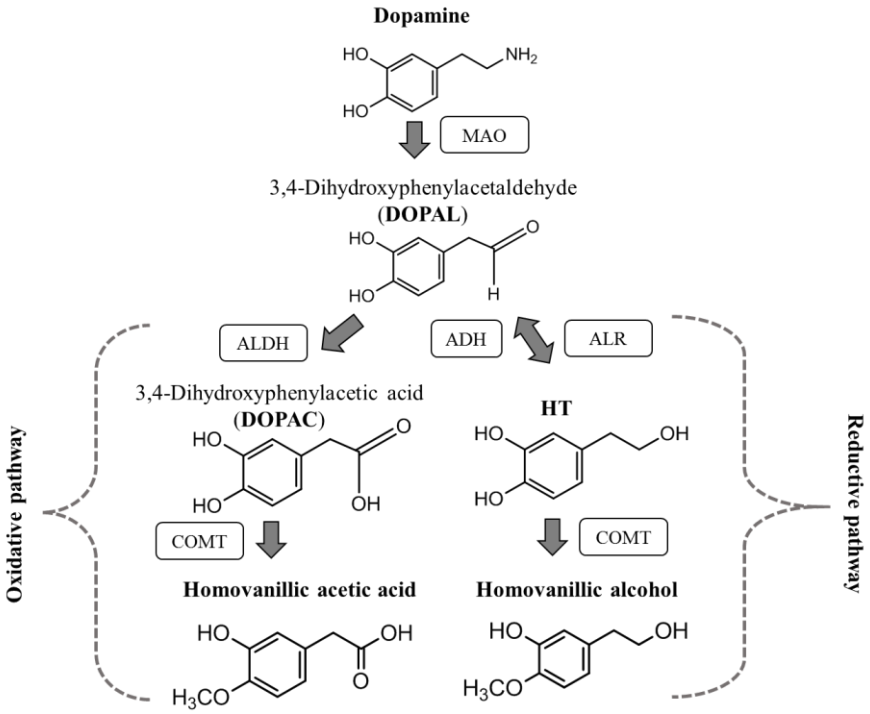

***Figure 32**: Endogenous biosynthetic pathway for HT formation through dopamine metabolism. MAO-B: monoaminooxidase B, ALDH: aldehyde dehydrogenase, COMT: catechol-O-methyltransferase enzyme, ALR: aldehyde/aldose reductases, ADH: alcohol dehydrogenase.*

Animal studies have shown that ethanol consumption creates a reductive environment which engenders a shift in dopamine oxidative metabolism and enhances the formation of HT instead of DOPAC [24]. The *in vivo* evidences have been confirmed by clinical trials where measurements in volunteers urine have shown an increase in HT excretion in sulfate form after wine intake [25,26].

HT is mainly absorbed in the intestine through bi-directional passive diffusion mechanism with an efficiency ranging from 75% up to 100% [27]. The absorption process depends on the used matrix for HT administration, being more effective in the form of OO, than in pure form [28]. *In vivo* studies have shown that also gender is a critical feature for final HT bioavailability, persisting for longer time in female rats [29]. HT has an intense and rapid absorption and its

plasma half-life is around 1-2 minutes and once absorbed it is strongly binded to high density lipoproteins acting as antioxidant and cardioprotective factor, when administered intravenously [30]. HT and its metabolites are characterized by high distribution abilities to tissues such as muscle, testis, liver, and brain (HT is able to cross the blood brain barrier) and are generally accumulated in kidneys and liver [31].

HT after is absorbed, it undergoes a rapid and intense metabolization. Initially, it is subjected to phase I metabolization inside enterocytes (phase I) and then recirculates in the liver to end in large intestine (phase II). Gut microbiota are the responsible modulator for absorption and transformation of HT and its metabolites. During phase I metabolism mainly oxidation reaction occurs, producing the major metabolic products; DOPAL and DOPAC [20]. During phase II metabolism, methylation reaction produces methoxy aldehydic and/or acidic derivatives and then sulfation and glucuronidation produce the corresponding metabolic sulfate/glucuronide conjugates of all the previous produced metabolites [20]. Moreover, in phase II metabolism and more specifically the alkaline conditions of human lumen, lead to the activity of an acetyl-transferase enzyme which can form HT-acetate and subsequently the corresponding sulfate product [32]. Also in a rat model a metabolite called *N*-acetyl-5-S-cysteinyl-HT has been identified in urine [33]. It has been found that HT and its conjugated metabolites are mainly excreted by the kidneys [34] approximately after six hours for the complete elimination from human body [20]. Metabolites from liver can be redirected back to duodenum where they can be transformed and reabsorbed. This recycling procedure leads to longer presence of HT and its metabolites in human body [35].

HT is easily detected in human urine in its free form and several coupled methodologies such as GC-MS and LC-MS have been proposed for quantification purposes [36,37]. From the

first reports it has been discovered that HT absorption and excretion levels are positively correlated with the administrated doses [38]. After the elucidation of HT metabolism in humans, its sulfate conjugate has been proposed as the most suitable biomarker for monitoring compliance in urine and plasma as well [37]. Nevertheless, other HT conjugates have been previously suggested and still used and mostly HT-glucuronides [38].

On the contrary, HT detection in human plasma is not an easy assignment. Radiolabeling of HT has uncovered its absorption and elimination in *in vivo* models estimating an absorption of 99% when administered orally in OO [28]. Its high binding affinity to plasma lipoproteins makes it almost undetectable in human plasma in its free form. Few quantification methodologies have been proposed via GC/LC-MS for the quantification of HT and selected conjugates [39]. However, for the detection usually several time-consuming steps are required in sample preparation process including derivatization reactions and expensive purification steps [40]. Low analytes recovery is the common element in the suggested methodologies and so far there is not an easy and efficient method for the quantification of HT in plasma.

In the present work a randomized bouble-blind intervention study was designed for the investigation of HT effect in overweight/obese women. For this purpose, an encapsulated HT enriched extract was developed and administered to 30 overweight/obese women. The HT extract derived from edible olives, with a final concentration of 2.5 mg HT per capsule. An analytical methodology was developed for capsules analysis and exact HT quantification thereof. Urine and blood samples were collected in three time points during a six-month intervention period. A validated method was developed for the quantification of HT in urine and the examination of the corresponding absorption and excretion levels during intervention. Continuously a UPLC-HRMS platform was integrated for the metabolomic analysis of urine and

blood samples as well. The derived data were subjected to MVA, which is considered an advanced tool for the treatment of the massive generated data of human metabolome analysis and contribute to the uncover of statistical significant metabolites. Statistical and optimization models were developed for blood and urine after studying and application of the appropriate parameters and algorithms respectively. The employed statistical process and chemometric tools in urine samples revealed metabolites which highlighted the followed metabolic pathway in the intervention groups (placebo and HT), while statistical significant blood biomarkers were revealed and appear to get altered after HT intake.

2. Materials and Methods

2.1.1 Chemicals and Reagents

Acetonitrile (ACN), *n*-hexane and HCl used for HT capsule pretreatment were of analytical grade (Fisher chemicals). ACN, water (H_2O) and acetic acid used for HT quantification in capsules were HPLC grade (Fischer chemicals). ACN and formic acid used for HRMS analysis were LC-MS grade (Fisher Chemical) and water (H_2O) was obtained from a milli-Q water purification system (Millipore, USA). The analytical reference standards, hydroxytyrosol (HT) and 2,4-Dinitrophenol (2,4-DNP) were purchased from Chembiotin (Greece) with purity > 99%.

2.1.2 Instrumentation

Quantification of HT in capsules was performed to an HPLC system equipped with a pump SpectraSystem P4000, autosampler SpectraSystem AS3000 and PDA SpectraSystem UV800. For the quantification of HT in urine extracts an Advance^{TM} UPLC system was used couple to an EVOQ^{TM} Elite Triple Quadrupole Mass Spectrometer (Bruker) equipped with a heated electrospray ionization source (HESI). Metabolomic analysis of urine and plasma was accomplished to an H class Acquity UPLC system (Waters, USA) coupled to a LTQ-Orbitrap XL hybrid mass spectrometer (Thermo Scientific, USA).

2.2 Capsules quantitative and qualitative analysis

Two different capsules were developed for the conduction of the intervention study; HT and placebo capsules. Both of them were soft capsules inducting refined OO with complete absence of biophenols as carrier. HT capsule was enriched in HT coming from the debittering by-product of edible olives, with final concentration 2.5 mg/capsule.

2.2.1 HT quantitative analysis

For the quantification of HT in capsule a special treatment was employed. Capsules outer cover was deconstructed with incubation for 90 min at 37°C with special pH conditions adjusted at 2 using HCl as acidic element. After the incubation, the solution was filtered and then directly analyzed via HPLC-DAD. For the quantitative analysis a Supelco Discovery HS C18 (25 cm x 4.6 mm, 5 μm) column was used. The gradient was consisted of H_2O + 0.2% acetic acid (AA) as solvent A and ACN as solvent B. The separation started with 2% of B and in seventeen minutes reached 30%. Finally, in tree minutes system returned to the initial conditions. The total flow rate was 1 mL/min and injection volume 20 μL. The total acquisition time was 20 minutes with λmax=280 nm. The same procedure was applied to placebo capsules as well. Capsules treatments and HPLC-DAD analysis were performed in triplicates. Spectra recording and data processing were carried out with ChromQuest™ 4.1 software.

2.2.2 UPLC-HRMS qualitative analysis of capsule

For compounds identification in the two type of capsules (HT and placebo) UPLC-Orbitrap-MS analysis was employed. Capsules were incised and the outer cover was separated from the inner content. The weight of the content was measured and then diluted in ACN and *n*-hexane in 1:1 ratio for defatting using liquid-liquid extraction. The ACN phase was collected and evaporated until dryness using rota evaporator.

For UPLS-Orbitrao-MS analysis, defatted extracts were prepared in the final concentration of 200 μg/mL diluted in 80:20 H_2O:MeOH solution. For the separation H_2O with 0.1% formic acid (FA) was used as solvent A and ACN as solvent B. The elution method started with 2% of B and stayed in these conditions for two minutes. The next sixteen minutes the percentage of B increased to 100% and maintained for three minutes. Finally, at twenty-ninth minute, A reached

the initial conditions and stayed for 4 minutes for system equilibration. An Acquity UPLC Peptide BEH C18 (100 mm x 2.1 mm, 1.7 μm) column was used for the analysis with stable temperature at 40°C. The measurements were performed with a total acquisition time of 25 minutes and a flow rate of 400 μL/min. The injection volume was 10 μL and the autosampler temperature was at 7°C. Mass spectra were obtained in negative and positive ion mode. For the negative ionization the capillary temperature was set at 350°C, capillary voltage at -30 V and tube lens at -100 V. Sheath and auxiliary gas were adjusted at 40 and 10 arb, respectively. For the positive ionization the above parameters were obtained and only capillary voltage and tube lens were adjusted to 40V and 120 V, respectively. Mass spectra were recorded in full scan mode in the range of 115-1000 *m/z*, with resolving power 30,000 at 500 *m/z* and scan rate 1 microscan per second. HRMS/MS experiments were obtained in data-depending method with collision energy 35.0% (q = 0.25). Anlysis was carried out and for both type of capsules for comparison purposes.

2.3 HT capsule administration to overweight/obese women

2.3.1 Study design

The study was carried out in the First Department of Propaedeutic and Internal Medicine of Medicine School of National and Kapodistrian University of Athens (NKUA). 38 overweigh and obese women with BMI 27-35 Kg/m^2 and waist circumference up to130 cm were randomized in a double-blind intervention study. Participants were divided into three groups; group A in which participants received 15 mg HT per day, group B in which participants received daily 5 mg HT and group C in which participants received placebo capsules. The intervention lasted six months and during the entire period participants followed the same dietary plan and record their actual diets and possible physical activity. At the baseline visit each participant was randomized in the

intervention and anthropometric measurements were carried out (weight and height for BMI estimation, perimeter of waist and hips and determination of body and visceral fat). The next visits were programmed in the first, the third and sixth month of the intervention, where participants provided urine and blood samples. The protocol was approved by the medical ethical committee of Medical School of NKUA. All participant gave written informed consent in order to participate in the current study. From the initial list of participants, 8 women were stepped back from the intervention and 30 women continued with capsules consumption.

2.3.2 Biofluid collection

Urine samples for HT quantification and metabolomics analysis were collected in the appropriate urine collection vessels and were stored at -80^{o}C before use. Blood samples were collected in EDTA vacuum tubes and were stored at -80^{o}C until subsequent analysis.

2.4 Quantitative determination of HT in human urine

For the quantification of HT in human urine an ultra high performance liquid chromatography coupled to a triple quadrupole mass spectrometer (UHPLC-Tq-MS) was used. A sensitive and accurate methodology was developed and then validated for the determination of the excretion levels of HT in two groups (group A and B) in time points t1, t3 and t6.

2.4.1 Samples for quantitative determination of HT in urine

Totally 53 urine samples coming from groups A and B in their time points (t1=1month, t3=3months and t6=6months) were included in the list for HT quantification via UHPLC-Tq-MS. Samples were collected in urine vessels before capsule consumption (overnight fasting) and stored at -80^{o}C until analysis day. Ultimately, 21 samples from group A and 19 samples from group B were forwarded for HT quantification. The rest 13 samples belong to pending

participants whose groups are still unknown because participants have not yet implemented the sixth month visit. Placebo samples were not quantified due to the absence of HT in placebo capsule. Table A13 tabulates the list of samples included in urine quantification accompanied by their code labels.

2.4.2 Urine sample preparation

Initially, samples were thawed in ice, homogenized and then 1.5 mL of them centrifuged at 12.000 rpm for 10 minutes at 4^{o}C. 50 μL of each sample code were added in an epperdorf (the rest volume was kept as an aliquot at -80^{o}C). Consequently, 200 μL of cold methanol were added and homogenized with vortex for 60 seconds. Finally, samples were centrifuged at 4^{o}C for 12 minutes in 14.000 rpm and supernatants were evaporated under vacuum conditions and centrifugation at room temperature until the complete dryness of the pellets. The derived residues were diluted in 100 μL MeOH:H_2O 60:40 and 5 μL of 2,4-Dinitrophenol (2,4-DNP) (IS) were added in the final concentration of 2 ng/mL. Samples were analyzed in triplicates with the developed UHPLC-Tq-MS method described below.

2.4.3 UHPLC-ESI-Tq-MS quantitative analysis

The mobile phase was consisted of a gradient system with H_2O and 0.1% (v/v) formic acid (A) and acetonitrile (B); the flow rate was set at 0.4 mL/min. Total analysis time was 10 min and the used chromatographic separation column was an Acquity® UPLC HSS T3 (Waters) (18 μm, 2.1 x 200 mm) heated at 40^{o}C. The elution system started with 2% B which reached 50% in 4 minutes. The next 2 minutes B reached 100% and stayed for 2 more minutes. At the ninth minute system returned to the initial conditions for 1 minuter for equilibrium. The injection volume was 5 μL and during analysis samples were stored at 10^{o}C.

Samples were ionized in negative mode with an ion spray voltage at 4000 V. The mass spectrometric parameters were: cone temperature, 250°C; cone gas flow, 25 units; heated probe temperature, 300°C; probe gas flow, 50 units; nebulizer gas flow, 50 units. The quantification of HT was conducted employing multiple reaction monitoring (MRM) mode and suitable collision energies. For HT the following transitions were monitored: 153.1>123.1, collision energy:14 as confirmation transition and 153.1>113.1, collision energy:6 as quantification transition. The above transitions were monitored for 4 minutes retention time (RT) window. For IS the following transitions were monitored: 183.1>109.2, collision energy:25; 183.1>137.0 collision energy:19 as confirmation and quantification transitions, respectively monitored for RT window of 4 minutes. Data were collected in centroid mode.

2.4.4 Preparation of standard solutions, calibration curve and quality control (QC) samples

Stock solution of HT and IS were prepared at a concentration level of 1 mg/mL in MeOH and stored at -20°C. Working solutions were prepared by diluting appropriate volumes of the analyte and IS stock solutions in a solution of H_2O:MeOH 60:40. Calibration points were built in matrix solution using 12 different concentrations of HT. The dynamic range of HT calibration curve was 0.1 ng/mL-100 ng/mL (100 pg/mL, 200 pg/mL, 500 pg/mL, 1 ng/mL, 2.5 ng/mL, 5 ng/mL, 12.5 ng/mL, 25 ng/mL, 50 ng/mL, 75 ng/mL and 100 ng/mL). IS final concentration was 2 ng/mL. As QC samples three concentration levels of the analyte and IS were prepared from the stock solutions, a low (1 ng/mL) a medium (25 ng/mL) and a high (100 ng/mL) and injected every 50 runs.

2.4.5 Matrix preparation

For the preparation of the matrix sample KA_20_t1 which belongs to placebo group and t1 was selected as appropriate time point. Matrix was prepared as all the other samples. This

procedure was followed individually for all the concentrations of the calibration curves and QC samples. Matrix samples were prepared as well in H_2O:MeOH 60:40.

2.4.6 Quantification and validation of the bioanalytical methodology

For the construction of the calibration curves the ratio of area of HT *vs* the area of the IS was used. The linearity was checked using partition least squares method and evaluation of the regression coefficient (R^2).

The validation of the method was performed in accordance to ICH quality guidelines "Validation of Analytical Procedures Q2 (R1)" [41], FDA [42] and EMA CHMP guidelines [43] for bioanalytical methodologies by evaluating the stability, specificity, linearity, precision, accuracy, lower limit of quantification (LLOQ) and the system suitability parameters.

2.4.6.1 Specificity-Recovery-Matrix effect

Specificity was evaluated by injecting five individually prepared matrix samples and investigation of the presence of possible interference at the corresponding RT of HT and IS. Recovery was determined at the three QC levels comparing the concentrations of HT and IS from pre-spiked samples with post-spiked samples. Matrix effect was assessed by comparing the % RSD of the peak area in the three QC samples in solvent and matrix solution.

2.4.6.2 Lower limit of quantification (LLOQ) and detection (LLOD)

LLOQ and LLOD were calculated based on the standard deviation and the slope of the respective calibration curve. Both parameters were estimated using the calibration curves and the signal of a blank using the equations below:

$$\text{LLOQ}= \frac{yblank+10\ \sigma}{b}$$

$$\text{LLOD} = \frac{yblank + 3\,\sigma}{b}$$

Where yblank is the background signal, b is the slope estimated from the calibration curve and σ is the standard deviation of the response.

2.4.6.3 Repeatability, intermediate precision and accuracy

Repeatability (within-run) and intermediate precision (between run) of the assay were evaluated based on and the standard deviation (SD) and relative standard deviation (%RSD) of the three concentration levels of QC run in five replicates. The rejection criteria was % RSD<20% for the low concentration and <15% for the medium and the high. Within-run accuracy and between-run were determined for QCs as the % standard error (% Er). The % deviation of the mean from the true value should be less than 20% for the low concentration and 20% for medium and high.

2.4.6.4 Robustness

The robustness of the method was evaluated incorporating alterations in analysis conditions within ±5% changes. Firstly, column temperature was set at 38ºC and 42ºC and secondly heated probe temperature was set at 285ºC and 315ºC. All experiments were performed in the medium QC concentration (25 ng/mL) calculating the chromatographic peak area of HT, the RT, 10% peak asymmetry and 10% peak width. Results are expressed as % RSD.

2.5 Metabolomic analysis of urine and blood samples

2.5.1 Samples for metabolomics study

The participants were divided in three sample groups. Two of them received HT in two different concentrations of HT, 15 and 5 mg per day and one more sample group received

placebo capsules. From all the participants urine and blood samples were collected in three time points; the first month (t1), the third month (t3) and the sixth (t6). Therefore, 73 urine samples and 75 blood samples were forwarded for metabolomic analysis. Table A14 in appendix illustrates in detail the analyzed samples.

2.5.2 Sample preparation

Urine samples were prepared in the same way as described in section 2.4.2. For the pretreatment of blood, samples were thawed in ice and then homogenized and centrifuged at 12.000 rpm for 10 minutes at 4^{o}C.

Unfortunately, because blood samples were stored directly to -80^{o}C without prior centrifugation, hemolysis supervened to all of them. For this reason, 50 μL of blood after dilution with H_2O in ratio 1:1 were mixed with 800 μL of cold MeOH and then vortexed for 60 seconds. Continuously, samples were centrifuged at 4^{o}C for 12 minutes in 14.000 rpm. Supernatants were collected and then mixed with *n*-hexane in ratio 1:1 for defatting purposes and the removal of the majority of cell membranes to the lipophilic *n*-hexane phase. The solutions were centrifugated in 3.500 rpm for 3 minutes for phase separation. Lower phases were evaporated under vacuum conditions and centrifugation at room temperature until the complete dryness of the pellets. The derived residues were diluted in 100 μL MeOH:H_2O 60:40.

QC pooled sample was prepared in the same way for urine and blood. Aliquots of all the samples were mixed and then extracted with the corresponding extraction methodology of each biofluid material.

2.5.3 UPLC-HRMS analysis

Urine samples acquisition. Urine extracts as well as the quality control (QC) pooled sample were analyzed with a LC gradient consisted of H_2O with 0.1% formic acid (FA) (solvent A) and ACN (solvent B). The elution method started with 2% of B which stayed for 2 minutes. In the next 16 minutes B reached 100% and stayed for 2 minutes. Finally, at 21st minute, system returned to the initial conditions and stayed for 4 minutes for system equilibration. A Thermo Hypersil Gold C-18 (50 mm x 2.1 mm, 1.9 μm) column was used for the separation, with a stable temperature of 40°C. The measurements were performed with a total acquisition time of 25 minutes and a flow rate of 400 μL/min. The injection volume was 10 μL and the autosampler temperature was at 7°C.

Mass spectra were obtained in negative ion mode using an electrospray ionisation source (ESI). The capillary temperature was set at 350°C, capillary voltage at -10 V and tube lens at -40 V. Sheath and auxiliary gas were adjusted at 40 and 10 arb, respectively. Mass spectra were obtained in negative and positive ion mode. For the negative ionization the capillary temperature was set at 350°C, capillary voltage at -30 V and tube lens at -100 V. Sheath and auxiliary gas were adjusted at 40 and 10 arb, respectively. For the positive ionization the above parameters were obtained and only capillary voltage and tube lens were adjusted to 40V and 120 V, respectively. Mass spectra were recorded in full scan mode in the range of 115-1000 *m/z*, with resolving power 30,000 at 500 *m/z* and scan rate 1 microscan per second. HRMS/MS experiments were obtained in data-depending method with collision energy 35.0% (q = 0.25). The system was calibrated externally every 50 injections.

Blood samples acquisition. Blood extracts as well as the quality control (QC) pooled sample were analyzed with a LC gradient consisted of H_2O with 0.1% formic acid (FA) (solvent

A) and ACN (solvent B). The elution method started with 2% of B which reached 70% in 4 minutes. In the next 6 minutes B reached 100% and stayed for 2 more minutes. In the next minute, system returned to the initial conditions for 2 minutes for system equilibration. An Acquity UPLC Peptide BEH C18 (50 mm x 2.1 mm, 1.7 μm) column was used for the separation, with a stable temperature of 40°C. The measurements were performed with a total acquisition time of 25 minutes and a flow rate of 400 μL/min. The injection volume was 10 μL and the autosampler temperature was at 7°C.

Mass spectra were obtained in negative ion mode using an electrospray ionisation source (ESI). The capillary temperature was set at 350°C, capillary voltage at -10 V and tube lens at -40 V. Sheath and auxiliary gas were adjusted at 40 and 10 arb, respectively. Mass spectra were obtained in negative and positive ion mode. For the negative ionization the capillary temperature was set at 350°C, capillary voltage at -30 V and tube lens at -100 V. Sheath and auxiliary gas were adjusted at 40 and 10 arb, respectively. For the positive ionization the above parameters were obtained and only capillary voltage and tube lens were adjusted to 40V and 120 V, respectively. Mass spectra were recorded in full scan mode in the range of 115-1000 *m/z*, with resolving power 30,000 at 500 *m/z* and scan rate 1 microscan per second. HRMS/MS experiments were obtained in data-depending method with collision energy 35.0% (q = 0.25). The system was calibrated externally every 50 injections.

2.5.4 Statistical process and chemometrics

UPLC-MS urine and blood injections were recorded with Xcalibur 2.2. Raw files (.raw, Thermo) were imported to MZmine 2.26 software for data processing. Peak lists were generated with centroid selection algorithm. For chromatogram building of the generated mass lists, 0.03 min was set as minimum time of span and 5 ppm for mass tolerance. Chromatogram

deconvolution module was employed and spectra were processed with local minimum search algorithm using R package. The minimum retention time range was set at 0.03 minute and peak width 0.05-0.5 minutes for urine and 0.03-0.8 for blood injections. Chromatograms were aligned and spectra were normalized regarding retention time with 0.05 minute tolerance. Join align method which aligns detected masses using a match score, calculated based on the mass and detection time of each peak was used. Finally, gap filing was implemented, using peak finder method. These lists were exported as asc file for import in SIMCA.

Both of the generated data tables were imported to SIMCA 14.1 (Umetrics, Sweden) software for statistical analysis. Mainly, Principal Component Analysis (PCA) and Orthogonal Partial Least Squares-Discriminant Analysis (OPLS-DA) were implemented for sample discrimination and identification of statistically important metabolites responsible for observed trends and classifications. For this purpose, Variable Importance in Projection (VIP) values of OPLS-DA models which rank variable contribution were estimated and evaluated. VIP scores >1 were considered as statistically significant.

The generated models were evaluated for their R2 and Q2 parameters indicating the measure of fit and the predictability, respectively. Only models with R2 values close to 1, Q2 values over 0.5 or models with lower R2 but close to Q2 value were accepted. Permutation test was also applied for further validation of the models. Similarly, only models which succeeded in the permutation test were used for data visualization and VIP calculations.

2.5.5 Structure elucidation workflow

Based on VIP calculations a list with significant features was created for each dataset and subjected to identification process. Initially, LC-HRMS chromatograms and their corresponding HRMS spectra (< 2 ppm) were investigated. Extraction ion method was used in parallel with

peak-to-peak selection affording the corresponding full scan spectra. Suggested Elemental Composition (EC) of each detected peak together with isotopic patterns and ring double bond equivalent (RDBeq) values were further used to confirm the proposed structures. Additionally, HRMS/MS spectra contributed to the identification of specific chemical entities based on in-house databases. Furthermore, on-line databases were used for additional structural information. More specifically, Human Metabolome Data Base (HMDB) (http://www.hmdb.ca/), METLIN Metabolomics Database (https://metlin.scripps.edu/), Kyoto Encyclopedia of Genes and Genomes (KEGG) (https://www.genome.jp/kegg/), ChemSpider free chemical structure database (http://www.chemspider.com/) and LIPID MASS (https://www.lipidmaps.org) lipidomics gateway were used. The obtained data were compared with those previously reported in literature.

3. Results and Discussion

Few studies have been conducted for the investigation of OO biophenols and more specifically HT in obesity. One human study was found in which an encapsulated olive leaf extract (containing 9 mg HT/capsule) was administered daily in men for evaluation of its effect on insulin sensitivity. The study revealed 15% improvement in insulin sensitivity and no effect on body composition [44]. On the other hand two other *in vivo* studies in obese mice showed a positive correlation of HT with anti-obesity effect after receiving HT by gavage (10 mg/Kg and 50 mg/Kg) [3,14]. Other studies conducted in rodents and rabbits which received HT by gavage in the form of OO or as a purified compound did not show any effect on weight loss; in these cases the administered doses were extremely low [45–47]. In the current study, HT was administered in soft capsules with final concentration of 2.5 mg/capsule (2 or 5 capsules/day).

3.1 Capsules quantitative and qualitative analysis

For the production of the enriched with HT capsule, OWW was used as raw material, due to its high content in HT (olivomed capsule). Extract was encapsulated with a soft outer cover and OO was used as carrier in HT and placebo capsule as well, based on the reports that HT is more effectively absorbed from humans when administered in OO matrix.[28]. The two type of capsules were identical to protect the double blindness of the study (Figure 33).

Figure 33*: Illustration of HT and placebo capsules.*

HT and placebo capsules were weighted and extracted to determine the total capsule weight, and content weight as well. The measurements revealed that HT capsules have an average weight of 0.7203 g and placebo 0.69846 g. The inner content was estimated at 0.5024g

and 0.6226 g respectively. Weight measurements were conducted for verification of the outward similarity of the two type of capsules.

3.1.1 HT quantitative analysis of capsules via HPLC-DAD

The used protocol for capsules dialysis aimed to the simulation of human stomach conditions (pH=2 and T=37ºC) in order to quantify the exact amount of HT released in human stomach after capsule consumption. The protocol was employed both to HT and placebo capsules to reassure the complete absence of HT in the latter capsule.

The quantification was based on an eight-point calibration curve constructed using the area of HT. The equation was y=87793x – 35339 with R^2=0.99998. After area integration in the appropriate RT, HT concentration was estimated at 2.47 mg HT per capsule. Placebo capsules have no traces of HT at all. The figure below depicts the HPLC-DAD chromatogram of the acidic treatment of HT capsule acquired at 280 nm.

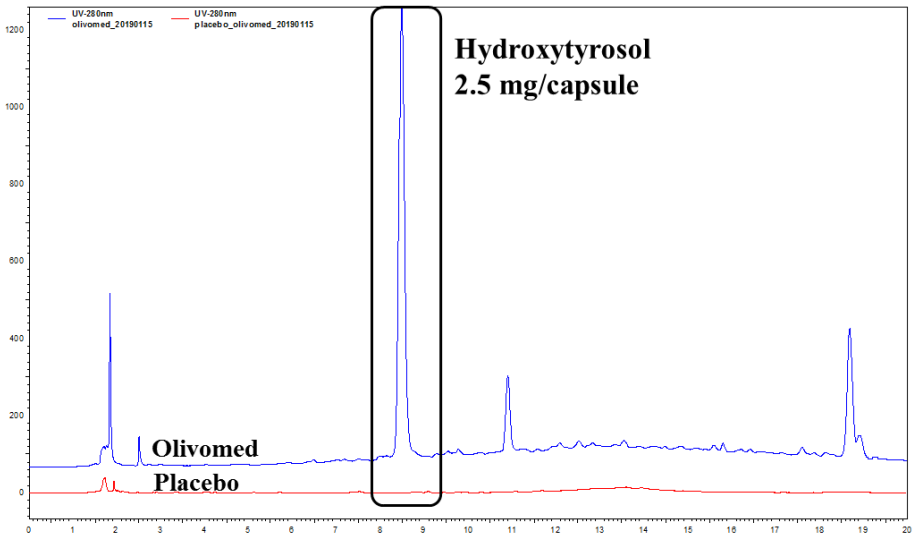

Figure 34: *HPLC-DAD chromatogram at 280 nm of HT capsule after dialysis in stomach conditions. HT is circled in red.*

3.1.2 UPLC-HRMS qualitative analysis of capsule

Inner contents of HT and placebo capsules were appropriate diluted and analyzed via UPLC-Orbitrap-MS for metabolites identification.

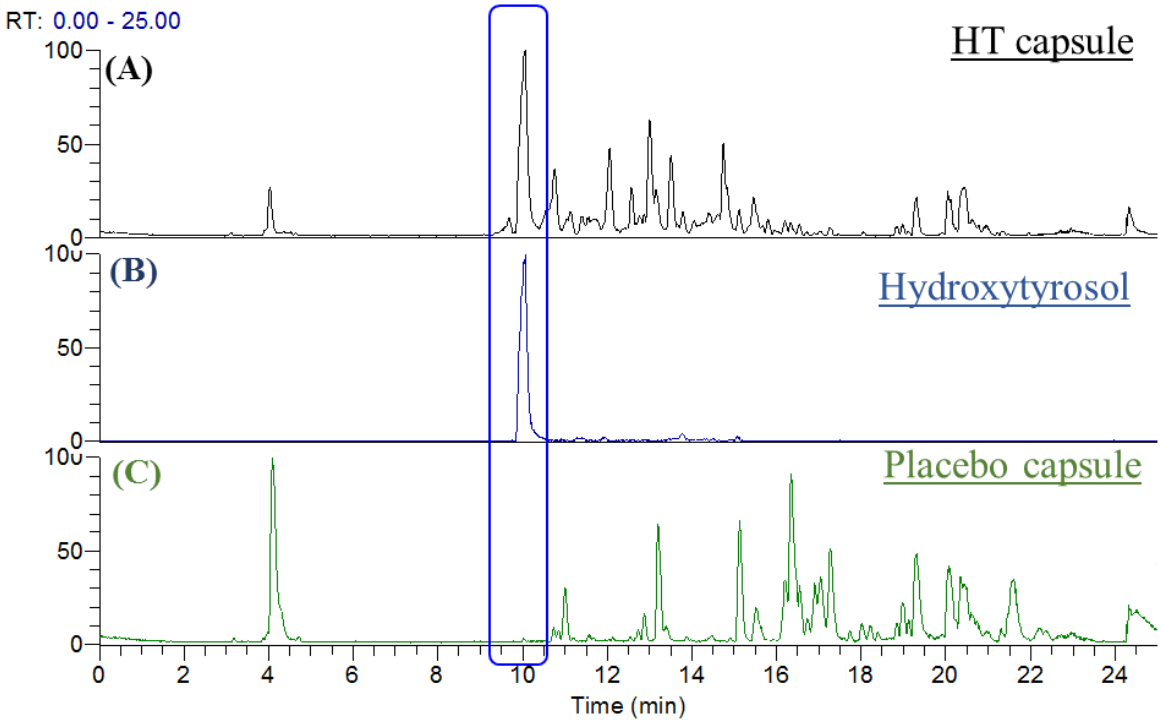

Figure 35: *Full scan chromatogram of HT capsule extract (A), extracted ion chromatogram of HT (B) and full scan chromatogram of placebo extract (C). HT is circle in blue.*

Figure 35 illustrates the full scan chromatogram of HT capsule extract (A), the extracted ion chromatogram of HT (B) and the full scan chromatogram of placebo extract (C). As it is obvious from the figure, HT constitutes the major peak in chromatogram A. However, in placebo capsule there is a complete absence of this compound. Figure 36 represents the full scan chromatogram of HT and the corresponding HRMS spectrum indicating HT pseudomolecular ion [M-H]- and its characteristic MS/MS fragment (MS2@153.056).

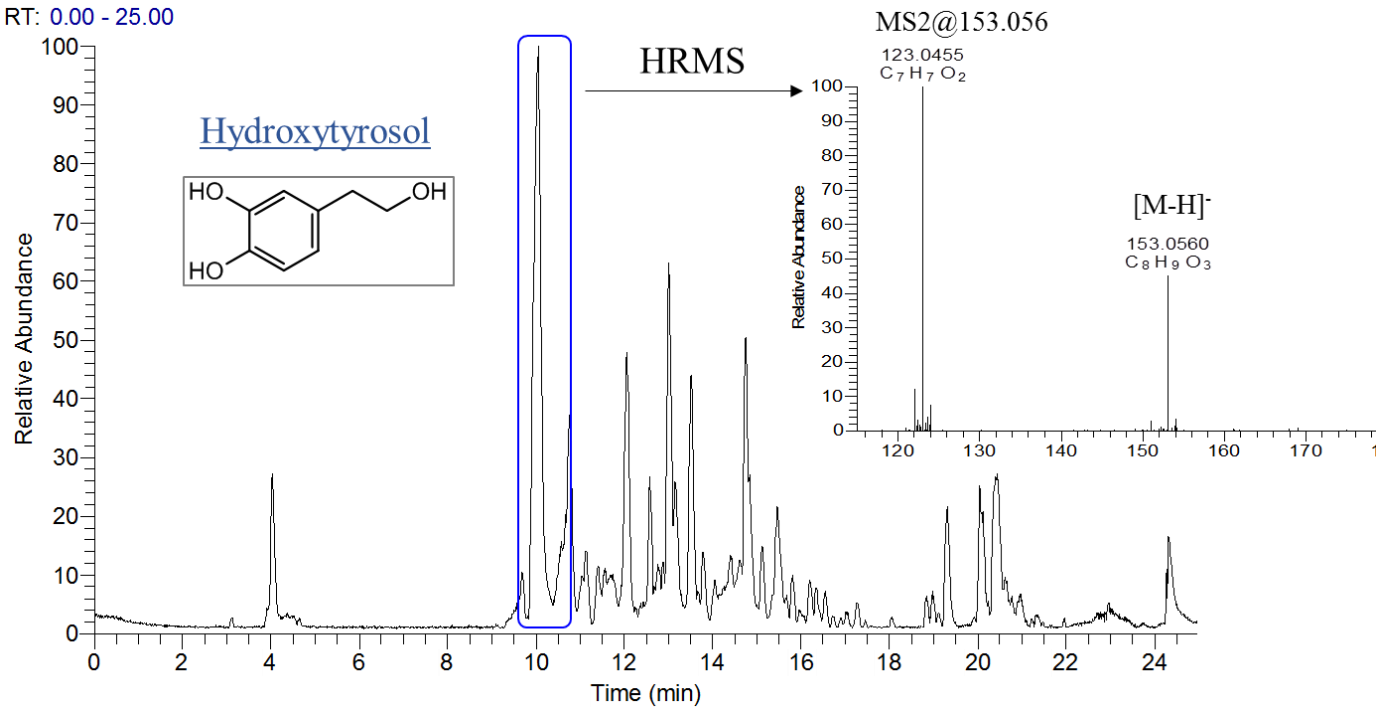

***Figure 36**: Base peak full scan chromatogram of HT capsule extract. At the right side of the chromatogram HRMS spectrum of HT is represented. [M-H]- corresponds to the pseudomolecular ion in negative ionization and MS2@ the respective MS/MS fragment of the pseudomolecular ion.*

Taking the advantage of the high resolving power of Orbitrap analyzer in combination with the separation of the UPLC dimension, identification of compounds was achieved with high confidence. Tools of elemental composition (EC) and ring and double bong equivalence (RDBeq) in parallel with the observed isotopic patterns and the high resolution of MS/MS spectra contribute together to the identification of compounds. Negative ion mode revealed better ionization of compounds and ultimately used for the identification process. The identified compounds of HT capsule extract are presented in Table 8 below. Totally 7 secondary metabolites were identified. The rest peaks of the chromatogram are agents contributing to the encapsulation of the extract and are common for both capsules. In detail, in HT capsule, HT (1) was identified with *m/z* 153.0561, EC: $C_8H_{10}O_3$ and RDB:4.5.

Additionally, dialdehydic form of decarboxymethyl elenolic acid (2) *(m/z*: 183.0665, $C_9H_{12}O_4$, 4.5), HT acetate (3) (*m/z*: 195.0656, $C_9H_{12}O_4$, 4.5), octadecanediooic acid (4) (*m/z*: 313.2379, $C_{18}H_{33}O_4$, 2.5), linoleic acid (5) (*m/z*: 279.2325, $C_{18}H_{32}O_2$, 3.5), palmitic acid (6) (*m/z*: 255.2328, $C_{16}H_{31}O_2$, 1.5) and oleic acid (7) (*m/z*: 281.2483, $C_{18}H_{33}O_2$, 2.5) were also detected. The identified metabolites 1-3 are typical biophenol metabolites of the enriched HT extract and metabolites 4-7 are characteristic fatty acids (FA) of OO which was used as carrier of the extract during encapsulation process. For this reason, placebo capsule is composed only from the metabolites 4-7 and does not contain at all biophenols. It has to be underlined that both kind of capsules contain the same OO as carrier and as a result the two capsules have the same FA composition. As it has been already mentioned, oleic acid has been reported as satiety factors [48]. The use of the same OO in capsules reassures that the obtained results of the study are caused from HT and not from the contained FA which are received from all the groups of the study.

Table 8: *Identified compounds in extract of the HT capsule. In columns are presented the detailed identification parameters.*

	***m/z* experimental**	***m/z* theoritical**	**RT**	**Elemental composition**	**RDB**	**Δ (ppm)**	**Name**
1	153.0561	153.0546	10.05	$C_8H_{10}O_3$	4.5	1.650	Hydroxytyrosol
2	183.0665	183.0652	12.06	$C_9H_{12}O_4$	4.5	0.917	Dialdehydic form of decarboxymethyl elenolic acid
3	195.0656	195.0652	13.19	$C_{10}H_{11}O_4$	5.5	0.963	Hydroxytyrosol acetate
4	313.2379	313.2373	18.82	$C_{18}H_{33}O_4$	2.5	-1.861	Octadecanedioic acid
5	279.2325	279.2319	20.09	$C_{18}H_{32}O_2$	3.5	-1.588	Linoleic acid
6	255.2328	255.2319	21.45	$C_{16}H_{31}O_2$	1.5	-0.719	Palmitic acid
7	281.2483	281.2475	21.60	$C_{18}H_{33}O_2$	2.5	-1.222	Oleic acid

3.2 HT capsule administration to overweight/obese women

Recent evidences have underlined the positive impact of HT to obesity and insulin resistance in high-fat diet (HFD)-fed mice [3]. Moreover it has been found that HT has beneficial effect on obesity by suppressing dose-dependently intracellular TG accumulation and the expression of adipogenesis-stimulating factors during adipocyte differentiation, promotes lipolysis in human primary visceral adipocytes during differentiation and decreases hepatic steatosis [49,50]. Only one human study was found in literature, in which overweight men received daily an encapsulated olive leaf extract containing 9 mg HT/capsule. However, participants did not experience any weight loss and only a positive association with insulin sensitivity was revealed [44]. In the current study, an enriched HT capsule was developed and administered in different doses in overweight/obese women in a six-month period.

3.2.1 Study design and sample collection

For the intervention 38 women were recruited with an average age of 49.47 years. The selection of female subjects was based on bibliographic data that HT persists longer in female subjects [29]. All of them enrolled as overweight or obese with BMI ranging from 27-35 kg/m^2 and stable weight (<5% variation during the past three months). Participants were randomized in three groups according to the administered HT dosage. Dosage administration was based on EFSA scientific health claim, daily polyphenols intake through olive oil and ultimate polyphenol absorption in humans. One group received the dosage described in EFSA health claim (5 mg/day) (low HT dosage), the second group three times higher the basic dosage (15 mg/day) (high HT dosage) and the last group received a placebo capsule. The table below describes the intervention groups and the capsule administration details. Ultimately, 8 women stepped out from the study and terminated capsules consumption and 30 continued until the sixth month of

the intervention. Ultimately 30 women participate in the study; 5 of them have not yet implemented the six-months period and for this reason their measurements have not been included in results representation and statistical process

***Table 9**: Description of intervention groups. For each group the total HT intake and capsule consumption per day is illustrated. In the last row the number of volunteers of each group is presented.*

Group	**Group A**	**Group B**	**Group C**
HT intake	15 mg HT/day	5 mg HT/day	0 mg/day
Capsule consumption (per day)	6 HT capsules	2 HT & 4 placebo capsules	6 placebo
Number of volunteers	8	9	8

All participants were consulted by dietitian to achieve uniformity in calories intake and evaluated by doctors in the first month of the intervention (t1), the third (t3) and the sixth (t6). Compliance in capsule consumption was evaluated by checking the empty blister packs when visiting the investigator. Measurements of body weight and body composition were carried out in each visit. The collected urine and blood samples were presented in detail in appendix (Table A14)

3.2.2 Anthropometric parameters of HT administration

Mean body weight loss, mean visceral fat loss and mean body fat loss were the used parameters for the determination of the effect of HT in overweight/obese women. Tables 10-12 below depict the measurements of the above parameters in the three time points of the intervention. In more detail, table 10 represents the mean body weight loss in kilograms (Kg) registered in each visit of the participants to the investigator. In the first month, group A which

received the high HT dosage lost 4.17 Kg, followed by group B and C which lost 1.21 Kg and 1.98 Kg, respectively. The third month of the study group A duplicated the loss and totally lost 8 Kg in average. The same trend was observed in group B and C which lost 2.77 and 4.00 Kg, respectively. At the last month of the intervention only group A lost more weight and overall participants lost 11.44 Kg in average after six months administration of HT. Group B and C did not lose any more weight and remain almost stable. It is notable that only participants of group A experienced body weight loss upper than 5% on the first month of the study and weight loss upper than 10% during the entire period of the study. Table A15 in appendix represents the statistical differences among groups.

***Table 10**: Mean body weight loss in kilograms (Kg) of the three groups in time point t1 (month 1), t3 (month 3) and t6 (month 6). Group A received 15 mg HT/day, group B 5 mg HT/day and group C received placebo.*

Mean body weight loss (Kg)	**1 month (t1)**	**3 months (t3)**	**6 months (t6)**
Group A	-4.17 (SD 1.85)	-8.00 (SD 3.89)	-11.44 (SD 4.01)
Group B	-1.21 (SD 1.03)	-2.77 (SD 2.11)	-2.73 (SD 2.43)
Group C	-1.98 (SD 0.83)	-4.00 (SD 2.00)	-2.33 (SD 2.87)
p	**0.010**	**0.005**	**<0.001**

Visceral fat loss is considered as a parameter of high importance in weight loss and study of obesity**.** Table 11 illustrates the loss of visceral fat of the three groups expressed in % percentage. In the first month of the study group A lost 1.87% visceral fat, while B and C groups appear the same levels of visceral fat loss being 0.22% and 0.58% respectively. At the third month again duplication of loss levels was observed. Group A lost 3.06% visceral fat and B and C 0.62% and 1.33 % respectively. The last month of the study all of the groups remain almost stable at the visceral fat loss.

***Table 11**: Mean visceral fat loss expressed as %. Results are expressed as mean values of groups A, B and C in time points t1, t3 and t6.*

Mean visceral fat loss (%)	**1 month (t1)**	**3 months (t3)**	**6 months (t6)**
Group A	-1.87 (SD 1.09)	-3.06 (SD 1.08)	-3.85 (SD 1.02)
Group B	-0.22 (SD 0.44)	-0.62 (SD 0.83)	-0.56 (SD 1.14)
Group C	-0.58 (SD 0.58)	-1.33 (SD 0.93)	-1.87 (SD 1.65)
p	**0.010**	**0.000**	**0.000**

Table 12 depicts the total mean body fat loss expressed in Kg. Group A lost 3.2 Kg in fat while in groups B and C the corresponding mean loss was 1.10 Kg and 2.46 Kg, respectively. In the third month the trend of duplication was observed again with fat loss of 6.60 Kg, 2.67 kg and 2.58 Kg for group A, B and C, respectively. The last month of the study like the previous parameters group A continued losing body fat and participants showed a total mean fat loss of 9.55 Kg. Groups B and C remained almost stable.

***Table 12:** Mean body fat loss expressed in Kg. Results are expressed as mean values of groups A, B and C in time points t1, t3 and t6.*

Mean body fat loss (Kg)	**1 month (t1)**	**3 months (t3)**	**6 months (t6)**
Group A	-3.20 (SD 1.06)	-6.30 (SD 3.08)	-9.55 (SD 2.43)
Group B	-1.10 (SD 0.99)	-2.67 (SD 1.85)	-2.06 (SD 1.72)
Group C	-2.46 (SD 1.78)	-2.58 (SD 2.69)	-2.13 (SD 2.66)
p	0.080	**0.017**	**0.000**

Based on the above data, body fat loss is also significant. After 6 months of HT intake, body fat loss followed similar pattern with body weight loss. It has to be underlined that group A lost 11.44 Kg in average, from which 9.55 Kg were loss in fat. This fat loss represents 83.5 % of the general weight loss. These results of HT effects in human weight loss are reported for the first time. A previous cohort study in overweight men did not show any effect of the

administered capsule, containing 9 mg HT/capsule [44]. This outcome could be correlated with the anthropometric measurements of group B of our study, which receive 5mg HT/day and did not show significant weight/fat loss. The dose of 15 mg/day (group A) seems to be effective, resulting in significant weight/fat loss. Bibliographically, the dose of 15 mg/day is reported for the first time and it has to be noted that this HT dose revealed anti-obesity effect in human. Moreover, adverse events were not reported with capsule consumption.

3.3 HT quantification via UHPLC-Tq-MS in urine

3.3.1 Sample preparation

For the sample preparation of urine samples ACN and MeOH were tested as extraction solvent system in pre-spiked samples with HT. MeOH results in 97-112% HT recovery with %RSD<10 (RSD=7.1%). ACN has recovery ranging from 70-93% and RSD>20% and for this reason was rejected as extraction solvent. Additionally, two different ratio of sample:MeOH were tested, 1:4 and 1:8, which result in the same recovery value. Ratio 1:4 was selected to decrease time in sample preparation procedure during the evaporation step.

3.3.2 Method development for UHPLC-ESI-Tq-MS

For the development of the chromatographic conditions MeOH and ACN were tested for analytes elution and ACN appeared better peak shape. Also addition of formic acid in water and 40^{o}C column temperature improve HT peak shape as well. The elution of HT and IS were adjusted in order to unfold a fast chromatographic analysis time, obviating the co-elution with other matrix compounds.

For the development of mass spectrometric parameters direct infusion of HT and IS in final concentration of 50 ng/mL and 20 ng/mL respectively were performed. Standards were tested in

negative and positive ionization. Both of them revealed better ionization in negative ion mode. MRM tool builder was used for the investigation of the appropriate collision energies to achieve optimal sensitivity and selectivity. Table 13 summarizes the selected parameters.

Table 13: *Summary of the used mass spectrometry and MRM method parameters for the quantification of HT and 2,4-DNP (IS) via UHPLC-Tq-MS.*

Mass spectrometry parameters						
Cone temperature (ºC)	**250**					
Cone gas flow (units)	**25**					
Heated probe temperature (ºC)	**300**					
Probe gas flow (units)	**50**					
Nebulizer gas flow (units)	**50**					
MRM parameters						
Compound	**Precursor**	**RT**	**RT window**	**Scan time (ms)**	**Product**	**Collision energy (v)**
HT	153.1	2.0	4	100	123.1	14
					113.1	6
2,4-DNP	183.1	4.5	4	100	109.2	25
					137.0	19

3.3.3 Quantification and validation of the bioanalytical methodology

Quantification of HT was performed using MRM method in negative ion mode. 2,4-DNP was used as IS, since it exhibits high and repeatable recovery and same chromatographic and ionization behavior like HT. 2,4-DNP shows high stability during analysis and it has not been described as an endogenous urine metabolite. Moreover, it does not interfere with HT. For these reasons it was selected as IS of the employed quantification methodology. Figure 37 illustrates the peaks of HT and IS in some of the injections used for calibration curves construction.

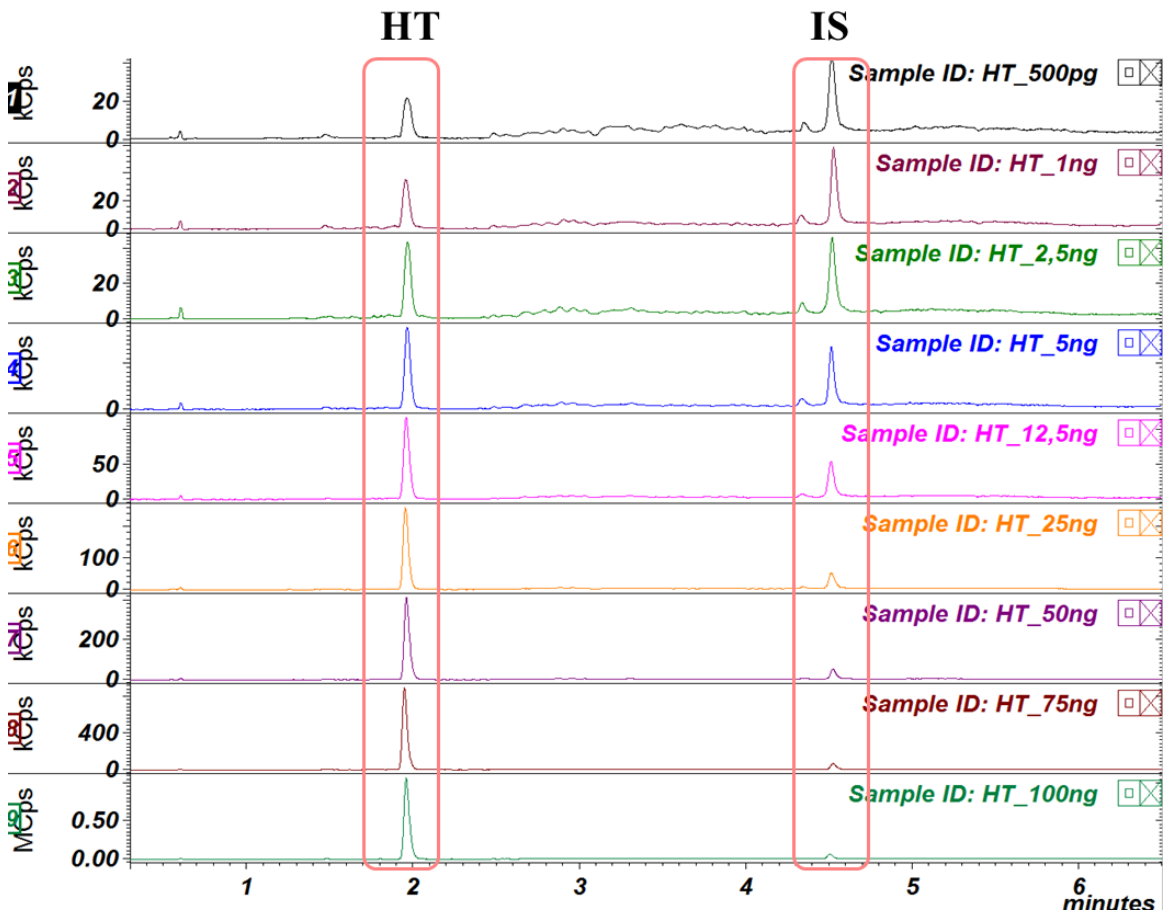

Figure 37: *UHPLC-Tq-MS chromatograms of nine calibration points of HT and IS (0.5 ng/mL, 1 ng/mL, 2.5 ng/mL, 5 ng/mL, 12.5 ng/mL, 25 ng/mL, 50 ng/mL, 75 ng/mL and 100 ng/mL). Peaks of HT and IS are annotated.*

For the construction of the calibration curves the ratio of the area of HT to the area of the IS was used. The linearity was checked using partition least squares method. The derived equation is: y = 0.148x + 06237 with correlation coefficient R^2=0.9997. The corresponding equation is presented in figure A29.

3.3.3.1 Specificity-recovery- Matrix effect

The specificity was evaluated and no interference from the endogenous urine metabolites was found to the corresponding RT of HT and IS. The matrix effect was assessed by comparing

the % RSD of the peak area in the three QC samples in solvent and matrix solution. Calculations displayed %RSD values < 10% for all the concentrations indicating that the construction of calibration curves in matrix does not affect the signal of the analyte. The recovery was determined in the three QC levels in five replicates with use of the equation below:

$$\%R = \frac{pre - spiked\ average\ area}{post - spiked\ average\ area}\ x\ 100$$

Recoveries were estimated over 94% for all the QC levels and render the employed methodology suitable for the quantification of HT in human urine.

3.3.3.2 Lower limit of quantification (LLOQ) and detection (LLOD)

LLOQ and LLOD were determined based on the given equations in section 2.4.6.2 of methods and materials. Particularly LLOQ was calculated at 0.04 ng/ml and LLOD at 0.03 ng/mL.

3.3.4.3 Repeatability, intermediate precision and accuracy

Repeatability, intermediate precision and accuracy were determined by analyzing five replicates at the three QC concentration levels. Repeatability and intermediate precision did not exhibit values over 8.3% and 13.4% respectively. Measured accuracy displayed %Er ±5.3% for all QC levels.

3.3.4.4 Robustness

The altered conditions to evaluate system robustness resulted in % RSD < 2% in both deliberate changed conditions. Change of column temperature caused an RT shifting with RSD=1.73 %, while change of the heated probe temperature caused RSD=0.47% in peak area calculations.

3.3.4 Measurements of HT in human urine

Fifty-three human urine samples were prepared and analyzed with the above discussed method for the quantitative determination of HT. For the quantification, groups A and B which received HT in different concentrations were forwarded for analysis. Placebo were not quantified due to the administration of placebo capsules, which did not contain HT at all. Quantification was based on a standard calibration curve prepared the same day of samples analysis. Previous research has shown that HT bioavailability in human body depends on the administered concentration [39,51]. The measured concentration depends on several factors such as the way of administration (ingestion of consumption), if it is administered with olive oil or as a separate substance and a critical parameter is urine collection (collection pre and post HT administration, fasting hours etc). These factors render difficult the establishment of specific excretion and absorption HT levels in human. In the current study, measurements between groups are characterized by high deviation due to the different water intake of participants during the day, which was obvious from sample colour and the different analyte intensities. Results are not normalized based on creatinine concentration in urine and the aim of the quantification was to investigate a possible trend of HT excretion during the sixth month period of intervention in the different groups. The figure bellow presents the concentration results of the participants grouped according to HT administration.

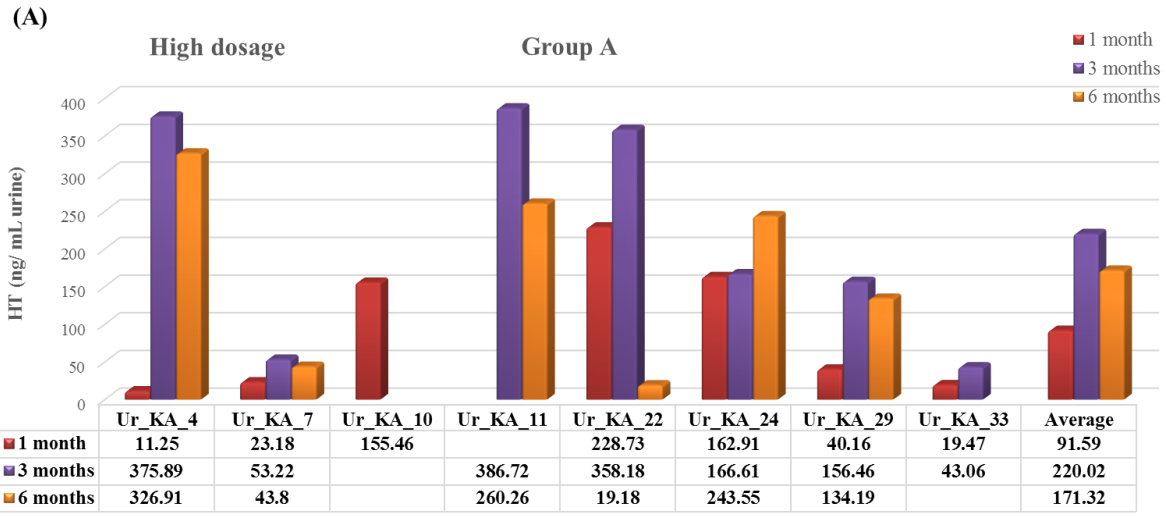

	Ur_KA_4	Ur_KA_7	Ur_KA_10	Ur_KA_11	Ur_KA_22	Ur_KA_24	Ur_KA_29	Ur_KA_33	Average
1 month	11.25	23.18	155.46		228.73	162.91	40.16	19.47	91.59
3 months	375.89	53.22		386.72	358.18	166.61	156.46	43.06	220.02
6 months	326.91	43.8		260.26	19.18	243.55	134.19		171.32

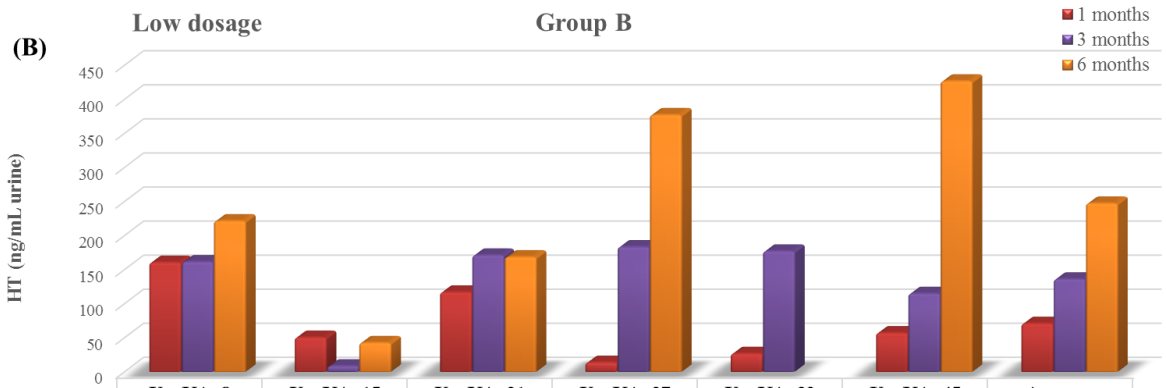

	Ur_KA_8	Ur_KA_15	Ur_KA_21	Ur_KA_27	Ur_KA_32	Ur_KA_45	Average
1 months	160.6	50.54	116.98	13.75	26.79	57.14	70.96
3 months	161.48	8.45	171.15	183.42	177.14	114.91	136.09
6 months	221.49	42.7	168.63	377.28		426.73	247.37

***Figure 38**: HT quantification in urine expressed in ng/mL urine. Graph A represents HT excretion in group A and graph B the corresponding excretion in group B. Red bars refer to t1, purple bars to t3 and orange bars to t6. Bellow graphs a table with the exact measurements is presented for each participant and the calculated mean value in the three time points.*

Concerning group A (figure 38A) HT highest concentration was found at 3 months showing an average concentration of 220.02 ng/mL urine. At the first month of the intervention HT was calculated at 91.59 ng/mL urine and at the sixth month at 171.32 ng/mL urine. The number of samples was low (n=8) and in some cases data were missing. As already mentioned there is a strong variability between individuals due to their different habits and most importantly

water consumption. Therefore, the average quantitative data are considered indicative of the excreted HT levels. In almost all women of group A the highest excretion was observed at the third month and then at the sixth there is a decline. Exception was participant with code Ur_KA_24, which appeared its highest concentration at the month six. Measurements of sample Ur_KA_7 were considerable low possible due to intake of high volume of water which caused high dilution of the sample. Although it is important that the trend was maintained. For the code Ur_KA_10 no urine samples were provided for the third and sixth month and for Ur_KA_33 for the sixth month.

Concerning group B (figure 38B), the highest excretion was found at six months being 247.37 ng/mL urine. In almost all of the participants, the highest concentration was measured at the sixth month with exception participant with code Ur_KA_15 which has extremely diluted samples and possibly due to the high dilution the highest concentration was observed on the first month. Also sample Ur_KA_21 showed almost the same concentrations for month three and six. For the code Ur_KA_32 no urine sample was provided for the sixth month.

It is notable that the highest concentration of HT is in the same level (220.02 ng/mL and 247.37 ng/mL for group A and B respectively) for the two HT treatments with a difference at the months that this concentration is detected. From this observation it can be hypothesized that participants of group B need approximately three more months to accumulate and thus to achieve the same HT excretion levels with group A. However, it is interesting that despite group B excreted the same HT amount with group A three months later, participants did not experience the respective weight and fat loss at this time point but remain stable at the anthropometric measurements (section 3.2.2). A rational explanation based on excretion values could be that the high HT dosage resulted in the faster weight loss of group A and for this reason group A was the

only group experienced weight loss, despite that group B received HT capsule as well. A possible extension of the intervention period may cause a weight loss to group B too. Consequently, it can be assumed that the recommended EFSA dosage (5 mg HT/day) could may have positive impact to the protection of blood lipids from oxidative stress but cannot contribute to weight loss. In the case of obesity, higher HT dosage seems to be more effective with strong positive impact in weight and visceral fat loss.

3.4 Metabolomic analysis of urine samples via UPLC-Orbitrap-MS

3.4.1 Samples for metabolomics study

The figure below presents the number of samples included in the statistical analysis grouped per treatment.

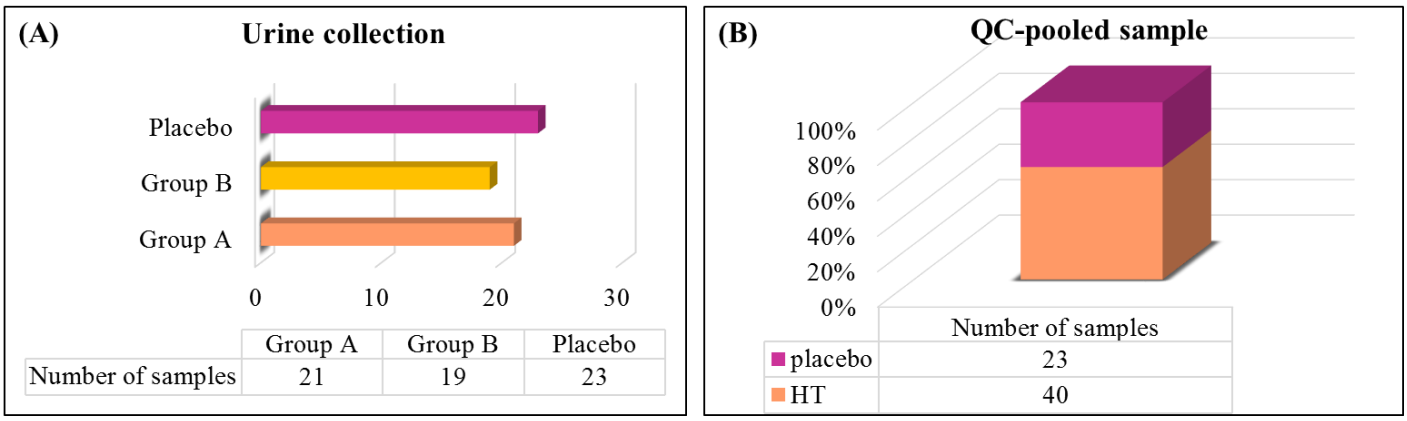

***Figure 39**: Representation of final urine collection. **(A)** presents in detail the collected samples per group; purple bar illustrates placebo samples, yellow bar samples from group B and light pink bar samples from group A. **(B)** presents the final composition of QC-pooled sample; purple part of the bar represents placebo samples and light pink the HT samples. Below each graph a detailed table describing the total sample collection in numbers is illustrated.*

Totally 40 samples were included in the metabolomic analysis coming from participants who received the HT treatment; 21 from group A and 19 from group B. Additionally, 23 samples

come from participants who received the placebo capsule. QC-pooled sample was prepared from the total number of samples (63 samples), meaning that QC is composed 63.5% from HT samples and 36.5 % from placebo samples. Pending samples that their identity group was not known were excluded from the statistical treatment.

3.4.2 Development of UPLC-HRMS methodology

For the development of the UPLC conditions, elution solvents, column temperature, and column characteristics were investigated. MeOH and ACN were tested as organic solvents and H_2O with and without FA were tested as aqueous phase. ACN resulted in better peak shape, together with acidified water and column temperature at 40^oC. Two different columns were tested; an Acquity UPLC Peptide BEH C18 (100 mm x 2.1 mm, 1.7 μm) and a Thermo Hypersil Gold C-18 (50 mm x 2.1 mm, 1.9 μm). The second column produced chromatograms with higher resolution.

Mass spectrometer parameters were optimized for the ionization of middle molecular weight compounds ~500 Da, which is the average weight of secondary metabolites. The aim was to achieve optimal ionization in a wide range of metabolites and develop a generic ionization methodology for negative and positive mode. The parameters described in section 2.5.3 were selected as more appropriate for this purpose.

3.4.3 Validation aspects

A QC-polled sample was prepared and injected every fifty runs to evaluate the repeatability of the analysis. The parameters of RT, mass accuracy and area were evaluated in each QC injection. For this purpose, three peaks were selected who had:

- different RT covering as possible the injection time

- different mass range to cover as possible the scanning mass range
- different levels for evaluation the parameter of area.

Hippuric acid (*m/z*: 178.0512, RT=4.82), cortolone-3-glucuronide (*m/z*: 571.2665, RT=7.59) and laurylsulfate (*m/z*: 265.1479, RT=9.60) were selected as the peaks satisfying RT, mass range and levels. Figure 40 illustrates a QC injection. The three selected compounds are annotated.

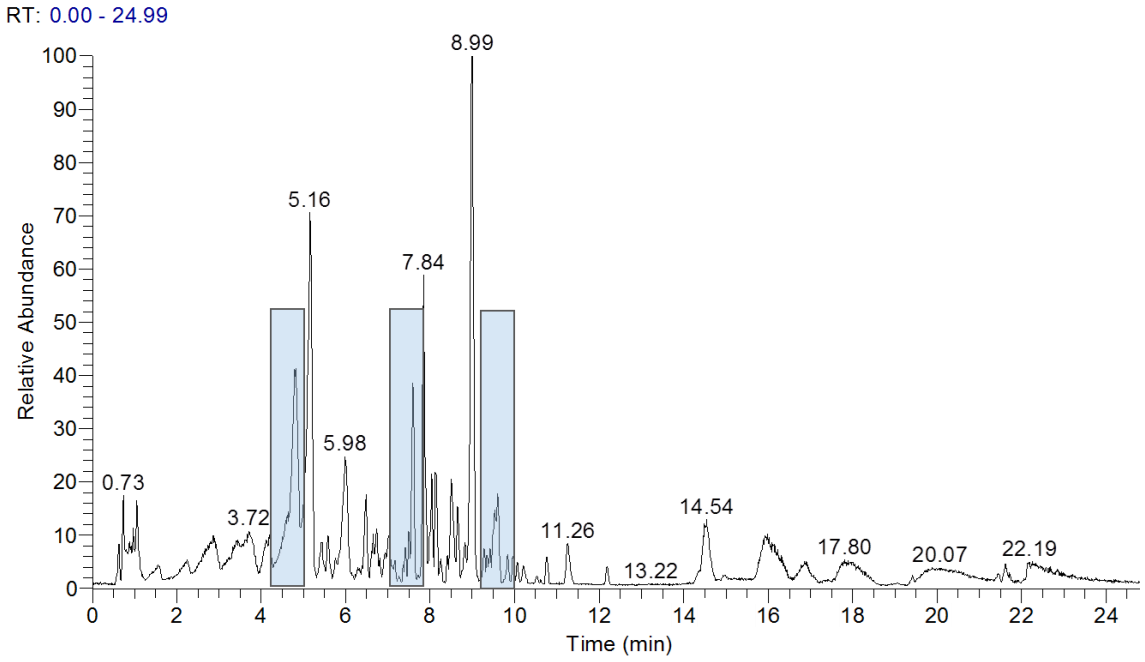

Figure 40: *UPLC-HRMS chromatogram of QC sample in negative ionization. Annotated peaks represent the selected compounds used for the evaluation of the repeatability of the analysis.*

Two evaluation criteria were subjected to each peak. Firstly, % RSD should be less than 1% for RT and 10% for area. Also accuracy should be less than 5 ppm. Hippuric acid, cortolone-3-glucuronide and laurylsulfate were evaluated for the above criteria. The figure below illustrates the %RSD of RT for the three selected metabolites. The same procedure was applied also for the parameter of area [42].

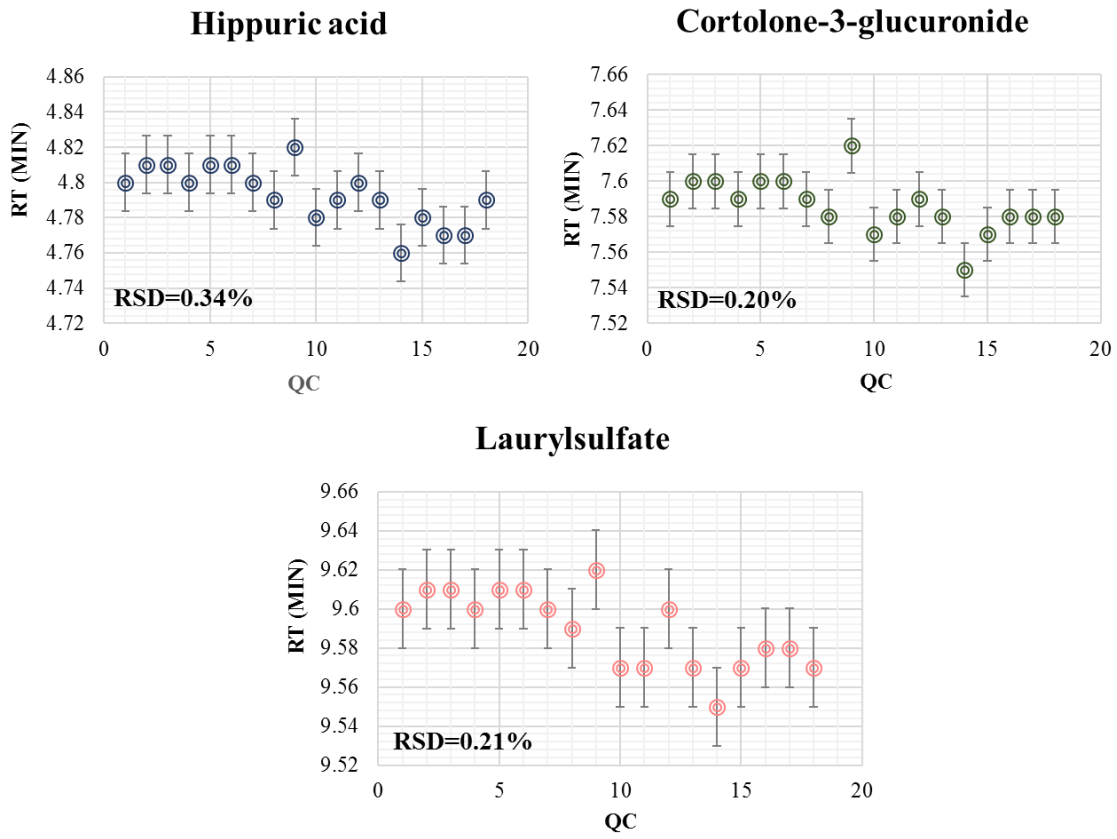

***Figure 41**: Representation of RSD (%) for RT of hippuric acid, cortolone-3-glucuronide and laurylsulfate in QC injections.*

As it is shown in the figure above RSD (%) values of the three metabolites were found 0.34% for hippuric acid, 0.20% for cortolone-3-glucuronide and 0.21% for laurylsulfate. The same estimations were performed for area parameter. In brief, the calculations showed %RSD for RT<0.4%, %RSD for area <8.2% and accuracy<2 ppm. The methodology was evaluated as accurate and repeatable for samples analysis. Moreover, injections and repetitions of each sample were randomized in the sequence to achieve more reliable evaluation of QC injections [42].

3.4.4 Chemometrics in urine samples

The statistical process started with unsupervised methods and particularly with PCA analysis in order to observe the data fitting, the existence of outliers and possible trends and variation between groups. Data were treated with UV and pareto to investigate the most appropriate scaling for data visualization. UV scaling found to produce models with better fitting parameters (R2 and Q2) and visualization plots and eventually selected for the statistical process. PCA analysis has been initially used to investigate the trends and the existence outliers in the two basic treatments; HT and placebo. The plot below represents the visualization of the total number of HT and placebo samples analyzed in negative ionization and treated with UV scaling.

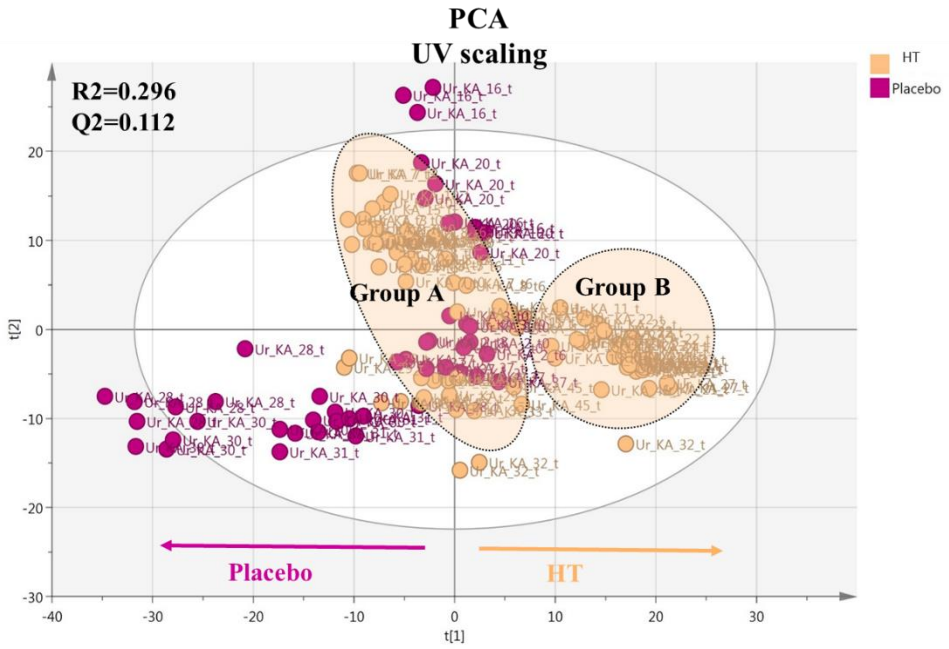

Figure 42: *PCA plot in UV scaling including the total number of samples. Observations are colored according to the administered capsule; purple for placebo and light pink for HT capsules. Fitting parameters are also depicted.*

The generated model resulted a plot with nine components and impotent data fitting. The scores values R2 and Q2 were significantly low, 0.296 and 0.112 respectively. Despite the low

fitting parameters, a weak trend of separation was observed on the first component between HT and placebo group. HT samples (light pink) tended to cluster on the right side of the first component and placebo samples (purple) on the left side. However, a considerable dispersion was observed in both groups. Placebo group revealed outliers coming from 3 different participants and time points (KA_16_t3, KA_28_t3 and KA_30_t6), while HT group had no outliers. Moreover, an additional tendency of forming two separate groups appeared between groups A and B of HT treatment.

For the further statistical exploration supervised methods were employed. Firstly, PLS treatment in UV scaling was performed defining HT and placebo treatment as Y qualitative parameters. With PLS treatment the fitting parameters were much higher (R2=0.985 and Q2=0.914). Both scores values were close to 1 and the one value close to the other indicating the improvement in data fitting and the high predictive power of the model.

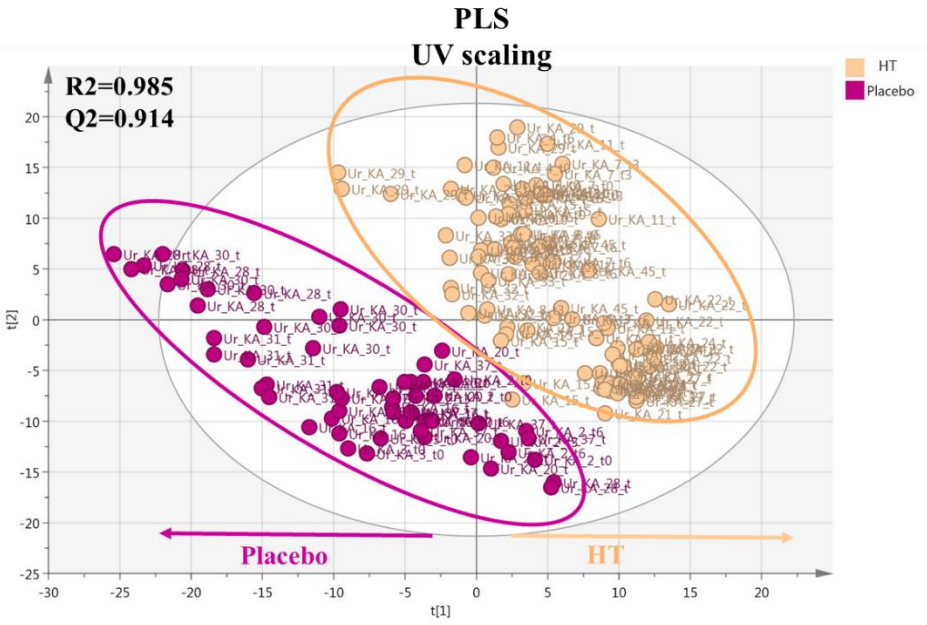

***Figure 43**: PLS plot in UV scaling including the total number of samples. Observations are colored and clustered according to the administered capsule; purple for placebo and light pink for HT capsules. Fitting parameters are also depicted.*

In the PLS plot a notable and stronger clustering was observed, although retaining the same trend of separation like the first constructed PCA plot. Both groups were characterized again by high dispersion, probably caused from the high metabolic deviation of each participant and the different metabolism of individuals placebo group disclosed outliers but in PLS only KA_28_t3 behaved as outlier. For this reason, the initial outliers of PCA plot were not excluded from the statistical process and the analysis continued with the total number of observations.

Continuously OPLS in UV was used to improve visualization. Using this treatment clear clusters were revealed between HT and placebo treatment and further grouping of HT into groups A and B. Nevertheless, in OPLS QC-pooled samples were imported to investigate the model visualization efficiency. QC samples were almost centralized revealing a discreet tendency towards HT cluster. This observation was normally expected given the fact that 63.5% of QC was consisted of HT samples. It has to be underlined that a distinct separation existed on the first component between HT treatment and placebo being retained in all the data treatments, supervised and unsupervised employed methodologies. Additionally, separation on the second component between groups A and B was also observed. Also in this treatment high fitting parameters were generated (R2=0.961 and Q2=0.815).

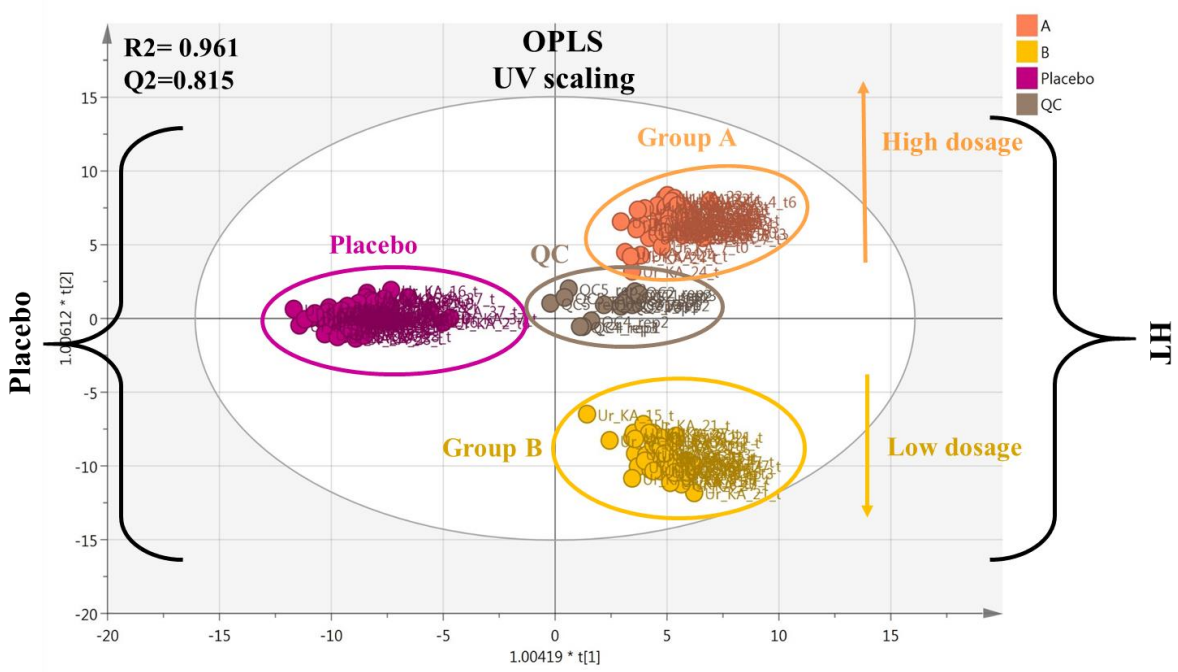

***Figure 44**: OPLS plot in UV scaling including the total number of samples. Observations are colored and clustered according to the administered capsule and dose; purple for placebo, yellow for group B, light pink for group A and grey for QC. Fitting parameters are also depicted.*

The above model was validated via the permutation test of Simca. Model passed the permutation test. Figure A30 presents in detail the R2 and Q2 intercepts for all the Y variables of the above OPLS plot (group A, group B, placebo and QC).

3.4.5 Metabolites identification

The aim of the current metabolomic approach is not only to investigate the clustering of different groups according to the capsule intake, but also to identify the variables, contributing to the clustering. In other words, to identify the statistical significant metabolites and potential biomarkers of HT intake. Loadings plot provide this information and in combination with VIP calculations can elicit the most statistical significant loadings of the model. After preliminary tests and chromatogram examination of individual samples belonging to groups A and B, turned

out that there were no significant metabolic differences between these groups and unambiguous results could be derived. In order to maximize the differentiation between groups an OPLS-DA plot was constructed using the two basic groups, HT and placebo. S-plot was prepared to investigate statistical significant metabolites between the two basic treatments and identify differential metabolites in each one.

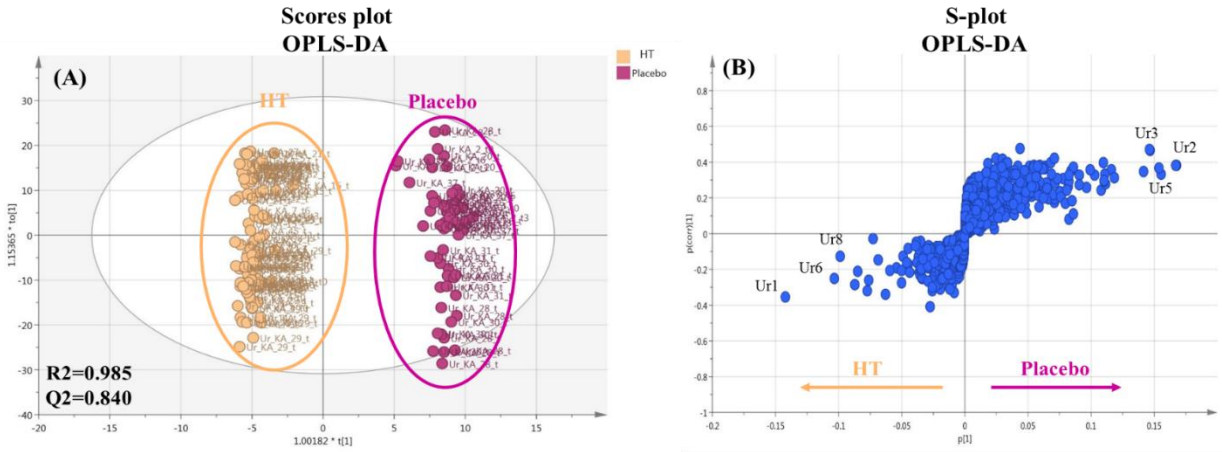

***Figure 45**: **(A)**: OPLS-DA scores plot of all samples in UV scaling. Observations are coloured according to the adminisered capsule; purple for placebo and light pink for HT. Fitting parameters are also depicted. **(B)** S-plot of the corresponding OPLS-DA scores plot. Statistical significant identified metabolites are annotated.*

Totally 105 features were calculated with VIP scores over 1. From this final list 30 compounds were identified in urine with decisive role in the metabolic pathway of each treatment. The list with the identified metabolites is presented in Table 14 below.

***Table 14:** Identified statistical significant metabolites of urine samples. For each metabolite a code number is given in the first column. Experimental m/z, name, elemental composition (EC), ring and double bong equivalent (RDB) and VIP value are illustrated. In the last column the belonging class of each metabolite is noted.*

#	Experimental *m/z*	Suggested molecule	EC	RDB	VIP	Group
Ur1	178.0512	Hippuric acid	$C_9H_9O_3N$	6.5	20.3404	HT

Ur2	194.0462	Hydroxyhippuric acid	$C_9H_9O_4N$	6.5	6.30864	Placebo
Ur3	367.1586	Epitestosterone sulfate	$C_{19}H_{28}O_5S$	6.5	5.59170	Placebo
Ur4	369.1733	5a-Dihydrotestosterone sulfate	$C_{19}H_{30}O_5S$	5.5	5.29357	Placebo
Ur5	181.0505	Homovanillic acid	$C_9H_{10}O_4$	5.5	5.20725	Placebo
Ur6	145.0616	Glutamine	$C_5H_{10}O_3N_2$	2.5	5.08479	HT
Ur7	261.0079	Homovanillic acid sulfate	$C_9H_{10}O_7S$	5.5	4.62802	Placebo
Ur8	187.0073	*p*-cresol sulfate	$C_7H_8O_4S$	4.5	4.15471	HT
Ur9	195.05226	1,3-Dimethyluric acid	$C_7H_8O_3N_4$	6.5	4.05979	Placebo
Ur10	245.0128	Homovanillic aldehyde sulfate	$C_9H_{10}O_6S$	5.5	3.97235	Placebo
Ur11	229.0544	Unknown	$C_{10}H_{14}O_4S$	4.5	3.70759	HT
Ur12	541.2665	Cortolone-3-glucuronide	$C_{27}H_{42}O_{11}$	7.5	3.63431	Placebo
Ur13	217.0181	Tyrosol-4-sulfate	$C_8H_{10}O_5S$	4.5	3.55331	Placebo
Ur14	191.0201	Citric acid	$C_6H_8O_7$	3.5	3.0914	Placebo
Ur15	203.0018	Methoxycatehol sulphate	$C_7H_8O_5S$	4.5	2.92597	Placebo
Ur16	274.0029	Hippuric acid sulfate	$C_9H_9O_7NS$	6.5	2.60944	Placebo
Ur17	128.0359	Pyroglutamic acid	$C_5H_7O_3N$	3.5	2.55335	Placebo
Ur18	173.0097	Aconitic acid	$C_6H_6O_6$	4.5	2.18325	Placebo
Ur19	265.1479	Lauryl sulfate	$C_{12}H_{26}O_4$	0.5	2.13303	Placebo
Ur20	263.1040	Phenylacetylglutamine	$C_{13}H_{16}O_4N_2$	7.5	1.98936	HT
Ur21	167.0215	Uric acid	$C_5H_4O_3N_4$	6.5	1.91047	Placebo
Ur22	151.0404	3,4-Dihydroxyphenylacetaldehyde	$C_8H_8O_3$	5.5	1.8488	Placebo
Ur23	245.0478	Unknown	$C_{10}H_{14}O_5S$	4.5	1.7337	HT
Ur24	123.0451	HT MS2	$C_7H_8O_2$	4.5	1.54178	HT
Ur25	227.0387	Unknown	$C_{10}H_{12}O_4S$	5.5	1.51326	HT
Ur26	465.2490	5-alpha-Dihydrotestosterone glucuronide	$C_{25}H_{38}O_8$	7.5	1.42304	HT
Ur27	243.0331	Unknown	$C_{10}H_{12}O_5S$	5.5	1.25191	HT
Ur 28	283.0829	*p*-crezol glucuronide	$C_{13}H_{16}O_7$	6.5	1.19395	HT
Ur29	259.0285	HT-acetate-4'-O-sulfate	$C_{10}H_{12}O_6S$	5.5	1.13281	HT
Ur30	343.1393	Homovanillic alcohol glucuronide	$C_{16}H_{24}O_8$	5.5	1.1057	HT

Overall, based on the above identified statistical significant metabolites of the dataset tyrosine/dopamine metabolic pathway seems to be altered from HT administration. However, each of the two basic treatments, HT and placebo, affected different subpathways and in each case different metabolites were upregulated or downregulated. In the case of placebo group, the classic dopamine metabolic pathway seems to be followed. Standard metabolites of this pathway were identified with high significance, such as 3,4-dihydroxyphenylacetylaldehyde, homovanillic aldehyde and homovanillic acid, accompanied with their methylated, sulfated and glucuronated products [20]. On the other hand, in the case of HT an overexpression pathway of three different normal urinary components was revealed. HT administration increased the final formation of thee phenol derived metabolites; hippruric acid, *p*-cresol and phenylaceytylglutamine [52].

In more detail, urine samples from placebo treatment disclosed that the metabolism of participants followed the classic phenylalanine pathway leading to the final formation of hydroxyhippuric acid (hydroxy-HA) and hippuric acid (HA) which are normal urinary components. Based on literature data and figure 32, the first produced dopamine metabolite, 3,4-dihydroxyphenylacetaldehyde (DOPAL), was identified in our statistical process with *m/z* 151.0401, chemical formula $C_8H_7O_3$ and RDB: 5.5. Consequently, homovanillic acid (*m/z* 181.0506, $C_9H_9O_4$, 5.5), homovanillic acid sulfate (*m/z* 261.0074, $C_9H_9O_7S$, 5.5) and homovanillic aldehyde sulfate (*m/z* 261.0074, $C_9H_9O_6S$, 5.5) were identified. In literature homovanillic metabolite and its products are considered as typical biomarkers of dopamine turnover in clinical chemistry, abundant in biological matrices [20]. Also other intermediate metabolites of the pathway were identified, tyrosol sulfate (*m/z* 217.0179, $C_8H_9O_5S$, 4.5) and methoxycatechol sulfate (*m/z* 203.0018, $C_7H_7O_5S$, 4.5). It has to be noted that the latest

metabolites were found in a relative small sample group and the corresponding metabolic reactions are regarded as minor pathways bibliographically [20]. This high metabolic divergence and the different metabolic reactions followed in the same metabolic pathway is attributed to the personal dietary and general habits followed by each participant. The final products of the pathway hydroxy-HA (*m/z* 194.0466, $C_9H_9O_4N$, 6.5) and HA sulfate (*m/z* 274.0029, $C_9H_8O_7NS$, 6.5) were identified. HA was detected as well in all the samples of the dataset, although it was not characterized as statistical significant metabolite of placebo group. Moreover, testosterone metabolites, methyluric acids, aconitic, citric acid, amino acids and fatty acids sulfates were identified as normally occurred urinary metabolites. Table A16 in appendix represents the identification parameters of the identified metabolites. The followed dopamine biosynthentic pathway enriched with the identified metabolic products for placebo is shown in the figure below.

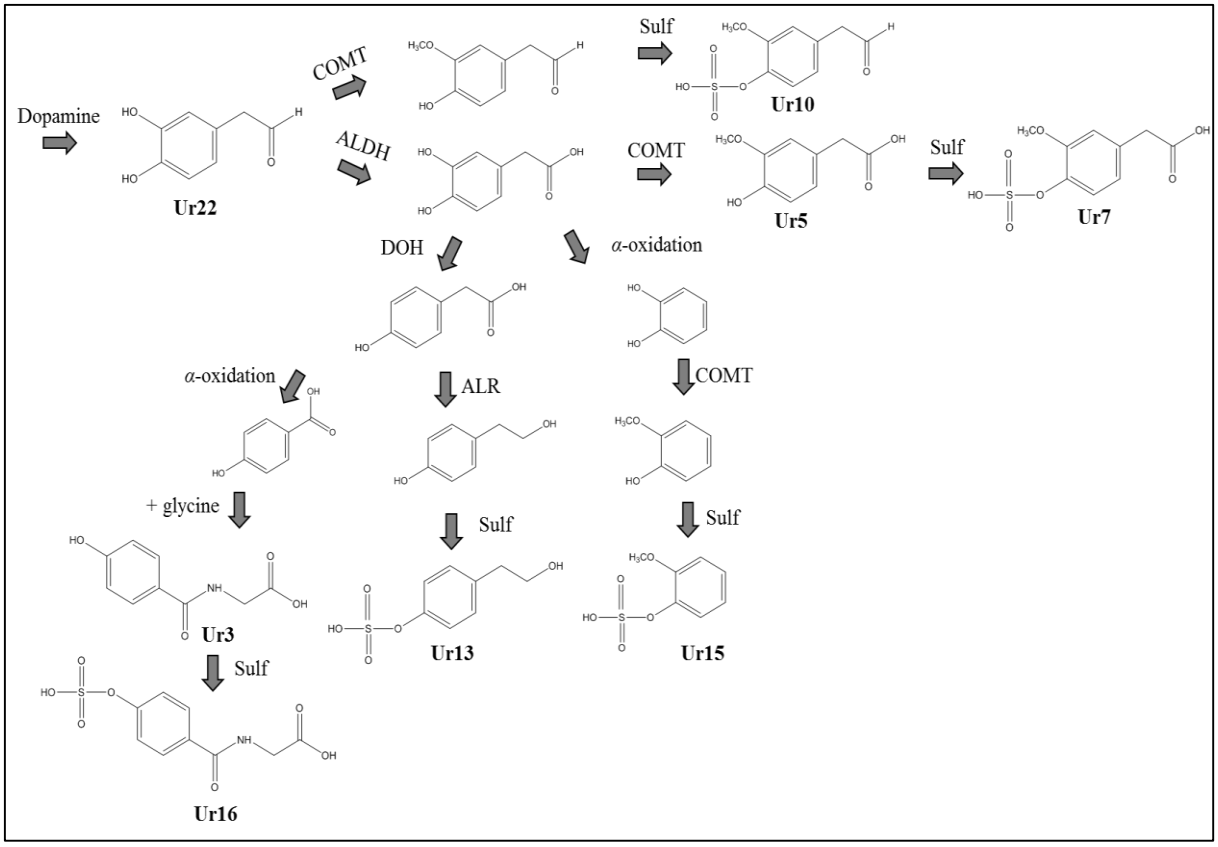

Figure 46: *Proposed metabolic pathway based on the identified metabolites of placebo group. The identified metabolites of the datset are annotaeted. COMT: catechol-O-methyltransferase , ALDH: aldehyde dehydrogenase, Sulf: sulphotransferase, DOH: dihydroxylase, ALR: aldehyde/aldose reductase.*

A different pathway was discovered in HT treatment due to the high phenol intake. Both A and B group seem to follow the same biosynthetic pathway. In this case phenylalanine pathway leads to the increased production of three different final metabolites; HA, *p*-cresol and phenylacetylglutamine (PAG). Based on literature, these three metabolites are characterized by bad reputation due to their association with toluene and benzene exposure and their use as indicators of such exposures in human urine [53]. However, recent evidences denote that increasing trends of these three metabolites are associated with reduced risk of metabolic

syndrome (MetS), through their influence in gut microbiome regulation [54] and phenols consumption [55].

HA acid was found as the metabolite indicating the highest statistical significance (VIP=24.1) in the whole dataset. It is worth to note that its concentration in human urine is directly associated with phenols consumption [55]. Hippuric acid (or hippurate) with *m/z* 178.0510, chemical formula $C_9H_9O_3N$ and RDB: 6.5 is the glycine conjugate of benzoic acid. The mean 24-h urinary excretion for HA has been measured via UPLC−MS/MS and found 6284.6 (4008.1) μmol/24-h in men and 4793.0 (3293.3) μmol/24-h in women (standard deviation shown in brackets) [56]. As it is obvious the excretion in the two genders is not the same and men exert higher concentrations in comparison to women.

HA biosynthesis is known since 1977 and requires two reactions carried out in mitochondrial matrix [57,58]. Initially, benzoic acid (produced from phenylalanine pathway) reacts with coenzyme A (CoA) and adenosine triphosphate (ATP) to form the intermediate complex benzoyl-CoA catalyzed by benzoyl-CoA synthase [59]. Consequently, this complex reacts with glycine which crosses the inner mitochondrial membrane to finally produce HA. The second reaction is catalyzed by benzoyl CoA: glycine N-acyltransferase [59,60] (Figure 47)

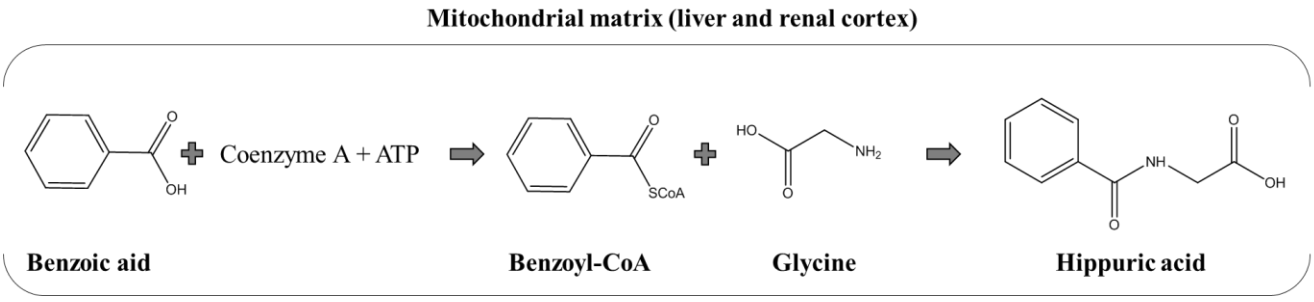

Figure 47: *Biosynthesis of hippuric acid in mitochondrial matrix.*

Studies have shown that dietary supplementation of phenolic compounds is associated with an increase in HA excretion in urine. Phase I and II metabolization of the consumed phenolic compounds lead to the increase of phenolic acid derivatives and thus HA [55].

Based on our findings (Table 14) and figure 32 the HT intake leads to the increased formation of DOPAC, which after dehydrogenases activity produces phenylacetic acid. After *α*-oxidation, benzoic acid is produced and finally HA is formed (Figure 48A).

Nevertheless DOPAC produces *p*-crezol and its derivatives, *p*-crezol sulfate (*m/z*: 187.0073, $C_7H_8O_4S$, 4.5) and *p*-crezol glucuronide (*m/z*: 283.0829, $C_{13}H_{16}O_7$, 6.5) which are also normally occurring urinary metabolites (Figure 48B) produced from tyrosine metabolic pathway [61]. *P*-cresol normally urinary excertion is 1002.5 (737.1) μmol/24-hr (men) and 1031.8 (687.9) μmol/24-hr (women), being in the same levels for the both genders [56]. Figure A31 in appendix presents in detail *p*-cresol biosynthesis through tyrosine pathway. The increased phenol administration leads the increased DOPAC production, which loses one hydroxyl group and after decarboxylation produces *p*-cresol. Because *p*-cresol is a product of the activity of intestinal bacteria, its excretion in urine is regarded as a marker of the proper population (in terms of bacteria species and number of each species) and activity of human microbiota [61].

The third overproduced compound is PAG (m/z: 263.1040, $C_{13}H_{16}O_4N_2$, 7.5). Like the other two compounds PAG is another microbial metabolite coming from phenylalanine pathway [62]. PAG is produced in the liver mitochondria after the reaction of phenylacetic acid with coenzyme A to form phenylacetyl-CoA. Subsequently, glutamine N-acetyl transferase catalyzes the reaction of glutamine with phenylacetyl-CoA for the final formation of PAG [62]. It is a normal urinary component and its mean excretion has been found 1283.0 μmol/24-hr in men and 1145.9 μmol/24-hr in women [56]. Phenylacetylglutamin concentration in urine is associated

with the excretion of nitrogenous wastes in human body like ammonia, urea, uric acid, and creatinine (uric acid found as a statistical significant metabolite for placebo group), produced from protein metabolism. In many animals, urine is the main route of excretion for such wastes through PAG and HA conjugation with glutamine and glycine, respectively [63,64]. In our study, the increased levels of DOPAC, caused by HT intake, led to the production of 3,4-Dihydroxyphenylpropanoic acid (DOPPAC) after carboxylation. DOPPAC can be then used either for *p*-cresol synthesis (figure A31) or can react with glutamine to form PAG (Figure 48C). It has to be noted that PAG shows better ionization in positive mode and higher VIP value in the corresponding model of positive ionization. Also the identified glutamine (*m/z*: 145.0616, $C_5H_{10}O_3N_2$, 2.5) of Table 14, appears the same RT with PAG and its detection is attributed to PAG fragmentation.

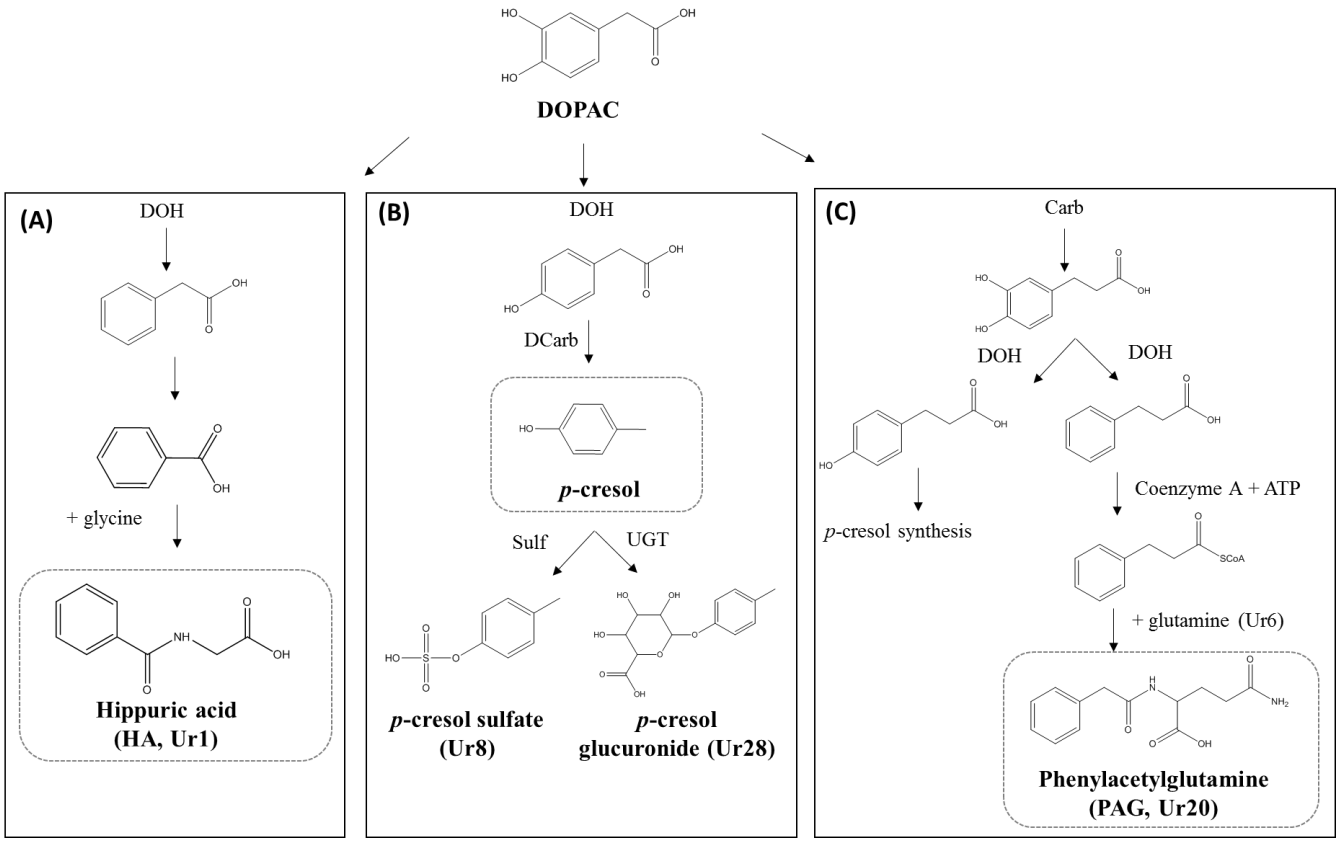

Figure 48: *Proposed metabolic pathway based on the identified metabolites of HT group. The identified metabolites of the datset are annotaeted. DOH: dihydroxylase, Dcarb: decarboxylase, Sulf: sulphotransferase, , UGT: glucurosyl-transferase, Carb: carboxylase.*

Moreover, HT-acetate sulfate, which is the sulfated product of HT-acetate is found as statistical significant metabolite in HT group. It has been reported that the alkaline conditions of human lumen induce the activity of acetyltransferase which catalyzes the transfer of acetyl group from acetyl-CoA to HT and finally form HT-acetate [65]. It has to be noted that in our study HT-acetate was detected in HT capsule and thus the production of HT-acetate sulfate could be derived either from HT metabolism either from the its direct consumption from the capsule. It is very important that HT-acetate has more lipophilic character in comparison to HT and pass easier the lipophilic cell membranes [65].

Another interesting finding of the statistical process is the identified metabolite Ur24 (*m/z*: 123.0451, $C_7H_8O_2$, 4.5) in HT groups. The interesting thing of this metabolite is that it has identical identification parameters with the characteristic MS2 fragment of HT and is eluted in the same RT with HT, after a standard HT injection with the same analytical methodology. This could signify the existence of HT in our samples, but probably binded to another chemical structure that is not well ionized or even its not identified. Also Ur24 could be an independent metabolite produced from phenols metabolization.

As it is shown in Table 14 also other compounds were encountered as statistical significant in HT groups, although they are considered as unknown metabolites. Specifically, metabolites Ur11 (*m/z*: 229.0554, $C_{10}H_{14}O_4S$, 4.5), Ur23 (*m/z*: 245.0478, $C_{10}H_{14}O_5S$, 4.5), Ur25 (*m/z*: 227.0387, $C_{10}H_{12}O_4S$, 5.5) and Ur27 (*m/z*: 243.0331, $C_{10}H_{12}O_5S$, 5.5) have not yet been referred in the literature. Although, the high resolving power of Orbitrap analyzer permits the determination of their chemical formula with confidence and thus their structure could be predicted. Based on the discovered biosynthetic pathways the chemical formula, RDB and MS/MS spectra, all of them are sulfated metabolites consisted of a benzene or phenol ring linked with a butyl carbon chain or propyl carbon chain plus on more methyl substitution. Additionally, the respective RT (Table A17) and their elution in non-polar systems implies the existence of an aliphatic chain with more than two carbons, which is normally found in our dataset and eluted in more polar systems. The possible structures indicate *p*-cresol biosynthetic pathway and it can be hypothesized that they are generated by tyrosine biosynthetic pathway (figure A31) in which is incorporated a dehydrogenation reaction and can explain the lack of two hydrogens and the existence of double bonds in Ur25 and Ur 27 which are possible produced from Ur11 and Ur23, respectively. Finally, a testosterone derivative Ur26 (*m/z*: 465.2490, $C_{25}H_{38}O_8$, 7.5) and

homovanillic alcohol glucuronide (*m/z*: 343.1393, $C_{16}H_{24}O_8$, 5.5) were characterized as statistical significant for HT groups.

In the above discovered pathway, all the identified metabolites are endogenous produced from dopamine and tyrosine pathways [20,66], with no reported effect until now on obesity. All of them are phenol derivatives and it can be assumed that the increased consumption of HT leads to overexpression of phenolic metabolites in human system. However, a recent study uncovered that increased levels of several endogenous metabolites, including hippuric acid, *p*-cresol and PAG were associated with reduced incidences of MetS [54]. This study adds further value to our outcomes and the need of further exploration of these three metabolites to human obesity and weight/fat loss has arisen. Previous *in vivo* experiments did not show any effect of HT in obesity [45–47]. However, the administered concentrations were low and the design of animal and human studies with higher HT intake is required for determination of the effect and relationship of the three metabolites in obese subjects as well as for the discovery of the mechanism which induces possible weigh/fat loss.

3.5 Metabolomic analysis of blood via UPLC-HRMS

Unfortunately, as it is already mentioned in methods and materials section all the collected blood samples were hemolyzed, because they were stored in -80^{o}C, before centrifugation for plasma obtainment. This accident impeded the sample preparation procedure and the subsequent metabolites identification. However, all of them were extracted as normal raw material for the generation of the total metabolic extract of blood.

3.5.2 Development of UPLC-HRMS methodology

For the development of the UPLC conditions, elution solvents, column temperature, and column characteristics were investigated. MeOH and ACN were tested as organic solvents and H_2O with and without FA were tested as aqueous phase. Using ACN a lot of peaks were not eluted and MeOH showed better elution abilities and thus selected as organic solvent. Acidified water with FA improved significantly peak shape and used as aqueous solvent. Column temperature was set at 40^{o}C to improve peak shape as well. Two different columns were tested; an Acquity UPLC Peptide BEH C18 (100 mm x 2.1 mm, 1.7 μm) and an Acquity UPLC Peptide BEH C18 (50 mm x 2.1 mm, 1.7 μm). The fist column produced chromatograms with higher resolution and selected for the separation.

The used mass spectrometric parameters were the same as urine HRMS optimized for generic ionization.

3.5.1 Samples for metabolomics study

Totally 43 samples were included in the metabolomic analysis coming from participants who received the HT treatment; 23 from group A and 20 from group B. Additionally, 20 samples came from participants who received the placebo capsule. QC-pooled sample was prepared from the total number of samples (63 samples), meaning that QC was composed 68.3% from HT samples and 31.7 % from placebo samples. Pending samples (n=12) that their identity group was not known were excluded from the statistical treatment.

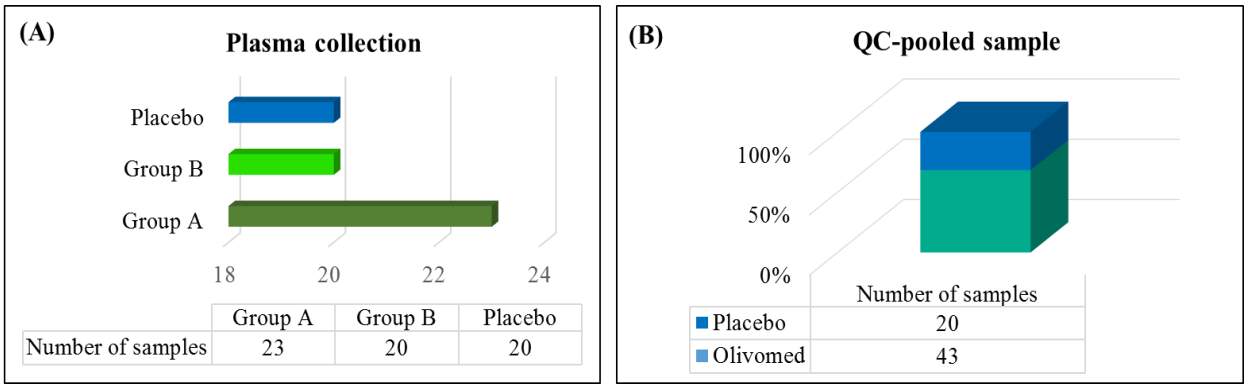

	Group A	Group B	Placebo
Number of samples	23	20	20

	Number of samples
Placebo	20
Olivomed	43

***Figure 49**: Representation of total blood collection. **(A)** presents in detail the collected samples per group; blue bar illustrates placebo samples, light green bar samples from group B and dark green bar samples from group A. **(B)** presents the final composition of QC-pooled sample; blue part of the bar represents placebo samples and green the HT samples. Below each graph a detailed table describing the total sample collection in numbers is illustrated.*

3.5.3 Validation aspects

A QC-polled sample was prepared and injected every fifty runs to evaluate the repeatability of the analysis. The parameters of RT, mass accuracy and area were evaluated in each QC injection. For this purpose, three peaks were selected who had:

- different RT covering as possible the injection time
- different mass range to cover as possible the scanning mass range
- different levels for evaluation the parameter of area.

P-cresol sulfate (*m/z*:187.0072, RT=2.70), epitestosterone sulfate (*m/z*:367.1586, RT=4.71) and 1-linoleoyl-2-docosadienoyl-sn-glycero-3-phosphoinositol (*m/z*:913.5815, RT=10.15) were selected as the peaks satisfying RT, mass range and levels. Figure 50 illustrates a QC injection. The three selected compounds are annotated.

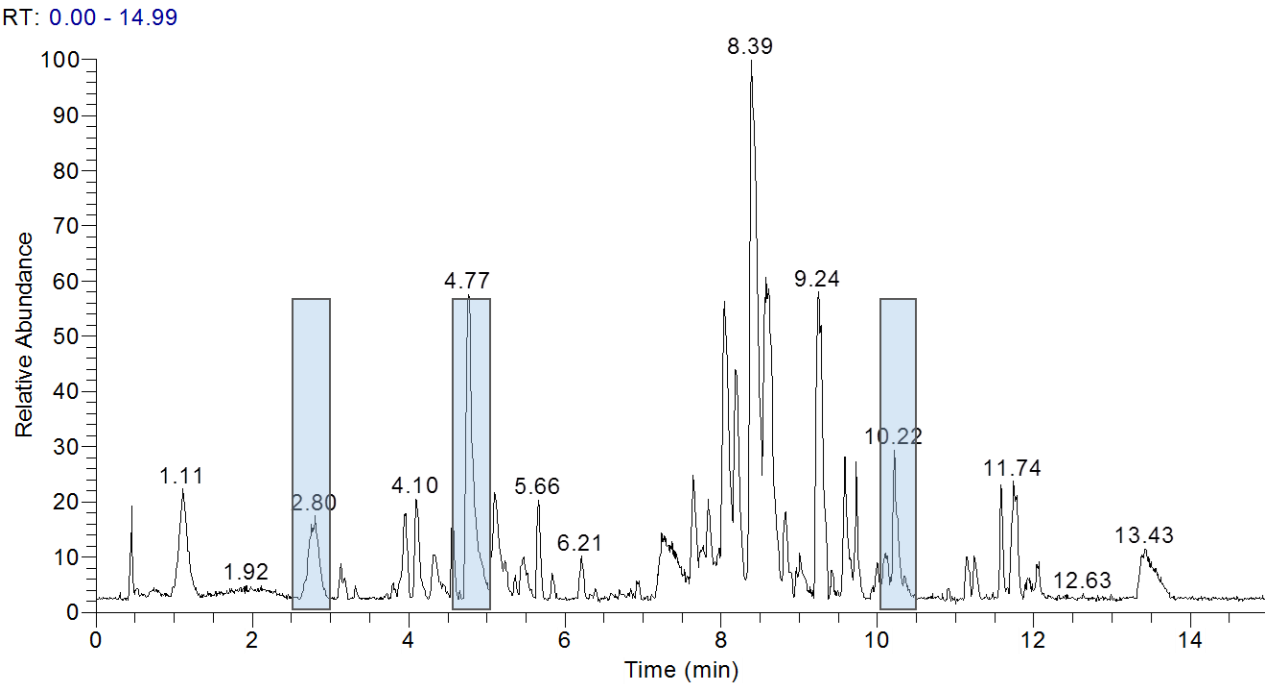

***Figure 50**: UPLC-HRMS chromatogram of QC sample in negative ionization. Annotated peaks represent the selected compounds used for the evaluation of the repeatability of the analysis.*

Two evaluation criteria were subjected to each peak. Firstly, % RSD should be less than 1% for RT and 10% for area. Also accuracy should be less than 5 ppm. *P*-cresol sulfate, epitestosterone sulfate and 1-linoleoyl-2-docosadienoyl-sn-glycero-3-phosphoinositol were evaluated for the above criteria. The figure below illustrates the %RSD of RT for the three selected metabolites. The same procedure was applied also for the parameter of area [42].

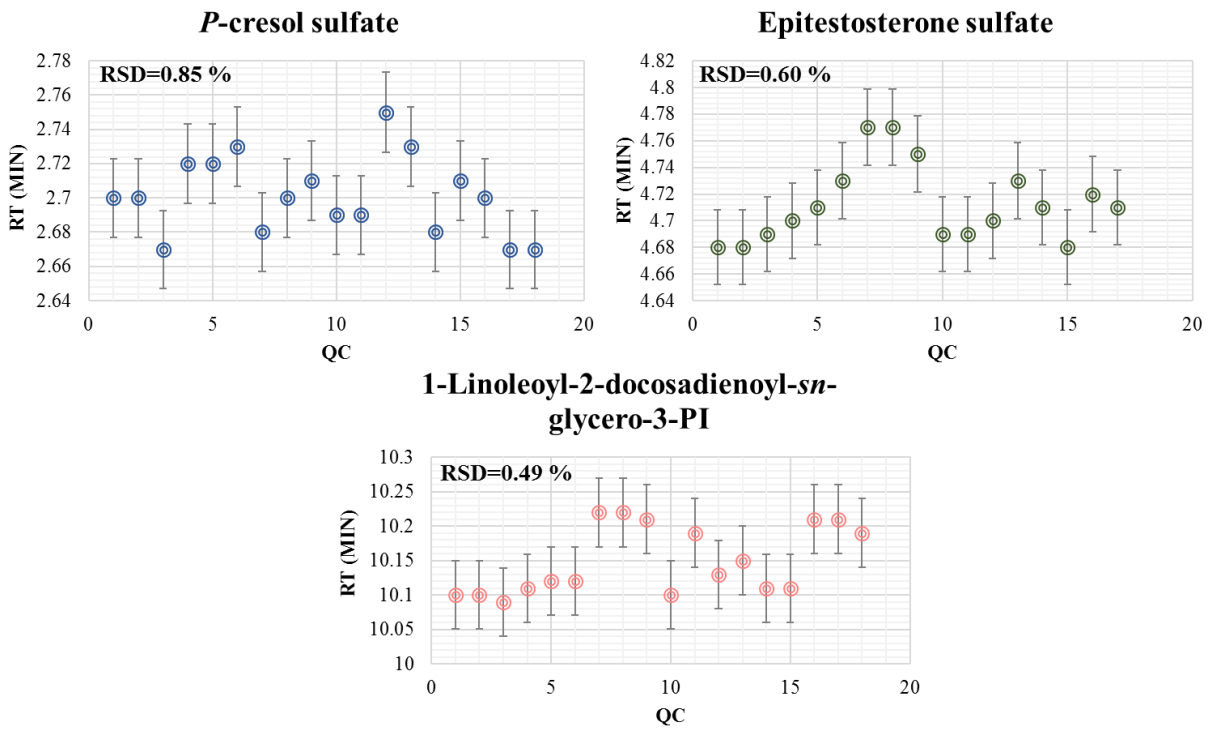

Figure 51: *Representation of RSD (%) for RT of p-cresol sulfate, epitestosterone sulfate and 1-linoleoyl-2-docosadienoyl-sn-glycerol-3-PI in QC injections.*

As it is shown in the figure above RSD (%) values of the three metabolites were found 0.85% for p-cresol sulfate, 0.60% for epitestosterone sulfate and 0.49% for l1-linoleoyl-2-docosadienoyl-sn-glycero-3-phosphoinositol. The same estimations were performed for area parameter. In brief, the calculations showed %RSD for RT<0.85%, %RSD for area <9.1% and accuracy<3.7 ppm. The methodology was evaluated as accurate and repeatable for samples analysis. Moreover, injections and repetitions of each sample were randomized in the sequence to achieve more reliable evaluation of QC injections [42].

3.5.4 Chemometrics in blood

Initially all observations were treated with unsupervised method to investigate data fitting and scaling. Data were analyzed with PCA in UV and Pareto scaling. In both scalings fitting was

not so good and the scoring parameters presented low values. The decision of the appropriate scaling was based on the visualization results and the outcomes that could be derived from the corresponding loadings plot. For these reasons UV scaling was rejected and pareto was used for PCA analysis. The figure below illustrates the corresponding PCA plot in pareto scaling including the total number of observations.

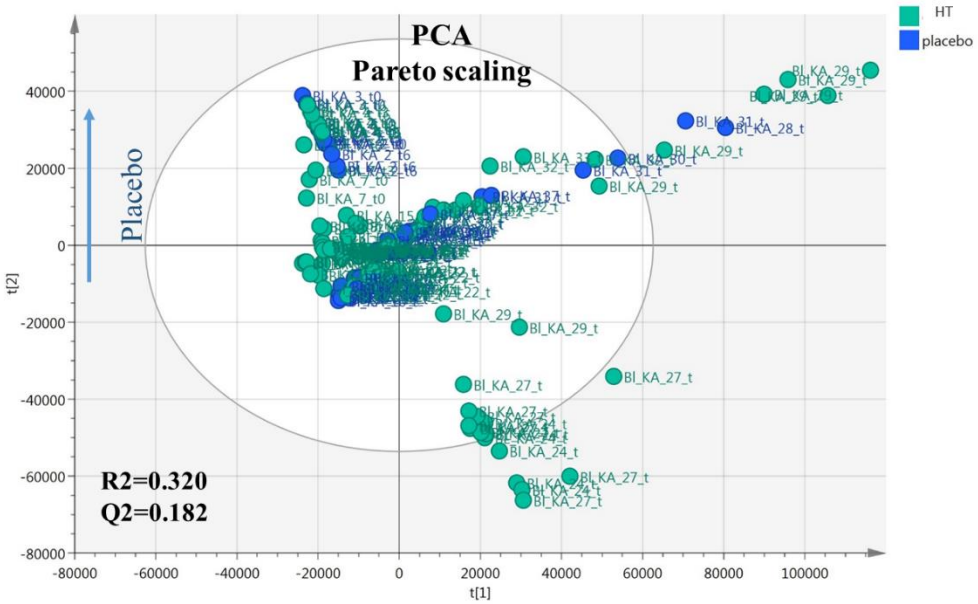

Figure 52: *PCA plot in pareto scaling including the total number of samples. Observations are colored according to the administered capsule; blue for placebo and green for HT capsules. Fitting parameters are also depicted.*

As it is shown in Figure 52 the trend of separation was not intense and fitting parameters were low (R2=0.320 and Q2=0.182), showing also a peculiar distribution of observations. The existence of many outliers was characteristic for HT group. The only observation of the plot was that placebo samples tend to aggregate at the upper part of the second component and no significant conclusion could be derived from the PCA model. Samples were characterized by high deviation and PCA found as impotent tool for the elicitation of the first remarks that can be used as guidance for the continuation of the statistical process. For this reason, the analysis

continued with PLS method and scaling parameter was tested again. In PLS, UV scaling resulted in much higher fitting parameters in comparison to pareto and as a result it was selected as scaling in PLS and the further data treatment as well. The figure below illustrates the corresponding plot in UV scaling.

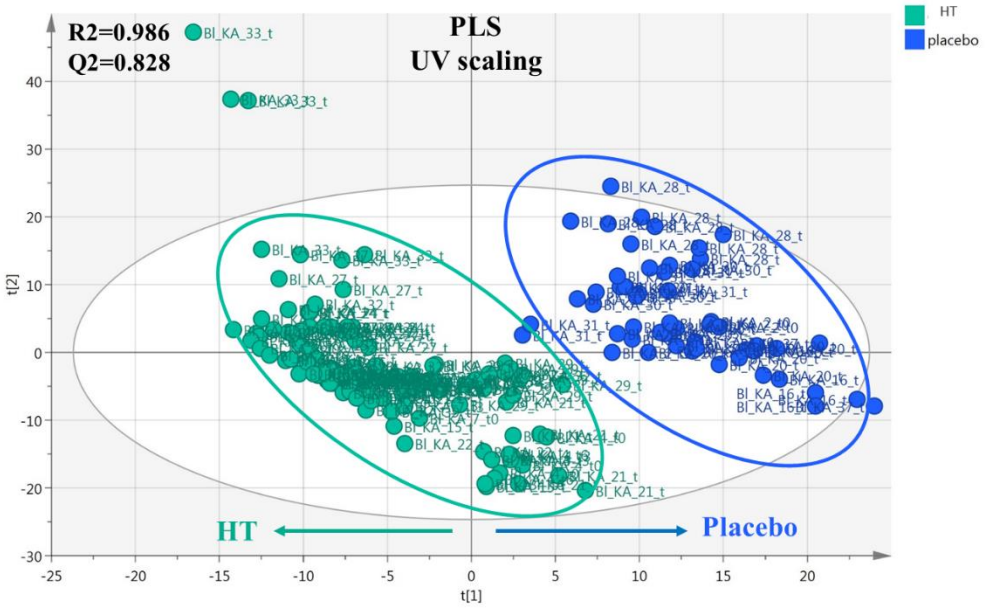

Figure 53: *PLS plot in UV scaling including the total number of samples. Observations are colored and clustered according to the administered capsule; blue for placebo and green for HT capsules. Fitting parameters are also depicted.*

Using PLS analysis fitting parameters were significantly improved (R2=0.986 and Q2=0.828) together with the grouping. Again HT treatment revealed outliers and specifically the sample with code KA_33_t3, which possessed significant distance from its group. For this reason, this sample was excluded for the data set. Another important remark is that there was a noticeable trend of separation on the first component between HT and placebo groups. In order to improve more the visualization, OPLS was applied in UV scaling. Additionally, in OPLS QC-

pooled samples were imported to the study to investigate their behavior in the dataset. The generated model is presented below.

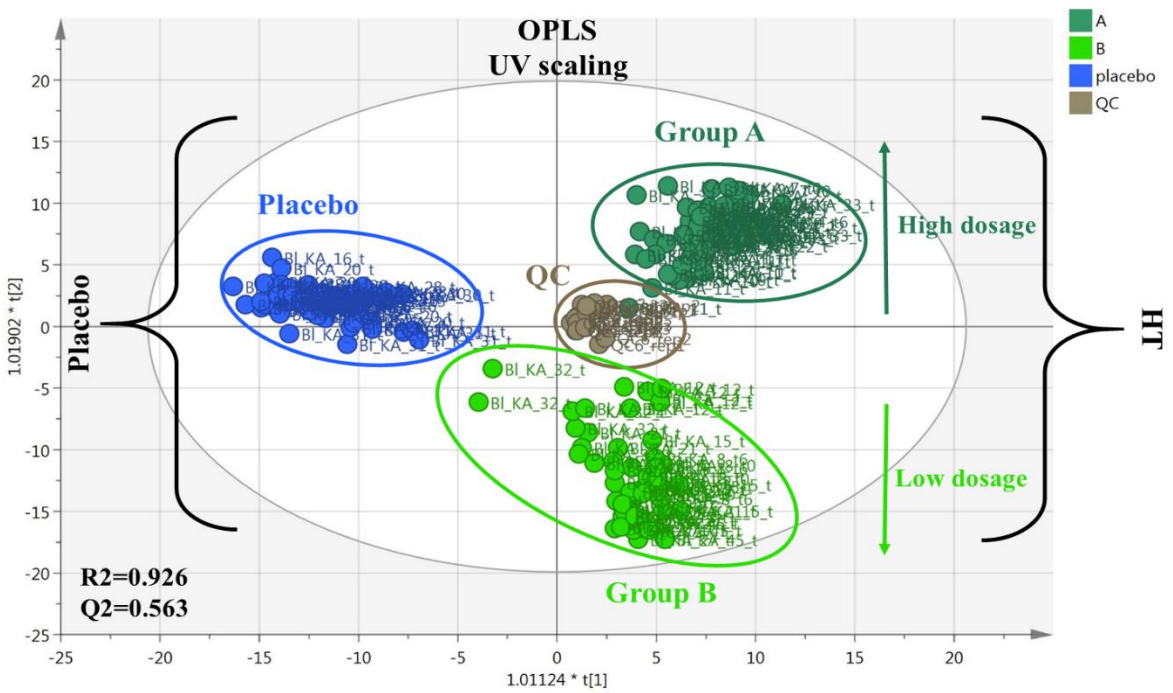

Figure 54: *OPLS plot in UV scaling including the total number of samples. Observations are colored and clustered according to the administered capsule and dose; blue for placebo, light green for group B, dark green for group A and grey for QC. Fitting parameters are also depicted.*

In OPLS model fitting parameter R2 is close to 1 and Q2 over 0.5. However, the two parameters are not the one close to the other and the predictivity of the model was considered low. It is remarkable that despite the low Q2 value, HT treatment (green-right side of the plot) differentiated from placebo group (blue-left side of the plot) on the first component. In parallel, the two HT treatments (group A and B) were discriminated on the second component. Group A signifying the high capsule dosage (15 mg/day) (dark green) was clustered at the upper part and low dosage samples (5 mg/day) (light green) at the lower part of the component. Also like urine

study, QC samples were not precisely centralized because in majority QC was composed from HT samples

3.5.5 Metabolites identification

For the investigation of the statistical significant metabolites, OPLS-DA analysis was employed to maximize the differentiation among groups. The treatment was based to the comparison of the two basic groups, HT and placebo to increase the discrimination capability. Based on preliminary results group A and B of HT did not present quality differences and they were characterized by the same features. For the study of the loadings, S-plot was constructed and VIP calculations were carried out to generate a list with the features influencing the model.

The first OPLS-DA plot between HT and placebo revealed outliers coming from both treatments. In particular, HT group revealed again outliers KA_33_t0 and t3 which behaved from the initial step as outliers. For this reason, these samples were excluded from the statistical analysis. Also KA_32_t6 and KA_37_t0 and t6 and KA_30_t3 were also excluded. Due to the poor data fitting, analysis in UV and pareto scaling was performed and investigation of the corresponding S-plot to select the best scaling for metabolites identification. Pareto scaling produced loadings plot with clear trends of metabolites and for this reason was selected despite having moderate Q2 value which indicated the low predictivity of the model.

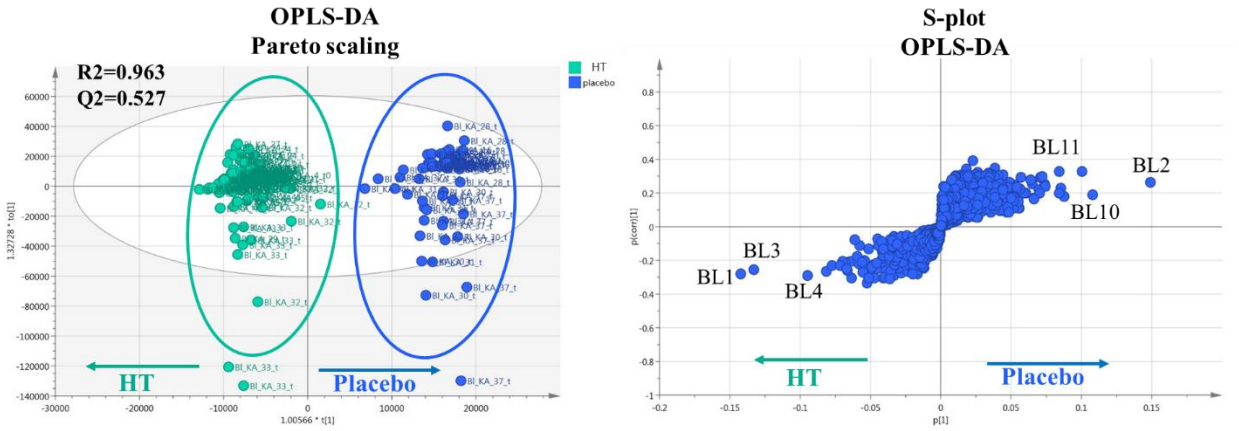

***Figure 55: (A)**: OPLS-DA scores plot of all samples in UV scaling. Observations are coloured according to the adminisered capsule; blue for placebo and green for HT. Fitting parameters are also depicted. **(B)** S-plot of the corresponding OPLS-DA scores plot. Statistical significant identified metabolites are annotated.*

Unfortunately, due to samples hemolysis VIP calculations generated a list with 1235 features with VIP scores over 1. The generated number of features was extremely high to study all the metabolites. After studying the first 100 features their *m/z* and the corresponding suggested EC revealed that most of them are compounds consisted of P and N indicating the intense existence of phospholipidic membranes or part of them in the extracts. In combination with the moderate predictive power of the model the perspective of the strong influence of the phospholipidic compounds to the model was rendered as possible. Table 15 presents the list with the identified compounds.

***Table 15**: Identified statistical significant metabolites of blood samples. For each metabolite a code is given in the first column. Experimental m/z, name, elemental composition (EC), ring and double bong equivalent (RDB) and VIP value are illustrated. In the last column the belonging class of each metabolite in noted.*

	Experimental *m/z*	**Suggested molecule**	**Elemental composition**	**RDB**	**VIP**	**Group**
BL1	281.2481	Oleic acid	$C_{18}H_{34}O_2$	2.5	10.628	HT
BL2	810.5277	1-stearoyl-2-arachidonoyl-sn-glycero-3-phosphoserine	$C_{44}H_{78}O_{10}NP$	7.5	9.51445	Placebo
BL3	395.2435	Hydroxy-16,16-dimethylprostaglandin E2	$C_{22}H_{36}O_6$	5.5	8.92886	HT
BL4	885.5472	1-oleoyl-2-homo-g-linolenoyl-sn-glycero-3-phosphoinositol	$C_{47}H_{83}O_{13}P$	7.5	8.04665	HT
BL5	464.3138	1-palmitoyl glycol-2-phosphocholine	$C_{23}H_{48}O_6NP$	1.5	7.96425	HT
BL6	283.2638	Stearic acid	$C_{18}H_{36}O_2$	1.5	7.412	HT
BL7	913.5815	1-linoleoyl-2-docosadienoyl-sn-glycero-3-phosphoinositol	$C_{49}H_{87}O_{13}P$	7.5	7.00679	HT
BL8	540.3298	1-(2-methoxy-octadecanyl)-sn-glycero-3-phosphoserine	$C2_5H5_2O_9NP$	1.5	5.78445	Placebo
BL9	524.2988	1-Stearoylglycerophosphoserine	$C_{24}H_{48}O_9NP$	2.5	5.36596	HT
BL10	500.2785	1-Arachidonyl-sn-glycero-3-phosphoethanolamine	$C_{25}H_{44}O_7NP$	5.5	4.74211	Placebo
BL11	367.1586	Epitestosterone sulfate	$C_{19}H_{28}O_5S$	5.5	4.20346	Placebo

BL12	544.2685	1-arachidonoyl-sn-glycero-3-phosphoserine	$C_{26}H_{44}O_9NP$	6.5	3.82733	Placebo
BL13	255.2329	Palmitic acid	$C_{16}H_{32}O_2$	1.5	3.6735	HT
BL14	786.5282	1,2-Dioleoylphosphatidylserine	$C_{42}H_{78}O_{10}NP$	5.5	3.62558	Placebo
BL15	187.0072	*p*-cresol sulfate	$C_7H_8O_4S$	4.5	3.46336	HT
BL16	303.2331	Arachidonic acid	$C_{20}H_{32}O_2$	5.5	3.14676	Placebo
BL17	265.1479	Lauryl sulfate	$C_{12}H_{26}O_4S$	0.5	2.9314	Placebo
BL18	269.2482	Palmitoleic acid	$C_{17}H_{34}O_2$	1.5	2.51477	HT
BL19	279.2332	Linoleic acid	$C_{18}H_{32}O_2$	3.5	2.49506	HT
BL20	369.1739	5a-Dihydrotestosterone sulfate	$C_{19}H_{30}O_5S$	5.5	1.99531	Placebo
BL21	435.2519	1-Oleoyl-lysophosphatidic acid	$C_{21}H_{41}O_7P$	2.5	1.56696	HT
BL22	229.0504	Unknown	C10H14O4S	4.5	1.42524	HT
BL23	448.3066	Glycochenodeoxycholic acid (bile acid)	$C_{26}H_{43}O_5N$	6.5	1.26083	HT

Overall 23 metabolites were identified. The presence of phospholipidic membranes in samples impeded considerably the identification step. Regardless the defatting step during extraction only unpolar metabolites were identified and none of HT metabolization products. The interesting part of identification was the detection of OO FA in HT treatment, which are included in HT capsule. Despite that placebo capsules contain also FA the corresponding samples were characterized only be phospholipids. From table 15 it can be assumed that HT treatment was characterized by the chemical categories of FA and phosphatidylinositols (PI). Also a prostaglandin derivative, a lysophosphatidic acid, a bile acid and two phenol derivatives were identified. On the other hand, placebo treatment was characterized by phosphatidylserines (PS), testosterone derivatives, lysophosphatidylethanolamine (LysoPE), one FA and one FA sulfate.

The compound with the highest significance was oleic acid (VIP=10.628) found in HT samples. Oleic acid (*m/z*: 281.2481, $C_{18}H_{34}O_2$, 2.5) is a monounsaturated fatty acid of OO (C18:1) and comprises almost 56-84% of its total FA content with known activity in decreasing LDL-cholesterol and increasing HDL-cholesterol in plasma [67]. Moreover, other FA contained in capsules were identified as statistical significant metabolites and specifically, stearic acid (*m/z:* 283.2638, $C_{18}H_{36}O_2$, 2.5) palmitic acid (*m/z*: 255.2329, $C_{16}H_{32}O_2$, 1.5), palmitoleic (*m/z*: 269.2482, $C_{17}H_{34}O_2$, 1.5) and linoleic acid (*m/z*: 279.2332, $C_{18}H_{32}O_2$,3.5). As it is already mentioned in the section of 3.1.2, these FA are constituents of HT capsule used as capsule carrier. Both groups of HT treatment were differentiated from placebo despite that these compounds are part of placebo capsule as well. It is noteworthy that oleic acid presented the highest intensities in group A, followed by group B which was in absolute accordance with the total capsule consumption of the two groups. Based on observational and cohort studies results populations with adherence to diets rich in MUFA (diet using OO as the only source of fat) like

Mediterranean diet is tightly associated with decreased obesity rates [68,69]. Recent data proved that dietary intake of oleic acid mobilizes intestinally-derived oleoylethanolamidea which is a lipid messenger of satiety [48]. Also oleic acid found to modulate gut microbiota composition towards a "lean-like phenotype", and polarises gut-specific immune responses mimicking the effect of a diet low in fat and high in polysaccharides content [70]. As a result, it can be assumed that the existence of MUFA, oleic acid, in capsules acted as a potential factor inducing satiety sense at participants.

Also in HT two PI derivatives were identified; BL4 (*m/z*: 885.5472, $C_{47}H_{83}O_{13}P$, 7.5) and BL7 (*m/z*: 913.5815, $C_{49}H_{87}O_{13}P$, 7.5). Their exact FA synthesis were discovered based on their $HRMS^n$ fragmentation (Table A17). PI are important lipids, both as a key membrane constituents and as participants in essential metabolic processes [71]. They are consisted of a phosphatidic acid backbone, linked via the phosphate group to inositol (hexahydroxycyclohexane). PI can have many different combinations of FA of varying lengths and saturation degree attached at the C-1 and C-2 positions. FA containing 18 and 20 carbons are the most common in our case, oleic and linoleic acid which were supplied via capsule. PI plasma existence in high concentration has been linked with the decrease of tracylglycerol concentration in obesity-model $Zuker^{(fa/fa)}$ rats[72], promotes cholesterol transportation and excretion [73] and anti-obesity effect in diet-induced obesity (DIO) mice, suggesting that PI improves liver function and reduces body fat and body weight [74].

BL3 metabolite (*m/z*: 395.2435, $C_{22}H_{36}O_6$, 5.5) is a prostaglandin derivative**,** in which the exact substitution of the hydroxyl group is not possible to be recognized in the basic prostaglandin E2 (PGE2) structure. Although based on the $HRMS^n$ data the hydroxyl group exists among C1-C5 (Table A17). BL3 was detected mainly in group A and some samples from

group B of HT treatment. Prostaglandins are naturally occurring prostanoids generated by the metabolism of arachidonic acid which is a major component of human lipidic membranes and plays a key role in membranes fluidity [75]. Specifically, prostaglandins are produced from the metabolization of free arachidonic acid produced from phospholipase A2 mediated hydrolysis. PGE2 has four G protein–coupled receptors: EP1 through EP4 [76]. Several studies have demonstrated the direct association of obesity with inflammation in adipose tissue characterized by hypertrophied adipocytes and increased production of proinflammatory cytokines and chemokines [77]. The inflammation is induced from the infiltration of adipose tissue by macrophages, which are primarily responsible for the inflammation response in this metabolic tissue [78]. Studies in LPS–treated human and murine macrophages have shown that PGE_2 suppresses the production of proinflammatory cytokines and chemokines via EP4 and suppresses chronic inflammation *in vivo* by mitigating macrophage activation during afflictions [79,80]. The above facts indicate that the increased levels of PGE2 derivatives in HT group, possible regulated the typical chronic inflammation disorders occurred by obesity.

BL21 (*m/z*: 435.2519, $C_{21}H_{41}O_7P$, 2.5) belongs to the category of lysophospatidic acids (LPA). LPAs are the simplest glycerophospholipids consisted of an acyl moiety esterified to the glycerol-3-phosphate backbone. BL21 was identified in HT groups and contained oleoyl in its structure, which was expected due to the identification of BL1 also as statistical significant biomarker. Like all glycerophospholipids, LPA are integral constituents of cellular membranes and are important signaling molecules as well [81]. Animal studies have demonstrated the association of increased LPA levels with obesity and insulin resistance [81], while in humans there are limited measurements. However a recent study highlightes that LPA is positively correlated with BMI [82].

Metabolite BL5 (*m/z*: 464.3138, $C_{23}H_{48}O_6NP$, 1.5) belongs to the category of lysophosphocholines (LysoPC). Generally, they have been postulated as biomarkers of the progression of different pathologies. *In vivo* investigations demonstrated that dysregulation of serum and hepatic levels of several LysoPCs occurs in rodents fed high-calorie diets [83–85]. Therefore, the examination of circulating levels of Lyso-PCs holds remarkable potential in the diagnosis of lipid disorders. This molecule was identified only in group A of HT and in relative high intensities in sample Bl_KA_33_t6. It is notable that t1 and t3 time points of this participant have been excluded from the statistical analysis because they behaved as outliers. This observation may indicate that the participant with this code may followed completely different dietary pattern and habits in comparison to the rest HT participants.

Finally, a bile acid (BL23, *m/z*: 448.3066, $C_{26}H_{43}O_5N$, 6.5) and two phenol derivative (BL15, *m/z*: 187.0072, $C_7H_8O_4S$, 7.5 and BL22, *m/z*: 229.0504, C10H14O4S, 4.5) were identified in HT treatment. It has to be underlined that BL15 and BL22 were found as statistical significant biomarkers in urine experiments in HT group, indicating the increased levels of these compounds in participants' biological fluids after capsule intake.

The major identified chemical category in placebo group is PS. PS are glycerophospholipids in which a phosphorylserine moiety occupies a glycerol substitution site. As is the case with diacylglycerols, glycerophosphoserines can have many different combinations of FA of varying lengths and saturation attached at the C-1 and C-2 positions. Phosphatidylserine is located entirely on the inner monolayer surface of the plasma membrane (and of other cellular membranes) and it is the most abundant anionic phospholipid. Therefore, phosphatidylserine may make the largest contribution to interfacial effects in membranes involving non-specific electrostatic interactions. Their role is to get exposed to cell membranes

and acts as an "eat me signal" during apoptosis, by prompting phagocytes to engulf the cells [86].

BL10 (*m/z*: 500.2785, $C_{25}H_{44}O_7NP$, 5.5) belongs to LysoPE in which one of the two acyl chains is missing. Generally, hemolysis is regarded as a possible reason for this acyl loss. Phosphatidylethanolamines (PE) have been found to be in increased levels in obese women with insulin resistance [87]. Also in placebo group BL16 (*m/z*: 303.2331, $C_{20}H_{32}O_2$, 5.5) which is a C-20 carbon carboxylic acid with 4 cis double bonds. BL16 is a major lipid component of cell membranes and usually one of the two acyl chains of glycerophospholipids structure. It has to be noted that the detected testosterone derivatives BL11 (*m/z*: 367.1586, $C_{19}H_{28}O_5S$, 5.5) and BL20 (*m/z*: 369.1739, $C_{19}H_{30}O_5S$, 5.5) were also found as statistical significant metabolites in urine placebo samples.

In contrast to urine, in blood samples metabolic pathways were not revealed. Samples hemolysis impeded significantly the identification step and few metabolites were identified coming from the capsule or endogenous formed. It is very important that in HT group a common metabolite in urine and blood was identified, *p*-cresol sulfate, which was suggested in the current study as a metabolite of high importance, requiring further exploration for its relavance in obesity. Moreover, MUFA capsule ingredients revealed as statistical significant, confirming previous studies denoting their effect on weight maintenance through modulation of gut microbiome [70]. Additionally, a category of compounds, phosphoinisitols, was revealed as significant in HT group, which has demonstrated anti-obesity effect in mice [74]. Further studies are required for observation of phenols variation in plasma and the combination of the results with urine metabolites for discovery of the followed mechanism causing weight/fat loss in human.

4. Conclusions

In the current study, different analytical platforms were employed for the investigation of human biological fluids after HT supplementation in a double-blinded study. After HT quantitative determination, urine and blood samples were analyzed for the investigation of human metabolome after daily administration of HT in standard doses. A six-months human intervention study was carried out consisted of the administration of HT in different doses and placebo capsules in 30 overweight/obese women. Anthropometric measurements were determined during the whole period and registration of the corresponding weight and fat loss. Participants lost 2-11 Kg depending on the treatment, followed by a total fat loss of 2-9 Kg. This the first human study where the designed protocol and administered HT doses, demonstrated anti-obesity effect and cause significant weight and fat loss in the group of participants receiving the high HT dose. The used capsules (HT and placebo) were characterized in terms of HT contained concentration and the description of their composition.

A highly sensitive and specific UHPLC-Tq-MS methodology was developed for the quantification of HT in human urine. Quantification results revealed an association between HT consumption and the excreted amount. An average value of 220.02 ng/mL was recorded after three-months administration of HT in the high dosage group (15 mg HT per day) and 247.37 ng/mL after six months administration of HT in low dosage (5 mg HT per day). The resulted concentrations revealed that the maximum excretion was in the same levels in both treatments with difference in the required period for the corresponding absorption and subsequent excretion. A double supplementation period was required for the low dose of HT (5 mg per day) for the excretion of the maximum recorded concentration. More specifically, in low dose a linear dose-response pattern was observed reaching the highest levels in 6 months of administration. In

contrast, in high dose which is also correlated with the observed weight/fat loss the highest levels are reached in 3 months showing a saturation effect. This is the first study investigating the role of HT supplementation and obesity, where an effect of HT saturation was recorder in human system.

Additionally, two different mass spectrometry based metabolomic approaches were developed for the investigation of HT biotransformation in human system and the corresponding followed biosynthetic pathways. Placebo and HT urine samples revealed two different biosynthetic pathways. Placebo group followed the standard dopamine pathway indicating as statistical significant features normally occurring components of dopamine pathway. On the other hand, study of HT samples exposed that HT supplementation leads to the overexpression of standard dopamine metabolites which subsequently form phenol and benzene urine derivatives. Specifically, hippuric acid, *p*-cresol and phenylacetylglutamine accompanied by the corresponding conjugated compounds produced through phase I and II metabolism were identified as major metabolites of this treatment. These metabolites are reported for the first time as final metabolites of HT supplementation, with a possible role in the mechanism of weight/fat loss. Also it has to noted that the three of them have been associated with toluene exposure and they are characterized by bad reputation in literature. Recent studies as well as the present study verify that these metabolites are generally overproduced, after phenol derivatives consumption and not only after exposure to organic solvents and the need of further exploration of these metabolites in human system and their possible anti-obesity effect was suggested. Plasma metabolomics revealed as statistical significant biomarkers capsule ingredients assuring the release and circulation of capsule ingredients in human biological fluids.

Overall, for the first time a double-blinded, placebo controlled human study was performed with administration of an encapsulated HT enriched extract in women for investigation of HT anti-obesity effect. For the first time weight/fat loss was recorded after HT supplementation which was analogous to the administered dose, indicating HT beneficial effect in overweight participants. Moreover, use of different doses and quantitative analysis in urine revealed novel data for the existence of HT saturation effect in human system. Metabolome investigation revealed the followed biosynthetic pathway and the biomarkers of HT administration in human urine. Three of them were correlated for the first time with HT supplementation and were suggested as the biomarkers playing key role in the corresponding weight/fat loss.

Bibliography

[1] W.H.O. (WHO), Obesity and Overweight, (2018). https://www.who.int/news-room/fact-sheets/detail/obesity-and-overweight.

[2] N.S. Mitchell, V.A. Catenacci, H.R. Wyatt, J.O. Hill, Obesity: overview of an epidemic, Psychiatr. Clin. North Am. 34 (2011) 717–732. doi:10.1016/j.psc.2011.08.005.

[3] Z. Liu, N. Wang, Y. Ma, D. Wen, Hydroxytyrosol Improves Obesity and Insulin Resistance by Modulating Gut Microbiota in High-Fat Diet-Induced Obese Mice , Front. Microbiol. . 10 (2019) 390. https://www.frontiersin.org/article/10.3389/fmicb.2019.00390.

[4] G.A. Bray, W.E. Heisel, A. Afshin, M.D. Jensen, W.H. Dietz, M. Long, R.F. Kushner, S.R. Daniels, T.A. Wadden, A.G. Tsai, F.B. Hu, J.M. Jakicic, D.H. Ryan, B.M. Wolfe, T.H. Inge, The Science of Obesity Management: An Endocrine Society Scientific Statement, Endocr. Rev. 39 (2018) 79–132. doi:10.1210/er.2017-00253.

[5] O. Castaner, A. Goday, Y.-M. Park, S.-H. Lee, F. Magkos, S.-A.T.E. Shiow, H. Schröder, The Gut Microbiome Profile in Obesity: A Systematic Review, Int. J. Endocrinol. 2018 (2018) 4095789. doi:10.1155/2018/4095789.

[6] P.D. Cani, M. Osto, L. Geurts, A. Everard, Involvement of gut microbiota in the development of low-grade inflammation and type 2 diabetes associated with obesity, Gut Microbes. 3 (2012) 279–288. doi:10.4161/gmic.19625.

[7] N.S. Boghossian, E.H. Yeung, S.L. Mumford, C. Zhang, A.J. Gaskins, J. Wactawski-Wende, E.F. Schisterman, B.S. Group, Adherence to the Mediterranean diet and body fat

distribution in reproductive aged women, Eur. J. Clin. Nutr. 67 (2013) 289–294. doi:10.1038/ejcn.2013.4.

[8] S. Bertoli, A. Leone, L. Vignati, G. Bedogni, M.A. Martinez-Gonzalez, M. Bes-Rastrollo, A. Spadafranca, A. Vanzulli, A. Battezzati, Adherence to the Mediterranean diet is inversely associated with visceral abdominal tissue in Caucasian subjects., Clin. Nutr. 34 (2015) 1266–1272. doi:10.1016/j.clnu.2015.10.003.

[9] C.L. Bendall, H.L. Mayr, R.S. Opie, C. Itsiopoulos, H.L. Mayr, R.S. Opie, C. Itsiopoulos, Central obesity and the Mediterranean diet : A systematic review of intervention trials, Crit. Rev. Food Sci. Nutr. 58 (2018) 3070–3084. doi:10.1080/10408398.2017.1351917.

[10] A.S. Dontas, N.S. Zerefos, D.B. Panagiotakos, C. Vlachou, D.A. Valis, Mediterranean diet and prevention of coronary heart disease in the elderly, Clin. Interv. Aging. 2 (2007) 109–115. https://www.ncbi.nlm.nih.gov/pubmed/18044083.

[11] E. Tripoli, M. Giammanco, G. Tabacchi, D. Di Majo, S. Giammanco, M. La Guardia, E. et al Tripoli, M. Giammanco, G. Tabacchi, D. Di Majo, S. Giammanco, M. La Guardia, The phenolic compounds of olive oil: structure, biological activity and beneficial effects on human health., Nutr. Res. Rev. 18 (2005) 98–112. doi:10.1079/NRR200495.

[12] N. Lemonakis, H. Poudyal, M. Halabalaki, L. Brown, A. Tsarbopoulos, A.-L. Skaltsounis, E. Gikas, The LC-MS-based metabolomics of hydroxytyrosol administration in rats reveals amelioration of the metabolic syndrome., J. Chromatogr. B, Anal. Technol. Biomed. Life Sci. 1041–1042 (2017) 45–59. doi:10.1016/j.jchromb.2016.12.020.

[13] V. Carito, S. Ciafre, L. Tarani, M. Ceccanti, F. Natella, A. Iannitelli, P. Tirassa, G.N. Chaldakov, M. Ceccanti, C. Boccardo, M. Fiore, TNF-alpha and IL-10 modulation

induced by polyphenols extracted by olive pomace in a mouse model of paw inflammation., Ann. Ist. Super. Sanita. 51 (2015) 382–386. doi:10.4415/ANN_15_04_21.

[14] K. Cao, J. Xu, X. Zou, Y. Li, C. Chen, A. Zheng, H. Li, H. Li, I.M.-Y. Szeto, Y. Shi, J. Long, J. Liu, Z. Feng, Hydroxytyrosol prevents diet-induced metabolic syndrome and attenuates mitochondrial abnormalities in obese mice., Free Radic. Biol. Med. 67 (2014) 396–407. doi:10.1016/j.freeradbiomed.2013.11.029.

[15] N. and A. (NDA) EFSA Panel on Dietetic Products, Scientific Opinion on the substantiation of health claims related to polyphenols in olive and protection of LDL particles from oxidative damage (ID 1333 , 1638 , 1639 , 1696 , 2865), maintenance of normal blood HDL-cholesterol concentrations (ID 1639), 9 (2011) 1–25. doi:10.2903/j.efsa.2011.2033.

[16] S.N. El, S. Karakaya, Olive tree (Olea europaea) leaves: potential beneficial effects on human health, Nutr. Rev. 67 (2009) 632–638. doi:10.1111/j.1753-4887.2009.00248.x.

[17] P. Kanakis, A. Termentzi, T. Michel, E. Gikas, M. Halabalaki, A.L. Skaltsounis, From olive drupes to olive OilAn HPLC-orbitrap-based qualitative and quantitative exploration of olive key metabolites, Planta Med. 79 (2013) 1576–1587. doi:10.1055/s-0033-1350823.

[18] C. Vilaplana-Pérez, D. Auñón, L.A. García-Flores, A. Gil-Izquierdo, Hydroxytyrosol and Potential Uses in Cardiovascular Diseases, Cancer, and AIDS , Front. Nutr. . 1 (2014) 18. https://www.frontiersin.org/article/10.3389/fnut.2014.00018.

[19] P. Mučaji, M. Nagy, A. Záhradníková, I. Holková, L. Bezáková, E. Švajdlenka, T. Liptaj, N. Prónayová, Polar constituents of Ligustrum vulgare L. and their effect on lipoxygenase activity, Chem. Pap. 65 (2011) 367–372. doi:10.2478/s11696-011-0015-4.

[20] J. Rodríguez-morató, A. Boronat, A. Kotronoulas, A. Pastor, E. Olesti, C. Pérez-mañá, O. Khymenets, M. Farré, R. De Torre, A. Boronat, A. Kotronoulas, J. Rodr, Metabolic disposition and biological significance of simple phenols of dietary origin : hydroxytyrosol and tyrosol, Drug Metab. Rev. Metab. Rev. 48 (2016) 218–236. doi:10.1080/03602532.2016.1179754.

[21] S.D. Angelo, C. Manna, V. Migliardi, O. Mazzoni, P. Morrica, G. Capasso, G. Pontoni, P. Galletti, V. Zappia, G.C. Nephrology, Pharmacokinetics and metabolism of hydroxytyrosol, a natutal antioxidant from olive oil, 29 (2001) 1492–1498.

[22] C.L. Xu, M.K. Sim, Reduction of dihydroxyphenylacetic acid by a novel enzyme in the rat brain., Biochem. Pharmacol. 50 (1995) 1333–1337. doi:10.1016/0006-2952(95)02092-6.

[23] A. Karkovi, T. Jelena, M. Barbaric, Hydroxytyrosol, Tyrosol and Derivatives and Their Potential Effects on Human Health, (2019).

[24] A.W. Tank, H. Weiner, Ethanol-induced alteration of dopamine metabolism in rat liver., Biochem. Pharmacol. 28 (1979) 3139–3147. doi:10.1016/0006-2952(79)90624-5.

[25] C. Perez-Mana, M. Farre, J. Rodriguez-Morato, E. Papaseit, M. Pujadas, M. Fito, P. Robledo, M.-I. Covas, V. Cheynier, E. Meudec, J.-L. Escudier, R. de la Torre, Moderate consumption of wine, through both its phenolic compounds and alcohol content, promotes hydroxytyrosol endogenous generation in humans. A randomized controlled trial., Mol. Nutr. Food Res. 59 (2015) 1213–1216. doi:10.1002/mnfr.201400842.

[26] C. Perez-Mana, M. Farre, M. Pujadas, C. Mustata, E. Menoyo, A. Pastor, K. Langohr, R. de la Torre, Ethanol induces hydroxytyrosol formation in humans., Pharmacol. Res. 95–96 (2015) 27–33. doi:10.1016/j.phrs.2015.02.008.

[27] M. Robles-Almazan, M. Pulido-Moran, J. Moreno-Fernandez, C. Ramirez-Tortosa, C. Rodriguez-Garcia, J.L. Quiles, Mc. Ramirez-Tortosa, Hydroxytyrosol: Bioavailability, toxicity, and clinical applications, Food Res. Int. 105 (2018) 654–667. doi:https://doi.org/10.1016/j.foodres.2017.11.053.

[28] K.L. Tuck, M.P. Freeman, P.J. Hayball, G.L. Stretch, I. Stupans, The in vivo fate of hydroxytyrosol and tyrosol, antioxidant phenolic constituents of olive oil, after intravenous and oral dosing of labeled compounds to rats, J. Nutr. 131 (2001) 1993–1996. https://www.scopus.com/inward/record.uri?eid=2-s2.0-0034931524&partnerID=40&md5=844b39a066086b7e52afa7ae3ef71a85.

[29] R. Dominguez-Perles, D. Aunon, F. Ferreres, A. Gil-Izquierdo, Gender differences in plasma and urine metabolites from Sprague-Dawley rats after oral administration of normal and high doses of hydroxytyrosol, hydroxytyrosol acetate, and DOPAC., Eur. J. Nutr. 56 (2017) 215–224. doi:10.1007/s00394-015-1071-2.

[30] S. Granados-Principal, N. El-Azem, R. Pamplona, C. Ramirez-Tortosa, M. Pulido-Moran, L. Vera-Ramirez, J.L. Quiles, P. Sanchez-Rovira, A. Naudí, M. Portero-Otin, P. Perez-Lopez, M. Ramirez-Tortosa, Hydroxytyrosol ameliorates oxidative stress and mitochondrial dysfunction in doxorubicin-induced cardiotoxicity in rats with breast cancer, Biochem. Pharmacol. 90 (2014) 25–33. doi:10.1016/j.bcp.2014.04.001.

[31] S. D'Angelo, C. Manna, V. Migliardi, O. Mazzoni, P. Morrica, G. Capasso, G. Pontoni, P. Galletti, V. Zappia, Pharmacokinetics and metabolism of hydroxytyrosol, a natural antioxidant from olive oil., Drug Metab. Dispos. 29 (2001) 1492–1498.

[32] L. Rubió, A. Macià, R.M. Valls, A. Pedret, M. Romero, R. Solà, A new hydroxytyrosol

metabolite identified in human plasma : Hydroxytyrosol acetate sulphate, Food Chem. 134 (2012) 1132–1136. doi:10.1016/j.foodchem.2012.02.192.

[33] A. Kotronoulas, N. Pizarro, A. Serra, P. Robledo, J. Joglar, L. Rubio, A. Hernaez, C. Tormos, M.J. Motilva, M. Fito, M.-I. Covas, R. Sola, M. Farre, G. Saez, R. de la Torre, Dose-dependent metabolic disposition of hydroxytyrosol and formation of mercapturates in rats., Pharmacol. Res. 77 (2013) 47–56. doi:10.1016/j.phrs.2013.09.001.

[34] F. Visioli, C. Galli, S. Grande, K. Colonnelli, C. Patelli, G. Galli, D. Caruso, Hydroxytyrosol excretion differs between rats and humans and depends on the vehicle of administration, J. Nutr. 133 (2003) 2612–2615. https://www.scopus.com/inward/record.uri?eid=2-s2.0-0042710935&partnerID=40&md5=7390ac68fecffd7596d7c2d89f73d615.

[35] M.-C. López de las Hazas, J. Godinho-Pereira, A. Macià, A.F. Almeida, M.R. Ventura, M.-J. Motilva, C.N. Santos, Brain uptake of hydroxytyrosol and its main circulating metabolites: Protective potential in neuronal cells, J. Funct. Foods. 46 (2018) 110–117. doi:https://doi.org/10.1016/j.jff.2018.04.028.

[36] E. Miro-Casas, M. Farre Albaladejo, M.I. Covas, J.O. Rodriguez, E. Menoyo Colomer, R.M. Lamuela Raventos, R. de la Torre, Capillary gas chromatography-mass spectrometry quantitative determination of hydroxytyrosol and tyrosol in human urine after olive oil intake., Anal. Biochem. 294 (2001) 63–72. doi:10.1006/abio.2001.5160.

[37] O. Khymenets, M.C. Crespo, O. Dangles, N. Rakotomanomana, C. Andres-Lacueva, F. Visioli, Human hydroxytyrosol's absorption and excretion from a nutraceutical, J. Funct. Foods. 23 (2016) 278–282. doi:https://doi.org/10.1016/j.jff.2016.02.046.

[38] F. Visioli, C. Galli, F. Bornet, A. Mattei, R. Patelli, G. Galli, D. Caruso, Olive oil phenolics are dose-dependently absorbed in humans., FEBS Lett. 468 (2000) 159–160.

[39] E. Miro-Casas, M.-I. Covas, M. Farre, M. Fito, J.O. O, T. Weinbrenner, P. Roset, R. de la Torre, Hydroxytyrosol disposition in humans., Clin. Chem. 49 (2003) 945–952.

[40] A. Pastor, J. Rodriguez-Morato, E. Olesti, M. Pujadas, C. Perez-Mana, O. Khymenets, M. Fito, M.-I. Covas, R. Sola, M.-J. Motilva, M. Farre, R. de la Torre, Analysis of free hydroxytyrosol in human plasma following the administration of olive oil., J. Chromatogr. A. 1437 (2016) 183–190. doi:10.1016/j.chroma.2016.02.016.

[41] A.I.C. on H. for Technical, R. Of, R. Pharmaceuticals, for human Use, Validation of Analytical Procedures: Text and Mthodology Q2 (R1), (2005).

[42] D. of H. and H.S. Food and Drug Administration, Bioanalytical Method Validation Guidance for Industry, (2013).

[43] E.M.A. (EMA), Concept/Recommendations Paper on the Need for a Guideline on the Validation of Bioanalytical Methods., (2008).

[44] M. de Bock, J.G.B. Derraik, C.M. Brennan, J.B. Biggs, P.E. Morgan, S.C. Hodgkinson, P.L. Hofman, W.S. Cutfield, Olive (Olea europaea L.) leaf polyphenols improve insulin sensitivity in middle-aged overweight men: a randomized, placebo-controlled, crossover trial., PLoS One. 8 (2013) e57622. doi:10.1371/journal.pone.0057622.

[45] M. González-Santiago, E. Martín-Bautista, J.J. Carrero, J. Fonollá, L. Baró, M. V Bartolomé, P. Gil-Loyzaga, E. López-Huertas, One-month administration of hydroxytyrosol, a phenolic antioxidant present in olive oil, to hyperlipemic rabbits

improves blood lipid profile, antioxidant status and reduces atherosclerosis development, Atherosclerosis. 188 (2006) 35–42. doi:https://doi.org/10.1016/j.atherosclerosis.2005.10.022.

[46] H. Jemai, I. Fki, M. Bouaziz, Z. Bouallagui, A. El Feki, H. Isoda, S. Sayadi, Lipid-lowering and antioxidant effects of hydroxytyrosol and its triacetylated derivative recovered from olive tree leaves in cholesterol-fed rats., J. Agric. Food Chem. 56 (2008) 2630–2636. doi:10.1021/jf072589s.

[47] E. Giordano, A. Dávalos, F. Visioli, Chronic hydroxytyrosol feeding modulates glutathione-mediated oxido-reduction pathways in adipose tissue: A nutrigenomic study, Nutr. Metab. Cardiovasc. Dis. 24 (2014) 1144–1150. doi:https://doi.org/10.1016/j.numecd.2014.05.003.

[48] G.J. Schwartz, J. Fu, G. Astarita, X. Li, S. Gaetani, P. Campolongo, V. Cuomo, D. Piomelli, The lipid messenger OEA links dietary fat intake to satiety., Cell Metab. 8 (2008) 281–288. doi:10.1016/j.cmet.2008.08.005.

[49] P. Illesca, R. Valenzuela, A. Espinosa, F. Echeverria, S. Soto-Alarcon, M. Ortiz, L.A. Videla, Hydroxytyrosol supplementation ameliorates the metabolic disturbances in white adipose tissue from mice fed a high-fat diet through recovery of transcription factors Nrf2, SREBP-1c, PPAR-gamma and NF-kappaB., Biomed. Pharmacother. 109 (2019) 2472–2481. doi:10.1016/j.biopha.2018.11.120.

[50] N. Wang, Y. Liu, Y. Ma, D. Wen, Hydroxytyrosol ameliorates insulin resistance by modulating endoplasmic reticulum stress and prevents hepatic steatosis in diet-induced obesity mice., J. Nutr. Biochem. 57 (2018) 180–188. doi:10.1016/j.jnutbio.2018.03.018.

[51] E. Miró-Casas, M.-I. Covas, M. Fitó, M. Farré-Albadalejo, J. Marrugat, R. de la Torre, Tyrosol and hydroxytyrosol are absorbed from moderate and sustained doses of virgin olive oil in humans, Eur. J. Clin. Nutr. 57 (2003) 186. https://doi.org/10.1038/sj.ejcn.1601532.

[52] T. Pallister, M.A. Jackson, T.C. Martin, J. Zierer, A. Jennings, R.P. Mohney, A. MacGregor, C.J. Steves, A. Cassidy, T.D. Spector, C. Menni, Hippurate as a metabolomic marker of gut microbiome diversity: Modulation by diet and relationship to metabolic syndrome, Sci. Rep. 7 (2017) 13670. doi:10.1038/s41598-017-13722-4.

[53] K. Kono, Y. Yoshida, H. Yamagata, M. Watanabe, Y. Takeda, M. Murao, K. Doi, M. Takatsu, Urinary excretion of cresol as an indicator for occupational toluene exposure., Ind. Health. 23 (1985) 37–45. doi:10.2486/indhealth.23.37.

[54] T. Pallister, M.A. Jackson, T.C. Martin, J. Zierer, A. Jennings, R.P. Mohney, A. Macgregor, C.J. Steves, A. Cassidy, T.D. Spector, C. Menni, Hippurate as a metabolomic marker of gut microbiome diversity : Modulation by diet and relationship to metabolic syndrome, Sci. Rep. 7 (2017) 1–9. doi:10.1038/s41598-017-13722-4.

[55] D. Krupp, N. Doberstein, L. Shi, T. Remer, Hippuric Acid in 24-Hour Urine Collections Is a Potential Biomarker for Fruit and Vegetable Consumption in Healthy Children and adolescents, J. Nutr. Nutr. Epidemiol. 142 (2012) 1314–1320. doi:10.3945/jn.112.159319.A.

[56] A. Wijeyesekera, P.A. Clarke, M. Bictash, I.J. Brown, M. Fidock, T. Ryckmans, I.K.S. Yap, Q. Chan, J. Stamler, P. Elliott, E. Holmes, J.K. Nicholson, Quantitative UPLC-MS/MS analysis of the gut microbial cometabolites phenylacetylglutamine, 4-cresyl

sulphate and hippurate in human urine: INTERMAP Study, Anal Methods. 4 (2012) 65–72. doi:10.1039/C1AY05427A.Quantitative.

[57] S.J. Gatley, S.A. Sherratt, The localization of hippurate synthesis in the matrix of rat liver mitochondria., Biochem. Soc. Trans. 4 (1976) 525–526. doi:10.1042/bst0040525.

[58] B.S.J. Gatley, The Synthesis of Hippurate from Benzoate and Glycine by Rat Liver Mitochondria, Biochem J. 166 (1977) 39–47.

[59] C. Petrus, S. Badenhorst, E. Erasmus, R. Van Der Sluis, C. Nortje, A. Aike, A new perspective on the importance of glycine conjugation in the metabolism of aromatic acids, Drug Metab. Rev. 46 (2014) 343–61. doi:10.3109/03602532.2014.908903.

[60] H.J. Lees, J.R. Swann, I.D. Wilson, J.K. Nicholson, E. Holmes, Hippurate: The Natural History of a Mammalian − Microbial Cometabolite, J. Proteome Res. 12 (2013) 1527–1546.

[61] K. Windey, V. De Preter, K. Verbeke, Relevance of protein fermentation to gut health, Mol. Nutr. Food Res. 56 (2012) 184–196. doi:10.1002/mnfr.201100542.

[62] J.W. Seakins, The determination of urinary phenylacetylglutamine as phenylacetic acid. Studies on its origin in normal subjects and children with cystic fibrosis., Clin. Chim. Acta. 35 (1971) 121–131. doi:10.1016/0009-8981(71)90302-0.

[63] S.W. Brusilow, Phenylacetylglutamine May Replace Urea as a Vehicle for Waste Nitrogen Excretion1, Pediatr. Res. 29 (1991) 147–150.

[64] M. Mokhtarani, G.A. Diaz, U. Lichter-konecki, S.A. Berry, J. Bartley, S.E. Mccandless, W. Smith, C. Harding, C. Le Mons, D.F. Coakley, B. Lee, B.F. Scharschmidt, Urinary

phenylacetylglutamine (U-PAGN) concentration as biomarker for adherence in patients with urea cycle disorders (UCD) treated with glycerol phenylbutyrate, Mol. Genet. Metab. Reports. 5 (2015) 12–14. doi:10.1016/j.ymgmr.2015.09.003.

[65] L. Rubio, A. Macia, R.M. Valls, A. Pedret, M.-P. Romero, R. Sola, M.-J. Motilva, A new hydroxytyrosol metabolite identified in human plasma: hydroxytyrosol acetate sulphate., Food Chem. 134 (2012) 1132–1136. doi:10.1016/j.foodchem.2012.02.192.

[66] Y. Saito, T. Sato, K. Nomoto, H. Tsuji, Identification of phenol- and p-cresol-producing intestinal bacteria by using media supplemented with tyrosine and its metabolites, FEMS Microbiol. Ecol. 94 (2018) 1–11. doi:10.1093/femsec/fiy125.

[67] F. Visioli, A. Poli, C. Gall, Antioxidant and other biological activities of phenols from olives and olive oil., Med. Res. Rev. 22 (2002) 65–75.

[68] C. Agnoli, S. Sieri, F. Ricceri, M.T. Giraudo, G. Masala, M. Assedi, S. Panico, A. Mattiello, R. Tumino, M.C. Giurdanella, V. Krogh, Adherence to a Mediterranean diet and long-term changes in weight and waist circumference in the EPIC-Italy cohort, Nutr. Diabetes. 8 (2018) 22. doi:10.1038/s41387-018-0023-3.

[69] M.A. Mendez, B.M. Popkin, P. Jakszyn, A. Berenguer, D. Chirlaque, A. Barricarte, E. Ardanaz, M. Dorronsoro, P. Amiano, A. Agudo, C.A. Gonza, Adherence to a Mediterranean Diet Is Associated with Reduced 3-Year Incidence of Obesity 1, J. Nutr. Community Int. Nutr. 136 (2006) 2934–2938.

[70] M. Di Paola, E. Bonech, G. Provensi, A. Costa, G. Clarke, C. Ballerini, C. De Filippo, M.B. Passani, Oleoylethanolamide treatment affects gut microbiota composition and the expression of intestinal cytokines in Peyer ' s patches of mice, Sci. Rep. (2018) 1–12.

doi:10.1038/s41598-018-32925-x.

[71] O.B. Clarke, D. Tomasek, C.D. Jorge, M.B. Dufrisne, M. Kim, S. Banerjee, K.R. Rajashankar, L. Shapiro, W.A. Hendrickson, H. Santos, F. Mancia, Structural basis for phosphatidylinositol-phosphate biosynthesis, Nat. Commun. 6 (2015) 8505. https://doi.org/10.1038/ncomms9505.

[72] B. Shirouchi, K. Nagao, N. Inoue, K. Furuya, S. Koga, H. Matsumoto, T. Yanagita, Dietary Phosphatidylinositol Prevents the Development of Nonalcoholic Fatty Liver Disease in Zucker (fa/fa) Rats, J. Agric. Food Chem. 56 (2008) 2375–2379. doi:10.1021/jf703578d.

[73] J.W. Burgess, T.A.-M. Neville, P. Rouillard, Z. Harder, D.S. Beanlands, D.L. Sparks, Phosphatidylinositol increases HDL-C levels in humans., J. Lipid Res. 46 (2005) 350–355. doi:10.1194/jlr.M400438-JLR200.

[74] K.O.S. Himizu, T.O.I. Da, H.A.T. Sutsui, T.O.A. Sai, K.A.O. Tsubo, N.A.O. Ku, Anti-obesity Effect of Phosphatidylinositol on Diet-Induced Obesity in Mice, J Agric Food Chem. 58 (2010) 11218–11225. doi:10.1021/jf102075j.

[75] X. Leng, H. Jiang, Effects of arachidonic acid and its major prostaglandin derivatives on bovine myoblast proliferation , differentiation , and fusion, Domest. Anim. Endocrinol. 67 (2019) 28–36. doi:10.1016/j.domaniend.2018.12.006.

[76] R.A. Coleman, W.L. Smith, S. Narumiya, International Union of Pharmacology classification of prostanoid receptors: properties, distribution, and structure of the receptors and their subtypes., Pharmacol. Rev. 46 (1994) 205–229.

[77] G.S. Hotamisligil, P. Peraldi, A. Budavari, R. Ellis, M.F. White, B.M. Spiegelman, IRS-1-mediated inhibition of insulin receptor tyrosine kinase activity in TNF-alpha- and obesity-induced insulin resistance., Science (80-.). 271 (1996) 665–668. doi:10.1126/science.271.5249.665.

[78] S.P. Weisberg, D. McCann, M. Desai, M. Rosenbaum, R.L. Leibel, A.W.J. Ferrante, Obesity is associated with macrophage accumulation in adipose tissue., J. Clin. Invest. 112 (2003) 1796–1808. doi:10.1172/JCI19246.

[79] K. Takayama, G.K. Sukhova, M.T. Chin, P. Libby, A novel prostaglandin E receptor 4-associated protein participates in antiinflammatory signaling., Circ. Res. 98 (2006) 499–504. doi:10.1161/01.RES.0000204451.88147.96.

[80] M. Minami, K. Shimizu, Y. Okamoto, E. Folco, M.-L. Ilasaca, M.W. Feinberg, M. Aikawa, P. Libby, Prostaglandin E receptor type 4-associated protein interacts directly with NF-kappaB1 and attenuates macrophage activation., J. Biol. Chem. 283 (2008) 9692–9703. doi:10.1074/jbc.M709663200.

[81] K. D'Souza, G. V Paramel, P.C. Kienesberger, Lysophosphatidic Acid Signaling in Obesity and Insulin Resistance, Nutrients. 10 (2018) 399. doi:10.3390/nu10040399.

[82] A. Michalczyk, M. Budkowska, B. Dolegowska, D. Chlubek, K. Safranow, Lysophosphatidic acid plasma concentrations in healthy subjects: circadian rhythm and associations with demographic, anthropometric and biochemical parameters., Lipids Health Dis. 16 (2017) 140. doi:10.1186/s12944-017-0536-0.

[83] H. Kim, J.H. Kim, S. Noh, H.J. Hur, M.J. Sung, J. Hwang, J.H. Park, H.J. Yang, M. Kim, D.Y. Kwon, S.H. Yoon, Metabolomic Analysis of Livers and Serum from High-Fat Diet

Induced Obese Mice, J. Proteome Res. 10 (2011) 722–731.

[84] H. Yeon, M.S. Kim, M.K.M. S, H. Min, P. Ph, J. Kim, D. Ph, E. Ji, K. Ph, C. Hwan, L. Ph, J. Han, Y. Park, D. Ph, Lysophospholipid profile in serum and liver by high-fat diet and tumor induction in obesity-resistant BALB/c mice, Nutrition. 30 (2014) 1433–1441. doi:10.1016/j.nut.2014.04.013.

[85] A. Caimari, R.M. Escorihuela, S. Sua, M. Sua, Impact of a cafeteria diet and daily physical training on the rat serum metabolome, PLoS One. 12 (2017) 1–19. doi:10.1371/journal.pone.0171970.

[86] K. Segawa, S. Nagata, An Apoptotic " Eat Me " Signal : Phosphatidylserine Exposure, Trends Cell Biol. 25 (2015) 639–650. doi:10.1016/j.tcb.2015.08.003.

[87] J.M. Wentworth, G. Naselli, K. Ngui, G.K. Smyth, R. Liu, P.E. O'Brien, C. Bruce, J. Weir, M. Cinel, P.J. Meikle, L.C. Harrison, GM3 ganglioside and phosphatidylethanolamine-containing lipids are adipose tissue markers of insulin resistance in obese women, Int. J. Obes. 40 (2016) 706–713. https://doi.org/10.1038/ijo.2015.223.

Appendix

Table A 13: *List of urine samples included in analysis for HT quantification via UHPLC-Tq-MS. The first column represents the given code to the participant and the second to fourth column the corresponding urine collection in the first (t1), third (t3) and sixth (t6) month of the intervention. Last column illustrates participant group.*

Participant code	t1	t3	t6	Group
Ur_KA_1	✓	✓	-	Pending
Ur_KA_4	✓	✓	✓	A
Ur_KA_7	✓	✓	✓	A
Ur_KA_8	✓	✓	✓	B
Ur_KA_9	✓	✓	✓	B
Ur_KA_10	✓	-	-	A
Ur_KA_11	✓	✓	✓	A
Ur_KA_14	✓	✓	-	Pending
Ur_KA_15	✓	✓	✓	B
Ur_KA_18	✓	✓	-	Pending
Ur_KA_21	✓	✓	✓	B
Ur_KA_22	✓	✓	✓	A
Ur_KA_24	✓	✓	✓	A
Ur_KA_27	✓	✓	-	B
Ur_KA_29	✓	✓	✓	A
Ur_KA_32	✓	✓	-	B
Ur_KA_33	✓	✓	-	A
Ur_KA_35	-	✓	-	Pending
Ur_KA_38	✓	✓	-	Pending
Ur_KA_39	✓	✓	-	Pending
Ur_KA_41	✓	✓	-	Pending
Ur_KA_45	✓	✓	✓	B
Sum	**53 samples**			

Table A 14: *List of urine and blood samples included in metabolomics analysis via UPLC-HRMS metabolomics. The first column represents the given code to the participant and the second to fourth column the corresponding urine and blood collection in the first (t1), third (t3) and sixth (t6) month of the intervention. Last column illustrates participant group.*

Patient code	**t1**		**t3**		**t6**		**Group**
	Urine	Blood	Urine	Blood	Urine	Blood	
KA_1	✓	✓	✓	-	-	-	pending
KA_2	✓	✓	✓	✓	✓	✓	P
KA_3	✓	✓	-	-	-	-	P
KA_4	✓	✓	✓	✓	✓	✓	A
KA_7	✓	✓	✓	✓	✓	✓	A
KA_8	✓	✓	✓	✓	✓	✓	B
KA_10	✓	✓	-	✓	-	-	A
KA_11	✓	✓	✓	✓	✓	✓	A
KA_14	✓	✓	✓	✓	-	-	pending
KA_15	✓	✓	✓	✓	✓	✓	B
KA_16	✓	✓	✓	✓	-	-	P
KA_18	✓	✓	✓	✓	-	-	pending
KA_20	✓	✓	✓	✓	✓	✓	P
KA_21	✓	✓	✓	✓	✓	-	B
KA_22	✓	✓	✓	✓	✓	✓	A
KA_24	✓	✓	✓	✓	✓	✓	A
KA_27	✓	✓	✓	✓	-	✓	B
KA_28	✓	✓	✓	✓	✓	✓	P
KA_29	✓	✓	✓	✓	✓	✓	A
KA_30	✓	✓	✓	✓	✓	-	P
KA_31	✓	✓	-	✓	✓	✓	P
KA_32	✓	✓	✓	✓	-	✓	B
KA_33	✓	✓	✓	✓	-	✓	A
KA_35	-	-	✓	✓	-	-	pending
KA_37	✓	✓	✓	✓	✓	✓	P
KA_38	✓	✓	✓	✓	-	-	pending
KA_39	✓	✓	✓	✓	-	-	pending
KA_41	✓	✓	✓	✓	-	-	pending
KA_45	✓	✓	✓	✓	✓	✓	B
Sum							
Urine	**73 samples**						
Blood	**75 samples**						

***Table A 15**: Representation of the statistical differences of body weight loss among groups A, B and C in the three time points of the intervention study.*

Statistical difference among groups	Body weight loss > 5%	Body weight loss > 10%
1 month (t1)	p=0.037	-
3 months (t3)	p=0.123	p=0.009
6 months (t6)	p=0.020	p=0.010

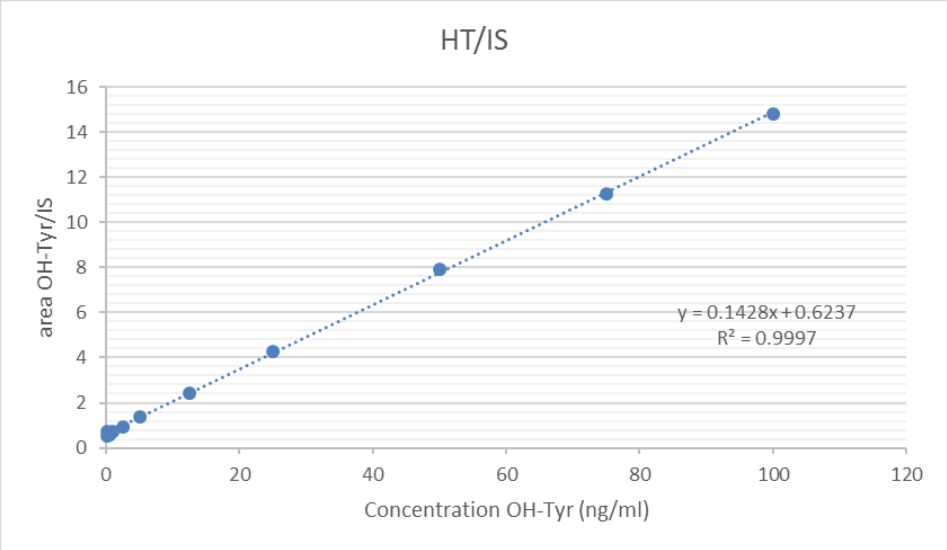

***Figure A 29:** Resulted equation of HT calibration curves. Horizontal axis represents the concentration of HT in ng/mL and the vertical axis the ratio of the HT vs IS.*

(A)

Y-variable	Intercepts
Group A	R2= (0.0, 0.819) Q2= (0.0, -0.354)
Group B	R2= (0.0, 0.819) Q2= (0.0, -0.354)
Placebo	R2= (0.0, 0.819) Q2= (0.0, -0.354)
QC	R2= (0.0, 0.819) Q2= (0.0, -0.354)

(B)

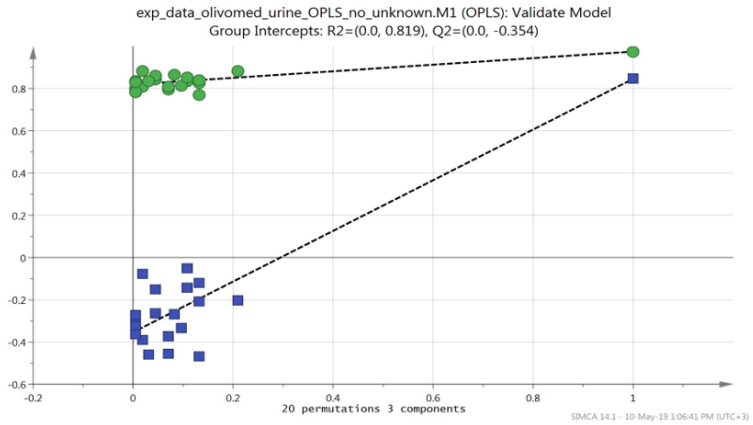

***Figure A 30**: **(A)** Representation of the results of permutation test describing R2 and Q2 intercepts for all the Y variables (group A, group B, placebo and QC) of the above OPLS urine plot. **(B)** Plot generated by permutation test.*

***Table A 16**: Identification parameters of statistical significant urine metabolites. Metabolite code (first column) as well as Δ value in ppm, RT and the corresponding MS/MS fragmentation are given.*

	Suggested molecule	**Experimental *m/z***	**Theoritical *m/z***	**Δ(ppm)**	**Elemental composition**	**RDB**	**RT**	**MS/MS (EC, RDBeq)**
Ur1	Hippuric acid	178.0512	178.0499	1.087	$C_9H_9O_3N$	6.5	4.79	134.0613 (C_8H_8ON, 5.5)
Ur2	Hydroxyhippuric acid	194.0462	194.0448	-1.734	$C_9H_{10}O_4N$	6.5	3.38	150.0564 ($C_8H_8O_2N$, 5.5)
Ur3	Epitestosterone sulfate	367.1587	367.1574	0.4425	$C_{19}H_{28}O_5S$	6.5	9.75	287.1805 ($C_{19}H_{27}O_2$, 6.5)
Ur4	5a-Dihydrotestosterone sulfate	369.1733	369.1730	-0.7840	$C_{19}H_{30}O_5S$	5.5	10.29	289.1609 ($C_{19}H_{29}O_2$, 5.5)
Ur5	Homovanillic acid	181.0510	181.0495	1.9196	$C_9H_{10}O_4$	5.5	4.18	121.0299 ($C_7H_5O_2$, 5.5)
Ur6	Glutamine	145.0616	145.0619	-1.968	$C_5H_{10}O_3N_2$	2.5	5.14	127.0514 ($C_5H_7O_2N_2$, 3.5)
Ur7	Homovanillic acid sulfate	261.0079	261.0063	1.7528	$C_9H_{10}O_7S$	5.5	4.97	181.0508 ($C_9H_9O_4$, 5.5)
Ur8	*p*-cresol sulfate	187.0073	187.0071	1.215	$C_7H_7O_4S$	4.5	5.96	107.0505 (C_7H_7O, 4.5) 79.9579 (SO_3, 0)
Ur9	1,3-Dimethyluric acid	195.0528	195.0513	2.033	$C_7H_8O_3N$	6.5	4.07	180.0290 ($C_6H_4O_3N_4$, 7.0)
Ur10	Homovanillic aldehyde sulfate	245.0128	245.0114	1.420	$C_9H_{10}O_6S$	5.5	5.43	165.0558 ($C_9H_9O_3$, 5.5)

Ur11	Unknown	229.0544	229.0540	1.5899	$C_{10}H_{13}O_4S$	4.5	8.94	149.0977 ($C_{10}H_{13}O$, 4.5) 79.9582 (SO_3, 0)
Ur12	Cortolone-3-glucuronide	541.2265	541.2643	0.157	$C_{27}H_{42}O_{11}$	7.5	7.59	523.2517 ($C_{27}H_{39}O_{10}$, 8.5) 335.2208 ($C_{20}H_{31}O_4$, 5.5)
Ur13	Tyrosol-4-sulfate	217.0179	217.0165	0.327	$C_8H_{10}O_5S$	4.5	7.05	137.0611 ($C_8H_9O_2$, 4.5)
Ur14	Citric acid	191.0198	191.0186	2.168	$C_6H_8O_7$	3.5	0.75	173.0090 ($C_6H_5O_6$, 4.5)
Ur15	Methoxycatehol sulphate	203.0018	203.0009	0.384	$C_7H_8O_5S$	4.5	5.55	123.0452 ($C_7H_7O_2$, 4.5)
Ur16	Hippuric acid sulfate	274.0029	274.0016	0.819	$C_9H_9O_7NS$	6.5	2.59	230.0125 ($C_8H_8O_5S$, 5.5) 194.0457 ($C_9H_8O_4N$, 6.5) 150.0562 ($C_8H_8O_2N$, 5.5)
Ur17	Pyroglutamic acid	128.0356	128.0342	2.528	$C_5H_7O_3N$	3.5	22.14	-
Ur18	Aconitic acid	173.0097	173.0081	2.5237	$C_6H_6O_6$	4.5	1.10	-
Ur19	Lauryl sulfate	265.1479	265.1468	0.575	$C_{12}H_{26}O_4S$	0.5	14.80	96.9606 (HSO_4, 0.5)
Ur20	Phenylacetylglutamine	263.1040	263.1026	0.848	$C_{13}H_{16}O_4N_2$	7.5	5.14	145.0624 ($C_5H_9O_3N_2$, 2.5)
Ur21	Uric acid	167.0215	167.0200	2.7952	$C_5H_4O_3N_4$	6.5	0.98	-

Ur22	3,4-Dihydroxyphenylacetaldehyde	151.0404	151.0390	1.937	$C_8H_8O_3$	5.5	6.42	107.0505 (C_7H_7O, 4.5) 93.0350 (C_6H_5O, 4.5)
Ur23	Unknown	245.0478	245.0478	-1.037	$C_{10}H_{14}O_5S$	4.5	6.89	165.0914 ($C_{10}H_{13}O_2$, 4.5)
Ur24	HT MS2	123.0451	123.0441	-0.073	$C_7H_8O_2$	4.5	5.34	-
Ur25	Unknown	227.0387	227.0373	0.347	$C_{10}H_{12}O_4S$	5.5	8.55	147.0818 ($C_{10}H_{11}O$, 5.5) 79.951 (SO_3, 0)
Ur26	5-alpha-Dihydrotestosterone glucuronide	465.2490	465.2483	-0.777	$C_{25}H_{38}O_8$	7.5	9.52	447.2371 ($C_{25}H_{35}O_7$, 4.5)
Ur27	Unknown	243.0331	243.0322	-0.137	$C_{10}H_{12}O_5S$	5.5	7.92	163.0764 ($C_{10}H_{11}O_2$, 5.5) 79.9579 (SO_3, 0)
Ur 28	*p*-cresol glucuronide	283.0829	283.0832	1.992	$C_{13}H_{16}O_7$	6.5	5.97	175.0249 ($C_6H_7O_6$, 3.5)
Ur29	HT-acetate-4'-O-sulfate	259.0286	259.0271	0.988	$C_{10}H_{12}O_6S$	5.5	7.38	179.0715 ($C_{10}H_{11}O_3$, 5.5)
Ur30	Homovanillic alcohol glucuronide	343.1394	343.1387	-0.431	$C_{16}H_{24}O_8$	5.5	8.42	175.0245 ($C_6H_7O_6$, 3.5)

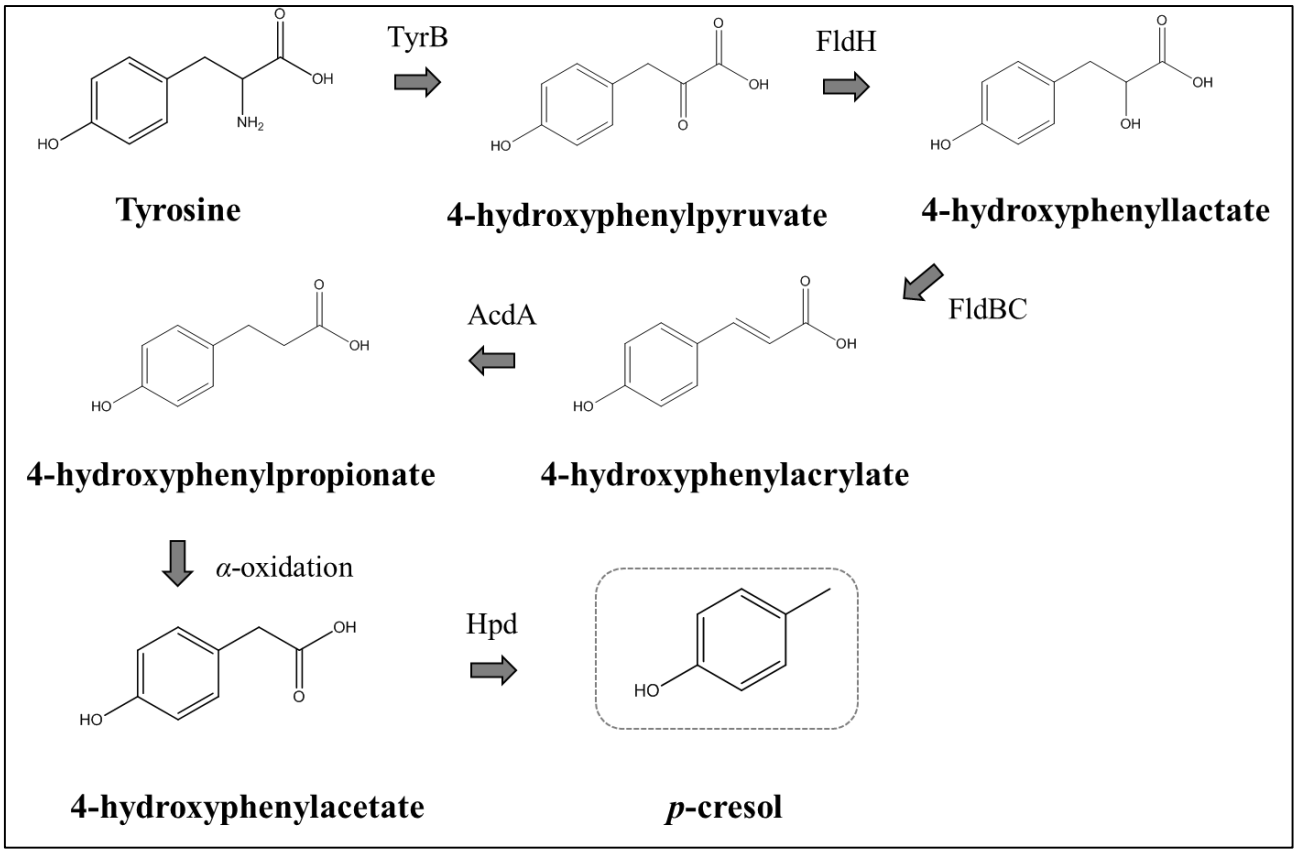

Figure A 31*: Biosynthesis of p-cresol. TyrB: tyrosine aminotransferase B, FldH: phenyllactate dehydrogenase, FldBC: phenyllactate dehydtatase, AcdA: acyl-CoA dehydrogenase, Hpd: hydroxyphenylacetate decarboxylase.*

Table A 17: *Identification parameters of statistical significant blood metabolites. Metabolite code (first column) as well as Δ value in ppm, RT and the corresponding MS/MS fragmentation are given.*

	Suggested molecule	**Experimental *m/z***	**Theoritical *m/z***	**Δ(ppm)**	**Elemental composition**	**RDB**	**RT**	**MS/MS (EC, RDBeq)**
BL1	Oleic acid	281.2485	281.2475	-0.475	$C_{18}H_{34}O_2$	5.5	10.03	263.2375 ($C_{18}H_{31}O$, 3.5)
BL2	1-stearoyl-2-arachidonoyl-sn-glycero-3-phosphoserine	810.5277	810.5280	-1.711	$C_{44}H_{78}O_{10}NP$	7.5	11.74	419.2561 ($C_{21}H_{40}O_6P$, 2.5)
BL3	hydroxy-16,16-dimethylprostaglandin E2	395.2435	395.2428	-1.068	$C_{22}H_{36}O_6$	5.5	5.82	277.1801 ($C_{17}H_{25}O_3$, 5.5)
BL4	1-oleoyl-2-homo-g-linolenoyl-sn-glycero-3-phosphoinositol	885.5472	885.5488	-3.018	$C_{47}H_{83}O_{13}P$	7.5	11.34	419.2558 ($C_{21}H_{40}O_6P$, 2.5) 283.2638 ($C_{18}H_{35}O_2$, 1.5)
BL5	1-palmitoyl glycol-2-phosphocholine	464.3138	464.3136	-1.740	$C_{23}H_{48}O_6NP$	1.5	9.96	403.2605 ($C_{21}H_{40}O_5P$, 2.5)
BL6	Stearic acid	283.2638	283.2632	-1.566	$C_{18}H_{36}O_2$	1.5	10.40	265.2533 ($C_{18}H_{30}O$, 2.5)
BL7	1-linoleoyl-2-docosadienoyl-sn-glycero-3-phosphoinositol	913.5814	913.5801	0.359	$C_{49}H_{87}O_{13}P$	7.5	10.15	605.3830 ($C_{31}H_{58}O_9P$, 3.5)
BL8	1-(2-methoxy-octadecanyl)-sn-glycero-3-phosphoserine	540.3298	540.3296	-1.577	$C_{25}H_{52}O_9NP$	1.5	8.74	480.3074 ($C_{23}H_{47}O_7NP$, 1.5)
BL9	1-Stearoylglycerophosphoserine	524.2988	524.2983	-1.071	$C_{24}H_{48}O_9NP$	2.5	9.45	437.2661 ($C_{21}H_{42}O_7P$, 1.5)

BL10	1-Arachidonyl-sn-glycero-3-phosphoethanolamine	500.2785	500.2772	0.475	$C_{25}H_{44}O_7NP$	5.5	7.97	303.2322 ($C_{20}H_{31}O_2$, 5.5)
BL11	Epitestosterone sulfate	367.1586	367.1574	0.333	$C_{19}H_{28}O_5S$	6.5	4.71	287.1807 ($C_{19}H_{27}O_2$, 6.5)
BL12	1-arachidonoyl-sn-glycero-3-phosphoserine	544.2685	544.2670	0.787	$C_{26}H_{44}O_9NP$	6.5	7.63	457.2351 ($C_{23}H_{38}O_7P$, 5.5)
BL13	Palmitic acid	255.2329	255.2319	-0.288	$C_{16}H_{32}O_2$	1.5	10.09	237.2221 ($C_{16}H_{29}O$, 2.5)
BL14	1,2-Dioleoylphosphatidylserine	786.5282	786.5280	-1.077	$C_{42}H_{78}O_{10}NP$	5.5	11.95	699.4952 ($C_{39}H_{72}O_8P$, 4.5)
BL15	*p*-cresol sulfate	187.0072	187.0060	0.520	$C_7H_8O_4S$	4.5	2.70	107.0506 (C_7H_7O, 4.5) 79.9579 (SO_3, 0)
BL16	Arachidonic acid	303.2331	303.2319	0.417	$C_{20}H_{32}O_2$	5.5	7.97	259.2426 ($C_{19}H_{31}$, 4.5)
BL17	Lauryl sulfate	265.1479	265.1468	0.025	$C_{12}H_{26}O_4S$	0.5	6.43	96.9606 (SO_3, 0)
BL18	Palmitoleic acid	269.2482	269.2475	-1.462	$C_{17}H_{34}O_2$	1.5	10.19	251.2368 ($C_{17}H_{31}O$, 2.5)
BL19	Linoleic acid	279.2332	279.2319	1.062	$C_{18}H_{32}O_2$	3.5	7.99	261.2220 ($C_{18}H_{29}O$, 4.5)
BL20	5a-Dihydrotestosterone sulfate	369.1739	369.1730	-0.672	$C_{19}H_{30}O_5S$	5.5	5.07	289.1611 ($C_{19}H_{29}O_2$, 5.5)
BL21	1-Oleoyl-lysophosphatidic acid	435.2519	435.2506	0.452	$C_{21}H_{41}O_7P$	2.5	8.33	152.9958 ($C_3H_6O_5P$, 1.5)

BL22	Unknown	229.0540	229.0529	0.118	$C_{10}H_{14}O_4S$	4.5	4.52	149.0975 ($C_{10}H_{13}O$, 4.5)
BL23	Glycochenodeoxycholic acid (bile acid)	448.3067	448.3057	-0.305	$C_{26}H_{42}O_5N$	6.5	6.11	287.1344 ($C_{10}H_{23}O_9$, 0.5)

General conclusions

Bioactive compounds from natural sources have an unfailing medicinal use for the prevention and treatment of human diseases. Industry exploiting health claims for many natural products, release dietary supplements in the market independently of the complete or incomplete research behind. OO holds two different health claims from EFSA and is characterized by plethora of bioactive ingredients with high pharmacological interest. Lately, several dietary supplements based on OO ingredients have been released in the market despite the insufficient research and published data for their efficacy and generally the impact on the human organism. In the current study a holistic research was conducted for the investigation of quality control of OO, the parameters affecting the content of specific bioactive compounds, their isolation for the performance of *in vitro* and *in vivo* experiments, the investigation of ADMET properties and finally a human intervention study. In the center of the research workflow was the development and application of mass spectrometry based methods and the use of different mass spectrometry platforms and metabolomic approaches for monitoring OO quality and OO based products, the exploration of their positive impact to health and elucidation of biophenols.

Initially, OO composition and the parameters affecting its quality were investigated. For this reason, more than 200 OO samples were attentively collected from the main olive oil producing areas of Greece, achieving the maximum representation of different factors known for their impact to OO chemical composition. Samples were extracted with IOC established methodology and analyzed via Folin-Ciocalteu for TPC determination. Average values for TPC were estimated according to geographical origin, production procedure and cultivation practice. Crete revealed the highest values for geographical origin, two phases decanters for production procedure and organic cultivation for cultivation practice. Subsequently samples were quantified

via HPLC-DAD for determination of HT, T, OLEA and OLEO content in OO. Crete showed high values for OLEA and OLEO and Peloponnese and Ionian islands for HT and T. It is interesting that Ithaca samples showed also high concentrations in OLEA and OLEO. Subsequently, two different high resolution mass spectrometry platforms (LC-Orbitrap and Flow injection MRMS) were developed for the determination of markers compounds affected by the parameters of origin, cultivation practice and production procedure. Totally 72 metabolites were identified as biomarkers and specific chemical categories were associated with the studied quality parameters such as oleic acid, oleuropein aglycon, elenolic acid, hydroxytyrosol etc. It should be highlighted, that the ability to isolate compounds from OO which are not commercially available strengthen considerably the identification confidence of marker compounds which is a critical drawback in NPs metabolic profiling studies. It has to be also noted that for the first time a mass spectrometry methodology without any sample preparation step, without the LC dimension analyzing together lipophylic and polar components providing a holistic quality control workflow for OO was developed.

Based on quantification results, an OO rich in OLEO and OLEA as well as in other biophenols was forwarded for biophenols isolations. Totally 8 biophenols were isolated from OO and tested with typical *in vitro* assays for cytotoxicity evaluation. Secoiridoids and specifically ligstroside aglycon were found more active in comparison to iridoids (elenolic acid and elenolic acid ethyl ester) and highly cytotoxic in doses over 1 μM. Interestingly, the 8S isomer of ligstroside aglycon was found as more potent compared to 8R. OLEO and OLEA as well as three TPFs (low, intermediate and high levels in OLEA and OLEO) were tested *in vitro* to human fibroblast cells and revealed their protective effect to oxidation stress. TPFs were also evaluated as dietary supplements to a *Drosophilla* model. Results indicated the long-term protective effect

in the fly model of aberrant activation of the insulin receptor adding thus further mechanistic knowledge on the reported healthy aging-promoting properties of EVOOs and the tested biophenols. Consequently, a PK experiment was designed and OLEO was administered to standard doses in a mouse model while plasma samples were collected in 10 time points. Due to the highly reactive and unstable nature of OLEA, it wasn't possible to be detected in plasma. However, degradation and/or biotransformation products were identified in different time points. Therefore, specific time points (relative Tmax) and concentration levels (relative Cmax) for OLEO phase I & II metabolites (oleocanthalic acid, tyrosol sulfate etc) were monitored and determined for the first time. Additionally, possible biotransformation reactions were described for the first time.

After EFSA health claim publication numerous HT products were released in the market. The lack of the appropriate investigation concerning the quality control of the realized products and the impact of HT to human metabolic system lead us to the design of a human intervention study, aiming the development of a holistic workflow for evaluation of an HT capsule anti-obesity effect and impact to human metabolome. Initially, HT capsules was analyzed for the determination its total ingredients and subsequently the exact quantitation of HT in capsule. The design of the study was based on EFSA suggested HT daily supplementation and the total absorption of phenols in human system. HT was administered in two different doses (5 and 15mg/day) to 30 overweigh/ obese women divided in three groups (high, low and placebo). HT supplementation showed a positive correlation with total weight and fat loss and participants lost from 2-11 Kg according to the received HT amount. It is important to note that the group receiving the high HT dose showed a significant weight loss (7-11 kg) as well as fat loss (7-9 Kg.) after six months of supplementation. Urine and blood samples were collected during

intervention (three time points, 1, 3 and 6 months) and HT was quantified in urine samples of volunteers using a triple quadrupole mass spectrometer. Additionally, untargeted metabolomic approach using high resolution mass spectrometry (Orbitrap analyser) was developed for discovery of marker metabolites in each group as well as exploration of HT metabolites and pathways analysis. Taking the advantage of the high resolving power of orbitrap analyzer the identification of compounds in different time points revealed HT metabolization products in blood and urine. Moreover, certain metabolites were identified to be altered in urine and blood samples indicating specific pathways activation in the three different groups. In the placebo group metabolites indicative of the classical dopamine pathway were identified. In contrast, in HT supplementation groups (both high and low dose) it seems that other branches are activated leading to the high production of hippuric acid, *p*-cresol and phenylacetylglutamine accompanied by the corresponding conjugated compounds produced through phase I and II metabolism. Moreover, a saturation effect was observed between the two HT doses offering useful information in respect to proper dose and time of the supplementation scheme.

Concluding OO one of the most important components of Mediterannean diet is a valuable source of active molecules. More research is needed to elucidate its composition and evaluation of biological propertied of its constituents in favor of human health

Development of a quality control method for EVOO

- *Mapping of Greek EVOO*
- *Quantification of 4 biophenols*
- *Correlation with geographical origin, cultivation practice and production procedure*
- *LC-MS (Orbitrap) and FIA-MRMS analysis of biophenols and intact EVOO*
- *Identification of 47 (biophenols) and 25 (intact EVOO) markers*
- *Correlation with quality parameters*

Biological evaluation of olive oil biophenols and Pk study

- ***8 biophenols** were isolated*
- *Secoiridoids found more potent to iridoids in a viability assay (MTT)*
- *C-8 configuration n seems important*
- *TPF, OLEO and OLEA were inactive in BJ normal cells (MTT) and protected cells from H_2O_2 mediated toxicity.*
- *Both, OLEO & OLEA **increase proteasome activity***
- ***TPF increases lifespan** of InRA^{1325D} overexpressing Drosophila tflies*
- *OLEO is not detectable in plasma (Pk study – 10 time points)*
- ***14** metabolites were identified and their relative content was monitored*
- ***Oleocantahlic acid** and **tyrosol sulphate** could serve as plasma markers for OLEO*

Double-blinded placebo study to obese women and markers identification

- *High HT group experienced **7-11 Kg total weight loss** and **7-9 kg total fat***
- *Low HT group & C (placebo) **did no loss weight** or fat*
- *Complete characterization of HT capsules*
- *HT quantified in urine using UHPLC-Tq-MS determined in 1, 3 and 6 months*
- *Average concentration was the same for high and low dose groups while Tmax different*
- *LC-HRMS & HRMS/MS metabolomics revealed clear clustering and identification of 30 biomarkers indicating different pathways for placebo and HT groups*